AEAT/ENV/R/1029 Issue 2

Modelling of Tropospheric Ozone Formation

A Final Project Report produced for the Department for Environment, Food and Rural Affairs on Contract EPG 1/3/143

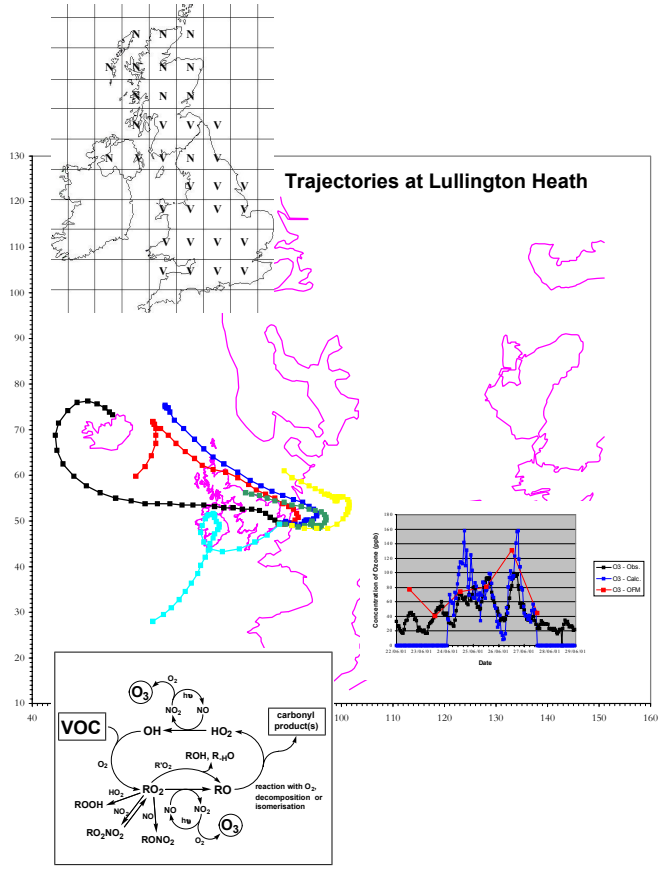

August 2002

AEAT/ENV/R/1029 Issue 2

Modelling of Tropospheric Ozone Formation

A Final Project Report produced for the Department for Environment, Food and Rural Affairs on Contract EPG 1/3/143

August 2002

Title	Modelling of Tropospheric Ozone Formation
Customer	Department for Environment, Food and Rural Affairs
Customer reference	EPG 1/3/143
Confidentiality, copyright and reproduction	
File reference	c:\my_documents\projects\ozone\reports\final_report_v3.doc
Report number	AEAT/ENV/R/1029
Report status	Issue 2

AEA Technology plc
E5 Culham
Abingdon
Oxon., OX14 3ED
Telephone 01235-463108
Facsimile 01235-463005

	Name	Signature	Date
Author	G D Hayman, M E Jenkin, M J Pilling, R G Derwent		
Reviewed by	G D Hayman		
Approved by	G D Hayman		

Executive Summary

The concentrations of ground-level ozone, a pollutant which affects human health, ecosystems and materials, widely exceeds environmental quality standards across the UK and Europe. Ozone is not emitted directly but is a photochemical pollutant formed when volatile organic compounds (VOCs) interact with nitrogen oxides under the influence of sunlight. The control of ground-level ozone concentrations is thus achieved by the control of emissions of VOC and NOx.

The non-linear nature of ozone production and loss requires the use of sophisticated chemical transport models to assess the effectiveness of actual and potential control measures. The aim of the project was thus to develop and improve predictive models for application to the formation of tropospheric ozone on a range of different geographical scales (*i.e.* global, regional and national). This overall project aim has been achieved.

No one model is capable of covering ozone formation on all the required scales from urban to global at a high spatial resolution or with the detailed treatment of chemistry and meteorology required. Thus, different but linked models are needed, as shown in Figure 1. As part of the present project, improvements have been made to existing models, such as STOCHEM or the Photochemical Trajectory Model, in terms of the chemical mechanisms or the emission inventories used. In addition, two new models - EUROSTOCHEM and the Ozone Source Receptor Model (OSRM) - have been successfully developed for application to the formation of tropospheric ozone and its control. The EUROSTOCHEM model provides greater spatial resolution than can be achieved using the parent STOCHEM model. The Ozone Source Receptor Model has been designed to supplement the ELMO model in some applications as it uses more realistic air mass trajectories. The models developed and improved in the project will provide the Department with a range of tools to assess ozone and its control on all the relevant spatial scales and at the appropriate level of detail.

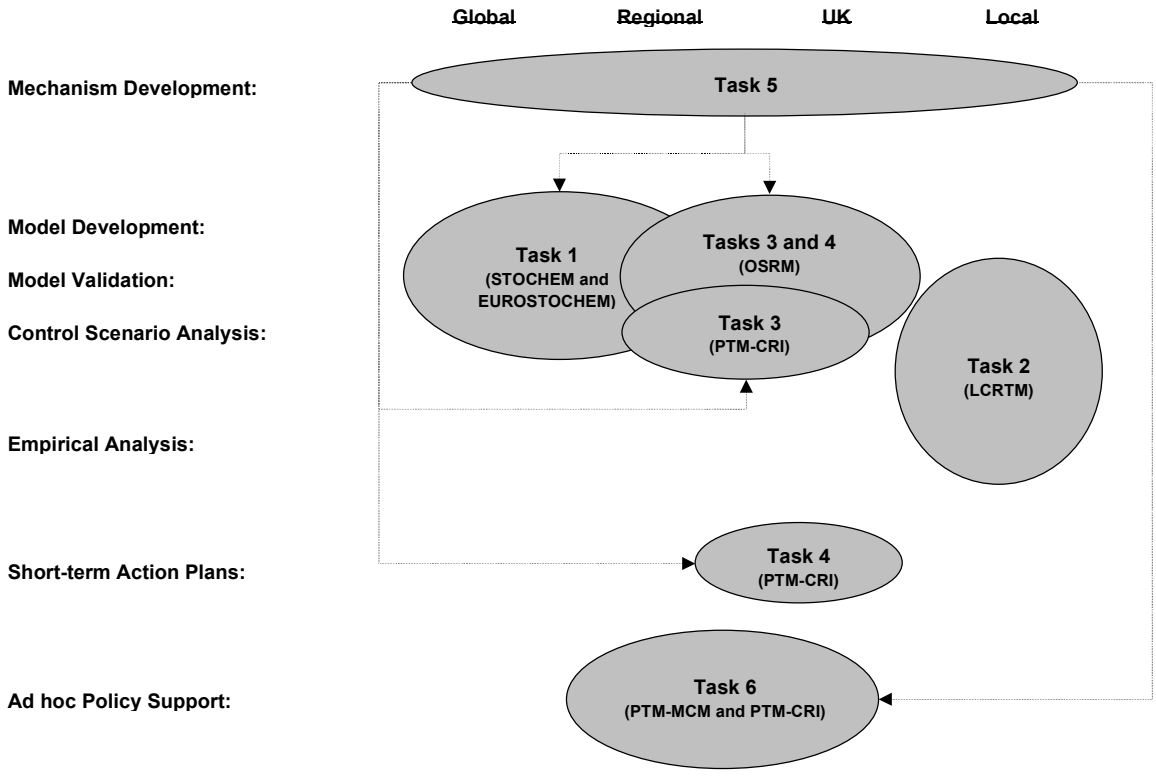

Figure 1 ***A Schematic Overview of the Spatial Domains covered by the Different Ozone Models Used in the Project, the Specific Activities Undertaken and their Relation to the 6 Main Project Task Areas.***

There are a large number of volatile organic compounds emitted from both anthropogenic and natural sources which contribute to ground-level ozone production. For example, the 1999 UK VOC Inventory considered 576 VOCs emitted from 250 source sectors. The contribution of individual compounds vary, a result of differing reactivities and structures. A key thrust of the present project has been to improve and/or expand the information available on key groups of compounds to increase the effectiveness of control measures or to target those sources which make the greatest contribution to ozone formation.

The Department for Environment, Food and Rural Affairs (DEFRA) has therefore let a contract to a consortium of groups (based at AEA Technology, the Meteorological Office, Imperial College and the University of Leeds) related to the development and application of predictive numerical models to describe the formation and control of ozone on regional and global scales. The detailed project objectives addressed a series of issues relating to:

Task 1. Global/regional modelling

Task 2. Urban ozone/nitrogen dioxide

Task 3. Scenario analysis

Task 4. Real-time ozone forecast model - short-term action plans

Task 5. Improvements to chemical and photochemical reaction schemes

Task 6. Policy support - national plan for VOCs/ozone

The key highlights and policy implications are summarised below:

Task 1: Global/Regional Modelling

Previous modelling work by the Meteorological Office using the STOCHEM global tropospheric chemistry model had indicated that the global ozone circulation could have a significant impact on regional ozone concentrations. The work had concluded that rising global ozone concentrations over the next few decades from increased Greenhouse Gas emissions could offset the reductions in ozone concentrations predicted on the European scale from control of VOC and NO_x emissions.

To improve these predictions, a nested model (EUROSTOCHEM) has been developed to calculate ozone concentrations over Europe at higher spatial and temporal resolutions than those achieved using the STOCHEM model. The performance of the EUROSTOCHEM model has been assessed by comparing the model output with ozone measurements made at UK and European ozone monitoring sites.

The EUROSTOCHEM model can reproduce the maximum hourly ozone concentrations observed daily at each site but was less successful at simulating the full diurnal behaviour. The model performance was generally found to be very good against a range of quantitative measures. The model exhibited the expected behaviour when the NO_x and VOC emissions used were separately reduced.

The modelling work has shown that much of the day-to-day variability in the maximum hourly mean ozone concentrations observed at a wide range of sites across Europe and across the British Isles is controlled by the global distribution and circulation of tropospheric ozone.

In general, the future global ozone build-up due to climate change will exert a major influence on the ozone concentrations around the median levels in the distribution of ozone hourly concentrations, with decreasing influences towards the minimum and maximum levels. In contrast, regional pollution control measures will tend to exert their major influence on the peak concentrations. Thus, for ozone concentrations close to median levels, the global build-up and regional pollution controls are calculated to affect the mean ozone concentrations by similar but opposite amounts. However, regional pollution controls were calculated to reduce maximum ozone concentrations significantly more than they were increased by the global-scale build-up.

Task 2: Urban Ozone/Nitrogen Dioxide

The reaction of ozone with NO is the major source of NO_2 in the troposphere. Ozone concentrations are depressed close to NO_x emission sources (in urban areas) by this reaction but increase downwind. The concentrations of NO_2 and O_3 observed are dependent on the initial amount of oxidant ($OX = O_3 + NO_2$) present together with the amount of NO_x emitted locally. Thus, regional and/or global changes in ozone will affect local concentrations of O_3 and NO_2. There are air quality standards for NO_2 and NO_2, as a secondary pollutant, will respond in a non-linear manner to control of the NO_x precursor emissions. It is important to define the NO_x-NO_2-O_3 relationship so that the level of emission reduction to achieve the required air quality standard can be determined.

Measurement data taken from ozone monitoring sites in London and the South East have been analysed to understand the NO_x-NO_2-O_3 relationship. The results indicate that there is a linear relationship between the concentrations of oxidant and NO_x. The intercept can be identified with the initial regional oxidant input and it follows the same seasonal pattern as observed in ozone concentrations. The slope was found to reflect the input of additional oxidant locally. There was no obvious seasonal pattern but there was a clear diurnal effect. Possible sources were identified as direct emissions of NO_2, photochemical and thermal processes.

An analysis of the maximum hourly NO_2 concentrations observed each day at the Marylebone Road site in 1999 confirmed that elevated regional scale oxidant formation can contribute to exceedences of the 105 ppb standard for NO_2 during summer months. The analysis clearly showed that such summertime exceedences can be well correlated with levels of oxidant at Rochester (the nearest rural site to London), and such an analysis provides a possible basis for improved prediction of such exceedences.

The relationship between annual mean concentrations of NO_x-NO_2-OX were analysed for 4 different site types (Central London background, Central London roadside, London suburbs and sites outside of London). The expressions derived for urban centre and background central London sites and sites outside central London are consistent with the expressions of Stedman (2001), with the inferred NOx thresholds which correspond to an annual mean NO_2 mixing ratio of 21 ppb (*i.e.* the WHO air quality guideline) consistently lying slightly higher. A number of sites were classified as 'intermediate', as they have partial roadside character, due to the influence of nearby roads. As expected, the data for these sites consistently lie at higher NOx than the generic expressions for the urban centre and background sites, but lower than the generic expression for roadside sites.

This analysis could also be used to assess the impact of climate change on the achievement of the annual air quality standard for NO_2. For every 0.1 ppb increase in background O_3 concentrations, an additional 0.12-0.22 ppb reduction would be needed in NO_x concentrations to achieve the NO_2 air quality standard.

The London Routine Column Trajectory Model was used to show that future annual mean NO_2 concentrations in central London will remain above the 21 ppb annual mean air quality target despite future planned reductions in road transport NO_x emissions. Furthermore, should global tropospheric ozone concentrations continue to increase, the annual mean air quality target will prove even more difficult to meet.

Task 3: Scenario Analysis and Task 4: Real-time Ozone Forecast Model - Short-term Action Plans (Using the PTM-CRI).

Ozone measurements have been analysed to provide information on the geographical origin and the temporal characteristics of episodes of elevated ozone concentrations over the UK. A Photochemical Trajectory model was subsequently used to understand the observed day-of-week dependence of ozone episodes. As a final part of this task, the photochemical trajectory model was used to investigate the effectiveness of a number of potential short-term control measures for periods when hourly ozone concentrations are forecast to exceed 120 ppb.

An analysis of the ozone concentration measurements made in 1988 and 1989 had previously shown that episodes of elevated concentrations of ozone over the UK were associated with air masses which had passed over continental Europe. For such air masses, the study concluded that about 50% of the

ozone could be attributed to emissions from sources on mainland Europe. Therefore, control of ozone concentrations over the UK would require concerted international action.

The analysis has been extended in the present project to take account of the larger dataset now available. Using ozone measurements made at 20 UK sites between 1992 and 1999, the present study provided further confirmation that episodes of elevated concentrations of ozone over the UK were associated with photochemically-aged air masses arriving in the UK from a broadly easterly or south-easterly direction, after passing over mainland Europe for a period of several days.

Analysis of monitoring data from the same sites over the period 1989-1999 demonstrate that ozone episodes are more prevalent at the end of the week, with the greatest numbers of hours $\geq$ 90 ppbv occurring on Fridays. *This has clear implications in terms of exposure and policy control.* Using the Photochemical Trajectory Model with the Common Reactive Intermediate mechanism (PTM-CRI), a likely explanation for the observed day-of-week dependence is the temporal dependence in the emissions of the ozone precursor species (VOC and NO_X) (which are greater on weekdays) and the multi-day timescale required for chemical processing and transport that lead to elevated ozone levels under photochemical episode conditions in the UK.

Many of the assessment models assume that the annual emission is released at a constant rate. The neglect of the variation in the temporal emission rates could compromise the ability of such models to reproduce the observed ozone behaviour. However, as a result of progressive changes in working practices and social habits, this effect may become less marked in the future, with the consequence that weekly cycles of pollution may become less noticeable.

The PTM-CRI was also applied to investigate the effectiveness of UK Short-term Action Plans. The design of the model is such that only a limited number of trajectories could be investigated. An episode occurring on 1st August 1999 at Barnsley Gawber (124 ppbv) was selected for investigation from the limited number of extreme ozone events now occurring. A number of possible emission control options were assessed. Removal of all UK anthropogenic precursor emissions resulted in a calculated decrease in peak ozone of 2.7 ppbv, which corresponds, on average, to a reduction of approximately 22 minutes in the exceedence duration. Potentially achievable action plans involving eliminating car use in the region of Rotherham/M1 and wider region of Nottinghamshire and South Yorkshire resulted in small changes in the peak ozone concentration. The study concluded that it was difficult to identify any realistic and beneficial UK short-term actions for the type of extreme ozone events which have been recorded in the UK in recent years.

Task 3: Scenario Analysis and Task 4: Real-time Ozone Forecast Model - Short-term Action Plans (Using the OSRM).

A new model - the Ozone Source-Receptor model - has been developed and applied during the present project. It is similar in concept to the ELMO model but has the advantage of higher spatial resolution, the use of realistic air mass trajectories and the option to allow the emissions to vary temporally. The model can be used to derive a range of ozone exposure metrics at 10 km resolution across the UK for different emission control scenarios.

The model was benchmarked against the PTM-MCM on a single trajectory and found to give similar concentrations for ozone and other key species involved in photochemical ozone production. The model performance was then evaluated by comparison with measurements made at UK ozone monitoring stations. The maximum hourly-mean ozone concentrations were derived for each day in 1997. The fraction of the calculated maximum daily ozone concentrations that lay within a factor of 1.5 below or 1.5 above the observed maximum ozone concentrations varied from 0.53 at Bottesford to about 0.77 at Strathvaich Dam.

Further evaluation of the OSRM performance was undertaken. The model was used to simulate the ozone, NO_x and NO_y measurements made at Lullington Heath and the nearby Barcombe Mills sites during a photochemical episode in June 2001. Model simulations were also undertaken using the PTM-CRI. The daily denuder measurements made at Barcombe Mills have provided an opportunity to test the ability of ozone photochemical models to simulate NO_y measurements. The performance of the two models is encouraging but further work is needed to optimise the formulation of the NO_y chemistry in the models. The performance of the OSRM is very comparable to that of the PTM-CRI, an accepted policy tool, for the trajectories and inventories used. Some of the discrepancy between

the models will be due to the different formulation of, for example, the chemical mechanism, the photolysis processes and the parameters characterising the boundary layer. These simulations have shown that the OSRM is fundamentally robust.

AOT40 maps were prepared for the UK using the OSRM to demonstrate its capability for UK-scale modelling. Although the absolute magnitudes were overestimated, the model-derived maps give a reasonable description of the observed spatial distribution, apart from the high values on the east coast of Scotland. The AOT40 maps calculated by the OSRM for the year 1998 have significantly lower values than those shown in the corresponding 1997 maps, which was consistent with 1998 being a lower pollution year than 1997. The OSRM model is thus able to reproduce the difference caused by the changes in the meteorology from 1997 to 1998.

The OSRM was used to investigate the relative response to 30% reductions in the emissions of NO_x and VOCs. The results indicated that a 30% reduction in the NO_x emissions have a greater influence on 40 ppb exceedence days at the UK Rural Ozone Monitoring Network sites compared with 30% reduction in the VOC reduction. For the higher O_3 exceedence thresholds, the results indicate a shift towards a greater response from VOC emission control. The responses agree reasonably well with those reported using the EUROSTOCHEM model, again providing confidence in the performance of the OSRM.

Task 5: Improvements to Chemical and Photochemical Reaction Schemes

The Master Chemical Mechanism is an important component of the work to assess the contribution that individual volatile organic compounds (and hence emission sources) make to ozone formation. This will assist the development of policies to identify and target the VOCs or source sectors for control.

During the present contract, major improvements have been made to the reaction mechanisms of aromatic compounds - an important class of ozone-producing VOCs. Revision of the photolysis rates has been carried out, particularly with regard to multifunctional carbonyl products formed in the aromatic systems. The Master Chemical Mechanism has also been expanded to include the important biogenic compounds - α and β pinene. The new reaction schemes for aromatic compounds and terpenes have been tested against measurements made in chamber studies and the latest version of the Master Chemical Mechanism is able to reproduce those measurements, giving confidence in the MCM.

Using the knowledge and understanding gained from developing the MCM, a reduced mechanism - the Common Reactive Intermediate (CRI) mechanism - has been derived from the Master Chemical Mechanism. The CRI mechanism treats the degradation of methane and 120 VOC using approximately. 570 reactions of 270 species (*i.e.* about 2 species per VOC). It thus contains only 5% of the number of reactions and 7% of the number of chemical species in MCM v2, providing a computationally economical alternative mechanism for use in the Photochemical Ozone Trajectory Model. The CRI mechanism has been benchmarked against the MCM and was shown to produce almost identical concentrations for key species (O_3, OH, NO_3, RO_2 and HO_2) to those calculated using the full Master Chemical Mechanism.

The Master Chemical Mechanism continues to be widely used and is increasingly accepted as the benchmark for an explicit chemical mechanism of hydrocarbon oxidation. Version 3 and earlier versions of the MCM are available on the MCM web-site hosted by the University of Leeds.

Task 6 : Policy Support

As part of Task 6, different versions of the photochemical trajectory model containing either the CRI or MCM mechanisms have been used to investigate the influence of a series of ozone precursor emissions controls on peak ozone levels typical of a UK photochemical episode.

Peak ozone concentrations have been simulated using the PTM-CRI for a series of year 2010 emissions scenarios related to the EU NECD, allowing the effectiveness of the different measures to be compared. Using an ozone episode occurring on the 31st July 1999 for this study, the influence of a series of the emissions scenarios on simulated peak ozone at the 8 southern UK sites was

determined. The present investigation of ozone precursor control scenarios using a representative case study allowed a number of conclusions can be drawn:

- Reductions in UK precursor emissions from 1998 to 2010 reference levels are calculated to have little or no effect on peak episodic ozone levels at locations to the east of the UK. Greater influences (up to 11% reduction) are calculated for locations on the west of the UK, or specific locations which are downwind of regions with particularly high UK emissions;

- Additional VOC reductions in the UK (1252 to 1200 kt a^{-1}) to meet the NECD target may have a small additional influence on selected downwind locations: further proposed reductions (1200 to 1150 kt a^{-1}) appear unlikely to have a major effect on peak episodic ozone levels. However, achievement of NECD targets throughout the EU (together with projected reductions in non-EU countries) were calculated to lead to a reduction of 20-25% in peak episodic ozone levels in the UK.

- The reduction of precursor emissions from 1998 to 2010 levels will be accompanied by a significant shift towards NO_X-limited conditions for episodic ozone formation.

It is likely that the actions taken to implement the United Nations Economic Commission for Europe VOC Protocol through EU Directives on motor vehicle emission controls has led to a reduction in the emissions of certain individual VOC species. In a separate modelling study undertaken in the project, a combination of the highly sophisticated Master Chemical Mechanism and speciated VOC inventories was used in the PTM for the standard Austria-UK trajectory. Ozone concentrations were calculated over a five day travel time in an air parcel which arrived at the England-Wales border. The peak ozone concentration calculated for the fifth and last day was 85.9 ppb. The UK PTM model was then rerun a further 124 times with the emission of each VOC species set to zero in turn. The difference in ozone concentrations was taken as an indication of the contribution to ozone formation of that VOC species. Some of the VOC species identified in motor vehicle emissions were found to be among the most prolific of all the VOC species in forming ozone.

If the contribution of each VOC to ozone production is combined with the observed trends in VOC concentrations, a downward trend in episodic peak ozone concentrations in north west Europe would have been expected during the 1990s. The present analyses should be extended to address the quantitative origins of the elevated ozone concentrations in terms of the VOC emissions from individual stationary source categories and the National Plan for VOCs and ozone.

Recommendations

A number of specific recommendations were identified to enable key policy issues associated with ground-level ozone to be addressed with greater reliability in the future. These were:

(1) There is a continued need for global modelling to investigate the linkage between regional and global-scale ozone and to assess the implication of climate change on the effectiveness of ozone policy control measures.

(2) The concentrations of NO_2 and ozone in the urban environment is an important policy issue in terms of population exposure and attainment of air quality standards. There is a need for detailed modelling of urban NO_2 and ozone using new approaches. The semi-empircal approach described above combined with regional scale modelling provides a possible way forward.

(3) The Ozone Source-Receptor Model (OSRM) is a powerful tool for assessing UK and European emission reduction strategies as it uses realistic air mass trajectories. It should be applied to investigate various UK and European emission reduction scenarios.

(4) The Master Chemical Mechanism is increasingly considered to be the benchmark mechanism to represent the oxidation of volatile organic compounds. To maintain its leading role in the field, it needs to be maintained and expanded. Specific developments include:

(a) ***Maintenance of the Master Chemical Mechanism:*** The chemistry of the existing 124 VOC in MCM v3 should be maintained to ensure that it incorporates the latest available information. A continued area of emphasis would necessarily be aromatic VOC for which new information is constantly becoming available.

(b) ***Maintenance of the MCM website***: The MCM website provides the opportunity to make the MCM available to the wider community, which has resulted in the mechanism being used by a number of groups outside the present consortium. This allows independent testing and validation, and provides independent feedback on the performance of the mechanism. The website should therefore should be updated periodically in line with developments in the mechanism.

(c) ***Expansion of the MCM***: The MCM should be expanded to include a number of additional VOC which potentially make an important contribution to ozone formation, and which cannot be reasonably represented by an existing VOC in the mechanism. This should include additional major biogenic VOC, such as 2-methyl-3-butene-2-ol (MBO) and limonene. In conjunction with this, it is recommended that an improved representation of biogenic emissions (magnitude and speciation) is required for the UK and NW Europe.

(d) ***Revision of Photolysis Rates***: Some appraisal and revision of photolysis rates has been carried out within the present programme, particularly with regard to multifunctional carbonyl products formed in aromatic systems. A complete review of the basis of photolysis rates should be carried out to reflect improvements in the database.

(e) ***Inclusion of Organic Aerosol Formation Processes***: For large, cyclic, unsaturated VOC (such as aromatics and monoterpenes), it is well established that secondary organic aerosol (SOA) is formed in conjunction with ozone. The inclusion of routes to the formation of secondary organic aerosol (SOA) should therefore be considered. This will assist the validation of schemes using chamber data (where SOA formation influences the time dependence of the gas phase species) and will also allow any impact of SOA formation on ambient ozone generation to be assessed.

(f) ***Development and Application of Related Chemical Mechanisms***: In addition to work on the MCM, the current programme has led to associated improvements in other schemes used in ozone models (*e.g.* STOCHEM) and the development of the CRI mechanism. The CRI mechanism should be updated, and a method should be developed for improving the representation of aromatic degradation. The CRI mechanism methodology also provides a basis for representing the chemistry of a large number of hydrocarbons in the speciated inventory which individually make small contributions, but which collectively represent a significant proportion of the 30% not currently covered by the MCM.

(5) There will be a continued need to use numerical models containing a detailed description to simulate ozone formation from each of the stationary VOC source categories.

Contents

Appendices

Acronyms

AEQ	Air and Environment Quality Division (DEFRA)
AOTx	Accumulated Ozone over a Threshold of x ppb
CLRTAP	(UN ECE) Convention on Long Range Transboundary Air Pollution
CRI	Common Reactive Intermediate (Chemical Mechanism)
DEFRA	Department for Environment, Food and Rural Affairs
DETR	Department of the Environment, Transport and the Regions
EC	European Commission
ELMO	Ozone Model developed by the Universities of Edinburgh/Lancaster and the Meteorological Office
EMEP	European Monitoring and Evaluation Programme
EPAQS	Expert Panel on Air Quality Standards
EUPHORE	European Photochemical Reactor (located at Valencia, Spain)
HYSPLIT	Hybrid Single-Particle Lagrangian Integrated Trajectory Model
LRCTM	London Routine Column Trajectory Model
MCM	Master Chemical Mechanism
MO	The UK Meteorological Office
NAEI	National Atmospheric Emission Inventory Programme
NAQS	National Air Quality Strategy
NECD	National Emission Ceilings Directive
NETCEN	National Environmental Technology Centre
NOAA	US National Oceanic and Atmospheric Administration
OSOA	Origin and Formation of Secondary Organic Aerosol
IPCC	Intergovernmental Panel on Climate Change
OSRM	Ozone Source-receptor Model
POCP	Photochemical Ozone Creation Potential
PORG	Photochemical Ozone Review Group
PTM	(Ozone) Photochemical Trajectory Model
QUARG	Quality of Urban Air Review Group
SOA	Secondary Organic Aerosol
SRES	Special Report on Emissions Scenarios (prepared by IPCC)
UNECE	United Nations Economic Commission for Europe
DMS	dimethyl sulphide $(CH_3)_2S$
HCFC	hydrochlorofluorocarbon
HFC	hydrofluorocarbon
NMVOC	non-methane volatile organic compound
NO	nitric oxide
NO_2	nitrogen dioxide
NO_X	oxides of nitrogen (= NO + NO_2)
O_3	ozone
OX	oxidant (=O_3 + NO_2)
RO_2	peroxy radical, derived from a VOC
PAN	peroxy acetyl nitrate
TIA	total inorganic ammonium
TIN	total inorganic nitrate
VOC	volatile organic compound

1 Introduction

1.1 BACKGROUND

During summertime, regional scale photochemical air pollution is a widespread phenomenon across much of north-west Europe. The UK frequently experiences photochemical pollution episodes, which are characterised by high levels of ozone and other photochemical pollutants (*e.g.*, peroxy acetyl nitrate, PAN). The production of elevated levels of ozone is of particular concern, since it is known to have adverse effects on human health, vegetation (*e.g.*, crops) and materials. Established air quality standards for ozone are currently among the most widely exceeded of any pollutant in the UK (EPAQS, 1994; AQS, 2000), and the formulation of control strategies is therefore a major objective of environmental policy.

Ozone is not emitted directly into the troposphere, but is a secondary photochemical pollutant formed from the sunlight-initiated oxidation of volatile organic compounds (VOC, for example hydrocarbons) in the presence of nitrogen oxides (NO_x). The control of ozone formation is thus achieved by the control of emissions of VOC and NO_x. Under conditions characteristic of photochemical pollution episodes, its formation and transport can occur over hundreds of kilometres, with the ozone concentration at a given location influenced by the history of the airmass over a period of up to several days. In addition to this, the increasing levels of ozone in the free troposphere on a global scale also influence regional scale photochemical processes as a result of providing an increasing background ozone level upon which the regional and national scale formation is superimposed. This effect has to be taken into account when assessing whether proposed air quality standards for ozone are likely to be achievable. Consequently, the control of ozone is an international problem requiring solutions agreed at an international level (UNECE, 1992; 1993; 1994).

The Department for Environment, Food and Rural Affairs (DEFRA) has previously supported a consortium of groups (based at AEA Technology, the Meteorological Office and the University of Leeds) on two projects related to the development and application of predictive numerical models to describe the formation and control of ozone on regional and global scales.

In the first (EPG 1/3/70), a Photochemical Trajectory Model (PTM) was developed, tested and applied as a tool for the analysis of ozone control strategies on a regional scale over Europe. The PTM incorporates the precursor VOC and NO_x emissions (in accordance with available speciated inventories), and describes the chemical development and transport of a boundary layer air parcel along pre-selected trajectories over Europe. Since the relation between precursor emissions and the concentration of ozone generated is complex, the simulation of ozone formation requires a detailed representation of the chemistry for a large number of simple and complex VOC which are known to be emitted into the boundary layer. This led to the development of the Master Chemical Mechanism (MCM) as a key component of the project (Jenkin *et al.*, 1997; Saunders *et al.*, 1997). The most recent version of the mechanism (MCM 2.0), is believed to be the most comprehensive description available of the chemical processes involved in photochemical pollutant formation, treating the degradation of methane and 122 non-methane VOC. The PTM has been applied particularly to the calculation of Photochemical Ozone Creation Potentials (POCP) for individual VOC (Derwent *et al.*, 1998; Jenkin and Hayman, 1999), and to the relative contributions to ozone formation made by different VOC emission categories (Jenkin *et al.*, 1999).

The second project (EPG 1/3/93) investigated the global and regional scale distribution of tropospheric ozone. The hypothesis that European regional scale ozone episodes are superimposed on top of a global-scale ozone baseline, that has itself been influenced by human activities, was examined. A global 3-D Lagrangian chemistry transport model, STOCHEM, to describe the global distribution of tropospheric ozone was therefore built and implemented as part of the project. This model has been applied to the emission situations appropriate to the pre-industrial and present day atmospheres and has provided clear evidence in support of increased levels of tropospheric ozone due to human activities. Using this model, and realistic future projections of global emissions to the year 2010 or thereabouts, it has been shown that European regional ozone concentrations may increase during the next decade. This increase may partially offset any likely improvement resulting from European regional pollution control policies.

The further refinement and policy application of the models developed in the previous programmes is a major component of the current work programme. In addition, the present programme was expanded to include an element of ambient data analysis and interpretation for ozone and nitrogen dioxide, and the development of new models to be applied to issues relating to ozone formation on regional and national scales.

1.2 STRUCTURE OF REPORT

In this final report, a detailed account of work undertaken on the project is presented. The report is structured as shown in Table 1.1 with sections on each of the six main task areas:

Task 1. Global/regional modelling
Task 2. Urban ozone/nitrogen dioxide
Task 3. Scenario analysis
Task 4. Real-time ozone forecast model - short-term action plans
Task 5. Improvements to chemical and photochemical reaction schemes
Task 6. Policy support - national plan for VOCs/ozone

Table 1.1 ***Structure and Contents of the Report.***

Section 1	Introduction:	Provides background information to the project and gives the structure of the report
Section 2	Project Overview	Provides an introduction to the project, the project objectives and their achievement, and the ozone models available to the project consortium
Section 3	Task 1: Global/Regional Modelling:	Describes the development, validation and application of the EUROSTOCHEM model. The impact of NO_x and VOC emission reduction and of future climate change scenarios are assessed.
Section 4	Task 2: Urban Ozone/Nitrogen Dioxide:	Describes the application of the LRCTM. The attainment of the NO_2 air quality standard is assessed. In addition, semi-empirical analysis and modelling has been undertaken to understand the relationship between NO_x-NO_2-O_3 concentrations in the urban environment.
Section 5	Tasks 3 and 4: Scenario Analysis and Short-term Action Plans using an Ozone Photochemical Trajectory Model:	Describes the application of the PTM-CRI to understand the geographical and temporal characteristics of elevated ozone concentrations over the UK and the effectiveness of possible policy control measures to address extreme ozone events.
Section 6	Tasks 3 and 4: Scenario Analysis and Short-term Action Plans using the Ozone Source-Receptor Model:	Describes the development, validation and application of the OSRM.
Section 7	Task 5: Improvements to Chemical and Photochemical Reaction Schemes:	Describes the expansion and improvements made to the Master Chemical Mechanisms and some applications.
Section 8	Task 6: Policy Support - National Plan for VOCs/Ozone:	Describes the effectiveness of possible policy control measures proposed by the UN ECE Gothenburg Protocol and the EU NCED and the contribution that individual VOCs make to ozone concentrations.
Section 9	Ozone Exposure Metrics	A review of a paper on the robustness of the AOT40 and other ozone exposure metrics and calculation of these metrics using UK ozone monitoring data.
Section 10	Publications:	List of scientific papers and other publications which have resulted from the project.
Section 11	Summary, Policy Implications and Recommendations:	A summary to indicate the major project highlights and the significance to policy development. A number of recommendations are identified to assist future policy development.
Section 12	Acknowledgements:	Acknowledgement of the support given by DEFRA and other funding agencies.
Section 13	References:	
Appendix 1	Detailed Project Objectives	Detailed description of the background to the project, its aim and specific objectives.
Appendix 2	Comparison of OSRM Calculations with Observed Ozone Concentrations:	Comparison of modelled and observed ozone concentrations for 1997 for 15 sites in the UK ozone monitoring network.
Appendix 3	The 125 VOC degraded in the Master Chemical Mechanism (MCM 3.0)	A list of the VOCs for which detailed degradation mechanisms have been
Appendix 4	A poster presented at the 15th Task Force Meeting of the UN/ECE ICP on Vegetation	The poster reviewed a paper on the robustness of the AOT40 and other ozone exposure metrics and calculation of these metrics using UK ozone monitoring data.

2 Project Overview

The project tasks and objectives are described (Section 2.1). As the major aim of the project was to develop new or to improve existing predictive models for ozone, a summary of the models used in the project is provided in Section 2.2. Section 2.3 summarises the extent to which the original project objectives were achieved.

2.1 PROJECT TASKS AND OBJECTIVES

The project objectives addressed a series of issues relating to:

Task 1. Global/regional modelling
Task 2. Urban ozone/nitrogen dioxide
Task 3. Scenario analysis
Task 4. Real-time ozone forecast model - short-term action plans
Task 5. Improvements to chemical and photochemical reaction schemes
Task 6. Policy support - national plan for VOCs/ozone

The work programme (given in detail on DEFRA's AEQ research website at http://www.aeat.co.uk/netcen/airqual/reports/research99_0/333.html) is provided in Appendix 1 and is broken down into the six main areas listed above.

2.2 THE AVAILABLE OZONE MODELS

The chemistry of ozone production and loss in the boundary layer and troposphere is highly non-linear. Numerical models are therefore needed to understand the chemistry of ozone production and loss, as well as to predict future concentrations in the light of actual, proposed or possible emission controls. No one model is capable of covering ozone formation on all the required scales from urban to global at a high spatial resolution or with the detailed treatment of chemistry and meteorology required. Thus, different but linked models are needed.

The aim of the proposed work was to develop new or to improve existing predictive models for application to the formation of tropospheric ozone on a range of different geographical scales (*i.e.*, global, regional and national) and its subsequent control. The outputs from the models would underpin the formulation of policy with regard to the air quality and ambient levels of ozone in the United Kingdom.

As part of the present project, improvements have been made to existing models, such as STOCHEM or the Photochemical Trajectory Model, in terms of the chemical mechanisms or the emission inventories used. In addition, two new models - EUROSTOCHEM and the Ozone Source Receptor Model (OSRM) - have been successfully developed for application to the formation of tropospheric ozone and its control. The EUROSTOCHEM model provides greater spatial resolution than can be achieved using the parent STOCHEM model. The Ozone Source Receptor Model has been designed to supplement the ELMO model in some applications as it uses more realistic air mass trajectories. The models developed and improved in the project will provide the Department with a range of tools to assess ozone and its control on all the relevant spatial scales and at the appropriate level of detail. An overview of the ozone models used (and related models), their features, capabilities and applications is presented in Table 2.1.

Table 2.1 ***Overview of the Ozone Models used in the Project, their Features, Capabilities and Applications.***

Model Description	Domain/Spatial Resolution/ Code and Solver	Chemistry/Emissions/Meteorology	Application/Advantages
STOCHEM (Meteorological Office) A 3-D global model of tropospheric ozone formation and acid deposition	➢ **Domain** - longitude: 180°W to 180°E; latitude = 90°N to 90°S; surface to 100 mbar. ➢ **Spatial Resolution** - 50,000 air parcels modelled giving an effective spatial resolution of 5° longitude by 5° latitude. ➢ **Code/Solver** - FORTRAN code; Iterative backward EULER solver with chemistry timestep of 300 s.	➢ **Chemistry** - 10 emitted VOCs; 70 species involved in 170 chemical and photochemical reactions; full diurnal chemistry. ➢ **Emissions** - global datasets of annual emissions of CH_4, VOCs, NO_x, SO_2, CO prepared by RIVM at 1° by 1° resolution for 1990; annual emission rates multiplied by monthly factor. ➢ **Meteorology** - air parcels advected by winds taken from a global meteorological dataset (spatial resolution: 1.25° longitude, 0.833° latitude and 12 unevenly-spaced levels in a hybrid vertical co-ordinate). Advection timestep = 3 hours. Winds interpolated linearly in time within the 6-hourly meteorological datasets, bi-linearly in the horizontal domain and using a cubic polynomial in the vertical.	➢ **Application** - study changes in atmospheric composition out to 2100 resulting from climate change. ➢ **Advantages** - linked to state-of-the-art climate models. - driven only by inputs and starting conditions. - includes feedbacks.
EUROSTOCHEM (Meteorological Office) A regional scale model nested within STOCHEM for tropospheric ozone formation and acid deposition	➢ **Domain** - longitude: 60°W to 60°E; latitude = 90°N to equator; surface to 100 mbar. ➢ **Spatial Resolution** - 500,000 air parcels modelled giving an effective spatial resolution of 150 km x 150 km. ➢ **Code/Solver** - FORTRAN code; Iterative backward EULER solver with chemistry timestep of 300 s.	➢ **Chemistry** - as STOCHEM. ➢ **Emissions** - global datasets of annual emissions of CH_4, VOCs, NO_x, SO_2, CO prepared by RIVM at 1° by 1° resolution for 1990; annual emission rates multiplied by monthly factor. ➢ **Meteorology** - air parcels advected by winds taken from a global meteorological dataset comprising a grid of 1.25° longitude, 0.833° latitude and 12 unevenly-spaced levels in a hybrid vertical co-ordinate. Advection timestep = 3 hours. Winds interpolated linearly in time within the 6-hourly meteorological datasets, bi-linearly in the horizontal domain and using a cubic polynomial in the vertical.	➢ **Application** - study changes in atmospheric composition out to 2030 but at a higher spatial resolution than that used in STOCHEM. - limited investigations of different emission control scenarios. ➢ **Advantages** - Can investigate impact of emissions in North America/Asia on European ozone. - Can link hemispheric and regional scales.
ELMO (Universities of Edinburgh/Lancaster and the Meteorological Office) Regional-scale boundary-layer photochemical ozone source-receptor model	➢ **Domain** - EMEP grid. ➢ **Spatial Resolution** - 10 km x 10 km receptor sites covering the UK. ➢ **Code/Solver** - FORTRAN code; Iterative backward EULER solver.	➢ **Chemistry** - as STOCHEM. ➢ **Emissions** - NAEI emissions of CH_4, VOCs, NO_x, SO_2, CO at 1 km x 1 km; EMEP emissions at 50 km x 50 km; emission control scenarios applied on a country-by-country basis ➢ **Meteorology** - uses linear 4-day air mass trajectories at 5° intervals around the compass rose for each UK receptor site; the ozone concentration on each trajectory is weighted by a pollution rose derived from the frequency with which UK ozone concentrations above 50 ppb occur from that wind direction.	➢ **Applications** - calculation of a range of ozone exposure metrics at 10 km resolution across the UK. - used to investigate different emission control scenarios for UK ozone. ➢ **Advantages** - focus on peak ozone and mean ozone levels.
Ozone Forecasting Model (AEA Technology) Boundary layer trajectory model	➢ **Domain** - EMEP grid. ➢ **Spatial Resolution** - Boundary layer air parcel of notional 10 km x 10 km horizontal dimensions. ➢ **Code/Solver** - Forward EULER	➢ **Chemistry** - Ozone production rate equated to the sum of the rates of reaction of OH with 20 VOCs multiplied by a constant OH concentration and the POCP of the VOC. ➢ **Emissions** - Constant emission rates. ➢ **Meteorology** - 4-day air mass trajectories provided by the Met Office for midday arrival times at 20 UK Ozone Monitoring sites.	➢ **Application -** provides daily forecasts of ozone concentrations at 20 UK sites. ➢ **Advantages** - simplified chemistry leads to very short run times but model only provides worse case concentrations.

Table 2.1 ***Overview of the Ozone Models used in the Project, their Features, Capabilities and Applications.***

Model Description	Domain/Spatial Resolution/ Code and Solver	Chemistry/Emissions/Meteorology	Application/Advantages
Photochemical Trajectory Model using the Master Chemical Mechanism (Meteorological Office/AEA Technology) Boundary layer trajectory model	➢ **Domain** - EMEP grid. ➢ **Spatial Resolution** - Boundary layer air parcel of notional 10 km x 10 km horizontal dimensions. ➢ **Code/Solver** - written as a FACSIMILE program, solved using a variable order GEAR solver.	➢ **Chemistry** - Version 3: 123 emitted VOCs; 4,500 species and 12,700 thermal and photochemical reactions; full diurnal chemistry. ➢ **Emissions** - Uses a combination of EMEP, CORINAIR and NAEI inventories providing annual emission estimates of CH_4, CO, VOCs, NO_x and SO_2 for years between 1994-1998; 1994 Biogenic Emission Inventory for Isoprene ; Constant or time varying emissions. ➢ **Meteorology** - uses either linear trajectories representing air mass trajectories for an idealised photochemical episode over the UK or air mass trajectories represented as (x,y) co-ordinates on the EMEP grid which have been derived off-line from meteorological datasets, *e.g.* the NOAA HYSPLIT or BADC datasets.	➢ **Applications** - development of POCP concept and calculation of POCPs; - assess contribution of individual VOCs and different VOC source sectors; -widely used to investigate different emission control scenarios on UK ozone to a coarse receptor grid. ➢ **Advantages** - The most detailed and comprehensive treatment of the oxidation of VOCs, thereby allowing the contribution of each VOC to ozone formation to be determined
Photochemical Trajectory Model using the Common Reactive Intermediate Chemical Mechanism (Imperial College/AEA Technology) Boundary layer trajectory model	➢ **Domain** - EMEP grid ➢ **Spatial Resolution** - Boundary layer air parcel of notional 10 km x 10 km horizontal dimensions ➢ **Code/Solver** - written as a FACSIMILE program, solved using a variable order GEAR solver.	➢ **Chemistry** - Version 3: 123 emitted VOCs; 270 species and 614 thermal and photochemical reactions; full diurnal chemistry. ➢ **Emissions** - Uses a combination of EMEP, CORINAIR and NAEI inventories providing annual emission estimates of CH_4, CO, VOCs, NO_x and SO_2 for years between 1994-1998; 1994 Biogenic Emission Inventory for Isoprene ; Constant or time varying emissions. ➢ **Meteorology** - uses either linear trajectories representing air mass trajectories for an idealised photochemical episode over the UK or air mass trajectories represented as (x,y) co-ordinates on the EMEP grid which have been derived off-line from meteorological datasets, *e.g.* the NOAA HYSPLIT or BADC datasets.	➢ **Applications** - multiple calculations to a specific receptor site; - used to investigate different emission control scenarios on UK ozone to a coarse receptor grid ➢ **Advantages** - Simpler chemical mechanism based on and derived from the MCM which leads to very short run times
OSRM (AEA Technology) A boundary layer regional scale photochemical ozone source-receptor model	➢ **Domain** - EMEP grid ➢ **Spatial Resolution** - 10 km x 10 km receptor sites covering the UK with higher resolution possible for urban areas ➢ **Code/Solver** - FORTRAN code; variable order GEAR solver.	➢ **Chemistry** - as STOCHEM ➢ **Emissions** - 1997 EMEP and 1998 NAEI inventories of NO_x, SO_2, CO and VOCs; 1994 Biogenic Emission Inventory for Isoprene; Option for constant or time varying emission rates. ➢ **Meteorology** - 4-day air mass trajectories derived from winds taken from a global meteorological dataset comprising a grid of 1.25° longitude, 0.833° latitude and 12 unevenly-spaced levels in a hybrid vertical co-ordinate. Advection timestep = 1 hour. Winds taken from 950 mbar pressure level, interpolated linearly in time within the 6-hourly meteorological datasets, bi-linearly in the horizontal domain.	➢ **Applications** - Calculation of a range of ozone exposure metrics at 10 km resolution across the UK; - used to investigate different emission control scenarios for UK ozone ➢ **Advantages** - higher spatial resolution and use of realistic air mass trajectories compared to the ELMO Model

A schematic diagram is presented in Figure 2.1, which shows the spatial domains covered by the different models, the main activities undertaken and the specific models which were used on the six project task areas. Figure 2.1 shows that the different modelling tools were largely complementary with little overlap.

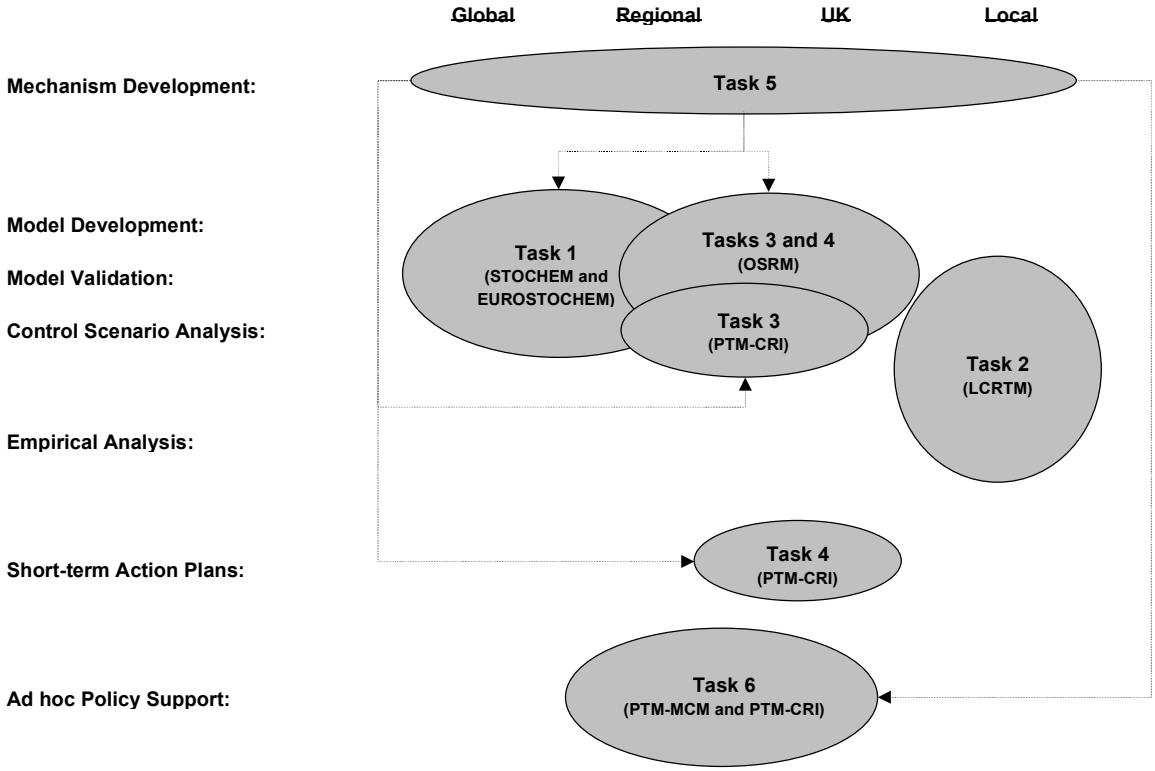

Figure 2.1 A Schematic Overview of the Spatial Domains covered by the Different Ozone Models Used in the Project, the Specific Activities Undertaken and their Relation to the 6 Main Project Task Areas.

2.3 OUTCOME COMPARED TO THE ORIGINAL OBJECTIVES

The detailed project objectives can be found in Appendix 1 and are also available from the DEFRA web-site hosted by AEA Technology. The address is:

http://www.aeat.co.uk/netcen/airqual/reports/research99_0/333.html

The project has achieved the objective to develop and apply a range of numerical models describing ozone production covering a range of spatial and temporal scales. The detailed objectives listed in Appendix 1 have been mostly achieved. Specific deviations are listed in Table 2.2.

Table 2.2 ***Achievement of and Reasons for Deviation from the Original Detailed Project Objectives.***

Task	Detailed Project Objective	Comment/Reason for Deviation
1. Global/Regional Modelling (see Section 3)	(a) The contractor should develop a modelling capacity to investigate the impacts of ozone precursor emissions emitted on the global scale on ozone levels in Europe and the United Kingdom. Information on European ozone concentrations should be available at a resolution of at least 50km.	Achieved through the development of the EUROSTOCHEM model. The spatial scale of the model results has been evaluated and has been found to comparable with that achieved in EMEP modelling, that is about 150 km. Further work will be required if the target spatial resolution of 50 km is to be achieved.
	(b) Furthermore, the model should be able to produce annual and monthly spatially disaggregated estimates of acid deposition, secondary aerosol concentrations (both sulphate and nitrate) and accumulated ozone above thresholds of 60 ppb and 40 ppb (*i.e.* AOT40s and AOT60s) at the same spatial resolution.	No progress has been made towards the production of annual and monthly disaggregated estimates of acid deposition at 50 km spatial resolution across Europe within STOCHEM or EUROSTOCHEM. Significant improvements would be required in the treatment of precipitation scavenging within STOCHEM and EUROSTOCHEM and the resources were not available to achieve them. To meet these objectives on acid deposition, global fields of SO_2, sulphate aerosol, NO, NO_2, nitric acid, nitrate aerosol, ammonia and ozone were passed from STOCHEM to the HARM model. The addition of these global model fields as an input to the HARM model has brought about a substantial improvement in the calculated deposition fields on the western seaboard of the British Isles. The objective of producing annual and monthly disaggregated estimates of secondary aerosol concentrations (both sulphate and nitrate) has been delivered through the development of the EUROSTOCHEM model. The detailed diurnal cycles observed in ozone at each EMEP and UK Rural Ozone Monitoring Network sites cannot be reproduced using the STOCHEM or EUROSTOCHEM models. The objective to calculate AOT40 and AOT60 metrics could not be met. To make progress, EUROSTOCHEM results have been expressed in an alternative and much more robust manner as 90 ppb, 60 ppb and 40 ppb exceedance days.
	(c) The contractor should investigate the feasibility of using land use dependent ozone deposition based upon the concept of stomatal conductivity (Mike Ashmore et al). This incorporates the influence of climatic factors on ozone take up by vegetation and may lead to more accurate model predictions.	Land use dependent ozone deposition based on the concept of stomatal conductivity has been used in STOCHEM and EUROSTOCHEM. However, the incorporation of these features has not led to the production of more accurate model predictions on the global or regional scale because the maps of land use and climatic factors are not currently available with sufficient coverage and reliability. Furthermore, it is doubtful whether an approach based on stomatal conductance would necessarily lead to a more accurate assessment of ozone critical levels and their exceedance in models because of the observed variations in the stability of the atmospheric boundary layer which is an important regulator of the ozone flux to vegetated surfaces.
	(d) The contractor should construct several realistic emissions scenarios for European and non-European Countries. These should be (i) current (1997), (ii) Current Reduction Plans for 2010, 2015 and 2020 (incorporating all countries' expected emissions reductions measures).	Although no progress has been made towards the construction of the global 1° latitude by 1° longitude emission fields that reflect the current reduction plans for European and non-European countries, a simplified representation was however constructed within EUROSTOCHEM to reflect the likely implementation of the UNECE Gothenburg Protocol.
	(e) For each of the scenarios in (d) the contractor should estimate the global and European contributions to acidic deposition and secondary aerosol and estimate AOT40 and AOT60 values on a grid cell basis. Data should be provided on an annual and monthly basis.	No progress has been made towards the construction of the global 1° latitude by 1° longitude emission fields reflecting current reduction plans that would be required to meet this objective.

Table 2.2 ***Achievement of and Reasons for Deviation from the Original Detailed Project Objectives.*** **(Continued)**

Task	Detailed Project Objective	Comment/Reason for Deviation
2. Urban Ozone/Nitrogen Dioxide	The contractor should be prepared to apply the results of this research regarding ozone changes (on the global, regional and national scales) to the consideration of future ozone and nitrogen dioxide concentrations in urban areas which are treated explicitly in DETR contract No. EPG 1/3/128 (DETR Nominated Officer is Dr Stephanie Coster).	Achieved. The LRCTM model has been used to assess the NO_x emission reductions required to meet target air quality in London, with and without increased global ozone levels in 2010. Required NO_x emission reductions increase from 72% to 75% on 1995 levels. Additional work undertaken to develop empirical O_3-NO_2-NO_x relationships from measurements made in the national monitoring networks (see Section 4.3).
3. Scenario Analysis	A tool is required which will allow the Department to analyse the benefits (*i.e.* changes in ozone climate) of implementation of possible European abatement strategies. Such a tool should be able to quantify changes in ozone levels relative to health based air quality standards in a spatially resolved manner across the UK.	Achieved through the development of the Ozone Source-Receptor Model (OSRM) (see Section 6)
	(a) To develop a model which can provide a representative description of the current and future ozone climate of the United Kingdom. The model should: ➢ reproduce current and historical ozone concentration fields based upon representative meteorology. ➢ be able to predict future ozone concentration fields resulting from various policies to reduce ozone precursor emissions in the UK and Europe. ➢ should provide results at a spatial resolution no worse than 10 km x 10 km. ➢ be able to estimate maximum hourly concentrations of ozone . ➢ be able to estimate the numbers of days on which EPAQS and WHO standards are exceeded (8-hour means equal to 50 ppb and 60 ppb respectively) ➢ incorporate anticipated changes in the distribution of urban ozone in the UK ➢ produce output in a form which will allow health based assessments to be undertaken of benefits resulting from particular emission reduction scenarios in the UK and Europe.	- OSRM was used to simulate the ozone concentrations observed at UK ozone monitoring sites during 1997. - Achieved using the PTM-CRI but the OSRM can in principle also achieve this objective (see Section 8.3.2). - Achieved by the OSRM - Achieved by the OSRM - Achieved by the OSRM - Facility in OSRM to cover urban areas at a higher spatial resolution - Post-processor module written to convert OSRM model output into a variety of ozone metrics.
	(b) Apply the model in a) to the estimation of health benefits (including exceedences of WHO and EPAQS air quality standards and maximum hourly concentrations) for up to 10 emissions scenarios to be chosen and developed in conjunction with the Department.	Not achieved but a limited number of emission scenarios were considered using the PTM-CRI.

Table 2.2 ***Achievement of and Reasons for Deviation from the Original Detailed Project Objectives.*** **(Continued)**

Task	Detailed Project Objective	Comment/Reason for Deviation
4. "Real-time" Ozone Forecast Model – "Short term Action Plans"	The Department requires a capacity to forecast ozone levels at a high spatial and temporal resolution. This forecasting tool should also be able to investigate the effects of various emissions control measures in the various source sectors on the forecast levels of ozone. These control measures could be both spatially and temporally varying. Ideally, any model should have the capacity to fulfil or take account of the criteria below, however, it is appreciated that such requirements may be technically out of reach or too onerous financially or time wise. The contractor should therefore propose the most practical solution available.	The OSRM has this capability. A limited study was undertaken using the PTM-CRI during the development of the OSRM (see Section 5.3).
	➢ Present hourly concentrations at a minimum 10 km grid square resolution for the whole of the UK.	The OSRM has this capability.
	➢ Work with the current NAEI contractor (and other organisations such as the London Research Centre) to develop speciated VOC emissions inventories on a 1 km grid square resolution. These inventories should also be resolved temporally to a minimum resolution of 1 hour. Similar inventories should also be prepared for NO_x and CO emissions.	Achieved.
	➢ Be capable of investigating the effect specific measures to reduce ozone precursor emissions (from a variety of sources with differing mixes of VOCs) at specific locations and times of the day.	The OSRM has this capability. A limited study was undertaken using the PTM-CRI during the development of the OSRM.
	➢ Investigate the feasibility of obtaining and utilising improved spatially and temporally disaggregated emissions data (ozone precursors) for Northern European countries such as Belgium, Netherlands, France and Germany.	Not achieved.
	➢ The model should be validated against monitoring data gathered during recent pollution episodes.	The OSRM was used to simulate the ozone concentrations observed at UK ozone monitoring sites during 1997.
5. Improvements to Photochemical Reaction Schemes (see Section 7)	(1) The Master Chemical Mechanism will be maintained and updated as follows:	
	➢ The degradation schemes for aromatic hydrocarbons will be updated in line with new kinetic and mechanistic data, as they become available. The particular features of aromatic degradation which have the most influence on ozone formation will be identified by performing appropriate POCP sensitivity studies.	New schemes developed for aromatic compounds and incorporated into version 3 of the Master Chemical Mechanism (see Section 7.3.3).
	➢ The representation of a number of gas-phase chemical processes will be updated in line with recently published kinetic and mechanistic data. This will include the following: (i) the reactions of OH with PAN species, (ii) the reactions of oxy radicals formed from degradation of esters and alkenes and (iii) the formation of excited oxy radicals from the reactions of some peroxy radicals with NO.	Achieved.
	➢ Photolysis rates of ozone and other inorganic and organic species will be updated in line with latest absorption cross-section and quantum yield data.	Some appraisal and revision of photolysis rates has been carried out, particularly with regard to multifunctional carbonyl products formed in aromatic systems.
	➢ The feasibility of incorporating or improving the description of the formation of secondary sulphate and nitrate aerosol will be assessed, with the additional aim of improving the representation of heterogeneous chemical processes of particular importance (*e.g.* the reaction of N_2O_5 with water).	This objective was deferred following the reduction in scope of the overall programme.
	➢ The updated MCM will be implemented into the Photochemical Trajectory Model (PTM), along with the latest amendments to the NAEI categorisation of sources. A limited degree of validation of the updates to the MCM/PTM will be performed using ambient observational data and environmental chamber data.	Achieved
	➢ The MCM website at Leeds University will be maintained and revised to include the updated MCM when completed.	Web-site maintained. Version 3 of the Master Chemical Mechanism released in 2001.

Table 2.2 ***Achievement of and Reasons for Deviation from the Original Detailed Project Objectives.*** **(Continued)**

Task	Detailed Project Objective	Comment/Reason for Deviation
5. Improvements to Photochemical Reaction Schemes	(2) Chemical schemes for use in the models will be constructed or updated. The performance of these schemes will be compared with that of the MCM using simple box models.	Achieved and Photochemical Ozone Creation Potentials compared (see Section 7.5).
6. Policy Support – National plan for VOCs/Ozone	After the 2nd NO_x protocol has been agreed (and the National Emissions Ceilings Directive adopted) there is likely to be a requirement for the Department to produce a National Plan to implement the emissions ceilings in the UK. The Department is likely to require policy support to cover the following aspects:	
	➢ How to maximise the ozone benefits accruing from the implementation of the rational Emission Ceilings Directive in the UK (*e.g.*, VOC management areas, controls on specific VOCs in certain locations, POCPs, *etc.*)	Support provided (see Sections 8.3, 8.3.2 and 8.3.4).
	➢ Provide support in the update of the UK Strategy to Reduce Emissions of Volatile Organic Compounds.	Support provided (see Section 8.3.5).

3 Global/Regional Modelling

3.1 SECTION SUMMARY

Previous modelling work by the Meteorological Office using the STOCHEM global tropospheric chemistry model had indicated that the global ozone circulation could have a significant impact on regional ozone concentrations. The work had concluded that rising global ozone concentrations over the next few decades from increased Greenhouse Gas emissions could offset the reductions in ozone concentrations predicted on the European scale from control of VOC and NO_x emissions.

To improve these predictions, a nested model (EUROSTOCHEM) has been developed to calculate ozone concentrations over Europe at higher spatial and temporal resolutions than those achieved using the STOCHEM model. The performance of the EUROSTOCHEM model has been assessed by comparing the model output with ozone measurements made at UK and European ozone monitoring sites.

The EUROSTOCHEM model can reproduce the maximum hourly ozone concentrations observed daily at each site but was less successful at simulating the full diurnal behaviour. The model performance was generally found to be very good against a range of quantitative measures. The model exhibited the expected behaviour when the NO_x and VOC emissions used were separately reduced.

The modelling work has shown that much of the day-to-day variability in the maximum hourly mean ozone concentrations observed at a wide range of sites across Europe and across the British Isles is controlled by the global distribution and circulation of tropospheric ozone.

In general, the future global ozone build-up due to climate change will exert a major influence on the ozone concentrations around the median levels in the distribution of ozone hourly concentrations, with decreasing influences towards the minimum and maximum levels. In contrast, regional pollution control measures will tend to exert their major influence on the peak concentrations. Thus, for ozone concentrations close to median levels, the global build-up and regional pollution controls are calculated to affect the mean ozone concentrations by similar but opposite amounts. However, regional pollution controls were calculated to reduce maximum ozone concentrations significantly more than they were increased by the global-scale build-up.

3.2 INTRODUCTION

Ozone concentrations in and around the major population centres of Europe have continued to exceed internationally accepted air quality standards and guidelines set to protect human health and to protect sensitive crops and vegetation (EU, 1992; EPAQS, 1994; AQS, 2000). A great deal of action has been taken by policy-makers to improve ozone air quality in the European region and much more is planned. Whether these actions will deliver the planned improvements in ozone air quality, depends on the adequacy of current understanding of the origins of the ozone present in the European atmosphere. Ozone at the surface may have had its origins in the stratosphere or formed by chemical reactions within the troposphere above the European atmospheric boundary layer, in the boundary layer over Europe from emissions within Europe or from emissions in other continents. Quantitative attributions of the origins of the ozone are entirely theoretical constructs and their accuracy depends on the adequacy and completeness of the models and their input data and the validity of the assumptions and simplifications made in their derivation.

A previous study using a global three-dimensional Lagrangian chemistry-transport STOCHEM model, pointed to there being an important coupling between the global and regional ozone

distributions in Europe (Collins *et al.*, 2000). It raised the possibility that the global-scale build-up in ozone over the next few decades may act to partially offset the reductions in ozone due to European regional emissions reductions. In this study, we have nested a regional model covering the European region within the above global model so that we can return to these same issues with a much finer spatial and temporal resolution.

3.3 NESTED MODEL APPROACH

3.3.1 The Nested Model Structure

The structure of the nested model is based on the global three-dimensional STOCHEM model that describes the chemical development of the troposphere by using 50,000 constant mass air parcels (Collins *et al.*, 1997). The motions of these air parcels are driven from global meteorological archives which contains fields of winds, temperatures, precipitation, cloud amounts and humidities at a 6-hourly time resolution. When the air parcels descend into the atmospheric boundary layer, they pick up emissions and undergo dry deposition. When air parcels enter the upper troposphere they also receive ozone and NO_y through stratosphere-troposphere exchange. Chemical and photolysis processes are driven with fully time-of-day-dependent chemical kinetic parameters. Wet scavenging and aerosol uptake are the main removal processes for water-soluble reaction products.

Nested within the global model domain there is an additional regional domain which covers the longitude range from 60°W to 60°E and the latitude range from the equator to the North Pole. This is the EUROSTOCHEM model domain which covers an area one sixth of the STOCHEM model domain. Whereas the global domain is filled with 50,000 constant mass air parcels, the regional domain contains 500,000 air parcels with one tenth of the mass of the global air parcels. Apart from the difference in mass of the air parcels, they undergo exactly the same processes of emissions, chemistry, deposition and exchange with the stratosphere.

The model experiments were performed by initialising the global STOCHEM model in October 1996 and running it forward using meteorological archives from an operational numerical weather prediction model until the end of December 1997. At the end of each month, a set of global model output files were written containing the mixing ratios of the principal model species. These files were used to start off the regional model. All the output described in this study was taken from the regional model at three hourly intervals. An imaginary cylinder was erected above each output location between the earth's surface and the top of the atmospheric boundary layer with a radius of 55 km. The output volume mixing ratio was taken to be the mean of the mixing ratios of that species averaged over all the air parcels within the imaginary output cylinder.

3.3.2 Advection and Dispersion Processes

In the global and regional models, the air parcels were advected according to winds taken from the Meteorological Office UM operational model, which are based on a grid of 1.25° longitude, 0.833° latitude and 12 unevenly-spaced η-levels in a hybrid vertical co-ordinate (topography and altitude). These fine resolution operational model archives covered the period from 1st October 1996 through to 31st December 1997. The advection timestep was set to three hours and new cell positions were calculated using a 4th order Runge-Kutta advection scheme. Winds were interpolated linearly in time within the 6-hourly meteorological datasets, bi-linearly in the horizontal domain and using a cubic polynomial in the vertical. The treatments of small-scale convection and interparcel exchange remain unchanged.

3.3.3 Chemistry

Both the global and regional models contain a full description of the fast photochemistry of the troposphere and the free radical reactions that process the emissions of the major tropospheric trace gases. There are 70 species in the chemical mechanism and they take part in over 170 chemical and photochemical reactions. The hydrocarbons modelled are methane, ethane, ethylene, propane, propylene, butane, toluene, o-xylene and isoprene together with their oxidation products such as peroxy radicals, hydroperoxides and carbonyls: formaldehyde, acetaldehyde, acetone, methylglyoxal and methylvinylketone. Photolysis rates for each time-step were obtained by interpolation in time between the appropriate values stored from the recalculation at intervals of 45 minutes. A chemistry timestep of 300 seconds was used in the backwards iterative solver.

Scavenging coefficients for large-scale and convective precipitation and the scheme to convert fractional scavenging rates to grid cell average rates remain unchanged from previous studies. No changes have been made to the treatment of dry deposition.

3.3.4 Treatment of Emissions

Emissions into the model are implemented as an additional term in the production flux for each species during each integration time-step, exactly as in the Collins *et al.* (1997) study. The emissions used are listed in Table 3.1. The man-made, biomass burning, vegetation, soil, oceans and 'other' are all surface sources based on two-dimensional (latitude, longitude) source maps. Stratospheric sources of ozone and nitric acid are calculated as two-dimensional inputs into the top model layer. The aircraft and lightning NO_x sources are three-dimensional. The man-made, paddy, tundra, wetland and 'other animal' sources (see Table 3.1) are held constant throughout the year at the yearly average value. The other sources vary by calendar month. After each advection timestep the surface emissions for a grid square are distributed equally over all the Lagrangian cells that are within the boundary layer in that grid square. If there are no cells within the boundary layer for a particular emissions grid square then those emissions are stored until a cell does pass through.

Table 3.1 ***The Global Emissions in Tg yr^{-1} from Each Source Category for Each Model Species used in the Model Calculations for the Present-day Atmosphere.***

Species	Human activities	Biomass burning	Vegetation	Soils	Oceans	Aircraft	Lightning	Others[2]
NO_x	21.0	8.0		5.6		0.5	5.0	
H_2	20.0	20.0		5.0	5.0			
CO	425.0	500.0	75.0		50.0			
CH_4	155.0	40.0			10.0			260.0
C_2H_4	17.0	10.0	20.0					
C_2H_6	6.0	6.5	3.5					
C_3H_6	21.0	5.0	20.0					
C_3H_8	6.5	12.0	2.0	0.5				
C_4H_{10}	47.0	2.0	8.0					
C_5H_8			506.0					
C_8H_{10}	4.7							
C_7H_8	14.0							
HCHO	1.0	5.0						
CH3CHO	0.3							

Notes: (1) Model emissions in Tg yr^{-1}, except NO_x and HNO_3, which are in Tg (N) yr^{-1}, and SO_2, which are in Tg (S) yr^{-1}; (2) Includes paddys (60 Tg yr^{-1}), tundra (50 Tg yr^{-1}), wetlands (65 Tg yr^{-1}), termites (20 Tg yr^{-1}), and other animals (85 Tg yr^{-1}).

The cells in our model are constrained to remain below 100 hPa by imposing a fixed lid to the model. In reality, they would travel to and from the stratosphere bringing high ozone and NO_y

concentrations down into the troposphere and losing species into the stratosphere. Upper boundary conditions have been set so that there is a total ozone flux into the model domain of 865 Tg over one year and a NO_y flux of one thousandth of the ozone flux by mass (as N), based on the study of Murphy and Fahey (1994), representing stratosphere-troposphere exchange.

3.3.5 Initial Concentrations

The global and regional model experiments described in this study, were started up from the assumed initial composition of the troposphere during October of the first model year and were run through to the end the next model year. All model concentrations were generated by the processes within the model without intervention, flux adjustment or the operation of fixed concentrations at any of the model boundaries. Initial conditions were set for methane, ozone and carbon monoxide using fields generated by a 2-D tropospheric model (Johnson and Derwent 1996).

3.3.6 Modelling Present and Future Ozone Levels

As the concentrations of the tropospheric source gases continue to increase following the growth of emissions from 1992 through to 2100, the STOCHEM model predicts that the human influence on past ozone levels continues into the future. A future trace gas emission scenario (B2) from the Intergovernmental Panel on Climate Change (IPCC) Special Report on Emissions Scenarios (SRES) (Nakicenovic *et al.*, 2000) was used to drive the global model for emission conditions appropriate to the year 2030. This scenario described the spatio-temporal evolution of the man-made emissions of NO_x, CO, methane, VOCs and SO_2. The global model meteorological archives for the year 2030 were generated from a transient experiment of the Hadley Centre coupled ocean-atmosphere HadCM3 model (Gordon *et al.*, 2000) driven by greenhouse gas and other forcing mechanisms appropriate to 2030 derived from the IS92a scenario. The regional model used the same fine resolution meteorological archives for both the 1990s and 2030 model experiments.

3.3.7 Modelling Secondary Aerosol Species

The global model STOCHEM and the regional model EUROSTOCHEM contain full and identical treatments of the formation, transport and removal of the secondary aerosol species: aerosol sulphate and nitrate. Aerosol sulphate is formed from the oxidation of sulphur dioxide (SO_2) and dimethyl sulphide (DMS) by in-cloud and gas-phase oxidation processes. In-cloud chemical processes involve the oxidation of SO_2 by hydrogen peroxide and ozone. The gas-phase chemical processes involve the oxidation of SO_2 by hydroxyl (OH) radicals and of DMS by both OH and nitrate (NO_3) radicals. Aerosol sulphate is formed by the nucleation of the sulphuric acid formed by the gas-phase processes or by evaporation of the cloud droplets in which the in-cloud oxidation has occurred. Aerosol nitrate is formed by scavenging of nitric acid (HNO_3) and nitrogen pentoxide (N_2O_5) by coarse particle sea salts or wind-blown dusts. Nitric acid is in turn formed by oxidation of nitrogen dioxide (NO_2) by OH radicals during daylight and nitrogen pentoxide is formed by the oxidation of NO_2 by ozone during nighttime.

3.4 EUROSTOCHEM MODEL PERFORMANCE

3.4.1 Evaluation Using Observations from the Mace Head Baseline Station

The EUROSTOCHEM model results have been carefully compared with the high frequency continuous monitoring data for methane, carbon monoxide and ozone collected at the Mace

Head atmospheric baseline station (Simmonds *et al.*, 1996) situated on the Atlantic Ocean coastline of Ireland, as shown in Figure 3.1. For much of the time, this monitoring station receives northern hemisphere maritime air masses which have travelled across the uninterrupted fetch of ocean and contain baseline levels of most trace gases. When the meteorological conditions change and regionally-polluted air masses are advected to Mace Head, then trace gas concentrations rise dramatically off their baselines and significant concentration excursions are observed. In this test of EUROSTOCHEM model performance, the aim has been to ascertain whether the model is able to capture these infrequent and sporadic concentration excursions caused by the switching between baseline maritime and European regionally-polluted air masses during the study period from 1st April to 31st August 1997.

Methane (CH_4) is a globally well-mixed trace gas with important sources in continental Europe arising from both from human activities and natural biogenic sources. The upper panel of Figure 3.1 illustrates a comparison of the EUROSTOCHEM CH_4 concentrations (shown as + signs), overlaid on the 40-minute observations, shown as a continuous line. For the sake of clarity, the model concentrations have been displaced downwards using an offset of 100 ppb. Allowing for the offset, both the model and observations agree accurately on the baseline level that was close to 1800 ppb in both time series during the study period.

The observations show sporadic excursions containing elevated CH_4 levels. Some of these excursions have been predicted in the regional model and line up exactly with the observed excursions. The magnitudes of the excursions in the model time series correspond closely with those in the observations. The agreement in the timing and magnitudes of the excursions between the model and the observations provides confidence that the long range transport of polluted air masses from continental Europe has been described quantitatively in EUROSTOCHEM.

However, a clear feature of the upper panel of Figure 3.1 is the much large number of excursions in the observed CH_4 time series compared with the model time series. This discrepancy highlights an important weakness in the EUROSTOCHEM model. There is a local source close to the Mace Head station in the surrounding peat bogs. Under daytime conditions and with a well-developed atmospheric boundary layer, these local sources are unimportant. However, during the summertime with near calm conditions, CH_4 emissions accumulate under shallow nocturnal inversions and cause many of the observed excursions. These processes are not modelled in EUROSTOCHEM and point to an important limitation of the nested model in its ability to handle local scale processes and influences.

Carbon monoxide (CO) is also a globally well-mixed trace gas with important man-made sources within continental Europe. It differs from methane in not having large local natural sources in the surrounding peat bogs and thus potentially simplifying the comparison between model and observations. The middle panel of Figure 3.1 illustrates the comparison of EUROSTOCHEM results (shown as + signs and displaced by 100 ppb) overlaid with the 40-minute CO observations (continuous line). The baseline in the observations declines from 150 ppb to 80 ppb over the study period whereas the model generates a rather constant baseline of about 115 ppb. In future work, the regional model initialisation should be made to reflect this observed seasonal cycle.

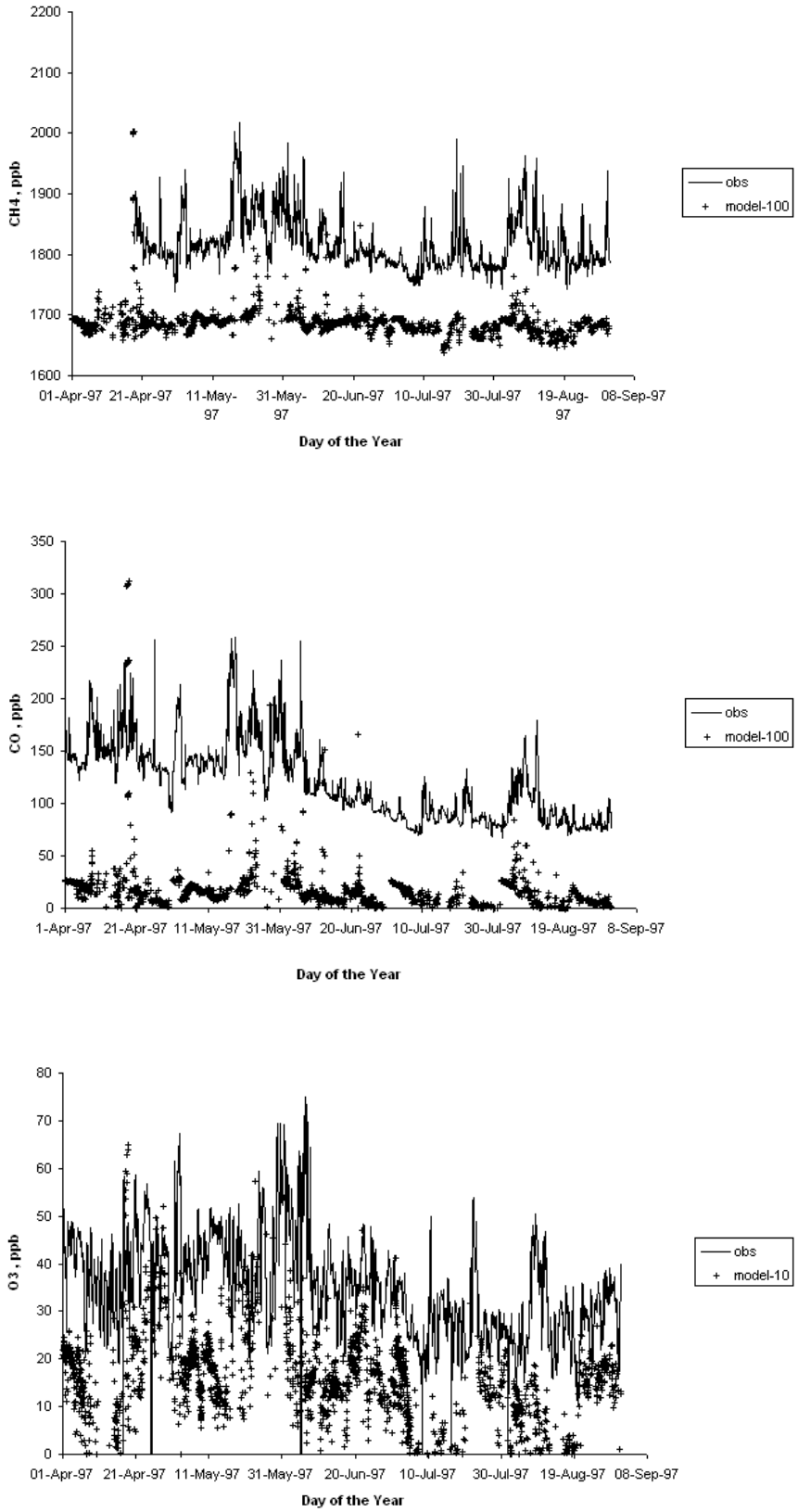

Figure 3.1 ***Comparison of Model Results with the Observations for April to August 1997 from the Mace Head Atmospheric Research Station for Methane (upper panel), Carbon Monoxide (middle panel) and Ozone (lower panel).***

The model CO excursions, caused by the advection of European regionally-polluted air masses to Mace Head, line up accurately with observed excursions and appear to have about the correct magnitude above their respective baselines. A marked downwards trend of about 3% per year has been noted in the observed CO excursions over the period from 1990 to 2000 and this has been attributed to reductions in European CO emissions following the widespread implementation of motor vehicle emission controls. The CO emissions employed in the EUROSTOCHEM model have a base year of 1990 that was at the beginning of the implementation of emission controls. On this basis it is to be expected that the model should overestimate, if anything, the observed CO concentration excursions. On this basis, therefore the EUROSTOCHEM simulations of the European regional pollution events appear quantitatively satisfactory in both timing and magnitude.

However, on occasions the model considerably underestimates the observed CO excursions. With CO, it is unlikely that local sources interfere significantly with the observations as it was with methane, and so some other explanation must be operating. It is likely that the combination of the coarse spatial resolution of the emission inventories, 5^{o} x 5^{o}, and the rather long advection time step employed, 3 hours, has meant that the EUROSTOCHEM model has failed to represent all of the CO transport events. During calm wind conditions, the density of air parcels is not sufficient to treat the local stagnation conditions that give rise to elevated CO levels.

Ozone is a highly reactive trace gas with a global distribution resulting from the complex interplay between photochemical production and destruction processes. Because of its short lifetime, its surface concentrations tend to be highly variable and this is clearly apparent in the time series for the study period (shown as the continuous line in the lower panel of Figure 3.1). Interestingly, the time series from the EUROSTOCHEM model (shown as + signs) also shows this heightened variability compared with CH_4 and CO. The model results appear to underestimate the observations by about 10 ppb during the early part of the study period but are exactly in line with the baseline in the observations at the end of the period. It would appear that the model is overestimating ozone destruction in air masses advected across the Atlantic Ocean during the spring. Alternatively, the model is not mixing in rapidly enough elevated ozone levels from aloft which have their origins in stratosphere-troposphere exchange. The representation of both of these processes may have been compromised by the regional model boundary that has been established in the western part of the North Atlantic Ocean.

The ozone baseline concentrations make a spectacular decline during the 5-9^{th} July caused by the advection of tropical air masses containing exceptionally low ozone concentrations to the Mace Head station in a southerly latitude transport event. This behaviour is captured quantitatively in both timing and magnitude by the EUROSTOCHEM model. Many of the remaining excursions in the observed time series are caused by the advection of photochemically-reacted air masses to the Mace Head station from continental Europe. Visual inspection of the model and observed time series points to the near simultaneous occurrence of these excursions and to the close similarity in their magnitudes. There are however some observed excursions which are not reproduced at all in EUROSTOCHEM. An explanation of these missed events must lie in the inadequate sampling of calm, anticyclonic regions in which ozone can accumulate and drift out to Mace Head. These problems with EUROSTOCHEM undersampling the frequency of photochemical events must clearly be borne in mind when considering the results presented in subsequent sections below. However, there appears to be no problems with the intensity of the photochemical episodes predicted by EUROSTOCHEM. Quantitative issues of model evaluation are however dealt with in further detail in the following section.

3.4.2 Evaluation against Observations from the EMEP Ozone Network

An important test of the nested model performance is whether it can reproduce the day-to-day variations in the observed ozone concentrations across Europe. A sub-set of 23 ozone monitoring sites have been selected from the European Monitoring and Evaluation Project (EMEP) ozone network (Hjellbrekke 1999) and the observational data selected for August 1997. This particular month was chosen because it contains the highest levels measured during 1997 at most of the sites and data are available for 100 monitoring stations. The sub-set of stations was selected so as to represent each country by one site, thereby ensuring a wide spatial distribution across Europe. Low elevation locations were preferred as opposed to mountaintop locations. All the sites are classified as remote rural locations, unaffected by local sources of pollution. The statistic chosen was the maximum hourly mean ozone concentration observed during each day, irrespective of the time of day. The maximum ozone concentrations during August 1997 varied between 57 ppb at Tustervatn, Norway and 100 ppb at Revin, France.

Figure 3.2 presents observed and model comparisons for each of the 23 sites for the maximum hourly mean ozone concentrations for each day during August 1997. The sites were grouped into the following categories of sites:

- Atlantic Ocean seaboard – Mace Head, Tustervatn, Monte Vehlo.
- North West Europe – Waldhof, Frederiksborg, Lahemaa, Virolahti, Harwell, Preila, Kollumerwaard, Aspreveten, Revin.
- Mediterranean - Roquetas, Aliartos, Montelibretti, Iskrba.
- Central and Eastern Europe – Illmitz, Taenikon, Kosetice, K-puszta, Jarczew, Shepeljovo, Starina.

Considering firstly the Atlantic Ocean seaboard sites, then the modelling results for Mace Head, Ireland follow closely the observed monthly pattern but overestimates the observations by up to10 ppb during the period 20-26th August. At Tustervatn in the north of Norway, the model follows the observations reasonably well except for two period of underestimation during August 4-9th and 12-16th. At Monte Vehlo in Portugal, the model underestimates the observations during the period August 2-17th and then follows the observations quite well.

At the sites in the north west Europe category, the modelling results follow the observations reasonably well. The model does an excellent job at the Harwell site in the United Kingdom. At Kollumerwaard in the Netherlands, the model follows the observations extremely well except for a period of underestimation during August 7-13th. At Frederiksborg in Denmark, the model follows the observed monthly pattern at the start and the end of the month but underestimates the observations during the period August 12-19th. At Waldhof in Germany, at Aspreveten in Sweden and Virolahti in Finland, the model follows the observations extremely well. At Lahemaa in Estonia the model indicates an ozone episode on August 22-23 which was not observed. At Preila in Lithuania, the model follows the observations reasonably well during the first 20 days then consistently underestimates the observations during the period August 21-30. At Revin in France, the model underestimates significantly the observations during the early part of the month then agrees well later in the month.

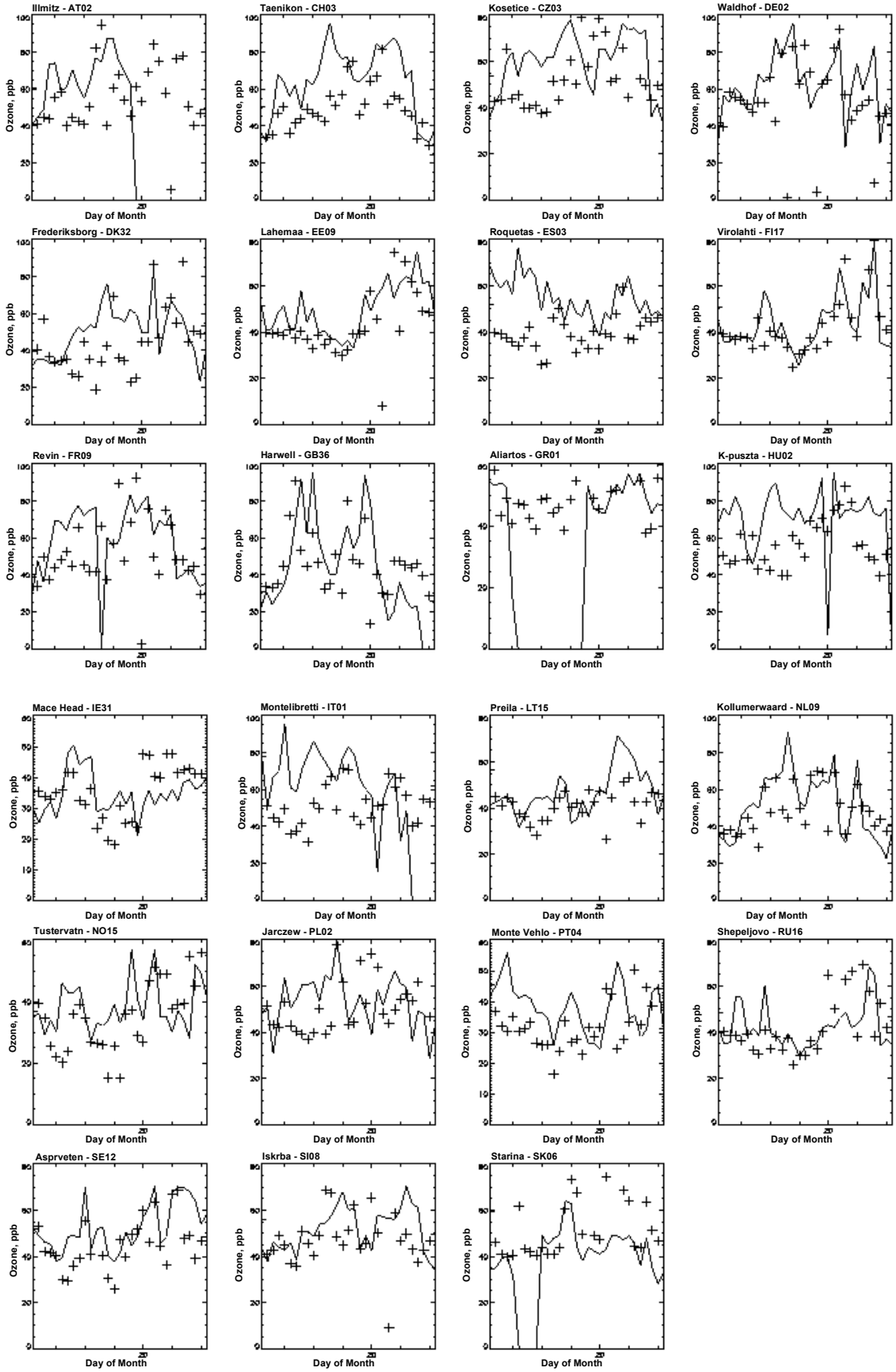

Figure 3.2 Comparison of Model Results with the Observations for August 1997 from the EMEP Monitoring Sites for Ozone.

At the Mediterranean sites, the model tends to show a significant underestimation of observed levels. At Roquetas in Spain and at Montilibretti in Italy, the model underestimates significantly the observations during the early part of the month then falls into line later in the month. Such data as there are for Aliartos in Greece are well simulated by the model. At Iskrba in Slovenia, the model does a really good job of simulating the observed pattern consistently throughout the month.

The comparison of model results with observations for the Central and Eastern European sites shows a generally poor level of model performance. At Kosetice in the Czech Republic, K-puszta in Hungary, Jarcsew in Poland and at Taenikon in Switzerland, the model shows a consistent pattern throughout the month that does not correspond well with the observations. At Illmitz in Austria, the model does a good job in explaining the occurrence of the observed peak in the middle of the month. At Starina in the Slovak Republic, the model does a good job of simulating the observed pattern during the first part of the month but considerably overestimates the observations during the period August 18-25th. At Shepeljovo in the Russian Federation, the model agrees well with the observations during the first part of the month and thereafter considerably overestimates them, particularly during the period August 20-24th.

Quantitative comparisons were performed on a site-by-site basis for i = 22 sites and for each of the j = 31 days between the observations, o_{ij}, and the model results, m_{ij}, using a range of statistics:

a. *bias* $= \frac{1}{31} \sum_{ij}(o_{ij} - m_{ij})$

b. *fractional bias* $= \frac{\sum_{ij}(o_{ij} - m_{ij})}{\sum_{ij} o_{ij}}$

c. *fraction of model maximum daily maximum concentrations* within the range from the 1.5 x observation and observation ÷1.5, *i.e.*, within a range of a factor of about two.

d. *normalised mean square error* $= \frac{\frac{1}{31} \sum_{ij}(o_{ij} - m_{ij})^2}{\frac{1}{31} \sum_{ij} o_{ij} \times \frac{1}{31} \sum_{ij} m_{ij}}$

e. *correlation coefficients* of the scatter plots of the model calculated concentrations *vs.* the 31 observations.

A summary of these statistics for each of the 22 sites is presented in Table 3.2. There are four sites that show less than 1 ppb mean bias between the model and the observations. These sites are spread amongst the site categories and include Mace Head (Atlantic Ocean seaboard), Waldhof and Virolahti (North West Europe) and Iskrba (Mediterranean). The sites with the worst bias, that is with more than 10 ppb mean underestimation, include the sites in the Mediterranean category: Roquetas and Montelibretti, and in the Central and Eastern Europe category: Illmitz, Taenikon and K-puszta. Starina appears to be an exception with a large model overestimation. The sites with the worst fractional bias appear to underestimate the observations by up to 30%.

Table 3.2 Summary of the Statistics of the Comparison of the Model Calculated Maximum Hourly Ozone Concentrations with the Observations from the EMEP Monitoring Network for August 1997.

Site		Bias (ppb)	Fractional bias	Fraction within a factor of 1.5	Normalised Mean Square Error	Coefficient of Determination R^2
Illmitz	AT	-12.1	-0.20	0.72	0.12	0.09
Taenikon	CH	-14.8	-0.26	0.71	0.13	0.45
Kosetice	CS	-6.5	-0.12	0.71	0.10	0.15
Waldhof	DE	0.3	0.005	0.86	0.08	0.31
Frederiksborg	DK	-5.2	-0.11	0.54	0.18	0.07
Lahemaa	EE	-2.3	-0.05	0.94	0.09	0.37
Roquetas	ES	-15.0	-0.32	0.58	0.16	0.00
Virolahti	FI	0.04	0.0001	0.97	0.04	0.57
Revin	FR	-7.3	-0.13	0.68	0.12	0.21
Harwell	GB	2.2	0.05	0.68	0.16	0.37
Aliartos	GR	6.7	0.13	0.84	0.07	0.07
K-puszta	HU	-19.7	-0.30	0.63	0.15	0.03
Mace Head	IE	0.27	0.008	0.94	0.06	0.12
Monte-libretti	IT	-12.9	-0.22	0.54	0.16	0.00
Preila	LT	-3.5	-0.08	0.90	0.06	0.28
Kollumerwaard	NL	-2.9	-0.06	0.84	0.08	0.39
Tustervatn	NO	-2.7	-0.07	0.73	0.12	0.10
Jarczew	PL	-1.3	-0.03	0.77	0.09	0.00
Monte Vehlo	PT	-5.6	-0.16	0.81	0.11	0.02
Shepeljovo	RU	1.6	-0.04	0.81	0.12	0.09
Aspreveten	SE	-6.0	-0.12	0.90	0.06	0.30
Iskrba	SL	0.6	0.01	0.84	0.10	0.05
Starina	SK	12.7	0.26	0.74	0.15	0.19

The fraction of model maximum hourly ozone concentrations within a factor of 1.5 below and 1.5 above the observed concentration, that is within about a factor of 2 range, varies from about 0.54 at Frederiksborg and Montelibretti to about 0.94 at Mace Head and Lahemaa. This indicates an acceptable level of model skill at all sites.

Correlation coefficients are often a useful measure of association and indicate that the model has captured well the monthly patterns in the maximum hourly ozone concentrations at Taenikon, Waldhof, Lahemaa, Virolahti, Harwell, Preila, Kollumerwaard, Aspreveten and Revin. Conversely, Table 3.2 indicates that at Illmitz, Roquetas, Aliartos, Montelibretti, Jarczew, Monte Vehlo, Shepeljovo and Iskrba the model has not reproduced at all well the detailed observed monthly pattern in these maximum hourly mean concentrations.

The evaluation tests for August 1997 show that there is a large spread in apparent model performance across the 23 sites. In general terms, model performance is best with the Atlantic Ocean fringe and north west European categories of sites and least best with the Central and Eastern European and Mediterranean categories of sites. Within each site category there is also significant variation in model performance. On this basis, it is difficult judge which deficiencies in the model formulation or input data are most likely to be important limiting model performance. It is likely that a complex interaction between the coarse spatial resolution of the emission inventories employed, 5^o x 5^o, in combination with problems with the meteorological fields under low windspeed conditions, is responsible for many of the limitations in model performance. The model results that follow must be evaluated in the light of the above experience. Whilst the model gives a reasonable guide to the observed day-to-day variations in

the maximum hourly mean ozone concentrations, individual maximum hourly values under particular meteorological conditions may be considerably in error.

3.4.3 Evaluation against Observations from the UK Rural Ozone Network

Having shown that the nested model shows some level of skill in predicting the maximum hourly mean ozone concentrations observed at a wide range of sites across Europe, attention is now focussed on sites within the British Isles. Observational data for August 1997 have been taken from the National Air Quality Information Archive for the 15 sites in the UK Rural Ozone Monitoring Network and have been compared carefully with the nested model results using the maximum hourly mean ozone concentrations as the appropriate metric for comparison purposes.

Figure 3.3 presents the observed and model comparisons for the 15 sites for each day during August 1997. The sites were grouped as follows:

- southern and western group – Yarner Wood, Somerton and Narberth,
- northern and western group –Aston Hill, Lough Navar, Great Dun Fell and Bush Estate,
- central and eastern group – High Muffles, Ladybower and Bottesford,
- southern and eastern group – Harwell, Sibton, Rochester and Lullington Heath,
- remote group - Strathvaich Dam.

Considering firstly the grouping of sites in the south and west, then the modelling results follow closely the observed pattern of daily ozone maxima at the Somerton site, particularly during the middle and end of the month. The model misses completely the observed ozone episode on the 9th August. At the Yarner Wood and Narberth sites, the model misses almost all of the observed ozone episodes. However, the range of model results overlaps closely with the observed range of daily ozone maximum concentrations.

At the northern and western sites, the model captures closely the observed daily patterns of ozone maxima. The model misses completely the observed ozone episode on the 11th August at Lough Navar and Great Dun Fell and on the 8th August and 16th August at Bush Estate. There is also a clear tendency for the model results to overestimate grossly the observed ozone daily maxima from the 20th August onwards at the Bush Estate, Great Dun Fell and Lough Navar sites.

The model generates a reasonable description of the daily pattern of ozone maxima for the sites in the central and eastern grouping. However, the model fails to predict the observed ozone episode that covered the extended period from the 5th to 13th August at High Muffles, Ladybower and Bottesford sites. The agreement is strikingly good at the southern and eastern sites, particularly at the Harwell and Lullington Heath sites. However, the model completely missed the observed ozone episodes on the 10th-13th August and 15th-17th August. Model performance at the remote Strath Vaich site appeared to be entirely satisfactory for the limited period over which the observations were avaialable. The comparison between the model and observations has been put on a quantitative basis in Table 3.3. There are three sites that show less than ± 2 ppb mean bias and these are Ladybower, Bottesford and Lullington Heath. The sites with the worst bias are Aston Hill and Great Dun Fell where the model overestimates grossly and Sibton and High Muffles where the model underestimates the observations. At the sites with the worst fractional bias, the model appears to overestimate (Great Dun Fell) or underestimate (High Muffles) the observations by ± 20 % or more.

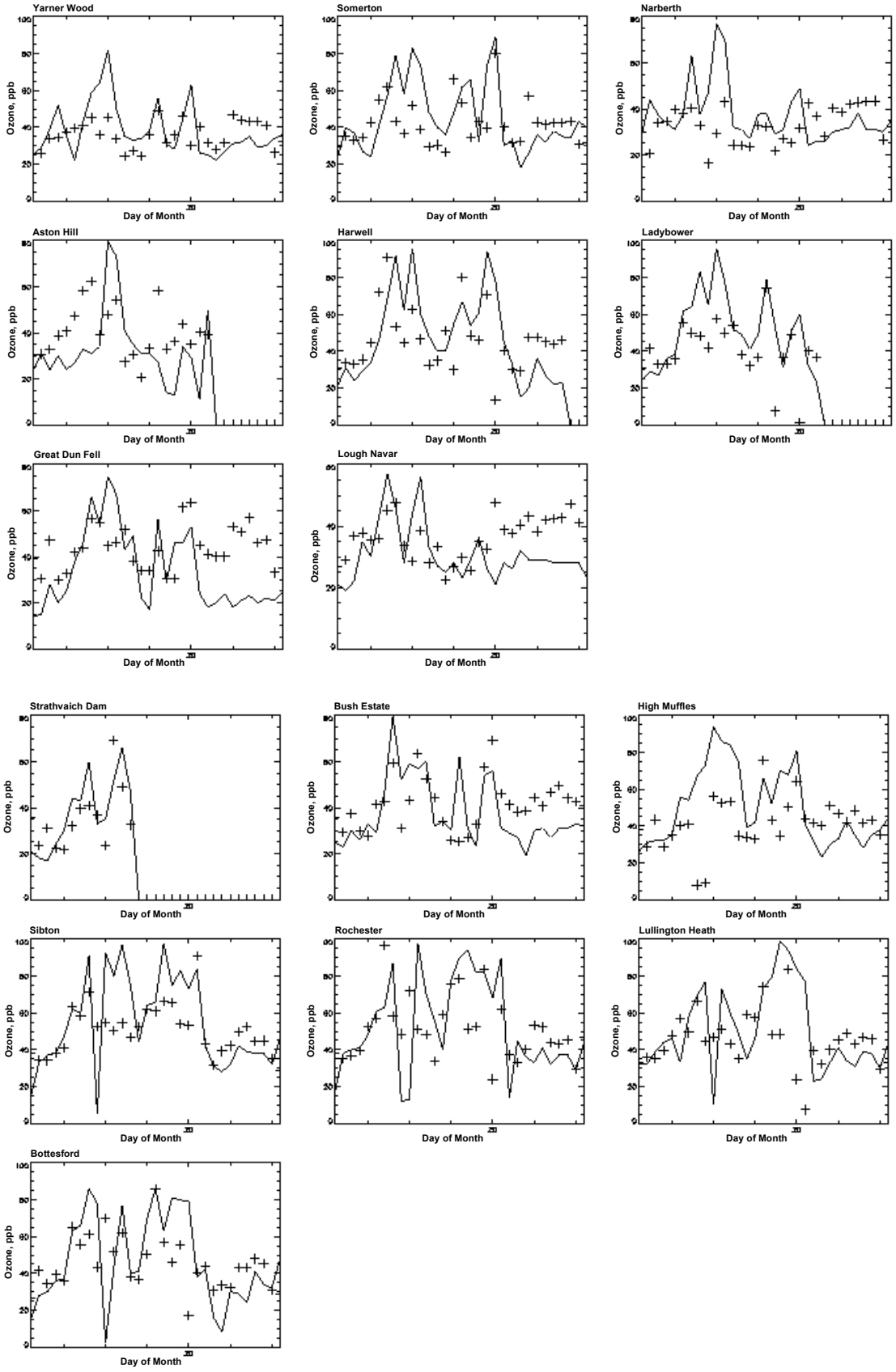

Figure 3.3 Comparison of Model Results with the Observations for August 1997 from the UK Rural Ozone Monitoring Network Sites for Ozone.

Table 3.3 Summary of the Statistics of the Comparison of the Model Calculated Maximum Hourly Ozone Concentrations with the Observations from the UK Rural Ozone Monitoring Network for August 1997.

Site	Bias (ppb)	Fractional bias	Fraction within a factor of 1.5	Normalised Mean Square Error	Coefficient of Determination R^2
Yarner Wood	-2.65	-0.071	0.80	0.142	0.105
Somerton	-3.29	-0.076	0.70	0.165	0.185
Narberth	-4.59	-0.131	0.70	0.197	0.0
Aston Hill	6.97	0.191	0.59	0.248	0.077
Lough Navar	5.39	0.161	0.77	0.114	0.068
Great Dun Fell	9.61	0.249	0.47	0.237	0.157
Bush Estate	3.82	0.097	0.87	0.188	0.257
Strath Vaich	-2.47	-0.068	0.85	0.114	0.410
High Muffles	-9.05	-0.200	0.70	0.275	0.044
Ladybower	-1.78	-0.036	0.61	0.182	0.217
Bottesford	-1.65	-0.034	0.80	0.125	0.504
Harwell	2.24	0.046	0.68	0.158	0.375
Sibton	-7.44	-0.138	0.77	0.135	0.474
Rochester	-4.44	-0.079	0.67	0.203	0.225
Lullington Heath	-1.78	-0.034	0.80	0.125	0.504

The fraction of modelled maximum hourly mean ozone concentrations that lay within a factor of 1.5 below or 1.5 above the observed maximum ozone concentrations varied from 0.47 at Great Dun Fell to about 0.87 at Bush Estate. This indicates an acceptable level of model skill at all sites.

The correlation coefficients in Table 3.3 indicate that the model has captured well the monthly pattern in the maximum hourly mean ozone concentrations at the Ladybower, Rochester, Bush Estate, Harwell, Strath Vaich, Sibton, Bottesford and Lullington Heath sites. Conversely, the model appears to perform poorly at Narberth, Aston Hill, Lough Navar and Yarner Wood.

The evaluation tests for August 1997 against the observations from the sites in the British Isles, show a large spread in apparent model performance. Within each category of sites there is significant variation in overall model performance. Well-performing sites against one yardstick may be adjacent to poorly-performing sites and it is difficult to discern any geographical pattern to either good or poor model performance. Hence it is difficult to judge which particular deficiences in the model formulation or input data are most likely to have limited overall model performance. Whilst the model appears to give a reasonable guide to the observed day-to-day variability in the maximum hourly mean ozone concentrations, individual modelled maximum hourly mean ozone concentrations may be considerably in error.

3.4.4 Evaluation of Model Calculated Secondary Aerosol Concentrations against Observations

An important test of EUROSTOCHEM model performance is whether it is able to reproduce the observed spatial variations in the concentrations of secondary aerosol sulphate and nitrate across Europe. A subset of 59 monitoring locations from the EMEP network were selected for August 1997. This sub-set was selected as before to ensure as wide a spatial coverage as possible across Europe from the available low elevation, rural site locations. The statistic chosen was the observed monthly mean concentrations.

The observations for August 1997 spanned the range from 1.9 μg S m^{-3} for Roquestas, Spain to 0.48 μg S m^{-3} for Bredkalen, Sweden (Hjellbrekke 1999). The EUROSTOCHEM model results spanned a somewhat wider range from 3.1 μg S m^{-3} at Neuglobosow, Germany to 0.1 μg S m^{-3} for Anholt, Denmark. The comparison between the EUROSTOCHEM model results and the observations was characterised by a bias of -0.19 μg S m^{-3} and a fractional bias of –0.17 over the 45 sites for which observations were available. The model results were within a factor of 1.5 up or down on the observations for 22 out of the 45 sites. The normalised mean square error was 0.48. All of these statistics confirm an acceptable level of EUROSTOCHEM model performance for aerosol sulphate, with a tendency to underprediction.

The scatter plot between observed and EUROSTOCHEM model calculated aerosol sulphate concentrations for the 45 sites for August 1997 is shown in Figure 3.4. There are three outlying points that indicate gross model underestimation and four outliers indicating gross underestimation. The set of three outliers represent stations in Germany: Neuglobosow, Langebrugge and Zingst. Presumably, the model results are gross overestimations because the model SO_2 emission inventory is for 1990 and the observations are for 1997. It is likely that the EUROSTOCHEM model results do not reflect the dramatic reductions in SO_2 emissions in the former German Democratic Republic during the period 1990-1997 which have led to a dramatic reduction in the observed levels of aerosol sulphate.

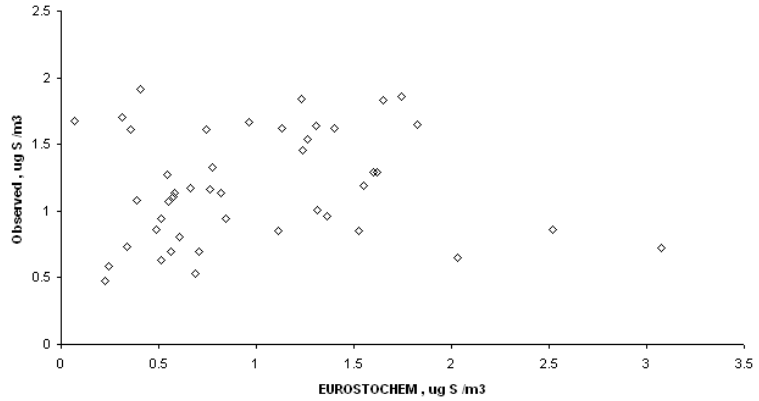

Figure 3.4 ***Scatter Plot of EUROSTOCHEM modelled vs. Observed Aerosol Sulphate Concentrations in μg S m^{-3} for August 1997 at EMEP sites.***

Three of the four outlying points that indicate gross underestimation in EUROSTOCHEM are located in Spain. Clearly, EUROSTOCHEM is unable to describe quantitatively the magnitude of the photochemical source of aerosol sulphate over the Iberian peninsular during August 1997. Taking these seven outlying points out of the scatter plot in Figure 3.4 and performing a least squares correlation of the observed *vs.* EUROSTOCHEM model results gives a R^2 value of 0.41 for the remaining 38 points. This indicates an adequate level of model performance for the EUROSTOCHEM model and it is well able to reproduce the observed pattern of spatial variation in aerosol sulphate across Europe during August 1997.

The reported observations for aerosol nitrate for August 1997 spanned the range from 1.32 μg N m^{-3} for High Muffles, North Yorkshire to 0.07 μg N m^{-3} for Bredkalen, Sweden. The EUROSTOCHEM model results spanned a somewhat smaller range from 1.0 μg N m^{-3} for Payerne, Switzerland to 0.08 μg N m^{-3} for Anholt, Denmark. The comparison between the EUROSTOCHEM results and the observations was characterised by a bias of –0.11 μg N m^{-3} and a fractional bias of –0.26 over the 34 sites for which observations were available. The model results were within a range of a factor of 1.5 up or down on the observations for 13 out of the 34 sites. The normalised mean square error was 0.54. All of these statistics confirm an

acceptable level of EUROSTOCHEM model performance for aerosol nitrate, with a tendency towards underestimation.

The scatter plot between observed and EUROSTOCHEM model calculated aerosol nitrate concentrations for the 34 sites for August 1997 is shown in Figure 3.5. There are two outlying points, one each indicating gross model underestimation and one model overestimation. The model grossly overestimated the observations at Payerne, Switzerland and underestimated them at Anholt, Denmark. These two points were removed from the scatter plot and a least squares regression analysis was performed indicating a R^2 value of 0.45 for the remaining 32 sites. This indicates an adequate level of model performance. EUROSTOCHEM is well able to reproduce the observed pattern of spatial variation in aerosol nitrate concentrations across Europe during August 1997.

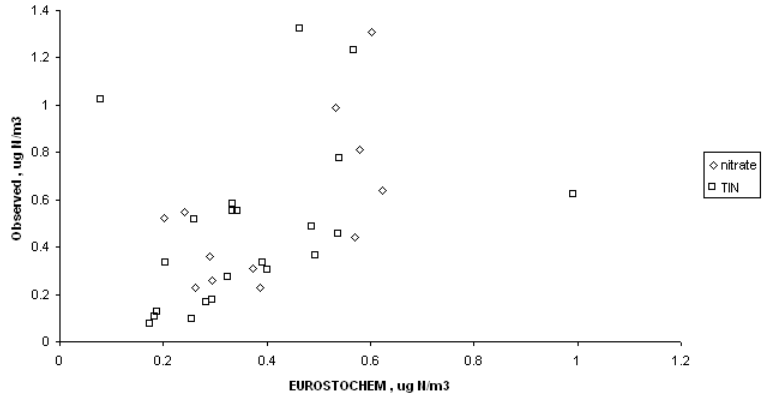

Figure 3.5 ***Scatter Plot of EUROSTOCHEM Modelled vs. Observed Aerosol Nitrate Concentrations in µg N m^{-3} for August 1997 at EMEP sites.***

There is a tendency for EUROSTOCHEM to underestimate the observed aerosol nitrate concentrations as indicated by the fractional bias estimate of –0.26 and the slope of the least squares regression through the scatter plot, Figure 3.5. It is difficult to know whether this underestimation is a cause for concern or not. Aerosol nitrate measurements are difficult to perform on a routine, network basis without introducing artefacts. Within the EMEP network, aerosol nitrate measurements have been superceded by those of total inorganic nitrate (TIN) which is the sum of nitric acid and aerosol nitrate[1]. However, these measurements may also be subject to artefacts. In Figure 3.5, the observations have been separated into observations of aerosol nitrate and those of TIN. However, there is no clear indication of any differences in slope between the scatter plots of model *vs.* aerosol nitrate or model *vs.* TIN.

A further consideration is that the EUROSTOCHEM model takes no account of the formation of fine particle ammonium nitrate. This should mean that the EUROSTOCHEM model results would necessarily underestimate the observations which include both fine particle ammonium nitrate and coarse particle sodium and calcium nitrate. Unfortunately there are no observational data for Europe with which to gauge how important it is to include or neglect ammonium nitrate formation.

[1] The TIN (and corresponding TIA) measurement programmes were replaced in the United Kingdom during 1999 by separate denuder measurements of the gaseous and aerosol nitrate components.

3.5 IMPACT OF CLIMATE CHANGE SCENARIO

3.5.1 Impact of Climate Change Scenario across Europe

To study the impact of the possible influence of the global build-up in greenhouse gases during this present century, the field of global ozone concentrations used to initialise the ozone concentrations in the regional model was changed from one appropriate to the 1990s to one for the year 2030 in the IPCC SRES scenario B2 (Nakicenovic *et al.*, 2000). The regional EUROSTOCHEM model was then rerun for the entire April to August 1997 period with the new ozone initialisation but with no change to the regional meteorological fields.

The influence of the global scale build-up in ozone between the 1990s and 2030 on the mean of the maximum hourly ozone concentrations calculated for each of the selected sites in the EMEP Monitoring Network is shown in Table 3.4. Mean maximum hourly ozone concentrations increase by between 1.5 and 2.9 ppb in the regional model. There is a tendency for the increments due to climate change scenario to be highest on the Atlantic Ocean fringes of Europe and least in north west and central Europe.

The climate change increments on a daily basis appear to be largest in magnitude on days closest to the mean and least on days with elevated ozone concentrations. This point is illustrated in Figure 3.6, where scatter plots are presented for each site of the daily increment due to the climate change scenario versus the maximum hourly ozone concentration for that day. The increments maximise in the middle of the range and tail off to higher or lower maximum ozone concentrations. The result is that the influence of the climate change scenario is greatest in the number of days that exceed 40 ppb, somewhat less in the number of days exceeding 60 ppb and virtually non-existent on the number of 90 ppb exceedance days, see Table 3.4. The change due to climate change scenario in the number of 40 ppb exceedance days varies between 4 and 20 days between the more polluted and least polluted sites. For the 60 ppb exceedance days, the changes lie in the range 0-10 days between the least polluted and the more polluted sites.

Table 3.4 ***Summary of the Model Experiments Studying the Impact of Climate Change on the Mean of the Maximum Ozone Concentrations at Sites in the EMEP Monitoring Network during April to August 1997. The Base Case numbers are shown followed by the Increment due to Climate Change in Parentheses.***

Site Name	Mean of Maximum Ozone Concentrations*, ppb	Number of Days with Exceedances over 40	60	90 ppb
Illmitz	58.3 (2.2)	142 (8)	58 (6)	5 (2)
Taenikon	60.5 (1.9)	137 (4)	48 (7)	7 (0)
Kosetice	58.1 (1.9)	145 (6)	57 (9)	5 (0)
Waldhof	64.0 (1.5)	149 (2)	68 (8)	13 (0)
Frederiksborg	47.3 (2.2)	101 (7)	19 (3)	2 (0)
Lahemaa	47.5 (2.6)	108 (14)	22 (3)	2 (0)
Roquetas	47.2 (2.8)	97 (19)	29 (5)	1 (0)
Virolahti	44.8 (2.7)	104 (20)	11 (5)	0 (0)
Revin	56.7 (2.0)	134 (8)	52 (4)	9 (0)
Harwell	53.1 (1.9)	125 (8)	44 (8)	3 (0)
Aliartos	55.5 (2.8)	138 (6)	51 (10)	3 (0)
K-puszta	59.5 (2.0)	146 (6)	59 (8)	8 (0)
Mace Head	41.9 (2.6)	86 (11)	13 (4)	0 (0)
Montelibretti	55.0 (2.0)	134 (5)	54 (4)	4 (0)
Preila	48.1 (2.4)	125 (8)	17 (3)	1 (0)
Kollumerwaard	53.5 (1.9)	128 (10)	42 (5)	2 (0)
Tustervatn	39.4 (2.9)	74 (13)	4 (0)	1 (0)
Jarczew	54.2 (2.1)	137 (6)	42 (3)	6 (0)
Monte Vehlo	42.7 (2.3)	78 (18)	18 (10)	1 (0)
Shepeljovo	45.0 (2.7)	104 (16)	10 (4)	1 (0)
Aspreveten	50.2 (2.4)	125 (13)	21 (6)	2 (0)
Iskrba	55.3 (2.0)	139 (5)	50 (7)	6 (0)
Starina	56.5 (2.4)	145 (4)	49 (6)	3 (1)

The influence of climate change scenario appears to come about because of the interplay of a number of factors. Those days with close to the average ozone levels appear to be well-ventilated days when winds advect northern hemisphere baseline air masses over much of north west Europe. On such days, changing the global ozone field exerts a large influence on these average ozone levels. Those days with higher than average ozone levels generally correspond to those with elevated ozone production, implying increased residence time over the emission source regions of North West Europe, increased travel times from the Atlantic Ocean and increased net ozone production over Europe. The influence of dry deposition over Europe is to decrease the influence of the initial ozone concentrations in those air parcels bringing elevated ozone concentrations. On these days, changing the global ozone field exerts only a small influence on these elevated ozone levels.

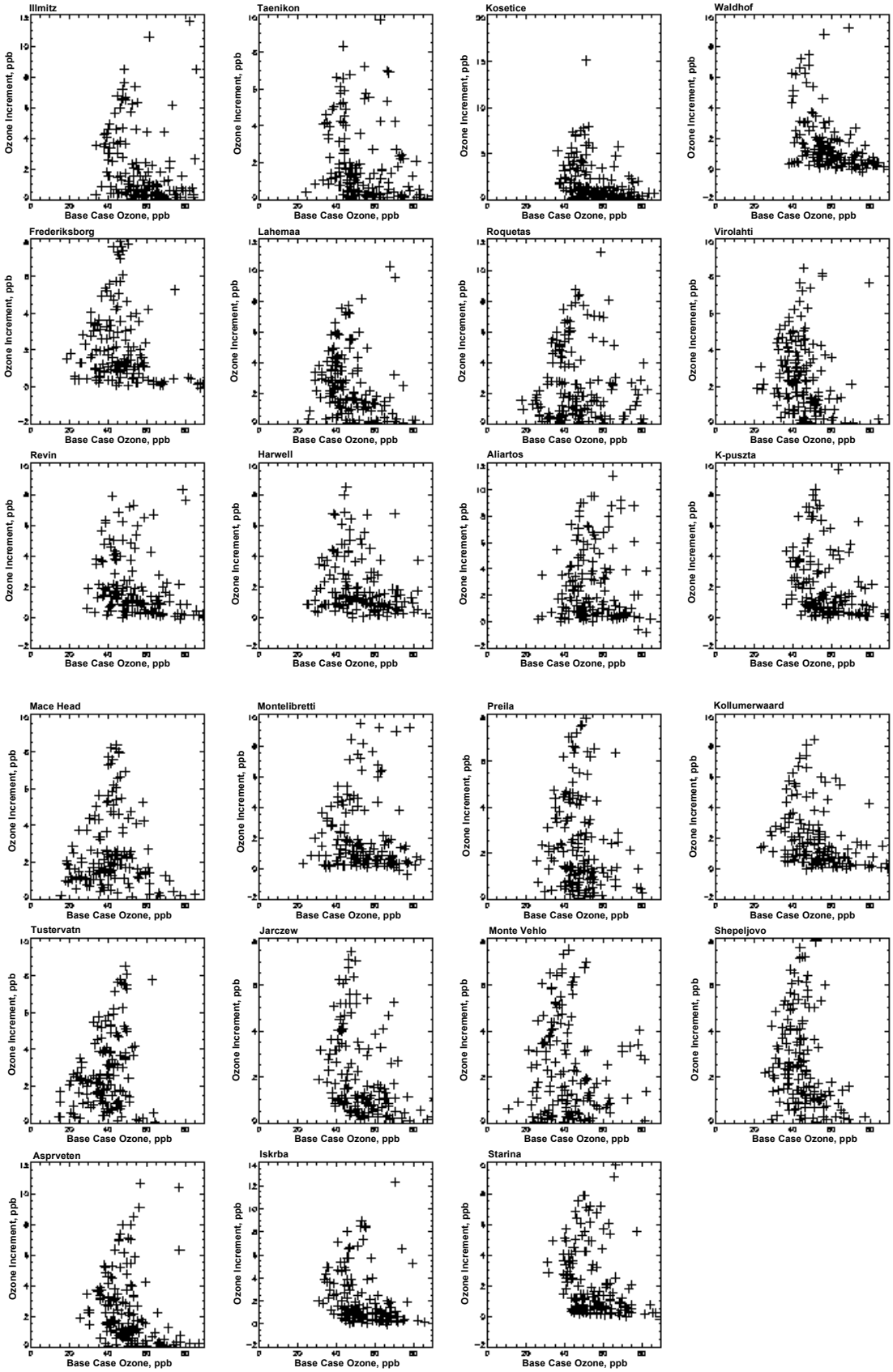

Figure 3.6 The Increments in Ozone Concentration at each selected EMEP Monitoring Network Site Plotted against the Base Case Ozone Concentration for the Climate Change Scenario.

3.5.2 Impact of Climate Change Scenario across the British Isles

The influence of the global scale build-up in ozone between the 1990s and 2030 on the mean of the maximum hourly mean ozone concentrations calculated for each site in the UK Rural Ozone monitoring network is shown in Figure 3.7. Mean maximum hourly mean ozone concentrations increase by between 1.9 and 2.6 ppb. There is a tendency for the climate increments to be higher at the more remote sites in Northern Ireland and Scotland and lower in the south-east of England.

Table 3.5 ***Summary of the Model Experiments Studying the Impact of Climate Change on the Mean of the Maximum Ozone Concentrations at Sites in the UK Rural Ozone Monitoring Network during April to August 1997. The Base Case numbers are shown followed by the Increment due to Climate Change in Parentheses.***

Site Name	Mean of Maximum Ozone Concentrations*, ppb	Number of Days with Exceedances over 40	60	90 ppb
Yarner Wood	48.3 (2.3)	102 (12)	30 (3)	1 (2)
Somerton	51.7 (2.1)	118 (7)	39 (7)	3 (0)
Narberth	42.0 (2.3)	74 (12)	14 (2)	1 (0)
Aston Hill	48.1 (2.1)	107 (12)	23 (5)	1 (0)
Lough Navar	44.2 (2.6)	95 (15)	17 (4)	1 (0)
Great Dun Fell	48.5 (2.1)	116 (9)	24 (4)	2 (0)
Bush Estate	45.4 (2.2)	100 (19)	15 (3)	2 (0)
Strath Vaich	41.9 (2.6)	80 (18)	10 (2)	1 (0)
High Muffles	47.4 (2.3)	113 (9)	23 (5)	2 (0)
Ladybower	51.9 (2.0)	127 (5)	34 (5)	2 (0)
Bottesford	53.0 (2.1)	130 (5)	43 (4)	4 (0)
Harwell	53.2 (1.9)	125 (8)	44 (8)	3 (0)
Sibton	52.0 (2.1)	128 (8)	33 (5)	3 (0)
Rochester	54.2 (2.0)	128 (10)	41 (6)	6 (0)
Lullington Heath	54.5 (2.0)	128 (10)	45 (4)	6 (0)

The climate change increments appear to be largest in magnitude on days with ozone concentrations close to the average and lowest on days with elevated ozone concentrations. This point is illustrated in Figure 3.7, where scatter plots are presented for each site showing climate increment for each day in relationship to maximum hourly ozone concentrations. The climate increments clearly maximize in the middle of the plot and tail off to both high and low concentrations, relative to the average.

Table 3.5 presents the impact of the climate change scenario on the number of 40 ppb, 60 ppb and 90 ppb exceedance days. The change in the number of 40 ppb exceedance days varies between 5 and 19 days with the largest increases in Northern Ireland and Scotland and the smallest in south-east England. For the 60 ppb exceedance days, the increases lie in the range between 3 and 8 days. These increases are significantly smaller than those reported for the EMEP network sites pointing to there being a clear difference between the behaviour found in the British Isles compared with the rest of Europe. There appeared be little impact due to climate change scenario of any consequence on the number of 90 ppb exceedance days found in the British Isles.

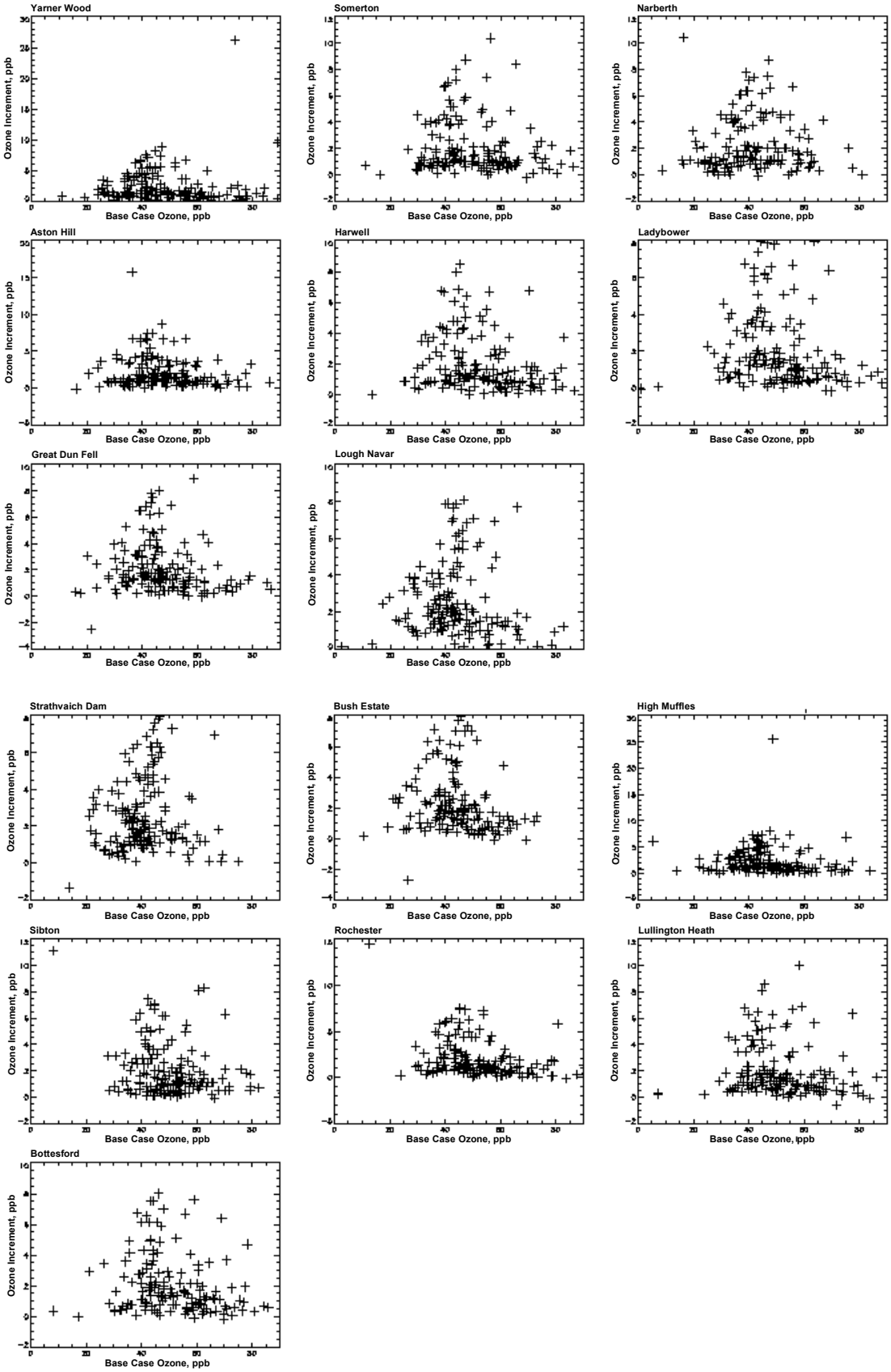

Figure 3.7 The Increments in Ozone Concentration at each UK Rural Ozone Monitoring Network Site Plotted against the Base Case Ozone Concentration for the Climate Change Scenario.

3.6 IMPACT OF REGIONAL POLLUTION CONTROLS

To investigate the impact of regional pollution controls on the ozone climate of Europe, two variants were made from the base case scenario. In the first of these, all surface man-made NO_x emissions in the regional model were reduced from their base case values by 30%. Natural NO_x sources such as lightning and soil emissions were left alone, as were biomass burning emissions in tropical regions. The same percentage reduction was applied across-the-board without spatial and temporal variation. The choice of this percentage reduction was arbitrary and has no regional policy significance. It happens to be a commonly used emission change in evaluating issues such as the NO_x- and VOC-sensitivities of photochemical ozone formation.

3.6.1 Ozone Responses to NO_x Emission Reductions

To illustrate the model responses to a 30% reduction in NO_x emissions, a scatter plot has been constructed for each selected site in the EMEP Monitoring Network showing how the model responses for each day between April and August 1997 vary with the maximum ozone concentration during that day, see Figure 3.8. At most sites, the ozone responses obtained by subtracting the maximum ozone concentration in the scenario case from the base case are positive, showing a decrease in photochemical production upon NO_x control. Model responses to NO_x control tend to increase with increasing base case ozone. That is to say, the days with the more highly elevated ozone levels show a larger response to NO_x emission reductions. Responses to NO_x emission reductions increase roughly linearly with base case ozone, implying that a 30% reduction in NO_x emissions is giving about a 10% reduction in maximum ozone levels. Photochemical ozone production is stimulated by increasing NO_x concentrations because they lead to the more efficient recycling of the HO_x free radicals. Higher NO_x levels ensure that the reaction of HO_2 + NO can compete more effectively against the free radical destruction reaction HO_2 + HO_2 + M. The photochemical chain reaction system works more effectively, ensuring that ozone production is stimulated as opposed to free radical destruction.

However, not all of the model responses to a reduction in NO_x emissions show decreases in ozone production, see Figure 3.8. At many sites, there are a substantial number of days when the model responses imply higher maximum ozone concentrations with the 30% NO_x reductions compared with the base case. This is a manifestation of the influence of NO_x levels on photochemical ozone production. Ozone production is certainly enhanced with increasing NO_x levels up to the point where the OH + NO_2 + M reaction competes against the OH attack on the hydrocarbon concentrations. Under these conditions, increasing NO_x concentrations inhibit ozone production and decreasing NO_x concentrations stimulate ozone production. Air parcels exhibiting this behaviour of increasing ozone production with decreasing NO_x levels are said to be VOC-sensitive. The sites that show this behaviour include: Illmitz, Taenikon, Kosetice, Waldhof, Roquetas, Revin, Montelibretti, Kollumerwaard, Iskrba and Starina. They tend to be the sites closest to the industrial and population centres of Europe.

There is a further mechanism by which NO_x emission reduction could lead to increased ozone levels and that is through reduced NO_x titration by way of the NO + O_3 reaction. However, with the coarse spatial resolution of the NO_x emission inventory used in this study, this mechanism is not an effective sink for ozone. The model responses to a 30% reduction in NO_x emissions at each of the UK Rural Ozone Monitoring Network sites are shown in Figure 3.9. These responses follow exactly the same patterns of behaviour as the selected EMEP Monitoring Network sites described above. The more remote sites: Lough Navar and Strath Vaich show only decreases in ozone due to 30% NO_x reductions whilst the remaining sites sometimes show ozone increases.

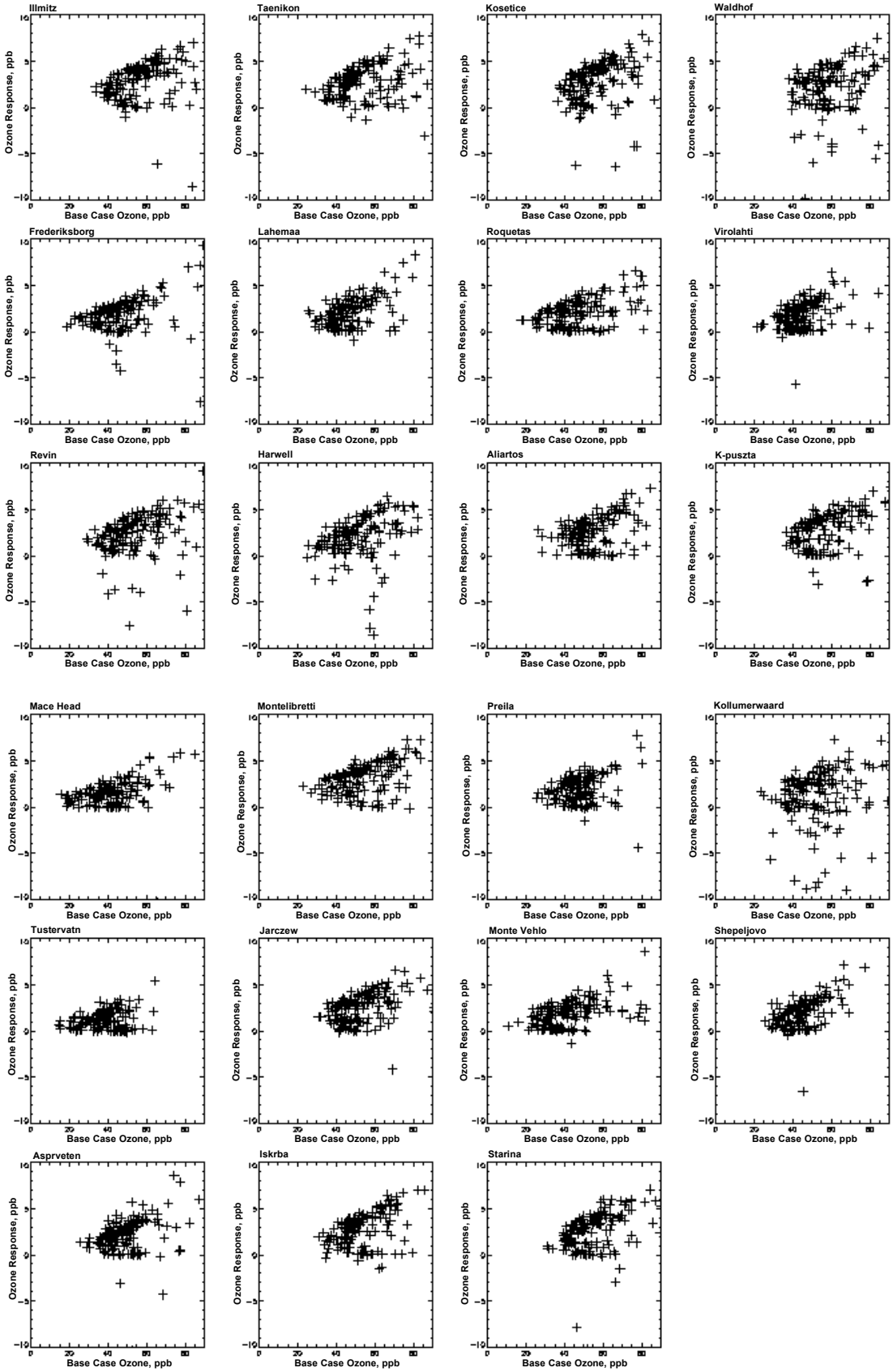

Figure 3.8 ***The Model Ozone Responses to 30% NOx Emission Reductions plotted against Base Case Ozone at Each Selected Site in the EMEP Monitoring Network.***

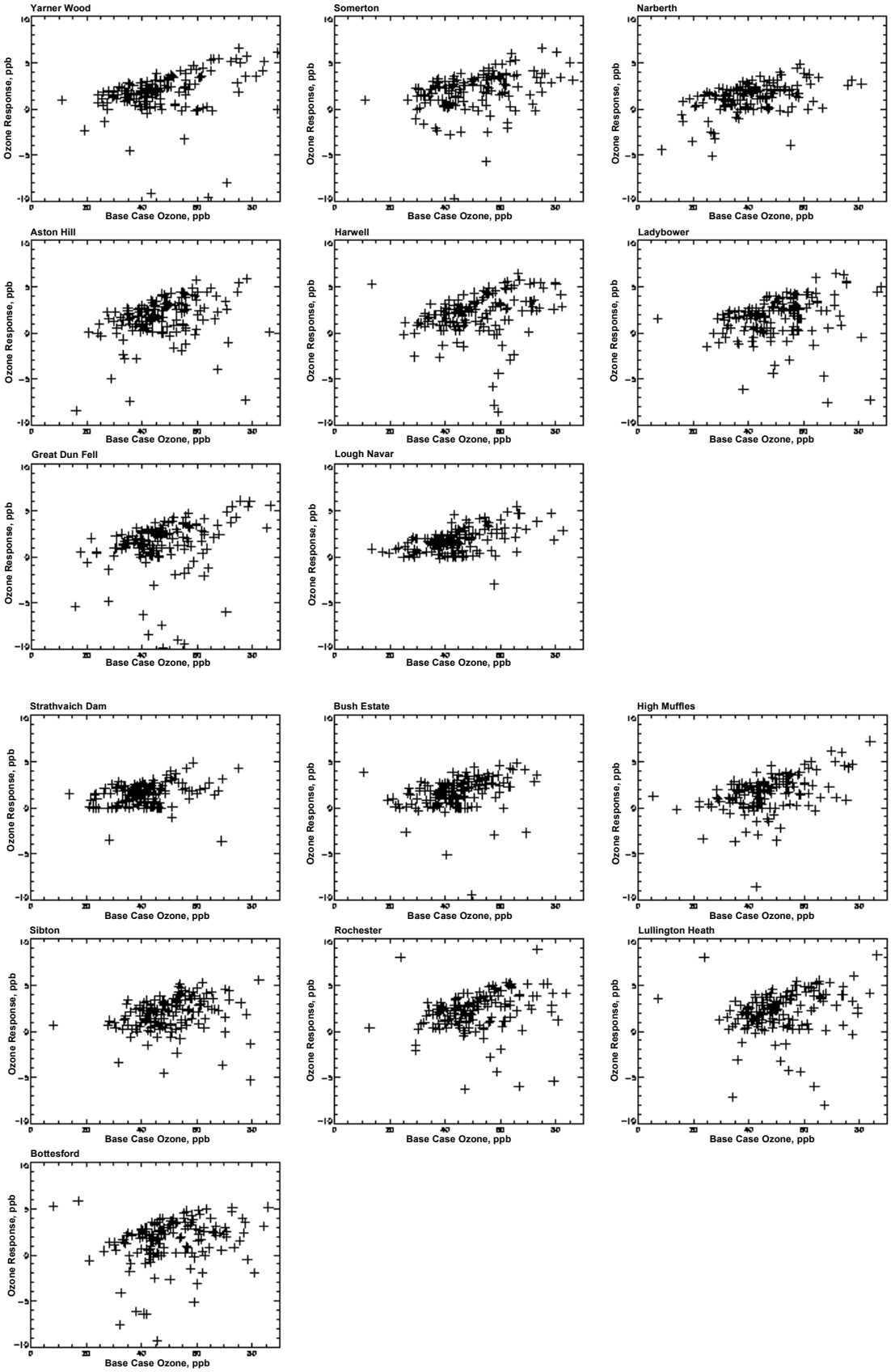

Figure 3.9 ***The Model Ozone Responses to 30% NO_x Emission Reductions plotted against Base Case Ozone at Each Site in the UK Rural Ozone Network.***

3.6.2 Model Responses to VOC Emission Reductions

The model responses (base case – scenario case) to a 30% reduction in VOC emissions are shown in Figure 3.10. At all the sites and on all the days, the model responses show that ozone production has been reduced in response to VOC controls. The model responses become increase with increasing base case ozone concentration and show a more or less linear relationship. This implies that a 30% reduction in VOC emissions produces about a 20% reduction in ozone levels, somewhat larger than that from a similar reduction in NO_x emissions.

Photochemical ozone production increases steadily with increasing VOC levels because of the more effective competition for the OH radicals between the VOCs and NO_2. There is no inhibition of ozone production by VOCs so that increased VOC emissions invariably imply increased ozone production and remarkably few of the points in Figure 3.10 are found below the axis.

The model responses to a 30% VOC reduction at each of the UK Rural Ozone Monitoring Network sites are shown in Figure 3.11. These responses follow exactly along the same lines as those for the selected EMEP Monitoring Network sites. A 30% VOC reduction produces up to a 20% reduction in ozone levels, with the exception of Lough Navar and High Muffles, where the responses are significantly smaller.

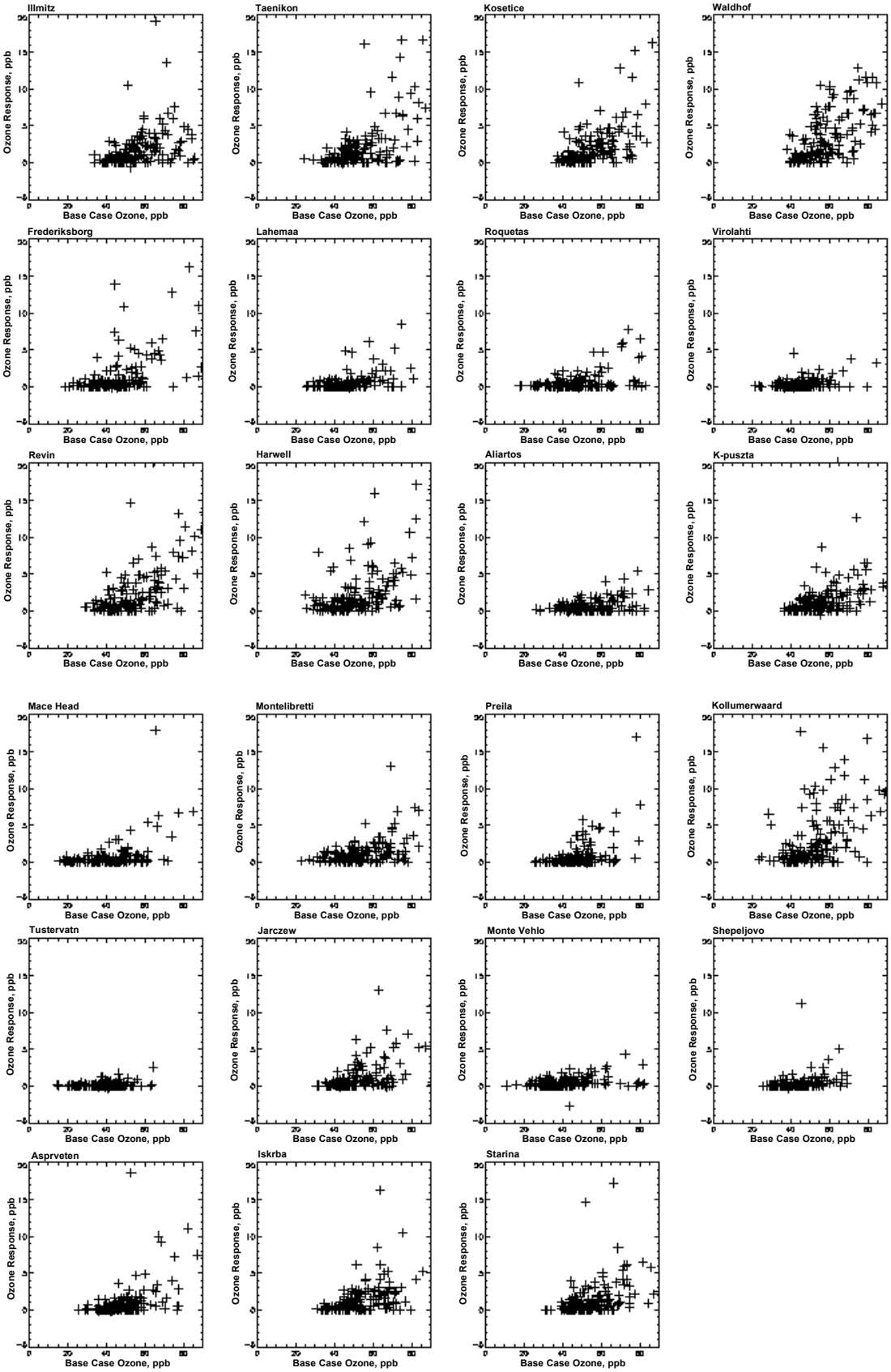

Figure 3.10 ***The Model Ozone Responses to 30% VOC Emission Reductions plotted against Base Case Ozone at each selected EMEP Monitoring Network site.***

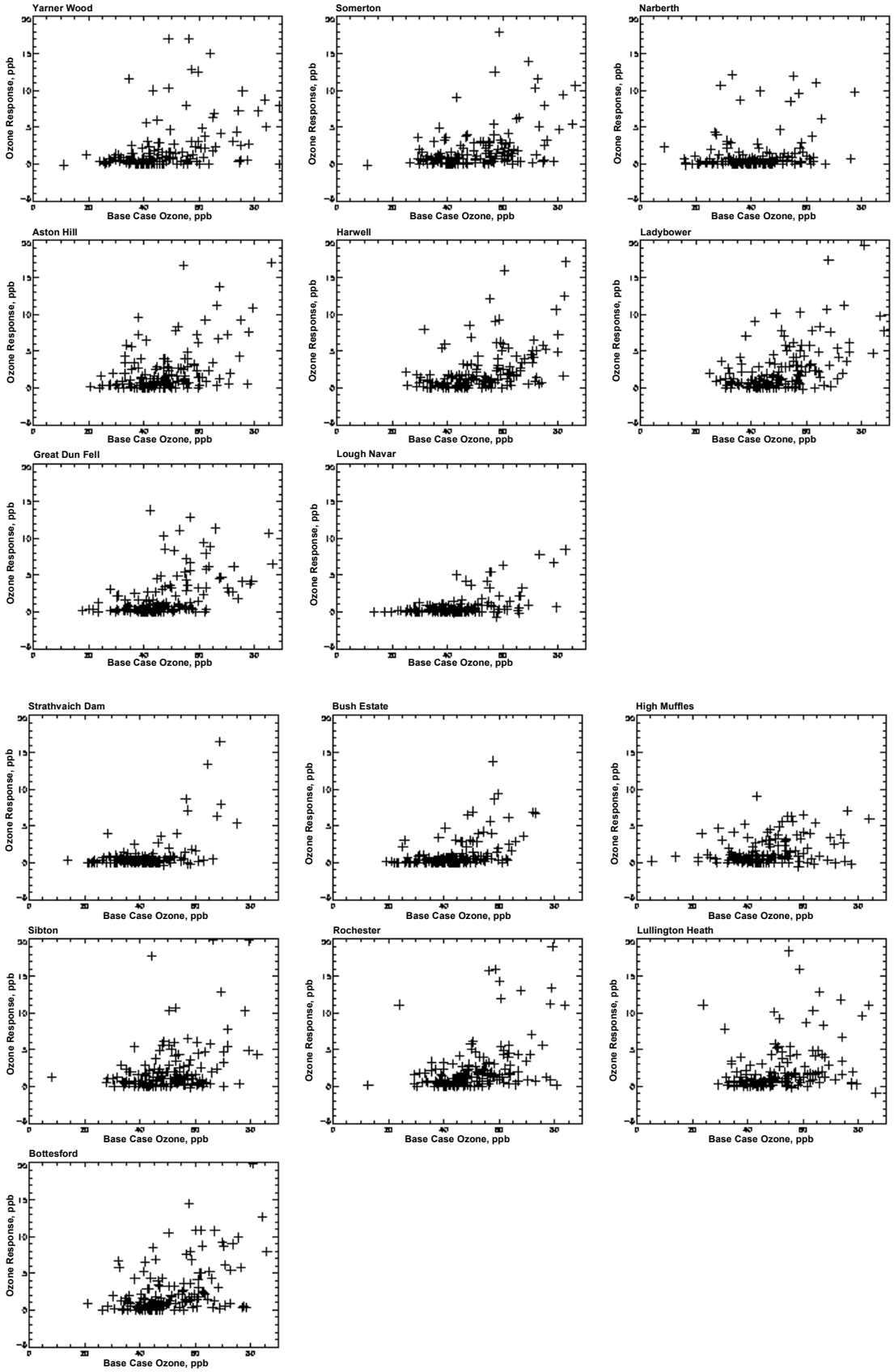

Figure 3.11 ***The Model Ozone Responses to 30% VOC Emission Reductions plotted against Base Case Ozone at Sites in the UK Rural Ozone Monitoring Network.***

3.6.3 NO_x *vs.* VOC Sensitivities

In Table 3.6, the model responses to 30% NO_x and VOC emission reductions have been quantified for selected sites in the EMEP Monitoring Network. Looking firstly at the mean of the maximum ozone concentrations, then 30% NO_x emission reductions have led to decreases in mean maximum ozone concentrations that ranged from about 1.0 to 3.1 ppb. In comparison, 30% VOC emission reductions lead to decrease of the order of 0.2 to 4.7 ppb. These decreases in mean ozone concentrations cover almost exactly the same range but with opposite sign as the model responses to climate change scenario as exhibited in Table 3.4.

Table 3.6 ***Summary of the Model Experiments Studying the Impact of NOx and VOC Emission Reductions on the Mean of the Maximum Ozone Concentrations during April to August 1997 at the sites in the EMEP Monitoring Network. The Model Responses to a 30% reduction in NOx Emissions are shown followed by the Responses to a 30% Reduction in VOC Emissions in Parentheses.***

Site name	Responses in Mean of Maximum Ozone Concentrations, ppb	Responses in Number of Exceedances Days 40 60 90 ppb
Illmitz	-2.8 (-2.1)	-9(-2) -11(-7) +2(0)
Taenikon	-2.7 (-2.7)	-8(-2) -7(-8) -2(-4)
Kosetice	-2.7 (-2.3)	-4(-2) -13(-8) -2(-2)
Waldhof	-2.0 (-4.7)	-6(-1) -7(-14) -1(-2)
Frederiksborg	-1.7 (-1.5)	-8(-5) 0(-3) +1(0)
Lahemaa	-1.8 (-0.9)	-12(-3) -6(-4) +1(-1)
Roquetas	-2.0 (-0.7)	-7(-1) -4(-2) 0(0)
Virolahti	-1.8 (-0.4)	-11(-2) -4(-2) 0(0)
Revin	-2.4 (-3.0)	-5(-5) -4(-6) -3(-4)
Harwell	-1.1 (-3.0)	-4(-6) -5(-7) +1(-2)
Aliartos	-2.6 (-0.7)	-6(-1) -10(-3) 0(0)
K-puszta	-2.9 (-1.8)	-4(0) -10(-6) -1(-2)
Mace Head	-1.5 (-0.7)	-10(-3) -4(-2) 0(0)
Montelibretti	-3.1 (-1.3)	-12(-3) -9(-6) -1(-1)
Preila	-1.9 (-1.0)	-9(-1) -3(-2) -1(0)
Kollumerwaard	-1.0 (-3.4)	-6(-7) -2(-14) -1(-2)
Tustervatn	-1.2 (-0.2)	-12(-1) -1(0) 0(0)
Jarczew	-2.7 (-1.4)	-5(-2) -8(-5) -4(-2)
Monte Vehlo	-1.8 (-0.5)	-14(-2) -6(-1) 0(0)
Shepeljovo	-1.9 (-0.6)	-10(-4) -3(-2) -1(0)
Aspreveten	-2.1 (-1.0)	-9(-3) -1(-3) 0(0)
Iskrba	-3.0 (-1.5)	-5(-1) -12(-9) -2(0)
Starina	-2.6 (-1.5)	-8(-1) -12(-5) 0(0)

Note (a) responses are calculated as (scenario case – base case) so that –ve numbers imply an ozone decrease due to emission reductions.

Then, examining the exceedance days statistics, 30% NO_x emission reductions appear to have a much larger influence on 40 ppb exceedance days at the EMEP sites compared with 30% VOC emission reductions. The decreases in 40 ppb exceedance days with 30% NO_x emission reductions appear to be similar in magnitude but of opposite sign to the model responses to climate change scenario. The opposite appears to be the case with the 60 ppb exceedance days statistics, where 30% VOC emission reductions appear to have a greater influence compared to 30% NO_x emission reductions. Again, the influence of the 30% VOC emission reductions is comparable to that of the climate change scenario but of the opposite sign. With the 90 ppb exceedance days, 30% VOC emission reductions lead to a decrease in exceedance days at all sites, whereas 30% NO_x emission reductions lead to both increases (Illmitz, Frederiksborg and

Lahemaa) and decreases (Taenikon, Kosetice, Waldhof, Revin, Montelibretti, Preila, Kollumerwaard, Jarczew, Shepeljovo and Iskrba). There was no widespread influence of climate change scenario on 90 day exceedance that was comparable at all to that from the NO_x or VOC emission reductions.

The corresponding model responses to 30% NO_x and VOC emission reductions have also been quantified for the UK Rural Ozone Monitoring Network sites in Table 3.7. The 30% NO_x emission reductions led to decreases in mean ozone concentrations that ranged from about 0.5 to 1.7 ppb. In comparison, 30% VOC reductions led to decreases from 0.8 to 3.6 ppb. These decreases were of a similar magnitude but opposite sign to the climate change scenario responses in Table 3.5.

Table 3.7 ***Summary of the Model Experiments Studying the Impact of NOx and VOC Emission Reductions on the Mean of the Maximum Ozone Concentrations during April to August 1997 at the sites in the UK Rural Ozone Monitoring Network. The Model Responses to a 30% reduction in NOx Emissions are shown followed by the Responses to a 30% Reduction in VOC Emissions in Parentheses.***

Site name	Responses in Mean of Maximum Ozone Concentrations, ppb	Responses in Number of Exceedances Days 40	60	90 ppb
Yarner Wood	-0.7 (-2.5)	-7(-11)	-2(-9)	+2(0)
Somerton	-0.5 (-2.7)	-10(-6)	-4(-9)	+2(-1)
Narberth	-1.0 (-1.7)	-6(-6)	-5(-5)	0(0)
Aston Hill	-0.7 (-2.7)	-3(-5)	-4(-7)	+2(-1)
Lough Navar	-1.7 (-0.8)	-11(-2)	-4(-1)	0(0)
Great Dun Fell	-1.1 (-2.3)	-9(-8)	-8(-8)	0(-1)
Bush Estate	-1.4 (-1.5)	-8(-3)	-2(-3)	0(0)
Strath Vaich	-1.4 (-0.9)	-11(-1)	-1(-3)	0(0)
High Muffles	-1.1 (-1.5)	-6(-6)	-2(-7)	0(-1)
Ladybower	-0.9 (-3.3)	-6(-8)	-4(-9)	+3(-2)
Bottesford	-1.0 (-3.6)	-8(-13)	-8(-14)	+1(-1)
Harwell	-1.1 (-3.0)	-4(-6)	-5(-7)	+1(-2)
Sibton	-1.6 (-2.4)	-6(-1)	-7(-10)	0(-1)
Rochester	-1.7 (-3.3)	-5(-2)	-7(-11)	+1(-3)
Lullington Heath	-1.6 (-3.2)	-5(-4)	-6(-9)	+2(-4)

Note (a) responses are calculated as (scenario case – base case) so that –ve numbers imply an ozone decrease due to emission reductions.

The model responses observed to the 30% NO_x and VOC emission reductions can be used to classify each day at each site. If the model response to the 30% NO_x reduction is more negative than that to the 30% VOC reduction then the day is classified as NO_x-sensitive. Conversely, if the model response to the 30% VOC reduction is more negative than that to the 30% VOC reduction then the day is classified as VOC-sensitive. Table 3.8 shows how many of the 152 days at each selected site in the EMEP Monitoring Network were classified as NO_x-sensitive on this basis. Most sites showed a preponderance of days classified as NO_x-sensitive on this basis. The exceptions were Waldhof, Kollumerwaard, Revin, Kosetice and Frederiksborg, which showed significantly fewer NO_x-sensitive days and by implication, more VOC-sensitive days.

If the day with the highest ozone concentration was examined at each site, then that day again could be classified as NO_x- or VOC-sensitive depending on the model responses on that day alone. Table 3.8 presents this classification under the column describing the sensitivity on the worst ozone day. On this basis, an equal number of sites were classified as NO_x-sensitive as VOC-sensitive. A final classification in Table 3.8 is based on the influence of emission reduction on the number of exceedance days. If 30% NO_x emission reductions produce a larger

reduction in the number of exceedance days compared with 30% VOC emission reductions, then that site is classified as NO_x-sensitive, and *vice versa*. Based on 90 ppb exceedance days, then almost all of the sites appear to be VOC- sensitive with the exception of Preila, Jarczew, Shepeljovo and Iskrba. These are all sites in the eastern part of the model domain and their exceptional NO_x- sensitivities reflect the relative spatial distributions of man-made VOC and NO_x emissions. VOC emissions are much lower in eastern Europe compared with NO_x emissions because of the decreased importance of motor vehicle emissions.

Table 3.8 ***NOx- and VOC Sensitivities of Each Selected Site in the EMEP Network during April to August 1997 based on Number of Days, Sensitivity on the Worst Ozone Day and Number of Exceedance Days.***

Site	Number of NO_x-Sensitive Days	Sensitivity on Worst Ozone Day	Sensitivity at Exceedance Days		
			40	60	90 ppb
Illmitz	127 out of 152	NO_x	NO_x	NO_x	VOC
Taenikon	122	VOC	NO_x	VOC	VOC
Kosetice	114	NO_x	NO_x	NO_x	VOC
Waldhof	78	VOC	NO_x	VOC	VOC
Frederiksborg	110	VOC	NO_x	VOC	VOC
Lahemaa	141	NO_x	NO_x	NO_x	VOC
Roquetas	146	NO_x	NO_x	NO_x	VOC
Virolahti	150	NO_x	NO_x	NO_x	VOC
Revin	100	VOC	VOC	VOC	VOC
Harwell	102	VOC	VOC	VOC	VOC
Aliartos	149	NO_x	NO_x	NO_x	VOC
K-puszta	135	NO_x	NO_x	NO_x	VOC
Mace Head	134	VOC	NO_x	NO_x	VOC
Montelibretti	141	VOC	NO_x	NO_x	VOC
Preila	133	NO_x	NO_x	NO_x	NO_x
Kollumerwaard	79	VOC	VOC	VOC	VOC
Tustervatn	139	NO_x	NO_x	NO_x	VOC
Jarczew	124	VOC	NO_x	NO_x	NO_x
Monte Vehlo	148	NO_x	NO_x	NO_x	VOC
Shepeljovo	146	NO_x	NO_x	NO_x	NO_x
Aspreveten	135	NO_x	NO_x	VOC	VOC
Iskrba	138	VOC	NO_x	NO_x	NO_x
Starina	131	VOC	NO_x	NO_x	VOC

The 30% NO_x reductions appeared to have a greater influence on 40 ppb exceedance days at the UK Rural Ozone Monitoring Network sites compared with 30% VOC reduction, see Table 3.9. The responses at Yarner Wood and Bottesford appeared to be much greater to 30% VOC reduction, however. In terms of 60 ppb exceedance days, both 30% VOC and NO_x reductions looked fairly comparable in effectiveness. The responses at Bush Estate, Strath Vaich and High Muffles looked significantly smaller compared with the other sites. Exceedance days at 90 ppb appeared to be decreased by 30% VOC reductions and increased by 30% NO_x reductions.

3.6.4 Comparison with Indicator Ratios

It is difficult to be certain about the assertions concerning the signs and relative magnitudes of the model responses to NO_x and VOC emission reductions. Sometimes, such model responses are critically dependent on model assumptions and it is difficult to be sure that they are robust. An approach has been developed for evaluating NO_x- and VOC-sensitivities based on indicator species (Sillman *et al.*, 1997). It has been found that model predictions of NO_x- and VOC-sensitivity were linked to the mid-afternoon concentration ratio of ozone to total oxidised nitrogen species, NO_z = HNO_3 + PAN + nitrate aerosol. These concepts have been extended

Table 3.9 ***NOx- and VOC Sensitivities of Each Selected Site in the UK Rural Ozone Monitoring Network during April to August 1997 based on Number of Days, Sensitivity on the Worst Ozone Day and Number of Exceedance Days.***

Site	Number of NO_x-Sensitive Days	Sensitivity on Worst Ozone Day	Sensitivity at Exceedance Days 40	60	90 ppb
Yarner Wood	109 out of 152	VOC	VOC	VOC	VOC
Somerton	105	VOC	NO_x	VOC	VOC
Narberth	105	VOC	VOC	VOC	VOC
Aston Hill	101	VOC	VOC	VOC	VOC
Lough Navar	137	VOC	NO_x	NO_x	VOC
Great Dun Fell	105	VOC	NO_x	VOC	VOC
Bush Estate	123	NO_x	NO_x	VOC	VOC
Strath Vaich	128	NO_x	NO_x	VOC	VOC
High Muffles	94	NO_x	VOC	VOC	VOC
Ladybower	84	VOC	VOC	VOC	VOC
Bottesford	86	VOC	VOC	VOC	VOC
Harwell	102	VOC	VOC	VOC	VOC
Sibton	100	VOC	NO_x	VOC	VOC
Rochester	99	VOC	NO_x	VOC	VOC
Lullington Heath	104	VOC	VOC	VOC	VOC

to include other concentration ratios in addition to $[O_3]/[NO_z]$. Broadly speaking, air parcels with $[O_3]/[NO_z]$ less than 8-10 were invariably found to be VOC-sensitive (ozone responses to VOC reductions greater than to NO_x reductions). Those with $[O_3]/[NO_z]$ greater than 8-10 were found to be NO_x-sensitive (ozone responses to NO_x reductions greater than those to VOC reductions).

We can evaluate the EUROSTOCHEM designations of NO_x- and VOC-sensitivity on this same basis. As each parcel reaches its arrival point in the EMEP Monitoring Network, the concentration ratio $[O_3]/[NO_z]$ is calculated in the base case and the ozone responses are available from the scenario cases. The results are plotted in Figure 3.12 and broadly speaking the plots show the expected behaviour. At high values of $[O_3]/[NO_z]$, the model responses to NO_x reductions are larger than VOC responses, (+ signs above x signs). Conversely, at low values of $[O_3]/[NO_z]$, model VOC responses are larger than NO_x responses (x signs above + signs). This ideal behaviour is clearly shown at Illmitz, Taenikon, Kosetice, Waldhof, Frederiksborg, Lahemaa, Revin, K-puszta, Kollumerwaard, Aspreveten, Iskrba and Starina.

There are however a few sites where $[O_3]/[NO_z]$ values rarely fall below 20 and the model responses appear to be entirely NO_x-sensitive over all the arrivals during the study period. These sites include Mace Head, Roquetas, Virolahti, Aliartos, Montelibretti, Preila, Tustervatn, Jarczew, Monte Vehlo and Shepeljovo. Again, this behaviour is entirely consistent with theoretical expectations.

The ozone sensitivity behaviour for each UK Rural Ozone Monitoring Network sites is shown in Figure 3.13. The classical turn-over between VOC- and NO_x-sensitivity at $[O_3]/[NO_z]$ ratios less than about 10 (Sillman *et al.*, 1997) is clearly shown at the Yarner Wood, Somerton, Harwell, Ladybower, Great Dun Fell, Strath Vaich, Bush Estate, High Muffles, Sibton, Lullington Heath and Bottesford sites. The EUROSTOCHEM model results for the UK sites appear to be entirely consistent with theoretical expectations.

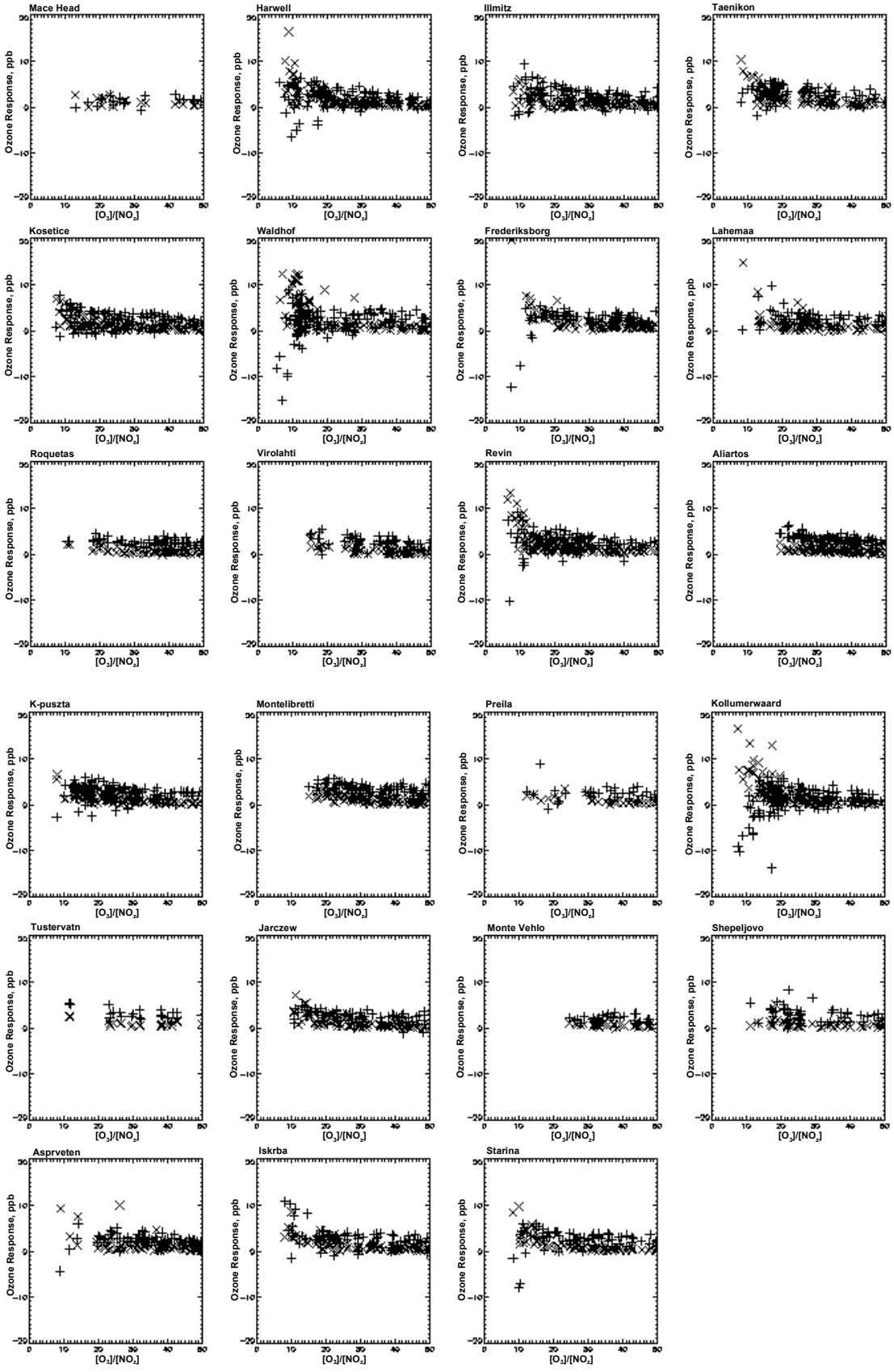

Figure 3.12 ***The Model Ozone Response to 30% NO_x (+ signs) and VOC (x signs) Emission Reductions plotted against $[O_3]/[NO_z]$ in the Base Case for Each Selected Site in the EMEP Monitoring Network.***

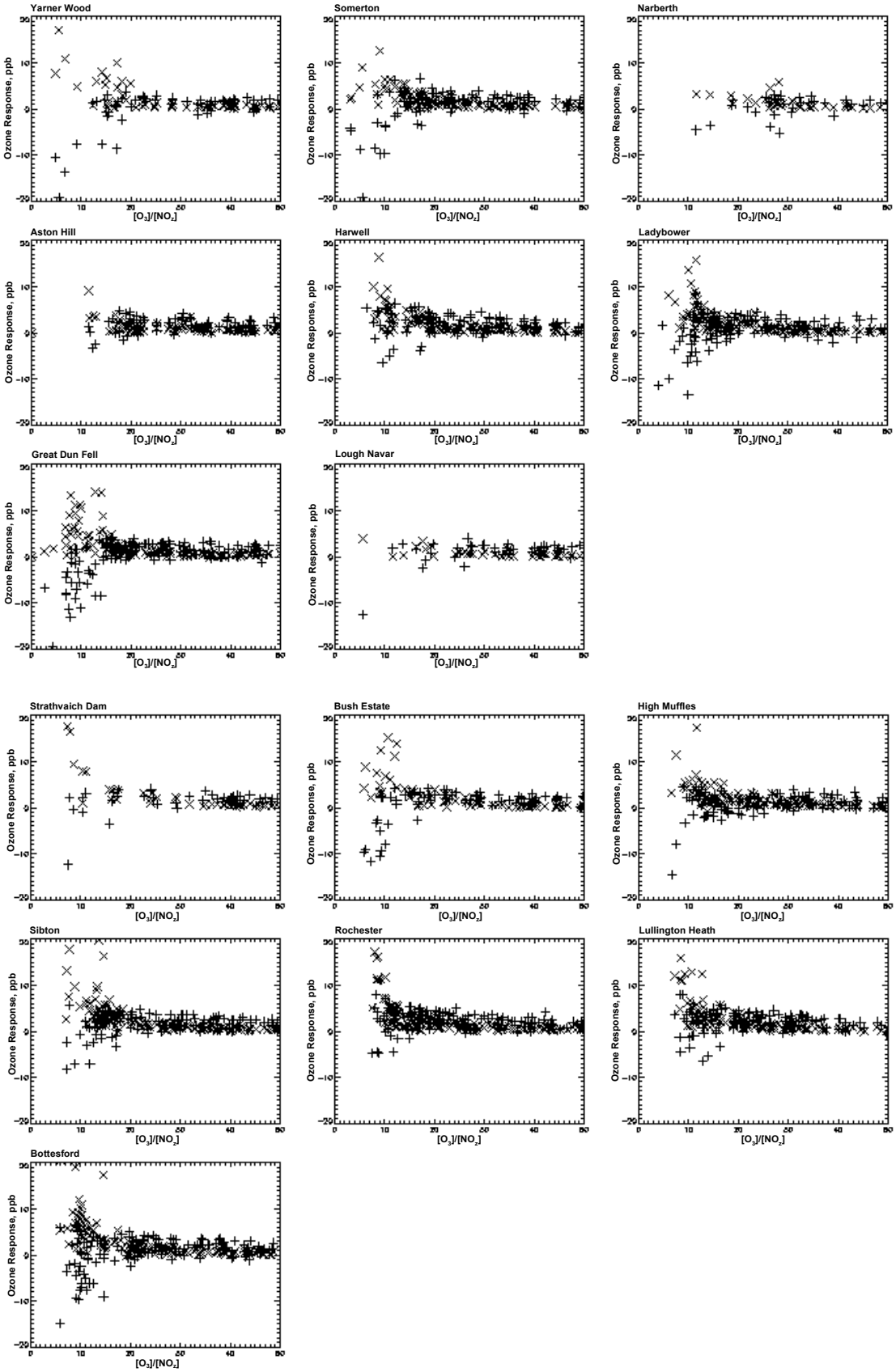

Figure 3.13 ***The Model Ozone Response to 30% NO_x (+ signs) and VOC (x signs) Emission Reductions plotted against $[O_3]/[NO_z]$ in the Base Case for Each Site in the UK Rural Ozone Monitoring Network.***

3.6.5 Modelling the Impact of the UNECE Gothenburg Protocol

Having established that the EUROSTOCHEM model is giving reasonable responses to NO_x and VOC emission reductions that are entirely consistent with theoretical expectations, it is appropriate to move on to the analysis of more realistic emission control scenarios. Ideally, emission control scenarios should be constructed for both European and non—European countries and these should address the current (1997) situation and current reduction plans for 2010, 2015 and 2020, incorporating the expected emission reduction measures for all countries and for all relevant trace gases. The resources have not been available to develop such a consistent set of emission fields and furthermore such emission fields have not become available from work carried out elsewhere.

To make progress, a simplified representation of the likely possible implementation of the UNECE Gothenburg Protocol has been constructed. The assumption has been made that in the Gothenburg scenario, European NO_x and VOC emissions from man-made sources would decline by 50% relative to the base case which correspond to 1990 emissions. The emission reductions were applied across-the-board and no changes were made to any of the other emission fields.

The maximum daily mean ozone concentrations were calculated using EUROSTOCHEM for the base case and Gothenburg scenarios, for each site in the EMEP and UK Rural Ozone Monitoring Networks, for each day of June and July 1997. The percentage reductions in the daily maximum ozone concentrations varied dramatically from day-to-day and from site-to-site. At the EMEP Monitoring Network sites, the Gothenburg scenario brought about reductions in daily maximum ozone concentrations in the range 0 - 30%. The average percentage reduction over the 1386 sites and days was 17%. At the UK Rural Ozone Monitoring Network sites, the Gothenburg scenario brought about an average reduction of 15% over the 911 sites and days.

Figure 3.14 presents a scatter plot of the model responses to the Gothenburg scenario *vs.* the base case daily maximum ozone concentrations for each EMEP Monitoring Network site and day during June and July 1997. The large day-to-day and site-by-site variations are clearly apparent from the Figure. However, despite the scatter, there is a clear tendency for the percentage reductions to increase with the daily maximum ozone concentration in the base case scenario. Figure 3.15 present a similar scatter plot for the UK Rural Ozone Monitoring Network sites and again similar behaviour is seen.

The Gothenburg scenario reduced the total number of 90 ppb exceedence days at the EMEP Monitoring Network sites from 57 to 18, from 633 to 305 for the 60 ppb exceedence days and from 1316 to 1278 for 40 ppb exceedence days. Clearly exceedence days were more dramatically reduced as the target exceedence threshold was increased. At the UK Rural Ozone Monitoring Network sites, the total number of 90 ppb exceedence days was reduced from 12 to 1, from 319 to 143 for the 60 ppb exceedence days and from 860 to 819 for the 40 ppb exceedence days.

In summary, a clear feature of the EUROSTOCHEM model responses to the UNECE Gothenburg Protocol scenario entailing 50% reductions in NO_x and VOC emissions was the dramatic day-to-day and site-by-site variations found in the percentage reductions in daily maximum ozone concentrations. Averaging over all 2297 sites and days during June and July 1997, a reduction of 17% in the daily maximum ozone concentrations was found for a 50% reduction in both NO_x and VOC emissions across-the-board in Europe.

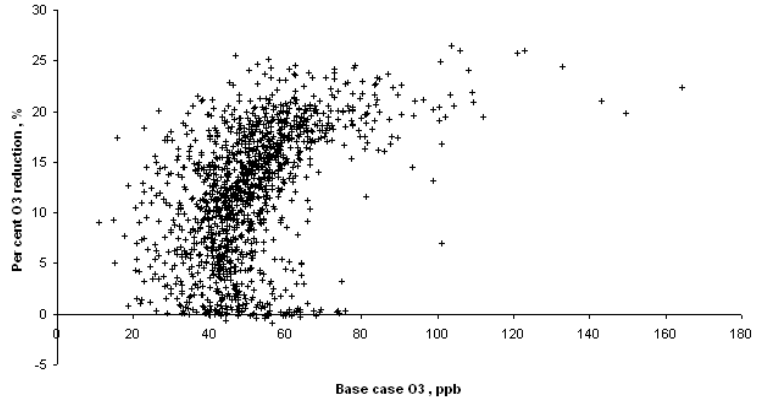

Figure 3.14 ***Scatter Plot of the Percentage Reductions in Daily Maximum Ozone Concentrations vs. Base Case Concentrations in EUROSTOCHEM at each EMEP Monitoring Network site during June and July 1997 following the Implementation of the Gothenburg Scenario.***

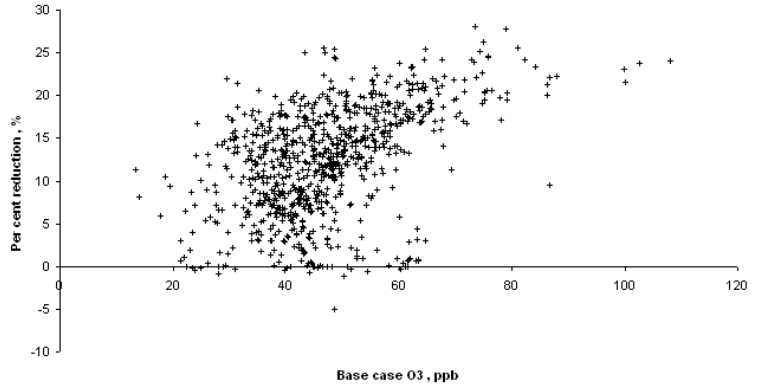

Figure 3.15 ***Scatter Plot of the Percentage Reductions in Daily Maximum Ozone Concentrations vs. Base Case Concentrations in EUROSTOCHEM at each UK Rural Ozone Monitoring Network site during June and July 1997 following the Implementation of the Gothenburg Scenario.***

3.7 DISCUSSION AND CONCLUSIONS

In this study, we have described how a European regional scale model has been nested inside a global 3-D Lagrangian chemistry-transport model using identical representations of the atmospheric processes in each model domain. A careful evaluation of the model results with observations at the Mace Head atmospheric baseline station with observations from 23 sites within the EMEP Monitoring Network and 15 sites within the UK Rural Ozone Monitoring Network has been carried out. From this evaluation, it has been concluded that the EUROSTOCHEM model exhibits considerable skill in describing the pattern of daily ozone maxima during the study period from 1st April through to 31st August 1997. However, the model was manifestly unable to resolve any of the local scale influences that affected ozone concentrations particularly during night-time. Also the model showed a tendency to underestimate the number of ozone peaks in the observed records because of the coarseness of the meteorological and emission fields employed. Those ozone peaks that were reproduced in the model, were modelled accurately to ±4 ppb, that is to say, within ±11 %. With these reservations in mind, the model was used to examine the likely impacts of the potential global ozone build-up by the year 2030 and the impacts of regional pollution control measures that aim to reduce NO_x and VOC emissions.

A conclusion of this study was that the likely impacts of the future global ozone build-up and regional pollution control measures would be quite different in different parts of the ozone concentration distribution. In general terms, the future global ozone build-up exerted a major influence on the ozone concentrations around the median levels in the distribution of ozone hourly concentrations, with decreasing influences towards the minimum and maximum levels. In contrast, regional pollution control measures exerted their major influence towards the

maximum levels in the distribution of ozone hourly concentrations. The result is that at levels close to median levels, the global build-up and regional pollution controls displaced the mean ozone concentrations by similar increments but with opposite signs. However, regional pollution controls reduced maximum ozone concentrations significantly more than they were increased by global scale build-up. In terms of exceedance days, global scale build-up and regional pollution controls had comparable impacts on the number of 40 ppb and 60 ppb exceedance days. Regional pollution control measures had a larger impact on the number of 90 ppb exceedance days compared with global scale build up.

This confirms our earlier study that pointed out that global scale build-up in ozone could offset the impact of regional pollution control measures on mean ozone levels in Europe. This may well be important where standards and guidelines have been set at the 40 ppb level for the protection of ecosystems. In this study we have confirmed these previous results and extended them to cover peak ozone levels. The impact of regional pollution control measures on peak ozone concentrations is unlikely to offset by global scale ozone build-up. This is the case at the 90 ppb level which is currently the level set for triggering public health warnings. However, we have found that where standards and guidelines have been set at the 60 ppb level for the protection of human health, then the influence of global scale build-up may still be important. It is still likely that global scale ozone increases may partially offset the reductions in the number of 60 ppb exceedance days due to regional pollution controls.

A further conclusion from this study concerns the importance of the global circulation and distribution of ozone in influencing the day-to-day variations in maximum ozone concentrations in Europe. By carefully taking into account in the EUROSTOCHEM model this global circulation and distribution, a reasonable description has been generated of the maximum hourly mean ozone concentrations at some sites across Europe. This points to the importance to be given to day-to-day variations in baseline ozone concentrations in the initialisation of ozone in regional modelling studies.

4 Urban Ozone/Nitrogen Dioxide

4.1 SECTION SUMMARY

The reaction of ozone with NO is the major source of NO_2 in the troposphere. Ozone concentrations are depressed close to NO_x emission sources (in urban areas) by this reaction but increase downwind. The concentrations of NO_2 and O_3 observed are dependent on the initial amount of oxidant ($OX = O_3 + NO_2$) present together with the amount of NO_x emitted locally. Thus, regional and/or global changes in ozone will affect local concentrations of O_3 and NO_2. There are air quality standards for NO_2 and NO_2, as a secondary pollutant, will respond in a non-linear manner to control of the NO_x precursor emissions. It is important to define the NO_x-NO_2-O_3 relationship so that the level of emission reduction to achieve the required air quality standard can be determined.

Measurement data taken from ozone monitoring sites in London and the South East have been analysed to understand the NO_x-NO_2-O_3 relationship. The results indicate that there is a linear relationship between the concentrations of oxidant and NO_x. The intercept can be identified with the initial regional oxidant input and it follows the same seasonal pattern as observed in ozone concentrations. The slope was found to reflect the input of additional oxidant locally. There was no obvious seasonal pattern but there was a clear diurnal effect. Possible sources were identified as direct emissions of NO_2, photochemical and thermal processes.

An analysis of the maximum hourly NO_2 concentrations observed each day at the Marylebone Road site in 1999 confirmed that elevated regional scale oxidant formation can contribute to exceedences of the 105 ppb standard for NO_2 during summer months. The analysis clearly showed that such summertime exceedences can be well correlated with levels of oxidant at Rochester (the nearest rural site to London), and such an analysis provides a possible basis for improved prediction of such exceedences.

The relationship between annual mean concentrations of NO_x-NO_2-OX were analysed for 4 different site types (Central London background, Central London roadside, London suburbs and sites outside of London). The expressions derived for urban centre and background central London sites and sites outside central London are consistent with the expressions of Stedman (2001), with the inferred NOx thresholds which correspond to an annual mean NO_2 mixing ratio of 21 ppb (*i.e.* the WHO air quality guideline) consistently lying slightly higher. A number of sites were classified as 'intermediate', as they have partial roadside character, due to the influence of nearby roads. As expected, the data for these sites consistently lie at higher NOx than the generic expressions for the urban centre and background sites, but lower than the generic expression for roadside sites.

This analysis could also be used to assess the impact of climate change on the achievement of the annual air quality standard for NO_2. For every 0.1 ppb increase in background O_3 concentrations, an additional 0.12-0.22 ppb reduction would be needed in NO_x concentrations to achieve the NO_2 air quality standard.

The London Routine Column Trajectory Model was used to show that future annual mean NO_2 concentrations in central London will remain above the 21 ppb annual mean air quality target despite future planned reductions in road transport NO_x emissions. Furthermore, should global tropospheric ozone concentrations continue to increase, the annual mean air quality target will prove even more difficult to meet.

4.2 INTRODUCTION

Owing to the chemical coupling of O_3 and NO_X, the levels of O_3 and NO_2 are inextricably linked. Consequently, the response to reductions in the emissions of NO_X is highly non-linear (*e.g.* QUARG 1993; PORG 1997), and any resultant reduction in the level of NO_2 is invariably

accompanied by an increase in the level of O_3. In addition, changes in the level of O_3 on a global scale potentially lead to an increasing background which influences local O_3 and NO_2 levels and the effectiveness of local emissions controls. It is therefore necessary to have a complete understanding of the relationships between O_3, NO and NO_2 under atmospheric conditions, if the success of proposed control strategies to achieve air quality standards and objectives for NO_2 (EPAQS, 1996; AQS, 2000) is to be fully assessed.

Analyses of existing monitoring data have been undertaken to determine whether the modelling work can be enhanced by the application of empirically-derived relationships between measured concentrations of O_3, NO_X and NO_2. In Section 4.3, monitoring data from a selection of southern UK sites have been used to investigate the relationships between ambient levels of O_3, NO and NO_2 as a function of NO_X, for levels of NO_X ranging from those typical of UK rural sites to those observed at polluted urban kerbside sites. Particular emphasis is placed on establishing how the level of 'oxidant', OX (taken to be the sum of O_3 and NO_2) varies with the level of NO_X, and therefore to gain some insight into the atmospheric sources of OX, particularly at polluted urban locations. The observed relationships between O_3, NO and NO_2 are also considered within the context of current understanding of their chemical coupling. An element of the work performed under Task 2 has involved the further application of the London Routine Column Trajectory Model (LRCTM) (see Section 4.4).

4.3 ANALYSIS OF THE RELATIONSHIP BETWEEN AMBIENT LEVELS OF OZONE, NO_2 AND NO

The analysis has focussed on selected locations in London and southern England, and has considered averaging intervals ranging between one hour and one year. Much of the analysis has concentrated on 1998 and 1999 data from four sites in central and west London, namely Marylebone Road (urban kerbside), Bloomsbury (urban centre), Hillingdon (suburban) and Teddington (urban background), and additional data from Reading, Berkshire (urban background) and Harwell, Oxfordshire (rural), allowing a wide range of NO_X levels (typically *ca.* 2 – 500 ppbv) to be considered. Some information about the location and characteristics of these sites is given in Table 4.1. For the analysis of annual mean data, additional London sites and additional years have also been considered, as discussed further below in Section 4.3.7.

Table 4.1 ***Information on Selected Sites used for Detailed Analysis of O_3, NO, NO_2 Relationships.***

Site	Location	Brief site description [1]	Annual mean NO_X (2000) [1,2]
Harwell	51.573°N 1.316°W	Rural site in field adjacent to Harwell Science Centre in Oxfordshire	9.4 ppbv
Reading	51.453°N 0.954°W	Urban background site in technical college grounds, 20 m from A4 dual carriageway	37 ppbv
London Teddington	51.422°N 0.339°W	Urban background site on rooftop in grounds of the National Physical Laboratory, about 500 m from nearest road	23 ppbv
London Hillingdon	51.496°N 0.461°W	Suburban site in residential area, 30 m from M4 motorway	73 ppbv
London Bloomsbury	51.523°N 0.129°W	Urban centre site in garden area surrounded by an enclosed square of busy roads between 40 and 140 m from the site	59 ppbv
London Marylebone Rd.	51.521°N 0.155°W	Kerbside site 1m from busy street canyon (50,000 vehicles per day)	210 ppbv

Notes: [1] More detailed information is available from the National Air Quality Information Archive at http://www.aeat.co.uk/netcen/airqual. [2] Although there is significant month-to-month variability, typical ranges in daily daylight averaged NO_X are as follows: Harwell, 2 – 20 ppbv; Reading, 15 – 150 ppbv; Teddington, 10 – 100 ppbv; Hillingdon, 15 – 300 ppbv; Bloomsbury, 40 – 250 ppbv; Marylebone Rd, 50 – 500 ppbv.

Much of the analysis has used 'daylight averaged' data for the sites in Table 4.1. The hours of daylight for each day in 1998 and 1999 were defined on the basis of sunrise and sunset times obtained from the 'astronomical applications' facility on the US Naval Observatory website (http://aa.usno.navy.mil/AA/). Because monitoring data are available at hourly resolution, daylight hours were defined as complete hours falling between sunrise and sunset and, where available, the corresponding data were averaged to provide a single value for each of O_3, NO and NO_2 for each site for each day in 1998 and 1999. If more than 25% of data for a particular day/site/pollutant were unavailable, an average value was not defined.

4.3.1 The Chemical Coupling of O_3, NO and NO_2

It is well established that the interconversion of O_3, NO and NO_2 under atmospheric conditions is generally dominated by the following reactions (Leighton, 1961),

$$NO + O_3 \rightarrow NO_2 + O_2 \quad (4.1)$$

$$NO_2 + h\nu\ (+O_2) \rightarrow NO + O_3 \quad (4.2)$$

which constitute a cycle with no net chemistry (*i.e.*, the overall effect of reaction (4.2) is the reverse of reaction (4.1)). These reactions therefore represent a closed system which has the overall effect of partitioning NO_X between its component forms of NO and NO_2, and oxidant (OX) between its component forms of O_3 and NO_2, but leaving the total mixing ratio of both NO_X and OX unchanged. During daylight hours, NO, NO_2 and O_3 are typically equilibrated on the timescale of a few minutes, a condition usually referred to as 'photostationary state'. The above cycle predicts that the photostationary state mixing ratios of the three species are related by the expression $[NO].[O_3]/[NO_2] = J_2/k_1$, where J_2 is the rate of NO_2 photolysis, and k_1 is the rate coefficient for the reaction of NO with O_3.

The observed variation of daylight average mixing ratios of O_3, NO and NO_2 with the total level of NO_X is shown in Figure 4.1 for November 1998 and 1999, using data from all 6 monitoring sites in Table 4.1. The lines in Figure 4.1 were calculated using a November daytime average value of $J_{3,2} = 2.9 \times 10^{-3}\ s^{-1}$ (51.5° N latitude) with the assumption of photostationary state. Clearly, this provides an adequate description of the daylight-averaged observations, consistent with the chemical coupling of these species being dominated by reactions (4.1) and (4.2).

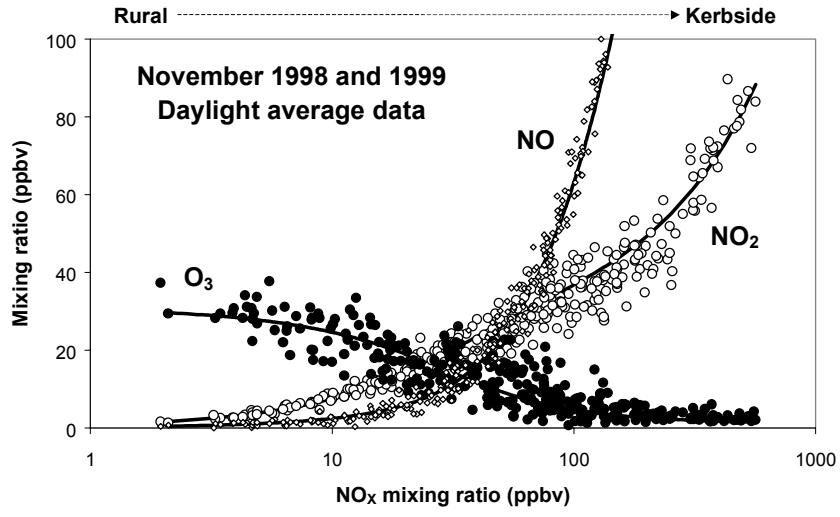

Figure 4.1 ***Variation of daylight average mixing ratios of O_3, NO and NO_2 with level of NO_X. Data are presented for each day of November 1998 and 1999 at the six sites listed in Table 4.1 (N.B. the NO_X axis is logarithmic). The lines were calculated with the assumption of photostationary state (see text).***

4.3.2 Local and Regional Contributions to Oxidant

The data in Figure 4.1 indicate that the NO_X crossover point occurs at about 60 ppbv NO_X. At lower levels, NO_2 is the major component of NO_X, whereas NO dominates at higher mixing ratios. The OX crossover point occurs at about 25 ppbv NO_X, with O_3 being the dominant form at lower levels, and NO_2 dominating at higher levels. This pattern is typical, although the precise crossover points vary with conditions (*e.g.*, with the value of J_2).

Figure 4.2 shows the same November 1998 and 1999 daylight data for O_3 and NO_2 on a linear NO_X scale. This clearly shows the interconversion of O_3 and NO_2 as a function of NO_X, but also indicates that NO_2 levels continue to increase with NO_X when O_3 is almost completely removed (*i.e.* at > *ca.* 100 ppbv NO_X). Indeed, Figure 4.3 shows that total OX appears to increase linearly with NO_X over the entire range considered, such that the level of OX at a given location has a NO_X-independent contribution, and a NO_X-dependent contribution. The former is effectively a *regional* contribution which equates to the regional background O_3 level, whereas the latter is effectively a *local* contribution which correlates with the level of primary pollution.

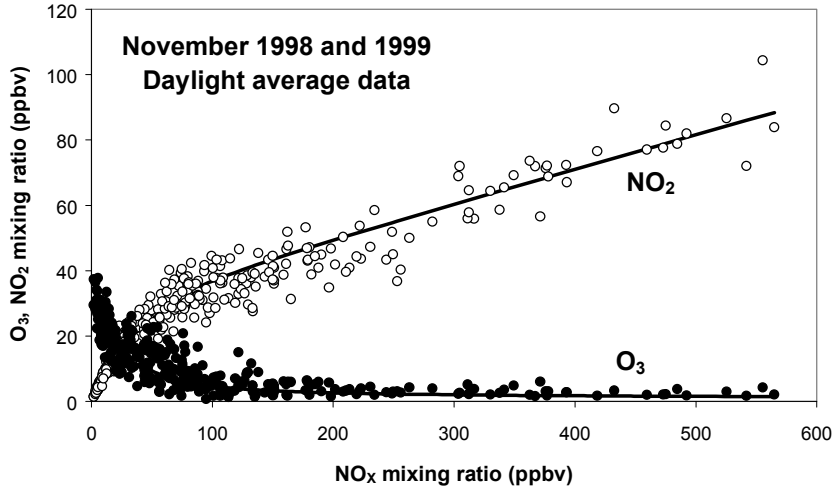

Figure 4.2 ***Variation of daylight average mixing ratios of O_3 and NO_2 with level of NO_X. Data are presented for each day of November 1998 and 1999 at 6 sites.***

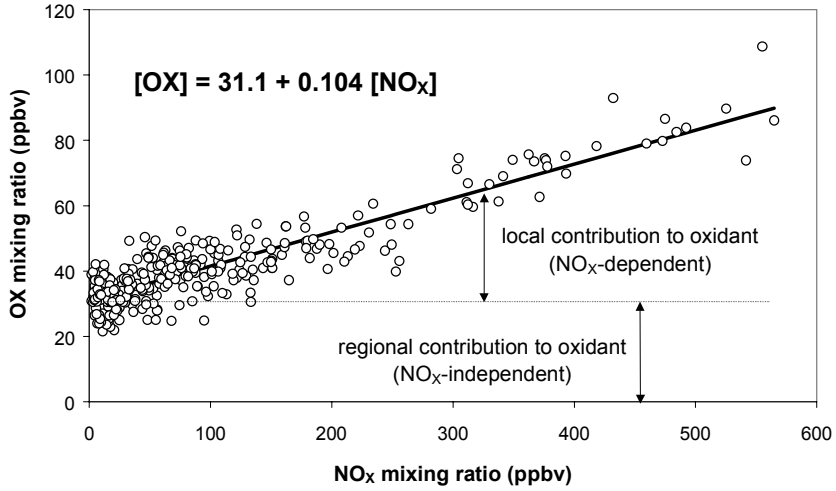

Figure 4.3 ***Variation of daylight average mixing ratio of OX with level of NO_X. Data are presented for each day of November 1998 and 1999 at 6 sites.***

Daylight average analyses were carried out for each month of the year, using 1998 and 1999 data combined. A similar dependence of OX on NO_X was observed for each month, although the data from the 'photochemical season' (April – September) showed significantly greater scatter than the winter months owing to a variation in the regional contribution resulting from

periodically elevated levels of O_3 during regional-scale photochemical events. The data for these months were therefore filtered to separate out 'ozone episode' days using the criterion that such days corresponded to a daylight average OX mixing ratio of > 50 ppbv at Teddington (the least polluted urban site considered). Figure 4.4 shows the results of the analysis using June data. This clearly shows that the level of OX at the complete range of sites was significantly elevated on episode days, as a result of the increased regional contribution, but that the local contribution (*i.e.*, the slope) was not significantly influenced.

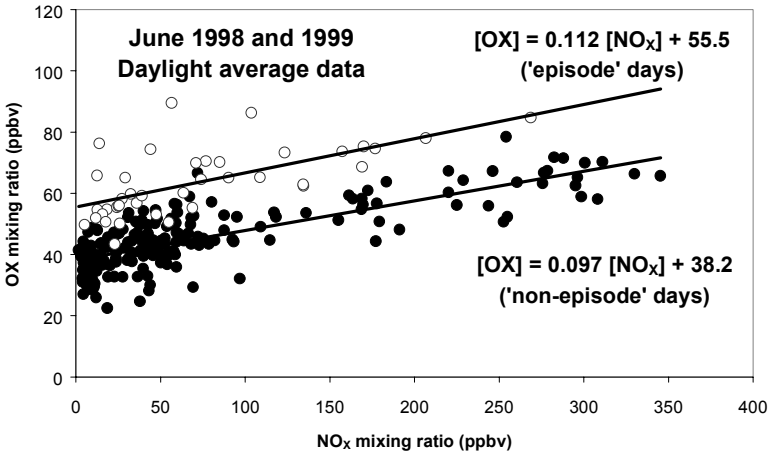

Figure 4.4 ***Variation of Daylight Average Mixing Ratio of OX with Level of NO_X. Data are Presented for Each Day of June 1998 and 1999 at 6 sites.***

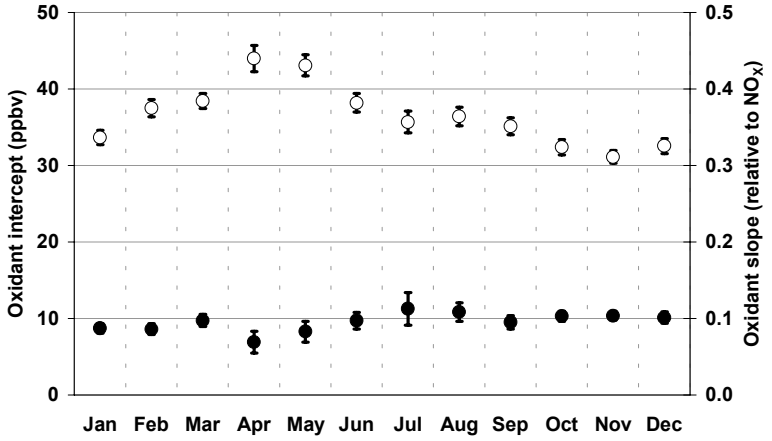

Figure 4.5 ***Seasonal variation of regional OX sources (OX intercept = open circles) and local OX sources (OX slope = filled circles). O_3 episode days (daylight average OX > 50 ppbv at Teddington) have been excluded from the analysis.***

The seasonal variation of the regional and local contributions are presented in Figure 4.5, with the parameters for April – September obtained from an analysis of non-episode days only. The regional contribution shows a seasonality with the characteristic springtime maximum observed for 'background' O_3 in the northern hemisphere (*e.g.*, see Monks, 2000). The local contribution shows remarkably little variation with season, and amounts to about 10% of the NO_X level throughout the year, based on an analysis of daylight averaged data for the 6 sites in Table 4.1. Clearly, therefore, this can lead to a substantial 'oxidant excess' at polluted locations.

4.3.3 The Impact of Regional-scale O_3 Episodes on Urban NO_2

Elevated levels of oxidant in the form of NO_2 at urban locations may therefore be generated either by having a large local source of oxidant (*i.e.* high NO_X levels), or by having a large regional source of oxidant in the presence of moderate NO_X levels. The former conditions typically prevail in wintertime episodes, when levels of NO_X of the order of 700 ppbv are required for the hourly threshold of 105 ppbv to be exceeded for NO_2. During summertime,

when boundary layer depths are much greater, such levels of NO_X are rare and NO_2 exceedences are only likely to occur when there is a large regional input of oxidant.

Figure 4.6 shows maximum hourly NO_2 and NO_X levels for each day in 1999 at Marylebone Rd., which clearly demonstrate these features. Exceedences of 105 ppbv for NO_2 during the winter months correspond to elevated NO_X. However, exceedences of the threshold continue at a similar frequency throughout the summer months, even though daily maximum NO_X levels are substantially lower. Figure 4.7 shows the same NO_2 and NO_X data plotted against each other. The data have been subdivided into three categories on the basis of the maximum level of OX measured at the rural site at Rochester on the Thames estuary in Kent. At this location, OX is mainly in the form of O_3, and provides an indication of the regional contribution. It is clear from Figure 4.7 that higher NO_2/NO_X ratios are observed at Marylebone Rd when this regional contribution to OX is elevated, and that exceedences of the 105 ppbv threshold can occur at moderate levels of NO_X.

4.3.4 Local Sources of Oxidant

Emissions of NO_2

The local, NO_X-dependent contribution to OX could result from a number of sources, the most obvious being direct emission of a proportion of NO_X in the form of NO_2. The dominant NO_X source in urban locations is road traffic exhaust. Available studies of combustion-related vehicular emissions indicate that the proportion of NO_X emitted in the form of NO_2 depends on vehicle and fuel type, and on driving conditions (*e.g.*, Heywood, 1988). For example, the output from diesel vehicles not only contains more NO_X generically, but is also likely to have a higher proportion of NO_X as NO_2. In addition the NO_2/NO_X ratio is likely to decrease at higher speeds when the engine is under greater load. Although it is probable, therefore, that NO_2 input from direct emission varies from one location to another, or from one time to another, as a result of varying vehicle fleet composition and driving speeds, an average figure of approximately 5% (by volume) is often quoted (*e.g.*, PORG 1997).

Thermal Chemical Sources

Direct emissions of NO_2 are therefore unlikely to account fully for the observed local oxidant contribution, suggesting that chemical sources are also likely to contribute. The termolecular reaction of NO with molecular oxygen,

$$2\,NO + O_2 \rightarrow 2\,NO_2 \qquad (4.3)$$

provides an additional thermal source of oxidant. The rate of this reaction is strongly dependent on the NO concentration, such that it is much more rapid at the elevated levels typical of those close to points of emission. For example, the time for 1% conversion of NO to NO_2 by this reaction is *ca.* 20 seconds at 100 ppmv NO in air, but increases dramatically as NO is diluted. At 500 ppbv NO (*i.e.* typical of the average at the high end of the range considered in the present analysis) the time for 1% conversion is *ca.* 1 hour. It is probable, therefore, that some NO to NO_2 conversion by reaction (4.3) occurs immediately after emission before the reaction is effectively halted (or at least significantly reduced in rate) by dilution.

Reaction (4.3) has certainly been postulated to make a major contribution to NO_2 formation in wintertime pollution episodes when a shallow inversion layer can lead to a combination of high

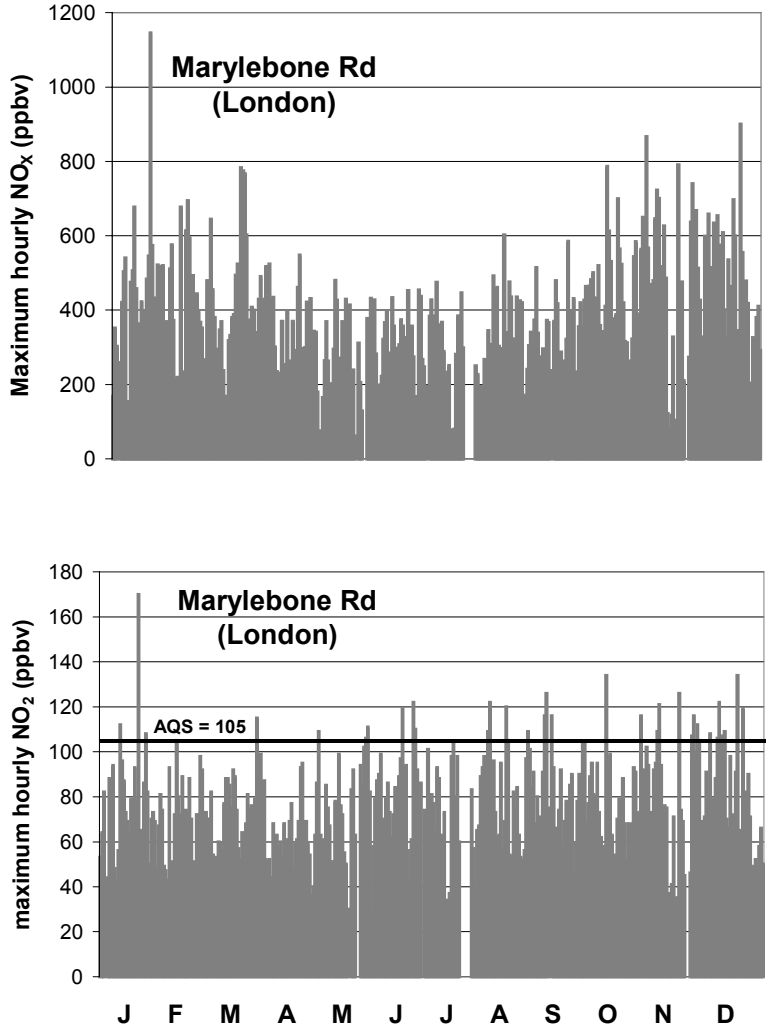

Figure 4.6 ***Maximum hourly levels of NO_X (upper panel) and NO_2 (lower panel) for each day of 1999 at Marylebone Rd, a kerbside site in London.***

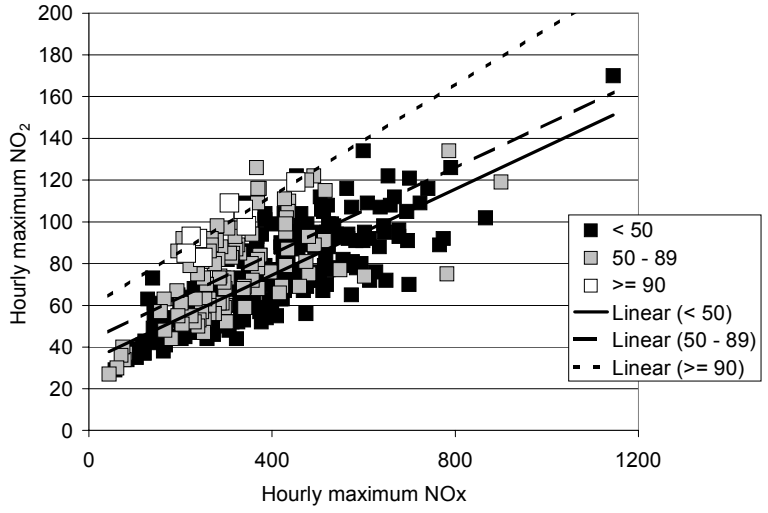

Figure 4.7 ***The relationship between maximum hourly NO_2 and NO_X at Marylebone Rd for each day in 1999, based on the data shown in Figure 4.6. The data have been grouped according to the maximum level of OX measured at the rural site at Rochester (see text).***

NO_X levels and stagnant air for periods of a day or more (*e.g.*, Bower *et al.*, 1994). In addition, previous analyses of data obtained at Cromwell Road, London in 1991 and 1992 (*e.g.*, QUARG, 1993) indicate a significant upward curvature in the NO_2 *vs.* NO_X relationship (which would also be expected in the OX *vs.* NO_X relationship) at NO_X levels greater than about 1 ppmv, suggesting that such levels are generally required for Reaction (4.3) to make a notable contribution to OX

generation. It should be noted that average NO_X levels of this magnitude are now rarely observed in the UK, even at roadside sites, owing to the influence of NO_X emission reductions from their peak value in 1991.

Photochemical Sources

Other possible NO_X-dependent sources of OX may derive from the concurrent emission of species which can lead to NO to NO_2 conversion. It is well-established that the sunlight-initiated, free radical catalysed degradation of VOC in the presence of NO_X leads to the oxidation of NO to NO_2 (*e.g.*, Atkinson, 1998; Jenkin and Clemitshaw, 2000). Consequently, the common-source emission of free radical precursors may provide additional sources of OX under polluted urban conditions. Two potential candidates are formaldehyde, HCHO (and possibly other carbonyls), and nitrous acid, HONO. HCHO is known to be emitted in road traffic exhaust (*e.g.*, PORG 1993), and there is some evidence for direct emissions of HONO (*e.g.*, Kurtenbach *et al.*, 2001; Martinez-Villa *et al.*, 2000). Each is comparatively photolabile, and may therefore lead to the generation of free radicals, and therefore NO-to-NO_2 conversion, in the sunlit atmosphere as shown schematically in Figure 4.8. The presence of reactive VOC in general allows closure of the well-established free radical propagated cycle, and the possibility that each photolysis event may lead to several NO-to-NO_2 conversions before free radical loss by an alternative reaction (*e.g.*, OH + NO_2; OH + NO).

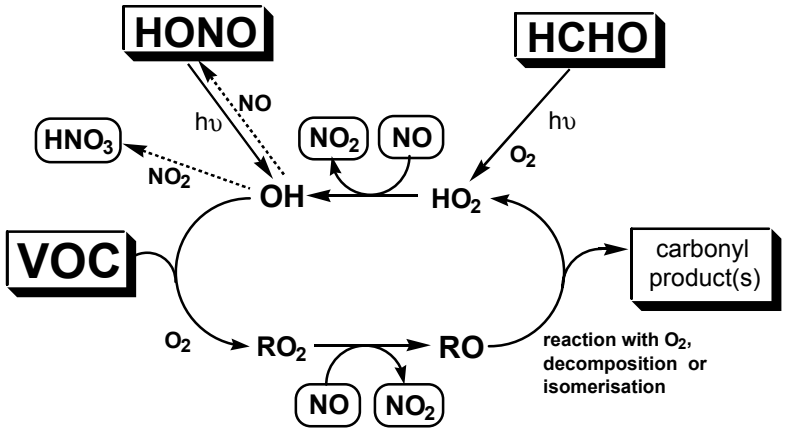

Figure 4.8 ***Schematic representation of the potential role of HONO and HCHO in initiating the free radical catalysed oxidation of VOC under polluted urban conditions, and the resultant oxidation of NO to NO_2.***

The potential importance of these species in leading to NO-to-NO_2 conversion depends on (i) their efficiency of photolysis to generate radicals, and (ii) on the 'chain-length' for NO_2 formation, *i.e.* essentially the number of free radical propagated cycles in Figure 4.8 which occur under the prevailing ambient conditions. The photolysis lifetime of HCHO in the southern UK is *ca.* 6 hours and 1 day under daylight-averaged midsummer and midwinter conditions, respectively. Consequently, it is unlikely that photolysis of emitted HCHO can have the major short-timescale impact required to contribute to the NO_X-dependent oxidant source presented here, although it is recognised that HCHO (which is formed more significantly from VOC oxidation) does ultimately make an important contribution to boundary layer radical production. HONO is significantly more photolabile, its photolysis lifetime being typically 15 and 40 minutes under daylight-averaged midsummer and midwinter conditions, respectively (PORG, 1997). Consequently, emitted HONO may be photolysed comparatively rapidly throughout the year to generate free radicals, with the subsequent efficiency of the cycle in Figure 4.8 depending mainly on the VOC/NO_X ratio. As described in detail previously (Jenkin *et al.*, 2001; Clapp and

Jenkin 2001), calculations carried out using the CRI-PTM (see Section 8.3.2) for representative southern UK conditions suggest that emission of HONO as *ca.* 1% of NO_X is sufficient to lead to an increase in the local OX contribution by *ca.* 3 - 4% throughout the year.

4.3.5 Diurnal Variations in OX-NO_X Relationship

The above analysis has so far considered daylight-averaged data. If photochemistry has an influence on OX levels at polluted locations, then a difference between daylight and night-time might be expected. Further analysis of the dependence of OX on NO_X for night-time averaged data indicates that the local contribution to oxidant is consistently 2-3% lower at night throughout the year (*e.g.* see the comparison of November daylight and night-time averaged data in Figure 4.2 and Figure 4.9).

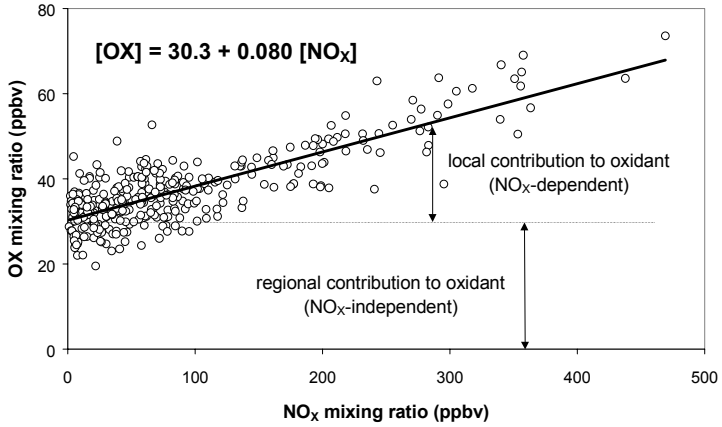

Figure 4.9 ***Variation of night-time average mixing ratios of oxidant (OX) with level of NO_X. Data are presented for each night of November 1998 and 1999 at the six sites listed in Table 4.1.***

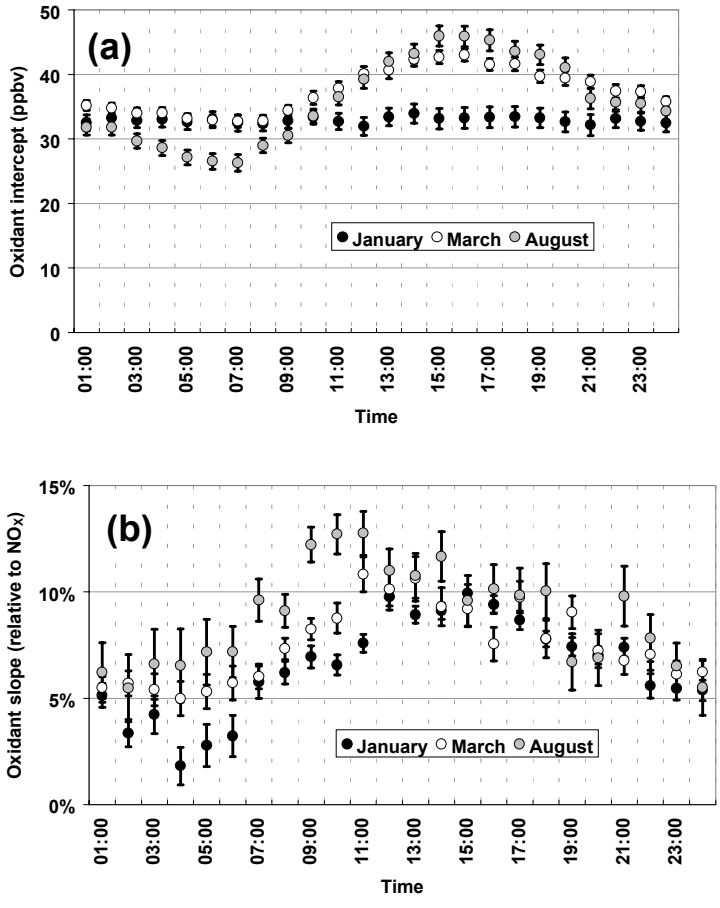

Figure 4.10 ***Hour-by-hour variation of (a) regional (i.e. NO_X-independent) source of OX, and (b) local (i.e. NO_X-dependent) source of OX, for selected months in 1999 (data are for hour ending with the given time).***

This analysis was further extended for selected months by investigating whether there is any hour-to-hour variation in the slope and/or intercept of the OX *vs.*. NO_X relationship. The corresponding data for January, March and August 1999 (shown in Figure 4.10) confirm that there is a distinct diurnal dependence in the local contribution to oxidant, providing further evidence for the role of photochemistry on a local scale throughout the year. The diurnal variation of the regional contribution is typical of that observed for O_3 at unpolluted sites (*e.g.* see PORG 1997), being almost absent in the winter, but showing an amplitude of about 20 ppbv in the summer.

4.3.6 Site-to-site Variations

The analyses presented above have made use of data from 6 monitoring sites with overlapping NO_X ranges to cover a wide range of conditions, and it is apparent (*e.g.* from Figure 4.1) that the data can largely be considered as a continuous dataset. However, some of the more polluted sites cover a comparatively wide range of NO_X (on a linear scale), and it is possible to perform similar analyses to those above for individual sites. The daylight averaged data from Marylebone Rd (typically 50-500 ppbv), Bloomsbury (typically 40-250 ppbv) and Hillingdon (typically 15 – 300 ppbv) have therefore been analysed, with the particular aim of comparing the magnitudes of the local (*i.e.* NO_X-dependent) oxidant sources at these sites.

Figure 4.11 summarises the results for Marylebone Rd and Bloomsbury for each month of the year. Whereas the local oxidant contributions at the two sites are comparable for most of the year, the data provide clear evidence that the local source is substantially greater in midsummer (July and August) at Bloomsbury. A possible reason for this is the contribution of summertime biogenic hydrocarbon emissions very locally to the Bloomsbury monitoring site. This site is located in a central London 'garden' surrounded by an enclosed square of busy roads. The gardens are generally laid to grass with many mature trees, providing the possibility of elevated emissions of reactive biogenic hydrocarbons (*e.g.* isoprene) in the summer months. Such emissions would increase the local VOC/NO_X ratio, and therefore the efficiency of the free radical catalysed cycle shown in Figure 4.8. In contrast, the Marylebone Rd site has no significant biogenic sources in the vicinity of the site.

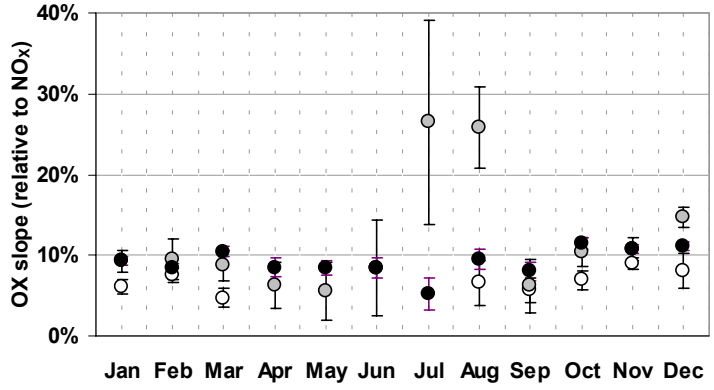

Figure 4.11 ***Comparison of local sources of oxidant at Marylebone Rd. (black), Bloomsbury (grey) and Hillingdon (white), based on daylight averaged data in 1998 and 1999. April-July data for Hillingdon unavailable due to low data capture for one of O_3, NO or NO_2 (see text).***

Hydrocarbon measurements are not made at the Bloomsbury site, so it is not possible to test this hypothesis directly. However, Figure 4.12 shows a comparison of isoprene and 1,3-butadiene data measured at the London Eltham site and Marylebone Rd. Similarly to Bloomsbury, the Eltham site has areas of grass and mature trees locally. Whereas 1,3-butadiene is believed to be solely of anthropogenic origin (primarily in vehicle exhaust), isoprene has contributions from

both exhaust emissions and biogenic sources. Figure 4.12 shows that the ratio isoprene/1,3-butadiene is consistently *ca.* 0.5 at both sites in the winter months (October – April). This figure is indicative of the relative emissions in vehicle exhaust, and is similar to previously reported values for locations in the UK, Canada and Switzerland (Burgess and Penkett, 1993; Derwent *et al.*, 1995; McLaren *et al.*, 1996; Reimann *et al.*, 2000). During the summer months, the ratio at Marylebone Rd remains approximately constant, whereas the ratio at Eltham increases significantly, maximising in July and August when biogenic sources are most important. Local biogenic hydrocarbon sources therefore have a significant influence on the VOC/NO_X ratio at Eltham, and the same may be true at Bloomsbury.

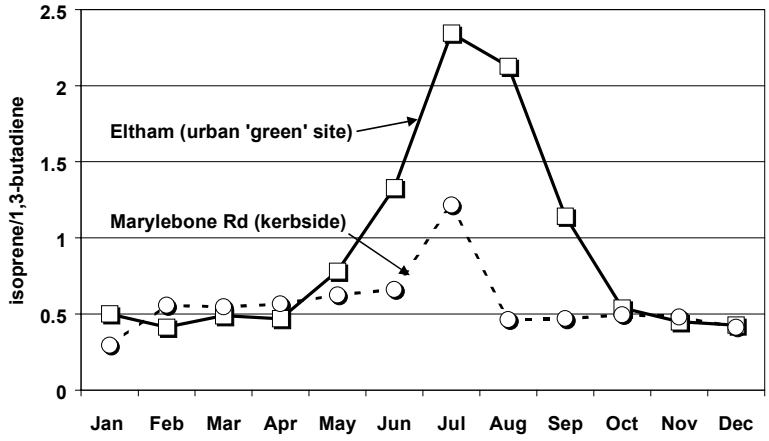

Figure 4.12 ***Comparison of monthly mean isoprene/1,3-butadiene ratios measured at Eltham and Marylebone Rd, as part of the DETR Automatic Hydrocarbon Network in 1998 and 1999. Based on data taken from AEA Technology website (http://www.aeat.co.uk/netcen/airqual).***

Figure 4.11 also compares the magnitude of the local oxidant source at Hillingdon with those observed at the other sites. Owing to poor data capture for one or more of O_3, NO and NO_2 during the months April-July, it is not possible to present OX *vs.* NO_X data for this site in isolation during those months. However, for the months for which comparison is possible, the local source of oxidant is consistently lower than at Marylebone Rd, typically by *ca.* 3-4%. Despite being in a suburban area, the Hillingdon site is comparatively polluted because it is located adjacent to the M4 motorway, which provides the major local source of NO_X. Consequently, the characteristics of the site are somewhat different from those of Marylebone Rd and Bloomsbury, at least in terms of the driving conditions of the traffic providing the local NO_X source. Whereas the traffic adjacent to the Marylebone Rd site, and in the vicinity of the Bloomsbury site, tends to be slow-moving or stationary, that adjacent to the Hillingdon site is generally moving significantly more rapidly. As discussed above in Section 4.3.4, it is probable that the proportion of NO_2 in the NO_X emitted from the faster moving traffic is lower, and this may explain the consistently lower local oxidant contribution at Hillingdon.

4.3.7 Analysis of Annual Mean Data

The analyses presented above have defined relationships between OX and NO_X on the basis of linear regressions of data obtained at a number of sites (or selected individual sites) on a large number of days. In principal, a similar analysis can be performed using annual mean data for sites where O_3, NO and NO_2 are measured.

The Relationship between Annual Mean OX and NO_X

Figure 4.13 shows how the annual mean levels of OX depend on NO_X for the majority of London sites where the required measurements are available, and for Reading and Harwell. Clearly, the same general trend to the previous analyses is observed, but the data show a

surprisingly large amount of scatter, given the level of averaging which has taken place. Closer inspection reveals that the scatter is primarily due to site-to-site variations, with a given site showing a reasonably consistent pattern from one year to another. This is, perhaps, more apparent in Figure 4.14, which shows only the data for the five urban and surburban sites considered in the previous analysis. In each case an associated regression line is presented, based on an intercept fixed at the value derived from analysis of the entire data set in Figure 4.13 (although analysis of the comparably large Bloomsbury data set alone provided an almost identical intercept). Figure 4.14 clearly shows a variation in magnitude of the local source of OX at Marylebone Rd, Bloomsbury and Hillingdon which is broadly consistent with the analysis presented in Section 4.3.2.

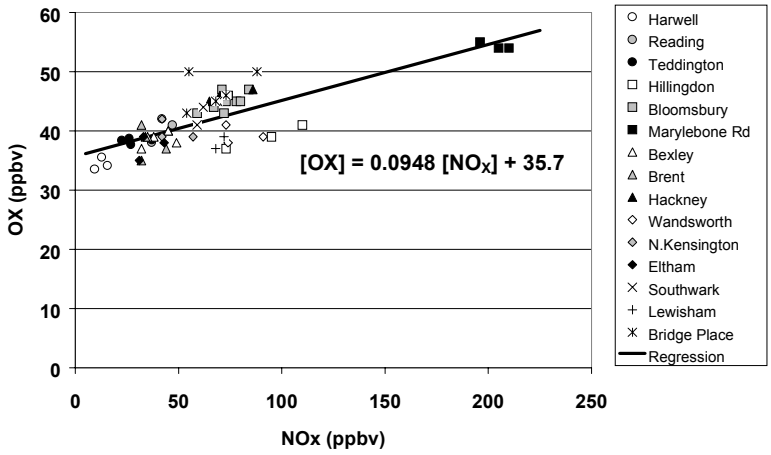

Figure 4.13 ***Variation of annual mean OX mixing ratio with NO_X for London sites where O_3, NO and NO_2 are measured, Reading and Harwell. The number of years of available data vary from one site to another, but all displayed data were obtained during 1992-2000.***

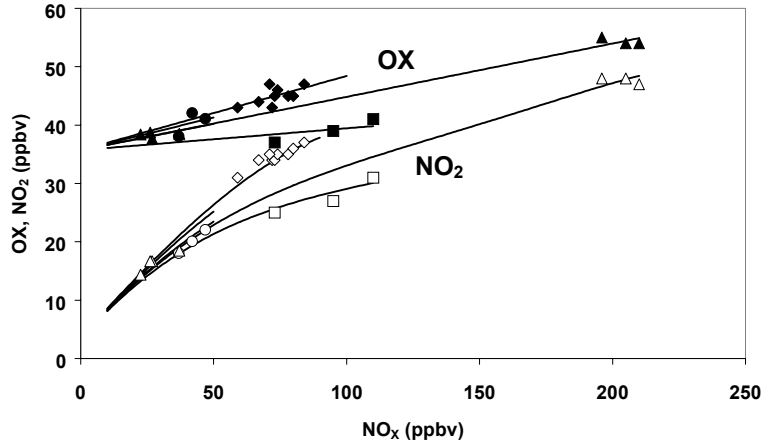

Figure 4.14 ***Annual mean OX (closed symbols) and NO_2 (open symbols) as a function of NO_X at Reading (circles), Teddington (triangles at low end of NO_X range), Hillingdon (squares), Bloomsbury (diamonds) and Marylebone Rd (triangles at high end of NO_X range). Lines are calculated from the expressions in Table 4.2.***

Oxidant Partitioning as a Function of NO_X

It has been recognised for some time that annual average NO_2 levels show a distinct variation from one site to another, even for sites for which the annual average NO_X is comparable (*e.g.* Stedman, 1999; Stedman *et al.*, 1998, 2000). The above analysis suggests that this is partly due to variations in the local sources of OX from one site to another, resulting from a number of possible factors (*e.g.* local driving conditions; vehicle fleet composition; local sources of biogenic hydrocarbons), as discussed in previous sections. However, also of importance is the precise partitioning of OX between its component forms of NO_2 and O_3. Figure 4.15 shows the fraction of OX which is in the form of NO_2, based on the annual average data for the sites in Figure 4.13. As expected, the data generally show that a progressively greater proportion of OX is in the form of NO_2 as the level of NO_X increases. However, the data appear to fall into two reasonably distinct groups, the first containing Hillingdon, Hackney, Wandsworth, Reading and

Marylebone Rd, and the second containing the remaining sites, which generally show higher NO_2/OX ratios. Although the reason for this distinction is not fully clear, such differences in the partitioning of NO_2 and O_3 presumably must relate (at least partially) to rates of, or the time available for, chemical processes. For example, a smaller proportion of OX might be expected to be in the form of NO_2 if either the photolysis rate (J_2) is notably higher at these sites (*e.g.* because they spend a greater proportion of the time out of the shade, or the local surfaces are of particularly high reflectivity), or if there is significantly less time for the conversion of emitted NO to NO_2 to occur because the air flow is less stagnant at these sites, or they are much closer to source. A short time-lag between emission and measurement most likely accounts for the lower ratios in the first group identified above: Marylebone Rd is a kerbsite site, Hackney and Wandsworth are first-floor sites overlooking busy roads, and the Hillingdon and Reading sites are in comparatively open locations 30 m and 20 m, respectively, from local traffic sources.

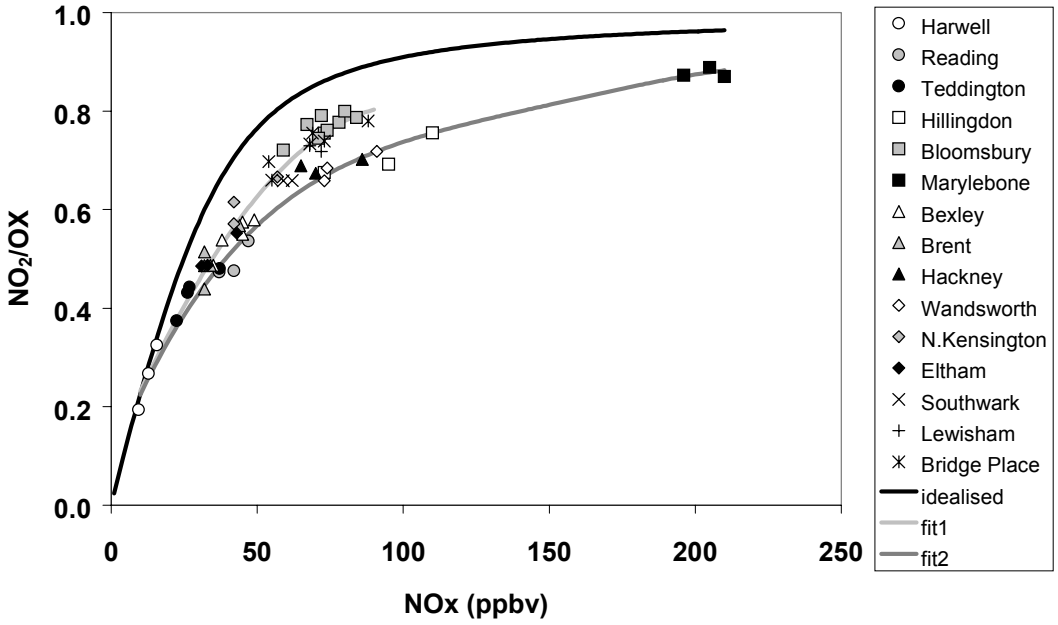

Figure 4.15 ***Variation of annual mean [NO_2]/[OX] as a function of NO_X for London sites where O_3, NO and NO_2 are measured, Reading and Harwell. The black line is the calculated idealised variation based on the assumption of photostationary state and a value of $J_{3.2} = 2.2 \times 10^{-3}$ s^{-1}, estimated from output of a two-stream isotropic scattering flux model (Hayman, 1997) for 51.5°N Lat. The precise form shows a very weak dependence on the applied OX vs. NO_X relationship which was taken to be the overall regression shown in Figure 4.13. The other lines are fitted polynomial expressions based on data for groups of sites (see text).***

On the basis of the photostationary state relationship (discussed in Section 4.3.1) it is possible to infer an expected variation of NO_2/OX. The idealised variation is also presented in Figure 4.15, based on an estimated annual average value of $J_{4.2} = 2.2 \times 10^{-3}$ s^{-1}. This shows the same general trend as the observed points, but lies consistently higher over the entire NO_X range. The normalised difference between the observed and calculated idealised values is shown in Figure 4.16, for the data from both groups of sites identified in Figure 4.15. This shows that the deviation between observed and idealised is lower at the ends of the NO_X range, maximising at approximately 40 ppbv NO_X. There are a number of reasons why this is the case. First, the idealised dependence describes how the partitioning of the oxidant components varies for a range of unique levels of NO_X, whereas each observed data point represents the mean of a large number of measurements at many NO_X levels. If a number of discrete measurements describes a curve of the form shown in Figure 4.15 then the mean of the measurements must lie below the curve. The deviation from the curve will be greater if the degree of curvature is greater.

Therefore, the deviation would be expected to be lower at the ends of the NO_X range (as observed), where the degree of curvature is lower. In addition to this, the deviation for a given site would be expected to be greater if the observed range of NO_X levels is greater. This will clearly contribute to variations from one site to another, and may be of particular relevance to Hillingdon for which the observed NO_X range is notably high.

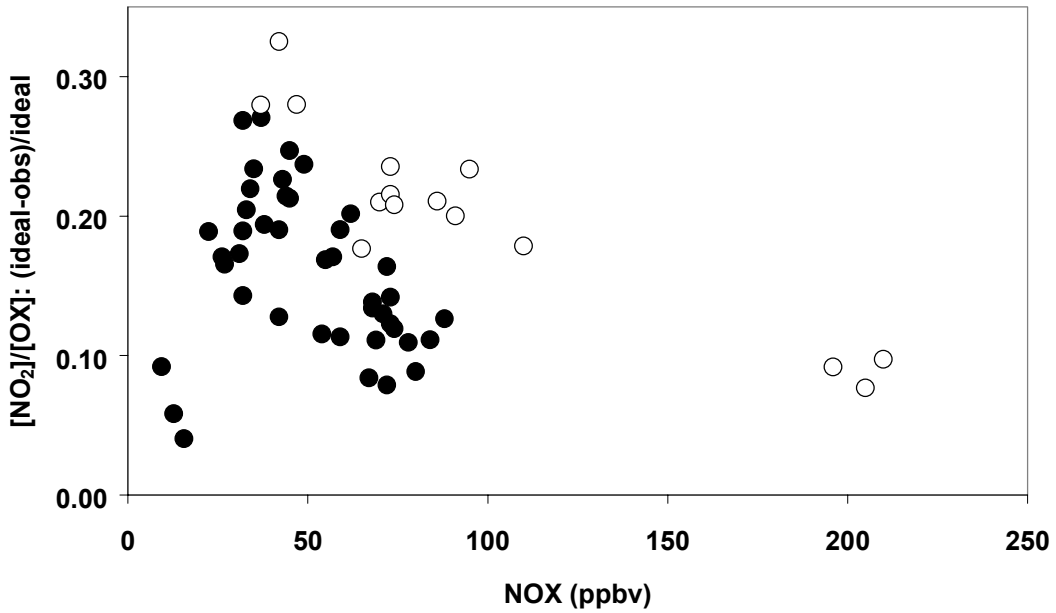

Figure 4.16 ***Normalised difference between the observed and idealised $[NO_2]/[OX]$ data presented in Figure 4.15 as a function of NO_X. Open circles: data from Hillingdon, Hackney, Reading, Wandsworth and Marylebone Rd. Closed circles: data from the remaining sites identified in Figure 4.15.***

It is also probable that chemical factors contribute to the observed deviation, as discussed above. The idealised curve assumes that the photostationary state relationship applies. Whereas this may be a reasonable assumption for daylight hours (*e.g.*, as shown in Figure 4.1), it is almost certainly not a good assumption for night-time (which accounts for 50% of the year). It is therefore unlikely that an idealised curve based on an annual average value of J_2 can give a fully quantitative indication of the expected partitioning in annual average NO, NO_2 and O_3. A particular problem arises at sites where intermediate levels of NO_X occur for a significant proportion of the time. At *ca.* 40 ppbv NO_X, the levels of NO and O_3 are predicted to be comparable, in the region of 10-15 ppbv. Consequently, neither species is in significant excess, and their reaction to form NO_2 (reaction (4.1)) approximates to second order kinetics. Under these circumstances, the reaction rate decreases significantly as the reaction proceeds. At night, therefore, the complete conversion of NO and O_3 to NO_2 at these intermediate NO_X levels has a very long time constant, even though the simple photostationary state relationship with $J_2 = 0$ (Section 4.3.1) would predict that O_3 and NO cannot co-exist at night, *i.e.*, that conversion to NO_2 occurs instantaneously. As a result, the idealised curve is likely to overpredict the proportion of OX in the form of NO_2, particularly for sites where NO_X levels are in the region of 40 ppbv for a significant proportion of the time.

Calculated Variation of Annual Mean NO_2 with NO_X

From the above discussion, it is clear that it is difficult to define theoretical expressions which quantitatively describe how the level of NO_2 varies with NO_X, even though the qualitative

behaviour is adequately explained by current understanding of the processes involved. The analysis suggests that it is possible to establish reasonably robust expressions which describe how the annual mean OX level varies with NO_X, and which take account of site to site variations (a series of such expressions is provided in Table 4.2 for each of the urban and suburban sites in Figure 4.13). However, the precise relationship between annual mean NO_2 and annual mean OX is subject to several varying factors, and it appears necessary to use fitted functions for groups of sites with particular characteristics. The data for the two groups shown in Figure 4.15 have therefore been used to derive the two polynomial expressions given in Table 4.2, and illustrated in the figure. The data for Harwell were included in both sets to allow the NO_X range to be extended to low levels.

Table 4.2 ***Summary of [OX] vs. [NO_X] and [NO_2]/[OX] vs. [NO_X] relationships, and NO_X thresholds derived from the analysis of annual mean data presented in Figure 4.13 and Figure 4.15 (see discussion in text).***

Site	Type	A [1]	[NO_2]/[OX] [2]	NO_X threshold [3]	
				This work	Carslaw (2001)
Bexley	Suburban	0.0771	Fit 1	39.4	
Bloomsbury	Urban Centre	0.1272	Fit 1	36.9	31.7
Brent	Urban BG	0.0616	Fit 1	40.3	
Bridge Place	Urban BG	0.1572	Fit 1	35.6	34.3
Eltham	Suburban	0.0477	Fit 1	41.2	
Hackney	Urban Centre	0.1391	Fit 2	40.4	
Hillingdon	Suburban	0.0375	Fit 2	48.6	
Lewisham	Urban Centre	0.0332	Fit 1	42.2	
Marylebone Rd	Kerbside	0.0914	Fit 2	43.5	
N Kensington	Urban BG	0.0873	Fit 1	38.8	36.9
Reading	Urban BG	0.1121	Fit 2	42	
Southwark	Urban Centre	0.1129	Fit 1	37.5	
Teddington	Urban BG	0.0902	Fit 1	38.7	
Wandsworth	Urban Centre	0.0449	Fit 2	47.8	

Notes

[1] Linear [OX] *vs.* [NO_X] relationships given by [OX] = A.[NO_X] + B, derived from data for each site presented in Figure 4.13. The regional OX contribution, B = 35.7 ppbv, is assumed site-independent and equivalent to that derived from the composite analysis of all sites.

[2] [NO_2]/[OX] *vs.* [NO_X] expressions are polynomial fits to data presented in Figure 4.15:

Fit 1: $[NO_2]/[OX] = (1.015 \times 10^{-1}) + (1.367 \times 10^{-2} [NO_X]) - (6.127 \times 10^{-5} [NO_X]^2) - (4.464 \times 10^{-8} [NO_X]^3)$: applicable range, 10 – 90 ppbv NO_X.

Fit 2: $[NO_2]/[OX] = (8.962 \times 10^{-2}) + (1.474 \times 10^{-2} [NO_X]) - (1.290 \times 10^{-4} [NO_X]^2) + (5.527 \times 10^{-7} [NO_X]^3) - (8.906 \times 10^{-10} [NO_X]^4)$: applicable range, 10 – 210 ppbv NO_X.

[3] Predicted NO_X threshold corresponding to an annual mean NO_2 of 21 ppbv

The expressions in Table 4.2 therefore allow [NO_2] *vs.* [NO_X] curves to be inferred for all 14 urban and suburban sites. This is illustrated in Figure 4.14 for the five sites included in the more detailed analysis presented in previous sections. For the most part, the resultant curves for NO_2 provide a good description of the data at each site, even though a slight bias may result from using expressions for NO_2/OX derived from fitting several sites to describe individual sites. The calculated variation of annual mean NO_2 with NO_X is also shown for all 14 sites in Figure 4.17, and the inferred NO_X thresholds which correspond to an annual mean NO_2 mixing ratio of 21 ppb (*i.e.* the WHO air quality guideline (WHO, 1994; 1995)) are also presented in Table 4.2. The NO_X thresholds for the sites considered show significant site-to-site variation, covering the range 35.6 - 48.6 ppbv. The results are thus broadly consistent with threshold values derived from existing NO_2 *vs.* NO_X relationships (Stedman 2001; Carslaw *et al.*, 2001). Those reported by Carslaw *et al.* (2001) for specific sites lie consistently slightly below the present values, but in reasonable agreement, as also shown in Table 4.2. Stedman (2001) derived three generic expressions to describe the NO_2 *vs.* NO_X relationship for 'central London sites', for 'sites outside central London', and for 'roadside sites', which are compared with the present expressions in

Figure 4.17. The present data for urban centre and background central London sites and sites outside central London are consistent with the expressions of Stedman (2001), with the inferred NO_X thresholds consistently lying slightly higher. As discussed above, a number of sites can be classified as 'intermediate', as they have partial roadside character, due to the influence of nearby roads. Logically, therefore, the present data consistently lie at higher NO_X than the generic expressions for the urban centre and background sites, but lower than the generic expression for roadside sites. The present data for Marylebone Rd (the only roadside site available for consideration by the analysis method) lie at significantly lower NO_X than the generic expression of Stedman. Although the NO_2-NO_X dependence provides a good description of the variation of the currently available narrow range, some systematic error may result from the necessary inclusion of Marylebone Rd in intermediate grouping in the present analysis.

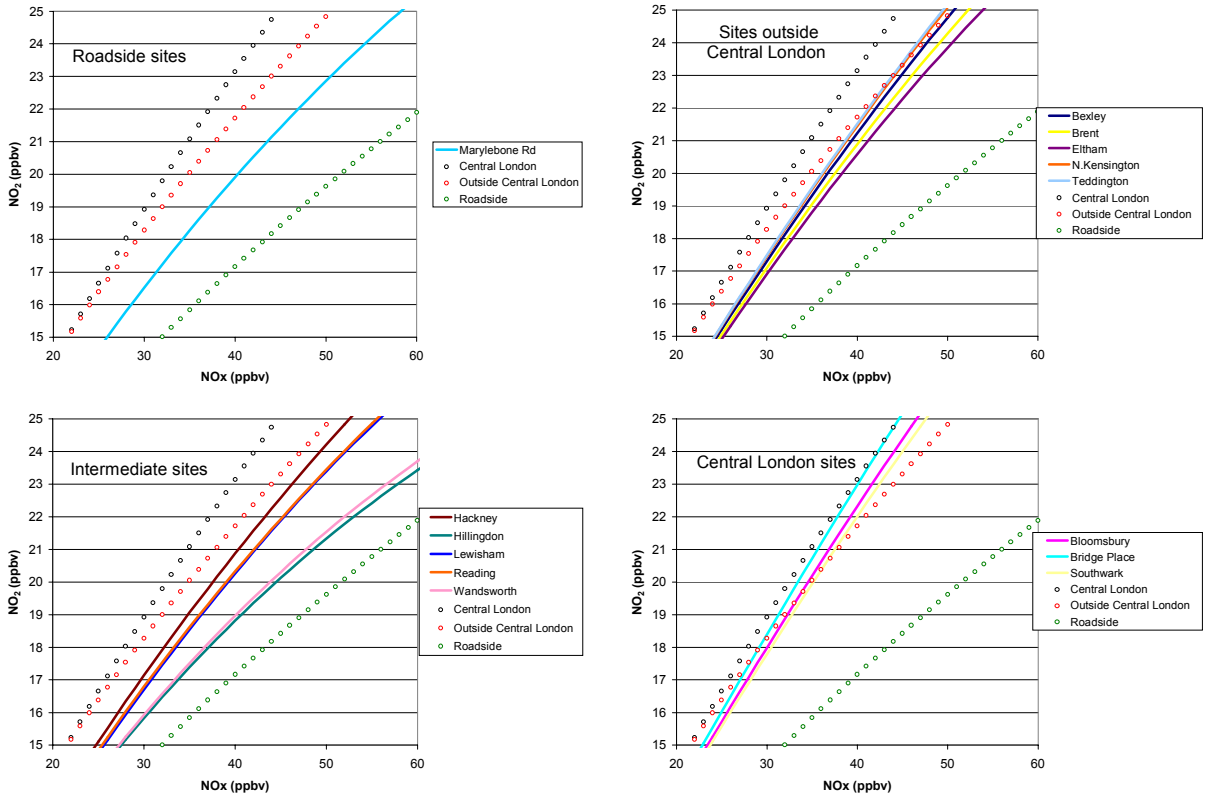

Figure 4.17 ***Inferred variation of annual mean NO_2 with annual mean NO_X at selected London sites and Reading, based on the parameters given in Table 4.2. In each panel, the generic expressions of Stedman (2001) for urban centre and background sites in central London and outside central London, and for roadside sites are also shown.***

Influences of Changes in the Regional Background O_3 Concentration

The information in Table 4.2 includes the annual mean NO_X thresholds corresponding to 21 ppbv NO_2 for the 5 urban and suburban sites for which data are presented in Figure 4.14. Based on year 2000 annual mean NO_X, the urban background sites (Teddington and Reading) are already below these thresholds, whereas the present analysis infers that NO_X levels at Hillingdon (suburban), Bloomsbury (urban centre) and Marylebone Rd need to be reduced from 2000 levels by factors of *ca.* 33 %, 37 % and 79 %, respectively, for the required *ca.*16 %, 32 % and 55 % reductions in annual mean NO_2 to be achieved. It should be noted, however, that this analysis is based on a single unchanging regional background oxidant level of 35.7 ppbv for the southern UK, which is reasonably consistent with available measurements for the latter half of

the 1990s. However, the results of the global modelling work performed by the Meteorological Office under Task 1 of the present programme (and presented in our previous report: Jenkin *et al.*, 2000a), suggest a gradual increasing ozone baseline from 34.3 ppbv in 1990 to 39.2 ppbv in 2030, based on the IPCC SRES emission scenario (A2 variant) (Nakicenovic *et al.*, 2000). This corresponds to an average increase of *ca.* 0.12 ppbv annum^{-1}, which needs to be taken into account when assessing future success in achieving air quality standards. Within the methodology defined above, it is also possible to account for changes in regional oxidant contribution by varying the parameter 'B' from the value of 35.7 ppbv used in the present analysis.

Figure 4.18 demonstrates how the NO_X level corresponding to an annual mean NO_2 of 21 ppbv varies with regional oxidant background up to a value of 37 ppbv, for the same five sites discussed above. These calculations suggest that for every 0.1 ppbv increase in regional oxidant background, additional site-dependent decreases in annual mean NO_X of between *ca.* 0.12 and 0.22 ppbv are required, for the NO_2 guideline of 21 ppbv to be achieved or maintained.

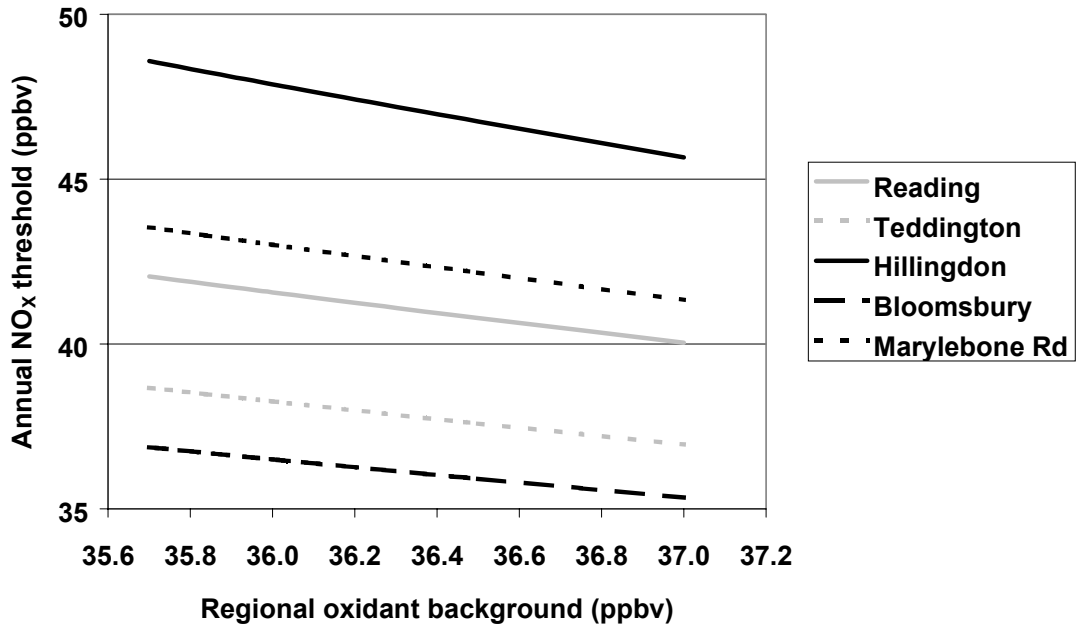

Figure 4.18 ***Calculated annual mean NO_X thresholds corresponding to annual mean NO_2 of 21 ppbv, as a function of regional oxidant background. Calculations are based on the expressions in Table 4.2, with the value of B varied between 35.7 and 37.0. Over this range, the observed variation is almost linear, and well described by the following expressions: Reading, NO_X threshold = 97.2 – 1.647 B; Teddington, NO_X threshold = 85.9 – 1.324 B; Hillingdon, NO_X threshold = 128.7 – 2.245 B; Bloomsbury, NO_X threshold = 78.8 – 1.176 B; Marylebone Rd. , NO_X threshold = 103.8 – 1.689 B.***

4.4 LONDON ROUTINE COLUMN TRAJECTORY MODEL (LRCTM)

4.4.1 Impact of Emission Reductions on Future NO_2 and Ozone Concentrations in London

The work performed within Task 2 of the work programme has also involved further application of the London Routine Column Trajectory model (LRCTM). In consultation with

DEFRA this work has focussed on the London conurbation, providing further results to support policy formulation on future NO_2 and ozone.

Detailed descriptions of the LRCTM model and its results are available elsewhere (Derwent 1999a, b). In these studies, the original London Research Centre NO_X emission inventory has been replaced with the 1996 NAEI 1km x 1km NO_X inventory, and emphasis has been placed on the special nature of the NO_2 concentrations in the central area of London. Scaling factors have been applied to the emissions from the road transport sector to generate NO_X emission inventories for the years 2005 and 2010. In all other respects, the model formulation and input data remain unchanged.

The model distributions of annual mean NO_2 and ozone concentrations across the central area of London for the years 1996, 2005 and 2010 are shown in Figure 4.19. The concentrations distributions for NO_2 show similar spatial patterns in each of the years whilst absolute concentrations decrease under the influence of emission controls. The spatial patterns indicate a local maximum due to stationary combustion sources in the East End of London and a broad maximum due to road traffic throughout the mapped region. The broad maxima decline steadily from 1996 through to 2010 under the influence of emission controls. The local maximum itself remains unchanged in magnitude although it appears to decrease because of the London-wide reduction in the broad maximum upon which it sits.

Averaging over the mapped region, annual mean NO_2 concentrations declined from 34.4 ppb in 1996 to 26.4 ppb in the year 2005 and to 23.3 ppb in the year 2010. The percentage decreases in annual mean NO_2 amounted to 23 % by 2005 and 32 % by 2010, much smaller decreases than assumed in the road transport emissions, 52 % and 68 % by the same years. NO_2 concentrations appear to fall much more slowly compared to road transport emissions because road transport is not the sole source of NO_X emissions in London and because changes in hourly mean NO_2 concentrations are not directly proportional to changes in NO_X emissions.

A major conclusion is that a substantial area within central London will remain with annual mean NO_2 concentrations above the 19 ppb air quality target in the year 2010, despite an assumed 68 % reduction in road traffic NO_x emissions relative to 1996.

The model distributions of ozone concentrations across the central areas of London are also shown in Figure 4.19. These distributions show maximum levels in the fringes of the maps and minimum levels towards the centres. This is consistent with ozone levels being controlled by the supply through advection from the regional background at the fringes of the maps and by depletion by reaction with nitric oxide emitted within the London conurbation.

Again, averaging over the mapped region, annual mean O_3 concentrations increased from 2.9 ppb in 1996 to 4.7 ppb in the year 2005 and to 5.8 ppb in the year 2010. The oxidant (O_x= $[NO_2]$ + $[O_3]$) concentrations accordingly steadily declined from 37.3 ppb in 1996 to 31.2 ppb in 2005 and to 29.0 ppb in 2010. The initially rapid decline in O_x between 1996 and 2005 is caused by the reduction in direct NO_2 emissions.

4.4.2 Impact of Global Ozone Increases on Future NO_2 Concentrations in London

Tropospheric ozone levels are thought to have increased in the northern hemisphere since pre-industrial times, through increased photochemical production, driven by human activities (Volz

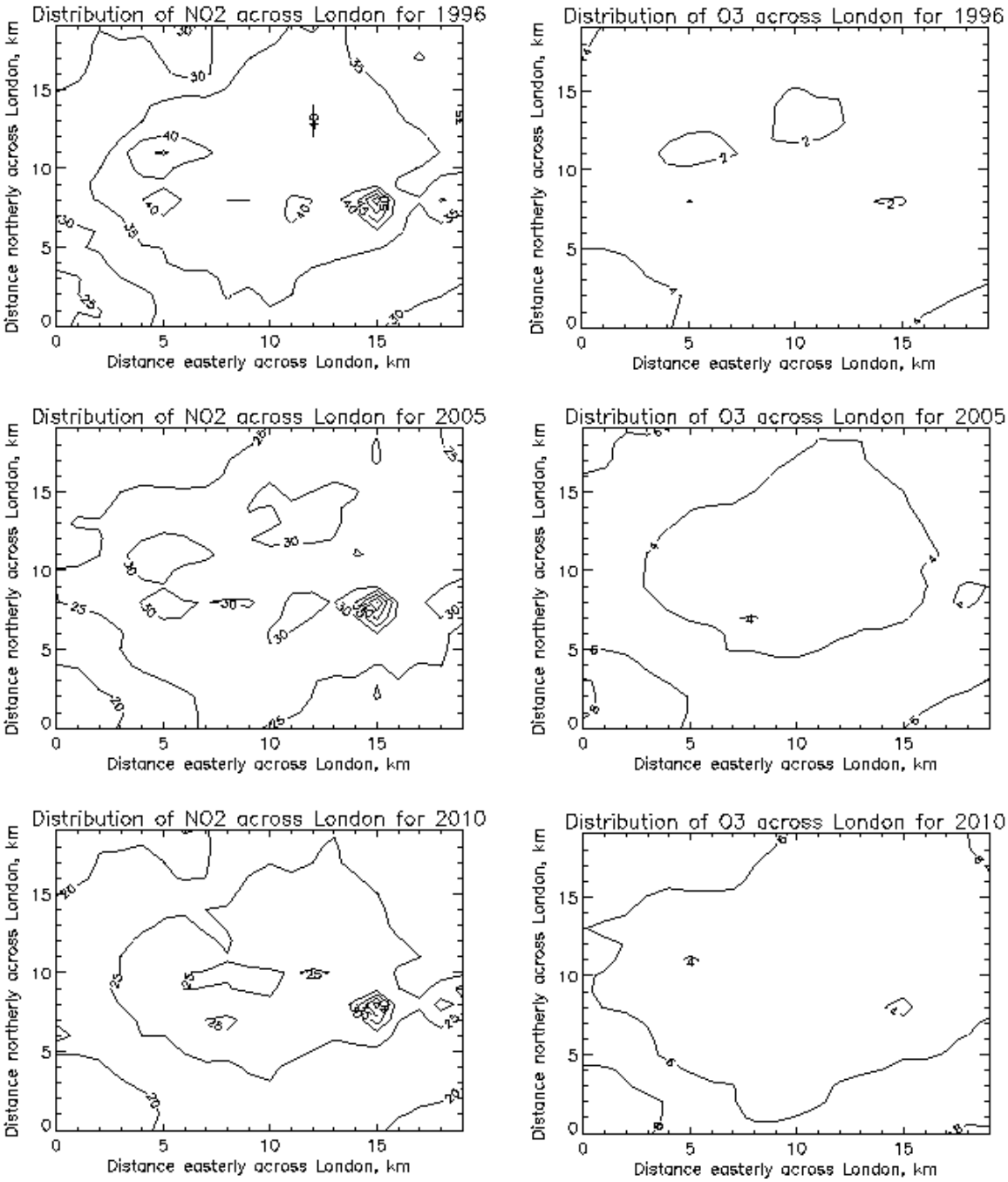

Figure 4.19 ***Modelled distributions of NO_2 in 1996, 2005 and 2010 (left-hand panels) and of O_3 in 1996, 2005 and 2010 (right-hand panels) using the LRCTM.***

and Kley, 1988). As the concentrations of the tropospheric source gases continue to increase following the growth of emissions from 1990 through to 2010, the STOCHEM model predicts that the human influence on past ozone levels should continue into the future. The monthly mean global surface ozone concentration for July increases from 20.93 ppb to 22.40 ppb, that is by 1.5 ppb, representing an increase of about 7 %. The increase is concentrated mainly in three main regions: Asia, southern Africa and south America. Decreases are found in eastern Europe, whereas slight increases are found in north America.

A general feature of the northern hemisphere surface ozone distribution is the "tongue" of ozone leaving the eastern seaboard of the north American continent and spreading across the

North Atlantic Ocean towards Europe. The "belt" of ozone stretches from Europe across the continental landmass and joins up with the ozone peaks over Asia. These features illustrate the long-range intercontinental scale of the ozone formation and transport processes in the lower troposphere as originally postulated by Parrish *et al.* (1993).

To quantify the potential for the increase in northern hemisphere baseline ozone levels across the British Isles by the year 2010, the seasonal cycles in ozone for western Ireland and southern England are compared in Figure 4.20. The small increases are separated out between the 1990 and 2010 scenario case and are plotted in Figure 4.21. The influence of north American sources is slightly more apparent in Ireland compared with southern England but an overall increase between the 1990 and 2010 scenario cases is clearly present. This amounts to about 2.6 ppb in western Ireland and about 2.1 ppb in southern England. A clear seasonal cycle is present in both the difference plots, see Figure 4.21.

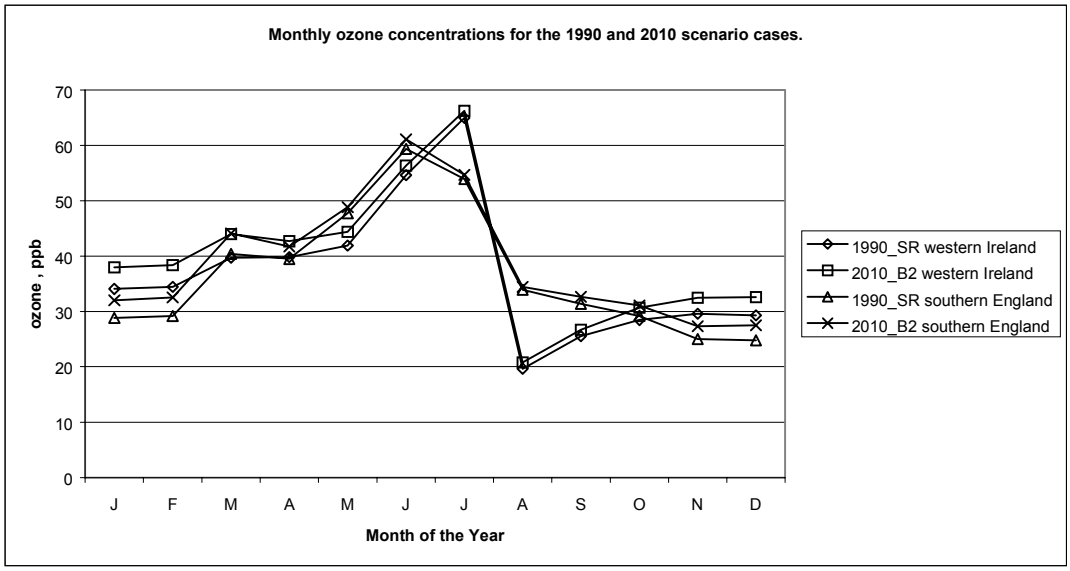

Figure 4.20 ***Monthly Mean Ozone Concentrations for Western Ireland and Southern England in the 1990 and 2010 scenario cases.***

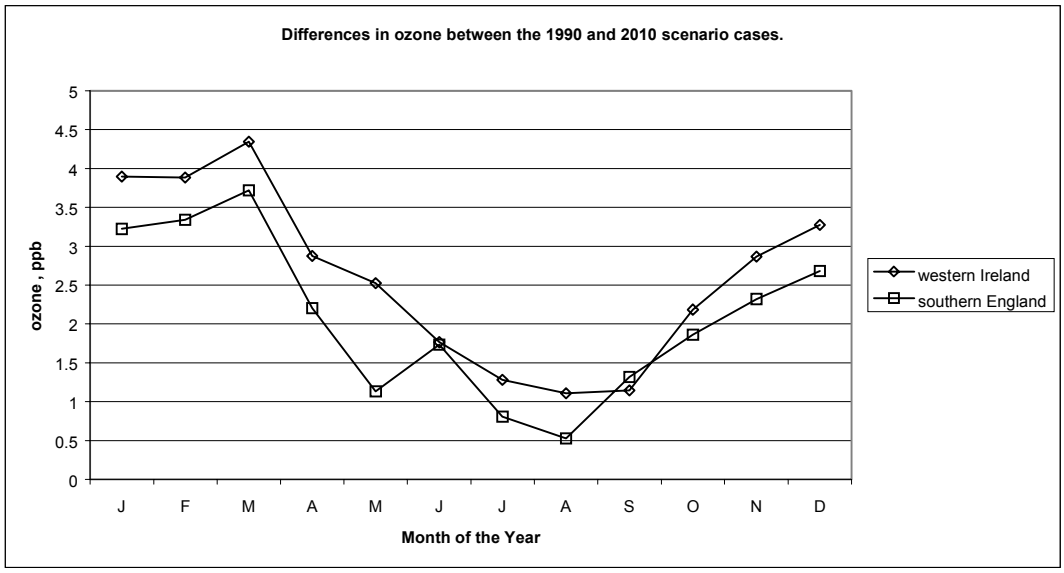

Figure 4.21 ***Differences in the Monthly Mean Ozone Concentrations between the 1990 and 2010 Scenario Cases.***

These monthly increments have been added to the hourly ozone concentrations monitored during 1995 at each of the rural ozone monitoring stations employed to initialise the ozone in each of the LRCTM air parcel trajectory calculations. The model experiments have then been rerun to determine the impact of this ozone increase on the NO_2 distribution within central London. As expected, Figure 4.22 shows that annual mean NO_2 concentrations increase in response to the global ozone increase.

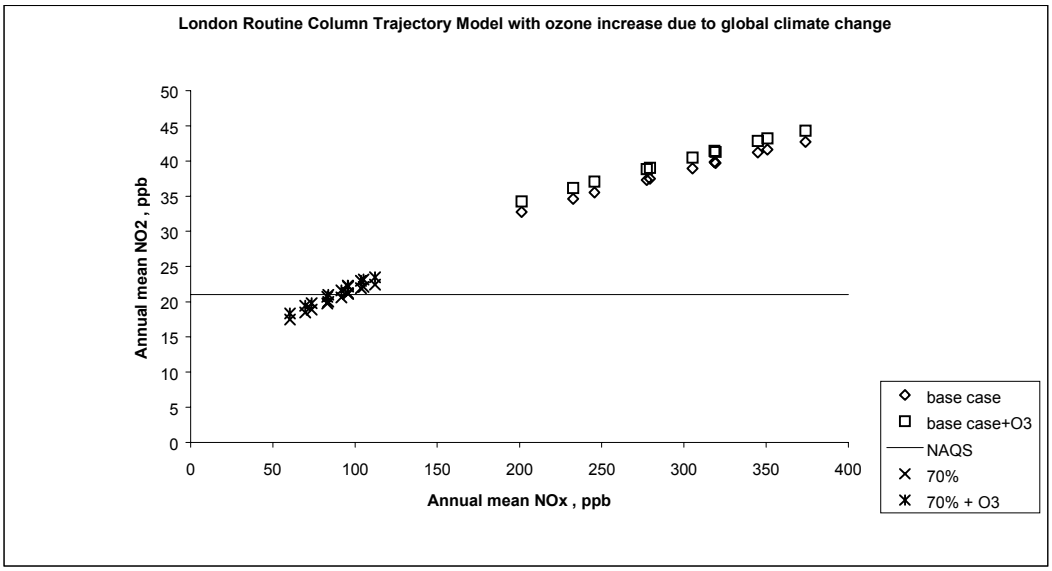

Figure 4.22 ***The influence of the Potential Increase in Global Baseline Ozone Levels between 1990 and 2010 on the Relationship between Annual Mean NO_2 and NO_x concentrations in the LRCTM and the Impact of Across-the-board 70 % NO_x Emission Reductions for a 10 equally-spaced Grid Points 1 km apart on a Transect through Central London.***

The annual mean of the monthly ozone increments in Figure 4.21 amounted to 2.07 ppb. In comparison, the annual mean NO_2 concentrations for the eleven grid points on the transect through central London increased by 1.57 ppb for the conditions of no NO_x emission reductions. The increase in NO_2 is thus somewhat less than the increase in global baseline ozone. This is because not all of the hourly values NO_2 concentrations at each grid point are limited by the availability of ozone initially present in the air parcel. Some of the hourly NO_2 concentrations, at some grid points, at both high and low NO_x levels, are limited by the magnitude of the NO_x emissions received into the air parcel.

The question remains as to whether additional NO_x emissions controls will be required if the same air quality target for NO_2 is to be met, despite an increase in global baseline ozone levels. This point is also addressed in Figure 4.22. This plot shows the influence of the global ozone baseline increase on the NO_2 concentrations at the 11 grid points for the year 2010 conditions of a 70 % reduction in NO_x emissions, with and without the global ozone increase. The influence of the global increase is much smaller for the conditions of a 70 % reduction in NO_x emissions, where the increase in annual mean NO_2 is only 1.0 ppb along the transect. Quite simply, fewer points are ozone-limited because with 70 % reduction in NO_x emissions, the availability of NO_x is much lower. Consequently, planned NO_x emission reductions yield a reduced improvement in NO_2 air quality with the increase in global ozone baseline concentrations.

The precise NO_x emission reduction requirement to meet a 21 ppb annual mean air quality target for NO_2 across a transect through London changes from 72% on 1995 levels to 75% for the conditions of increased global ozone levels.

5 Scenario Analysis and Short-term Action Plans using an Ozone Photochemical Trajectory Model

5.1 SECTION SUMMARY

As part of this task, ozone measurements have been analysed to provide information on the geographical origin and the temporal characteristics of episodes of elevated ozone concentrations over the UK. A Photochemical Trajectory model was subsequently used to understand the observed day-of-week dependence of ozone episodes. As a final part of this task, the photochemical trajectory model was used to investigate the effectiveness of a number of potential short-term control measures for periods when hourly ozone concentrations are forecast to exceed 120 ppb.

An analysis of the ozone concentration measurements made in 1988 and 1989 had previously shown that episodes of elevated concentrations of ozone over the UK were associated with air masses which had passed over continental Europe. For such air masses, the study concluded that about 50% of the ozone could be attributed to emissions from sources on mainland Europe. Therefore, control of ozone concentrations over the UK would require concerted international action.

The analysis has been extended in the present project to take account of the larger dataset now available. Using ozone measurements made at 20 UK sites between 1992 and 1999, the present study provided further confirmation that episodes of elevated concentrations of ozone over the UK were associated with photochemically-aged air masses arriving in the UK from a broadly easterly or south-easterly direction, after passing over mainland Europe for a period of several days.

Analysis of monitoring data from the same sites over the period 1989-1999 demonstrate that ozone episodes are more prevalent at the end of the week, with the greatest numbers of hours $\geq$ 90 ppbv occurring on Fridays. *This has clear implications in terms of exposure and policy control.* Using the Photochemical Trajectory Model with the Common Reactive Intermediate mechanism (PTM-CRI), a likely explanation for the observed day-of-week dependence is the temporal dependence in the emissions of the ozone precursor species (VOC and NO_X) (which are greater on weekdays) and the multi-day timescale required for chemical processing and transport that lead to elevated ozone levels under photochemical episode conditions in the UK.

Many of the assessment models assume that the annual emission is released at a constant rate. The neglect of the variation in the temporal emission rates could compromise the ability of such models to reproduce the observed ozone behaviour. However, as a result of progressive changes in working practices and social habits, this effect may become less marked in the future, with the consequence that weekly cycles of pollution may become less noticeable.

The PTM-CRI was also applied to investigate the effectiveness of UK Short-term Action Plans. The design of the model is such that only a limited number of trajectories could be investigated. An episode occurring on 1st August 1999 at Barnsley Gawber (124 ppbv) was selected for investigation from the limited number of extreme ozone events now occurring. A number of possible emission control options were assessed. Removal of all UK anthropogenic precursor emissions resulted in a calculated decrease in peak ozone of 2.7 ppbv, which corresponds, on average, to a reduction of approximately 22 minutes in the exceedence duration. Potentially achievable action plans involving eliminating car use in the region of Rotherham/M1 and wider region of Nottinghamshire and South Yorkshire resulted in small changes in the peak ozone concentration. The study concluded that it was difficult to identify any realistic and beneficial UK short-term actions for the type of extreme ozone events which have been recorded in the UK in recent years.

5.2 THE ORIGIN AND DAY-OF-WEEK DEPENDENCE OF PHOTOCHEMICAL OZONE EPISODES IN THE UK

5.2.1 Introduction

It is well documented that the emissions of a variety of pollutants display strong weekly cycles which lead to variations in air quality from one day to another (*e.g.* Elkus and Wilson, 1977; Karl, 1978; Bower *et al.*, 1989; Altshuler *et al.*, 1995; Pryor and Steyn, 1995; Broennimann and Neu, 1997; Diem, 2000; Wilby and Tomlinson, 2000) and which may be responsible for similar variations observed in meteorological parameters such as rainfall, sunshine and temperature (*e.g.*, Ashworth, 1929; Wilby and Tomlinson, 2000). The observed levels of emitted (i,e., primary) pollutants tend to show weekly patterns which directly reflect the day-to-day variations in their local emissions. For secondary pollutants (formed from chemical processing of primary pollutants), the patterns are less predictable since chemical factors also need to be taken into account. In the specific case of ozone, the situation is particularly complex, because it has a global background level upon which regional and local chemical processes (which may either produce or destroy ozone) are superimposed.

As a result of this complexity, weekly patterns in ozone levels display differences between urban and rural locations (*e.g.* PORG, 1993), and also variations with prevailing meteorological conditions (Broennimann and Neu, 1997). The majority of reported studies have tended to concentrate on average levels for different days of the week at sites with significant local pollution. These studies have consistently demonstrated that ozone levels tend to be higher at weekends, particularly on Sundays, than on weekdays (*e.g.*, Graedel *et al.*, 1977; Bower *et al.*, 1989; Altshuler *et al.*, 1995; Pryor and Steyn, 1995; Pont and Fontan, 2001). This may reasonably be explained by decreased local emissions of NO_X at the weekends, and a corresponding increase in ozone because of its reduced local removal by reaction with NO. Indeed, clear anti-correlations with average NO_X levels have been reported (Pryor and Steyn, 1995), and the day-of-week variation in average ozone levels has been shown to be essentially absent at remote rural locations in the UK (*e.g.* PORG, 1993).

It is well-established, however, that ozone is produced from the sunlight-initiated chemical processing of emitted volatile organic compounds (VOC) and NO_X (*e.g.*, Sillman, 1999; Jenkin and Clemitshaw, 2000). Under conditions characteristic of photochemical pollution episodes in north-west Europe, ozone formation and transport can occur over hundreds of km, with the ozone concentration at a given location typically influenced by the history of the airmass over a period of up to several days. Consequently, the level of ozone is strongly influenced by the meteorological conditions and the level of input of VOC and NO_X into the airmass prior to arrival. Owing to the timescale for ozone formation and transport under such conditions, the weekly pattern for 'elevated ozone events' is unlikely to be the same as that observed for average ozone levels, or for levels under unfavourable conditions for ozone formation. Indeed, reported studies have demonstrated that there tends to be a distinctly different pattern, with lower weekend ozone levels, when either favourable meteorological conditions (Broennimann and Neu, 1997), or summertime data at selected locations (Elkus and Wilson, 1977; Diem, 2000) are considered separately.

The analyses presented in the present section focus specifically on photochemical ozone events, when hourly mean levels of ozone ≥ 90 ppbv (*i.e.* the 'information threshold') have been recorded at UK monitoring sites. Initially, back trajectories associated with all such events at 20 sites over the period 1992-1999 are presented, to indicate the origins of air masses typically

associated with ozone episodes in the UK. An analysis of data from 1989-1999 for the same sites is then presented to determine the number of hours the 90 ppbv threshold has been reached or exceeded as a function of day of the week. Finally, the CRI-PTM is used to investigate the influence of temporal variations in precursor emissions on simulated levels of ozone at 8 southern UK rural sites, under the conditions of the photochemical episode on 31 July 1999. The simulated variation of ozone levels at the site locations with day of week is compared with the general pattern observed at rural sites in the UK.

5.2.2 Airmass Origins

Archived monitoring data were used to identify days on which the 90 ppbv threshold was reached or exceeded over the period 1992-1999 at the 14 rural and 6 urban sites identified in Figure 5.1. These sites were selected as they form the basis of the UK ozone forecasting network (Stedman *et al.*, 1997), for which archived back-trajectory data are also available. The employed trajectories are derived from the UK Meteorological Office NAME model (*e.g.* Ryall *et al.*, 1998), and are isobaric at 950 mb.

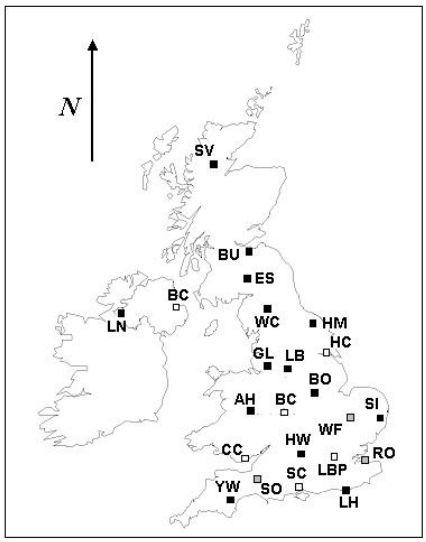

Figure 5.1 ***Locations of the UK network sites considered in the present study. Black and white squares are the 14 rural and 6 urban sites, respectively, used in the analyses of ozone episode air mass origins and the temporal variation of ozone threshold exceedences. Grey squares are the additional southern UK rural sites used in the trajectory modelling case study. Key to abbreviations is given in Tables 1 and 2.***

The trajectories associated with each ozone episode day at each site were therefore identified, with each trajectory representing the flow of air to the given site over a period of 96 hours prior to arrival at midday. The results for all 20 sites combined are shown in Figure 5.2. The data clearly show that the highest levels of ozone at the UK sites tend to occur on days when the back trajectories have 'looped' over mainland Europe and arrive in the UK from a broadly easterly or south-easterly direction. Under such conditions, the airmass receives a plentiful supply of ozone precursor emissions from populated regions during the 96 hour time period prior to arrival at the UK sites. Given that such trajectories are also typical of those established during stable anticyclonic conditions, the corresponding high solar intensity promotes the photochemical processing of the emissions which leads to ozone generation. The data presented in Figure 5.2 are also fully consistent with the results of a previous analysis of trajectories associated with elevated ozone levels in the UK for the summers of 1988 and 1989 (Stedman and Williams, 1991).

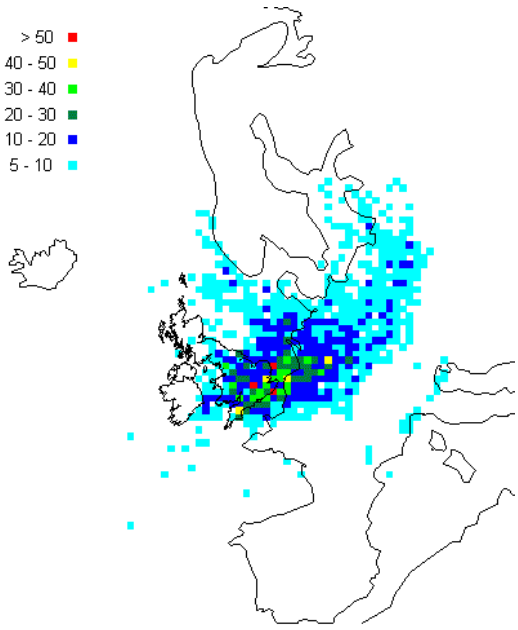

Figure 5.2 ***A combined plot of all 96-hour back trajectories arriving at the 20 UK sites shown in Figure 5.1 (black and white squares) at noon on days on which the 90 ppbv threshold was reached or exceeded. The data are presented in terms of the number of occasions a given EMEP 50km x 50km grid square was traversed in the 96 hour period prior to an observed ozone exceedence during 1992-1999 (see text). The plot contains 178 trajectories.***

5.2.3 Day-of-week Dependence of Ozone Exceedences

Archived data from the 20 sites in Figure 5.1 for the period 1989-1999 were analysed to investigate the number of hours the 90 ppbv information threshold was reached or exceeded on each day of the week. The majority of information is available for the rural sites, many of which have been running for the entire 11 year period considered. The results show a distinct temporal pattern, repeated at many of the sites, which indicate that ozone exceedences are more prevalent towards the end of the week. Data for five of the long-running southern UK rural sites (*i.e.* those collecting data throughout the period 1989-1999) are also plotted in Figure 5.3, together with the total for all the rural sites listed in Table 5.1.

On the basis of the data obtained at all rural sites, the number of hours of exceedence clearly maximises on Fridays, with Saturdays and Thursdays also having a greater number of hours than other days. A similar pattern is also obtained at many of the individual sites. For example, 4 of the 5 sites for which data are given in Figure 5.3 have the greatest number of hours exceedence on Fridays, with the remaining site having slightly more on Saturdays. However, there are some interesting differences between the sites. Those further to the west (Yarner Wood and Aston Hill) have a well defined single maximum at the end of the week (Thursday – Saturday), whereas the central southern UK site (Harwell), and those to the east (Sibton and Lullington Heath) appear to have an additional maximum earlier in the week.

The available ozone exceedence statistics are much less plentiful for the urban sites (Table 5.1), partly because none of the sites has data for the complete period 1989-1999 (and there are fewer sites), and partly because the generally higher levels of NO_X partition a greater proportion of the available oxidant into the form of NO_2. However, the limited data do show an end of week maximum. Compared with the rural sites, however, Saturdays and Sundays appear to be relatively more important, leading to a maximum on Saturdays, rather than Fridays: this can be explained by lower local NO_X emissions at the weekend, as discussed above for the analysis of mean data. However, there is also a marked contribution to the exceedences on Tuesdays, which actually have the greatest number of hours, based on the limited statistics.

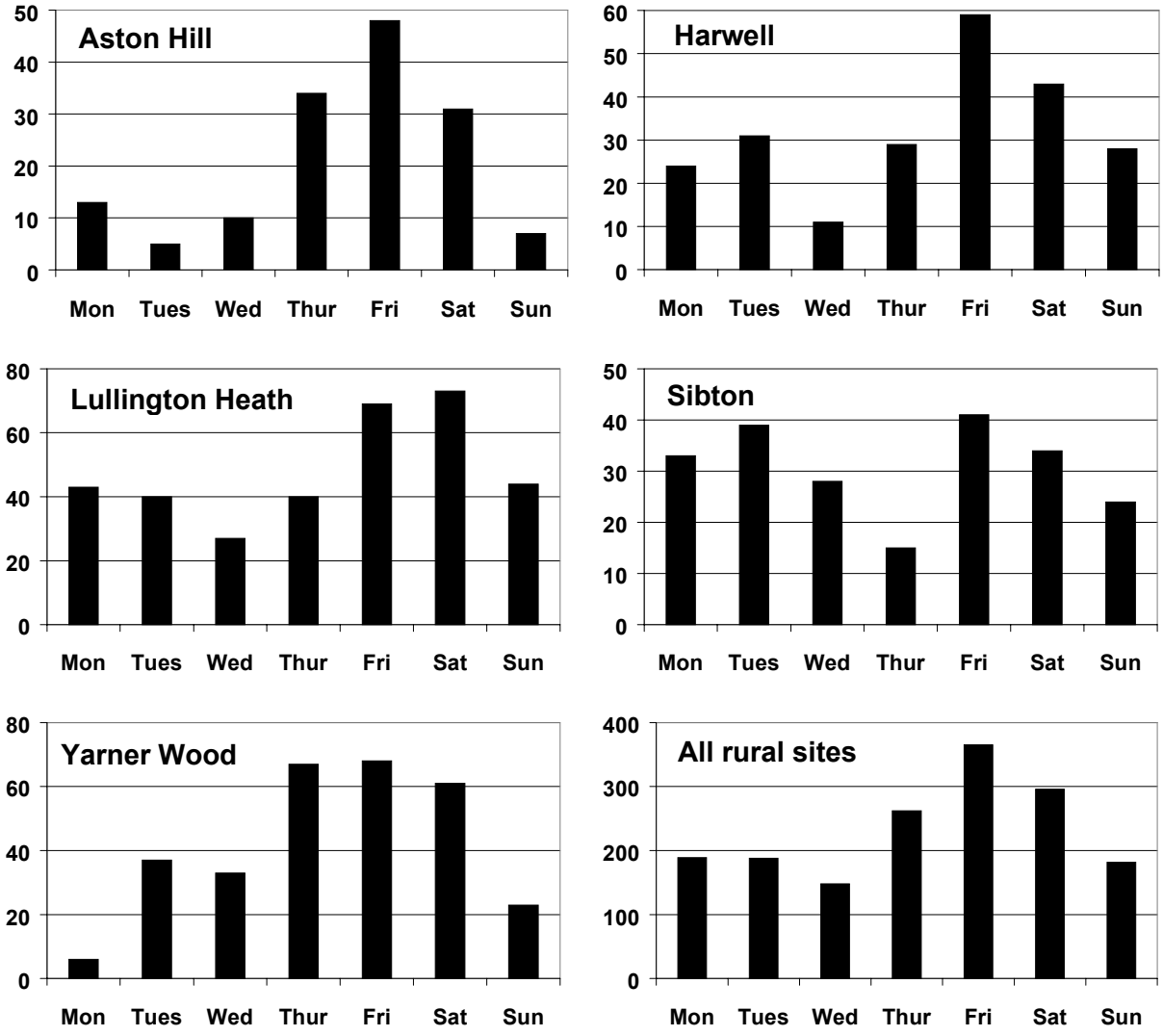

Figure 5.3 ***Number of hours with ozone ≥ 90 ppbv on each day of the week at selected long-term rural sites in the UK over the period 1989-1999, and the total number of hours by day of week at the 14 rural sites (black squares) in Figure 5.1.***

The prevalence of ozone episodes towards the end of the week is most likely a consequence of the day-of-week dependence of ozone precursor emissions. Other factors which contribute to the occurrence of ozone episodes are either invariant with day of week (*i.e.*, in the case of chemical parameters) or are equally likely to occur on each day of the week (*i.e.*, in the case of appropriate meteorological conditions), assuming the analysis has considered a sufficiently large number of days. The possibility of meteorological variability was tested for a limited number of the southern UK sites using the archived trajectories for each day of the summer months (April-September) in the years 1992-1999. As expected, no evidence was found for airmass arrival from an easterly or south-easterly direction being more prevalent towards the end of the week (*i.e.*, on Thursdays to Saturdays), confirming that the observed day-of-week dependence of extreme ozone events is not a result of meteorological variability.

Available information indicates that precursor VOC and NO_X emissions are generally greater on weekdays than on weekend days, as discussed further below. Consequently, for identical meteorological conditions, it is likely that the rate of ozone production is greater on weekdays than it is on weekend days. If the ozone concentration at a given point under summertime

anticyclonic conditions is assumed to be influenced by the airmass history over a period of about five days (*i.e.* typical of transport times across Europe), then a day of week dependence in peak ozone concentration would indeed be expected, with the maximum occurring on Friday. This is essentially because the integrated precursor emissions over a five day period are greater for the period Monday-Friday than for any other five day period. To test this hypothesis, the CRI-PTM has been used to investigate the formation of ozone along trajectories arriving at 8 southern UK rural sites, for the conditions of a recent ozone episode.

Table 5.1 ***Ozone threshold exceedence statistics: a summary of number of hours with ozone ≥ 90 ppbv on each day of the week at 20 rural and urban sites in the UK (1989-1999).***

Number of hours ≥ 90 ppbv threshold (1989 - 1999)								
Site	**Type**	**Mon**	**Tue**	**Wed**	**Thu**	**Fri**	**Sat**	**Sun**
Aston Hill (AH)	Rural	13	5	10	34	48	31	7
Bottesford (BO)	Rural	2	1	3	14	21	8	11
Bush (BU)	Rural	6	2	0	6	2	0	1
Eskdalemuir (ES)	Rural	5	0	6	5	6	0	1
Glazebury (GL)	Rural	8	2	0	4	7	2	11
Harwell (HW)	Rural	24	31	11	29	59	43	28
High Muffles (HM)	Rural	16	12	16	14	13	15	7
Ladybower (LB)	Rural	15	17	4	22	17	27	15
Lullington Heath (LH)	Rural	43	40	27	40	69	73	44
Lough Navar (LN)	Rural	7	0	0	3	1	0	0
Sibton (SI)	Rural	33	39	28	15	41	34	24
Strath Vaich (SV)	Rural	0	0	0	0	0	0	0
Wharley Croft (WC) [1]	Rural	11	2	10	9	13	2	10
Yarner Wood (YW)	Rural	6	37	33	67	68	61	23
Belfast Centre (BC) [2]	Urban	0	0	0	0	0	0	0
Birmingham Centre (BHC) [2]	Urban	0	2	0	0	2	1	0
London Bridge Place (LBP) [3]	Urban	0	3	0	0	4	9	4
Cardiff Centre (CC) [4]	Urban	1	11	0	6	10	7	7
Hull Centre (HC) [5]	Urban	0	3	0	0	0	0	0
Southampton Centre (SC) [5]	Urban	0	0	0	0	0	1	1
Total	Rural	189	188	148	262	365	296	182
Total	**Urban**	1	19	0	6	16	18	12
Total	**All**	**190**	**207**	**148**	**268**	**381**	**314**	**194**
Notes: [1] Until Nov. 1994; [2] Since Mar. 1992; [3] Since Jul. 1990; [4] Since May 1992; [5] Since Jan. 1994.								

5.2.4 Trajectory Modelling of Ozone Exceedences

A Case Study of 8 Rural Sites: Saturday 31 July 1999

The most severe UK photochemical ozone episode in 1999 occurred at the end of July and beginning of August, with the highest aggregate concentrations measured at southern UK rural sites on Saturday 31 July. This date was therefore selected for a case study, using the 8 southern UK rural sites listed in Table 5.1. The 8 sites include the 5 long-running sites for which data are presented in Figure 5.3. As indicated in Table 5.2, elevated ozone levels were recorded throughout the southern UK, with peak levels exceeding the 90 ppbv threshold at 5 sites.

The meteorological conditions on 31 July 1999 were typical of those associated with elevated levels of ozone in the UK, as described in Section 5.2.2. Figure 5.4 shows the 96-hour trajectories arriving at the 8 sites at 1600 hr on 31 July 1999. It should also be noted that, for the prevalent conditions, the Harwell site was positioned directly downwind of London, and therefore was influenced by a large injection of pollution comparatively late in the trajectory.

Table 5.2 ***Observed peak ozone mixing ratios at 8 southern UK sites on Saturday 31 July 1999, and those simulated using the Photochemical Trajectory Model.***

Site	Observed peak ozone (ppbv)[1]	Simulated peak ozone (ppbv)[2]
Aston Hill, AH (Powys)	98	93.9
Harwell, HW (Oxfordshire)	100	92.0
Lullington Heath, LH (Sussex)	111	102.0
Rochester, RO (Kent)	92	101.5
Sibton, SI (Suffolk)	Not measured	102.2
Somerton, SO (Somerset)	89	88.5
Wicken Fen, WF (Cambridgeshire)	92	81.3
Yarner Wood, YW (Devon)	77	68.7
[1] based on hourly mean; [2] see text		

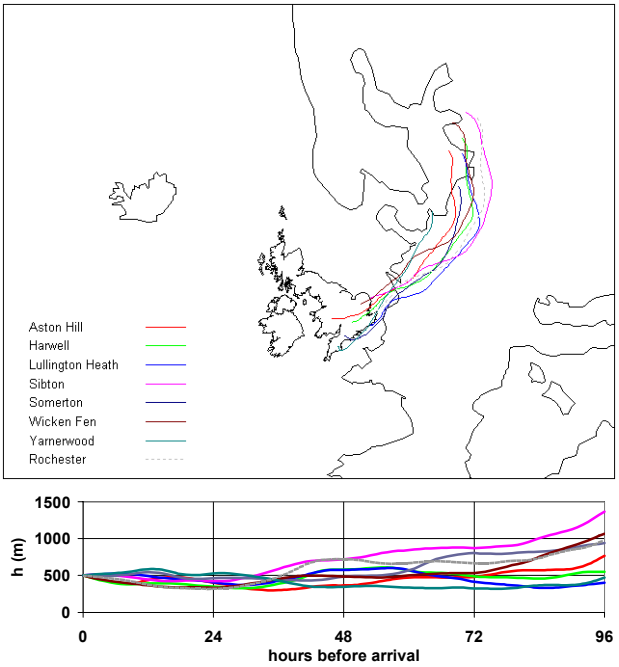

Figure 5.4 ***96-hour trajectories arriving at 8 southern UK rural sites at 1600 hr on 31 July 1999. The trajectories were obtained from the NOAA interactive on-line service (http://www.arl.noaa.gov/ready/hysplit4.html) using the model vertical velocity option. The altitude profile indicates that the trajectories were likely to be largely in the boundary layer over the timescale of interest, and therefore collecting emissions from ground level sources.***

The Photochemical Trajectory Model

The CRI-PTM is described in detail in Section 7.4. For the present investigation, a number of updates were made to the model. The UK emissions maps for VOC, NO_X, CO and SO_2 were updated to the NAEI 1998 data. For other European countries, the existing inventories (based on EC CORINAIR and EMEP) were scaled so that the country totals were consistent with the latest figures available on the EMEP website (http://www.emep.int/) at the time of the analysis (generally corresponding to 1997). The input of biogenic VOC was based on the data of Simpson *et al.* (1995).

The temporal variations applied to the emissions of VOC and NO_X were based on those estimated recently for the UK by Jenkin *et al.* (2000b). In that study, single representative profiles describing the seasonal, day-of-week and hour-of-day variations in emissions were assigned to each of over 180 source categories included in the NAEI. Where possible, the profiles were based on available temporally resolved data (*e.g.*, fuel consumption, electricity generation, traffic volume statistics), which can be related to emissions. The day-of-week factors indicate that the total emissions of either anthropogenic VOC or NO_X are similar on each of the weekdays, but tend to show a very small progressive increase through the week, being about 4% and 3% higher, respectively, on a Friday compared with Monday. However, the emissions at the weekend are significantly reduced. Compared with the average of the weekdays, the emissions of anthropogenic VOC are *ca.* 24% lower on Saturday and 31% lower on Sunday, and those of NO_X are *ca.* 25% lower on Saturday and 32% lower on Sunday.

The model was used to simulate the chemical development over a 96 hour period along the 8 trajectories arriving at the UK sites at 1600 hr (Figure 5.4). The model was therefore initialised at 1600 hr on day 1 of the trajectory, arriving at the end point at 1600 hr on day 5. The trajectories were obtained from the NOAA on-line service: http://www.arl.noaa.gov/ready/hysplit4.html.

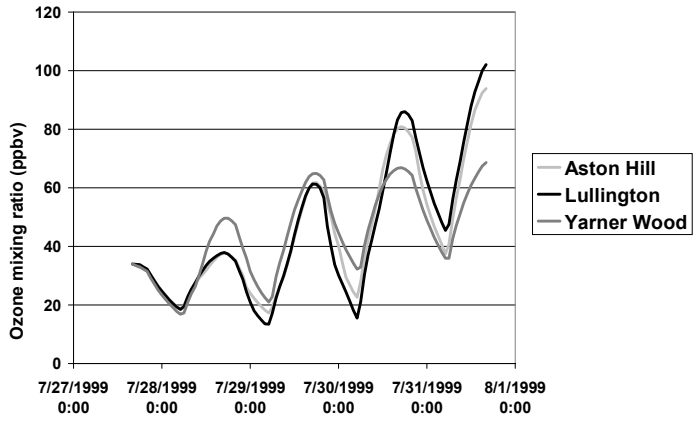

Figure 5.5 ***Simulated time evolution of ozone over a 96-hour period prior to arrival at Aston Hill, Lullington Heath and Yarner Wood at 1600 hr on Saturday 31 July 1999. In each case, the ozone mixing ratio was initialised at a regional background level of 34 ppbv.***

Results and Discussion

To allow comparison of simulated and observed ozone levels, the model was initially run such that the trajectories were initialised with day 1 as Tuesday and with arrival at the end points on Saturday (*i.e.* to concur with the actual arrival day). The corresponding time evolution of ozone along selected trajectories is shown in Figure 5.5, and the simulated mixing ratios at the end points for all 8 trajectories are presented in Table 5.2, along with those observed. In general terms, the agreement is reasonably good, with the difference between observed and calculated levels (obs-calc) ranging from –9.5 ppbv at Rochester to +10.7 ppbv at Wicken Fen. For the 7 sites for which comparison is possible, the model correctly calculates Lullington Heath to have the highest ozone mixing ratio, and Yarner Wood to have the lowest.

The influence of artificially varying the arrival day was then investigated. Seven calculations were therefore performed for each trajectory to calculate the peak ozone mixing ratio at each site, with the final day corresponding, in turn, to each day of the week. The results are shown in Figure 5.6. With the exception of Harwell, all sites show a similar pattern, with the highest mixing ratio generally calculated for arrival on a Friday. For Rochester and Sibton, however, the mixing ratios calculated for Friday and Saturday are essentially identical, with that calculated for Thursday only very marginally lower. The minimum calculated peak ozone at these 7 sites

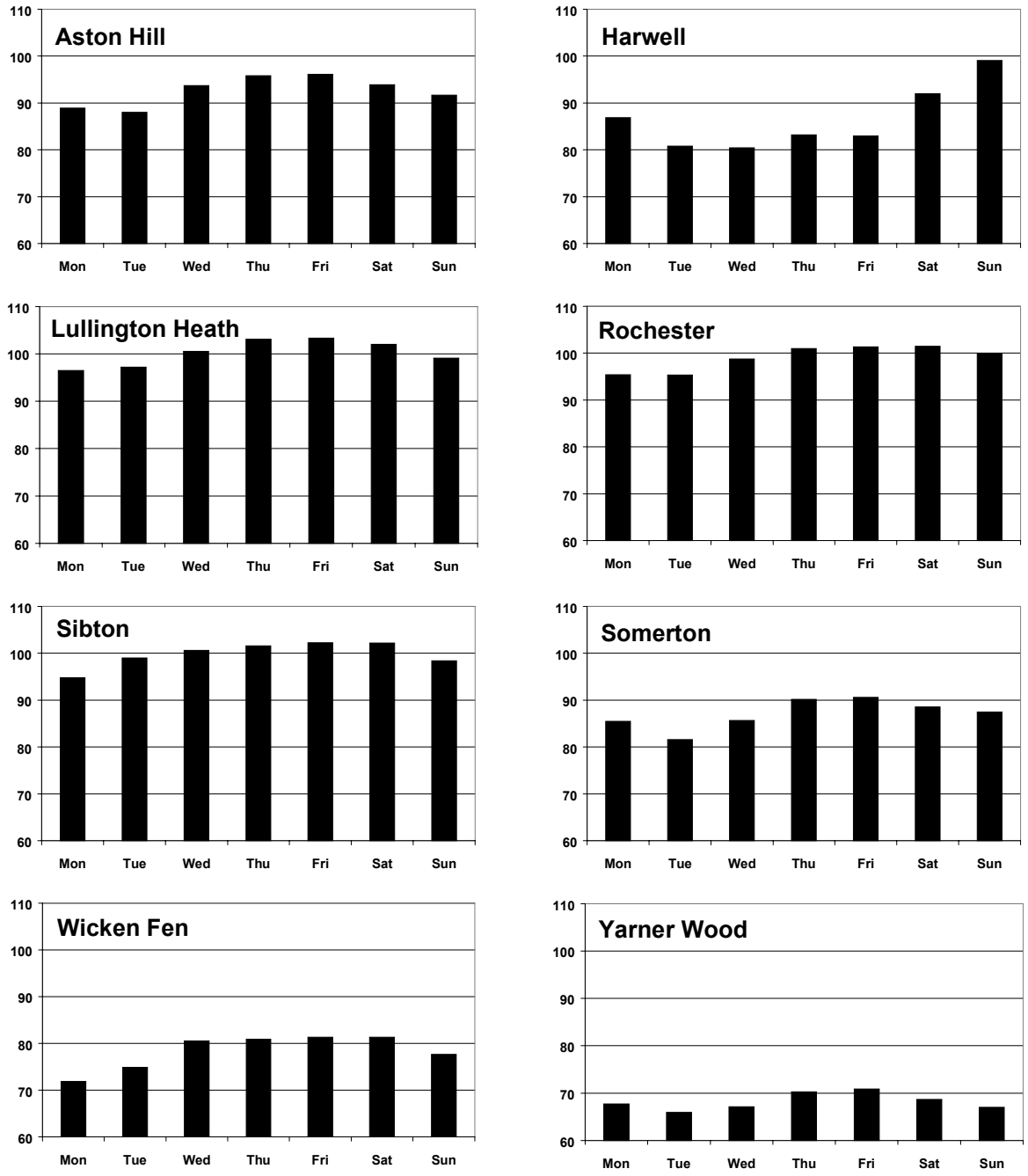

Figure 5.6 ***Variation of simulated peak ozone mixing ratios (in ppbv) at 8 southern UK sites with day of week. Note that y-axis scale is 60-110 ppbv in each case.***

(usually on a Monday or Tuesday) is typically about 7 or 8 ppbv lower. The calculations for Harwell show a distinctly different pattern to those observed at the other sites, with significantly higher peak ozone levels calculated on Saturday and Sunday. As mentioned above (and shown in Figure 5.4), the trajectory to Harwell on 31 July 1999 passes directly over central London a few hours before arrival, and therefore receives a significant injection of pollution comparatively late in the trajectory. Under these circumstances, the air mass is strongly VOC limited, with ozone production being very sensitive to the VOC/NO_X ratio and also inhibited by high absolute levels of NO_X. Consequently, the ozone formation in the latter stages of the trajectory is calculated to be greater on the weekend days when the absolute levels of NO_X injected as the air mass passes over London are lower.

The simulations were each initialised with a regional background mixing ratio of 34 ppbv ozone. As it is possible that the initial ozone may possess a small day-to-day variation, further calculations were performed to test the sensitivity of the simulated level of ozone at the arrival points to varying the initial mixing ratio. The results indicated that the final mixing ratio was very insensitive to this variation, typically increasing by less than 2 ppbv when an initial mixing ratio of 50 ppbv was used instead of 34 ppbv. Consequently, the final mixing ratio is mainly determined by chemical processing of emissions along the trajectory path.

In general terms, the results presented in Figure 5.6 are consistent with the observed prevalence of ozone episodes on Fridays, as the highest peak ozone level is calculated for Fridays at most sites. However, the observational statistics are in terms of the 'number of hours the 90 ppbv threshold is reached or exceeded', whereas the PTM output defines an instantaneous peak mixing ratio at the end point of a trajectory. Data from the air quality archive was therefore analysed to see if there is a relationship between observed peak ozone mixing ratio, and the number of consecutive hours a given threshold is exceeded. Data for the 8 rural sites considered in the present study over the period 1989-1999 are presented in Figure 5.7. These show there is a distinct relationship between the peak ozone mixing ratio (≥ 90 ppbv) in a given episode and the number of consecutive hours ≥ 90 ppbv. A linear regression analysis implies that the two quantities may be related by the following expression:

$$\text{Hours} \geq 90 \text{ ppbv} = 0.216(\pm 0.009).[O_3]_{peak}(\text{ppbv}) - 18.0(\pm 1.0) \qquad \text{(i)}$$

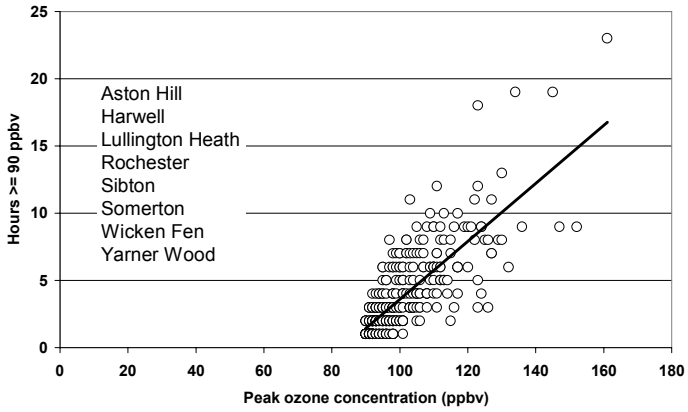

Figure 5.7 ***The observed relationship between the peak ozone mixing ratio (≥ 90 ppbv) in a given episode and the number of consecutive hours ≥ 90 ppbv, on the basis of data from the 8 rural sites over the period 1989-1999.***

Although the plot apparently shows a large amount of scatter, it presents data from 331 events with many coincident data points close to the regression line. Consequently, the relationship is reasonably well determined, with comparatively small standard deviations in the slope and intercept. This expression was used, therefore, to infer the number of hours ≥ 90 ppbv at each of the 8 sites, from the calculated ozone peak values. The results for the 6 sites where the 90 ppbv threshold was calculated to be achieved on at least one day of the week are shown in Figure 5.8, along with the combined total for these sites.

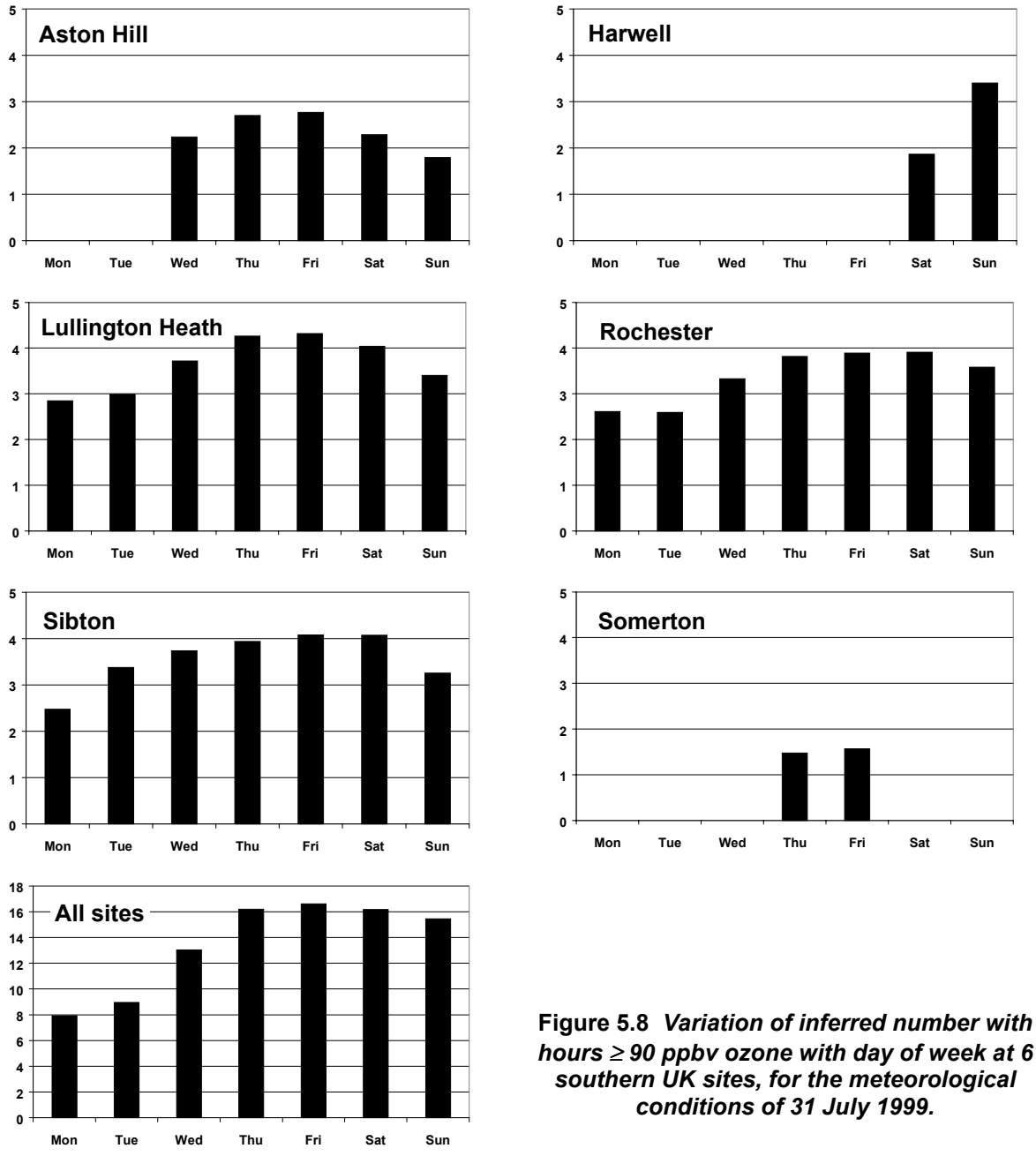

Figure 5.8 ***Variation of inferred number with hours ≥ 90 ppbv ozone with day of week at 6 southern UK sites, for the meteorological conditions of 31 July 1999.***

The total for all sites recreates some of the features of the observed general pattern of exceedences with day of week shown for all rural sites in Figure 5.3. In particular, Friday is identified as the day with most hours exceedence, the inferred number of hours being about a factor of two greater than on Monday and Tuesday. Certain other features are not recreated, however, in particular the comparatively small number of hours exceedence observed on Wednesdays and Sundays (Figure 5.3). Although the 31 July 1999 episode is reasonably typical of ozone episodes in the UK, it must be stressed that it is a case study which may not yield all the features which might be obtained if calculations were performed for a large number of similar (but certainly not identical) photochemical pollution events. In the present case, the calculated total figure for Sunday in Figure 5.8 is clearly greatly influenced by the individual contribution of Harwell and may therefore overestimate the relative probability of ozone exceedences on Sundays in general. It is difficult, however, to put forward an explanation for the observed

Wednesday minimum within the context of the day of week emissions variation estimated in the recent study of Jenkin *et al.* (2000b) and applied in the case study presented here.

5.2.5 Conclusions

The analyses presented above have provided information on the geographical origins and day-of-week dependence of extreme ozone events in the UK, when hourly mean levels of ozone have reached or exceeded the information threshold of 90 ppbv. The trajectories associated with such events at 14 rural sites and 6 urban sites in the UK over the period 1992-1999 show that the highest levels of ozone occur under summertime anticyclonic conditions, when photochemically-aged air masses arrive in the UK from a broadly easterly or south-easterly direction, after passing over mainland Europe for a period of several days.

Analysis of monitoring data from the same sites over the period 1989-1999 demonstrate that ozone episodes are more prevalent at the end of the week, with the greatest numbers of hours ≥ 90 ppbv occurring on Fridays. Relative to Fridays, the number of hours exceedence on the other days are: Sundays 51%, Mondays 50%, Tuesdays 54%, Wednesdays 39%, Thursdays 70%, Saturdays 82%.

The observed day-of-week dependence is believed to result from the temporal dependence in the emissions of the precursor VOC and NO_X (which are greater on weekdays) and the multi-day timescale required for chemical processing and transport to lead to elevated ozone levels under photochemical episode conditions in the UK. This hypothesis is broadly supported by the results of a case study using the CRI-PTM, which includes a full representation of seasonal, day-of-week and hour-of-day variations in precursor emissions, based on a recent appraisal (Jenkin *et al.*, 2000b).

Both the monitoring data presented in Figure 5.3, and the data used to infer the temporal variations of precursor emissions (Jenkin *et al.*, 2000b) have major contributions from measurements made in the early to mid 1990s. As a result of progressive changes in working practices and social habits, it is possible that the day-to-day variations in emissions (particularly the weekday-weekend difference) may become less marked in the future, with the consequence that weekly cycles of pollution may be come less noticeable.

5.3 SHORT-TERM ACTION PLANS

5.3.1 Extreme Ozone Events (≥ 120 ppbv) in the UK

The proposed inclusion of 'short-term action plans' in the EU Directive relates specifically to extreme episodic ozone events, where there is a risk of exceedence of the alert threshold (240 μgm^{-3} =120 ppbv) for three or more consecutive hours. In order to use the PTM to investigate the possible impact of action plans, it is necessary to identify when and where such events have occurred, and to establish that the model can recreate the observed ozone level with some degree of success for a representative event. Figure 5.9 and Figure 5.10 provide some statistics on the occasions during the period 1989-1999 when the ozone hourly average reached or exceeded 120 ppbv at UK monitoring sites[2]. Figure 5.9 shows that the severity of the ozone

[2] One recorded extreme event (157 ppbv at Redcar at 1500 hr on 12 August 1997) is omitted from Figure 5.9 and Figure 5.10 because it is believed to be anomalous. On this occasion, ozone apparently built up to this peak value from a level of 72 ppbv over a 3 hour period (only 1 hour ≥ 120 ppbv) and dropped to 79 ppbv in the following

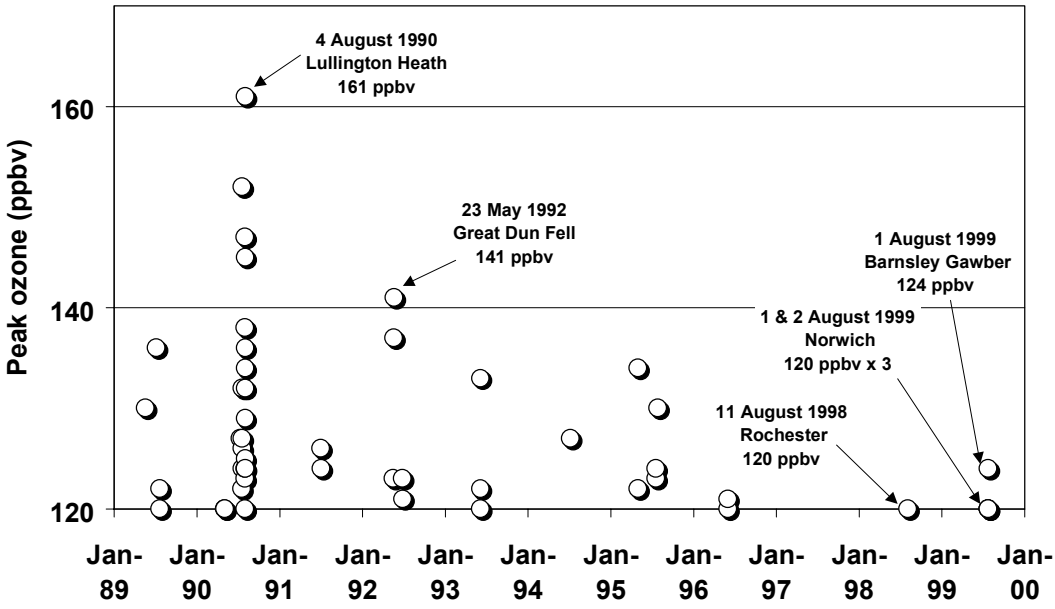

Figure 5.9 ***Reported Peak Ozone Mixing Ratios on Occasions when 120 ppbv was Reached or Exceeded at UK AURN sites.***

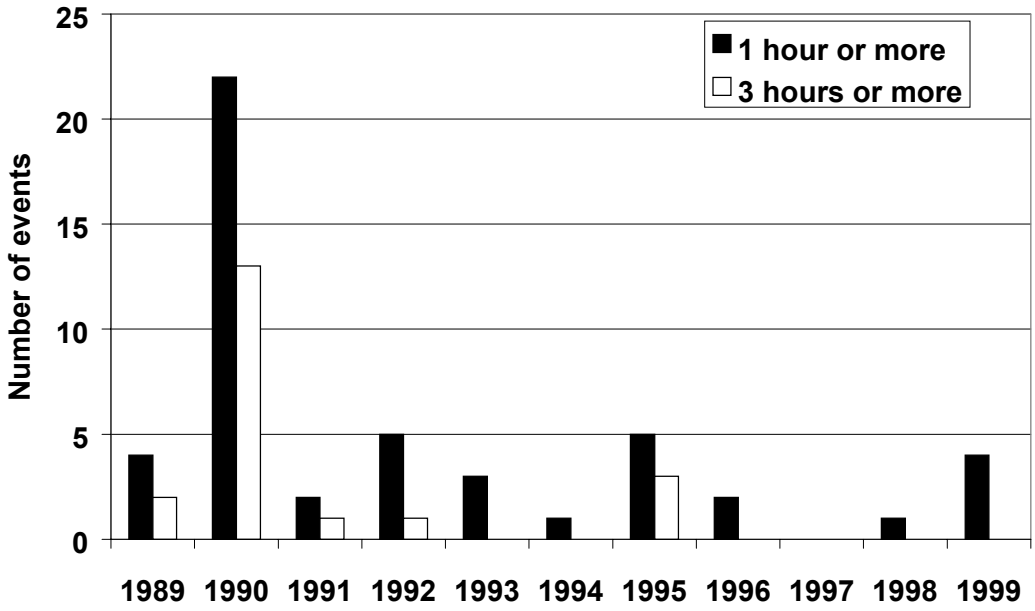

Figure 5.10 ***The number of extreme ozone events (hourly average ≥ 120 ppbv) occurring at UK sites during each of the years 1989-1999. The number of events ≥ 1 hour and ≥ 3 hours duration are shown.***

exceedences has tended to decline over this period (*e.g.* 140 ppbv has not been exceeded since 1992), and Figure 5.10 shows that, despite an increase in 1999, the frequency of the ozone exceedences has generally fallen. It should also be noted that the number of ozone monitoring

hour. The level of total oxidant (ozone + nitrogen dioxide) apparently changed from 185 ppbv at 1500 hr to 85 ppbv at 1600 hr. The level of ozone at High Muffles (a rural site 40 km south of Redcar) was between 80 and 84 ppbv for the period 1300-1600 hr. It seems likely, therefore, that the Redcar ozone measurement was subject to some unidentified interference between 1300 and 1500 hr on 12 August 1997.

sites has increased throughout the period such that an unchanging situation would have been expected to result in an increase in the number of recorded events per year. It appears, therefore, that the required conditions for extreme ozone events to occur are much rarer than in the early 1990s. For example, ozone levels ≥ 120 ppbv were recorded for 76 site-hours during 1990-94, but for only 24 site-hours during 1995-99, despite the increase in the number of sites. Although significant year-to-year variation is clearly apparent, the overall picture is consistent with an underlying decrease in the severity and frequency of extreme ozone events in the UK.

Figure 5.10 also shows the number of recorded events of three or more hours duration during 1989-1999, *i.e.* those for which consideration of short-term action plans would have been warranted. This shows that there have been no such events for six of the last seven years of the period, emphasising that events of this duration are very rare indeed.

The anotations in Figure 5.9 identify the location and date of a number of ≥ 120 ppbv events, including the five most recent in 1998 and 1999. For four of these five events, 120 ppbv was reached (but not exceeded) for a single hour. Three of these exceedences were at Norwich Centre on 1 and 2 August 1999, and one was at Rochester on 11 August 1998. Figure 5.11 shows a corresponding 96-hour trajectory arriving at Norwich at 1900 hr on 1 August, illustrating the broadly westerlyairflow (*i.e.* easterly winds) typically associated with UK ozone episodes.

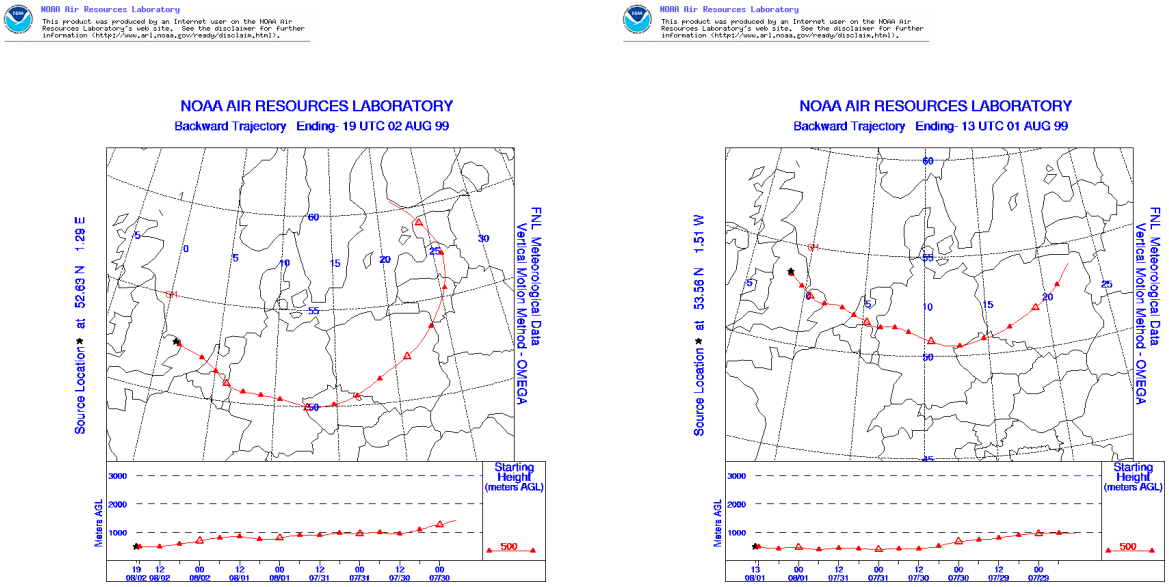

Figure 5.11 ***96-hour trajectories to Norwich Centre (1900 hr 2 August 1999) and Barnsley Gawber (1300 hr on 1 August 1999), which correspond to reported hourly average ozone ≥ 120 ppbv at these sites. The trajectories were obtained from the NOAA interactive on-line trajectory service (http://www.arl.noaa.gov/ready/hysplit4.html).***

Both Norwich and Rochester are close to the east coast of the UK and are likely to be barely influenced by UK precursor controls under episodic conditions (see also Section 8.3.2). The remaining event at Barnsley Gawber at 1300 hr on 1 August 1999 was the most severe in the UK in recent years (124 ppbv), although still only lasting for a single hour. An associated 96-hour trajectory is also shown in Figure 5.11, indicating that the airflow passed over the UK for the final 18 hours prior to arrival. For much of this time, the trajectory path travelled over rural areas of Suffolk, Norfolk and Lincolnshire and therefore did not receive particularly significant precursor emissions (as shown from the integrated NO_X emissions in Figure 5.12). However, the final six hours travel involved passage over the general area of Worksop (Nottinghamshire)

and Rotherham (S.Yorkshire) and into the M1 corridor, prior to arrival at Barnsley Gawber, about 1 hour downwind of Rotherham. This event was therefore selected for further investigation using the PTM.

5.3.2 Simulation of an Extreme Ozone Event

The PTM/CRI mechanism (1998 ref scenario, see Section 8.3.2) was used to simulate the chemical development along the 96-hour trajectory arriving at Barnsley Gawber shown in Figure 5.8. Because of the idealised diurnal boundary layer variation in the model, the simulated ozone maximum generally occurs at *ca.* 1600 hr: consequently the calculation was initialised at 1600 hr on 28 July for arrival at 1600 hr on Sunday 1 August (*i.e.*, even though the observed maximum occurred at 1300 hr). Under these conditions, the simulated ozone mixing ratio at the trajectory end point was 118 ppbv, compared with the observed maximum of 124 ppbv. In order to provide a base case simulation, the VOC emissions throughout the model domain were slightly increased (by *ca.* 6%), to bring the simulated mixing ratio at the end point up to 124 ppbv.

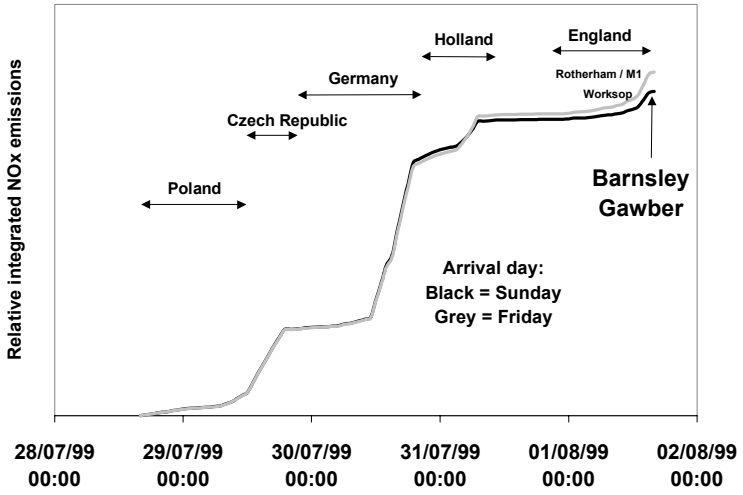

Figure 5.12 ***Integrated emissions of NO_X (on an arbitrary scale) along the 96-hour trajectory arriving at Barnsley Gawber shown in Figure 5.11. Emissions based on 1998 ref scenario with arrival day as Sunday and Friday.***

The variation of simulated ozone at the end point with day of week was investigated. In contrast to the results of the calculations presented in Section 5.2, the variation from one day to another was found to be very small on this trajectory, the simulated mixing ratios in ppbv being: Monday (123.6), Tuesday (121.0), Wednesday (122.4), Thursday (122.6), Friday (122.4), Saturday (122.4), Sunday (124.0). This lowered sensitivity almost certainly results from the limited emissions received along a significant portion of the trajectory path (*i.e.* the North Sea and rural eastern England).

As indicated from the temporal emissions variations presented in Figure 6.2, Sunday arrival corresponds to the lowest precursor emissions on the final day, whereas Friday arrival corresponds to the highest. This is highlighted in Figure 5.12, which compares the integrated NO_X emissions for arrival on the two days. In order to maximise the contribution of UK emissions to those received along the trajectory, further calculations were carried out with the arrival day assumed to be Friday. A set of 11 investigated precursor control measures is listed in Table 5.3. Of these, only two are realistically feasible: the remainder are to test the sensitivity of the simulated ozone level to purely illustrative measures.

Table 5.3 ***Summary of precursor control measures investigated. Measures 1 – 9 are illustrative. Measures 10 and 11 represent a potentially achievable action.***

	Control measure
1	No UK emissions of anthropogenic VOC or NO_X
2	UK emissions of anthropogenic VOC or NO_X doubled
3	No anthropogenic VOC emissions in the region of Rotherham/M1 [1]
4	No NO_X emissions in the region of Rotherham/M1 [1]
5	No anthropogenic VOC or NO_X emissions in region of Rotherham/M1 [1]
6	No anthropogenic VOC emissions in Nottinghamshire or South Yorkshire [2]
7	No NO_X emissions in Nottinghamshire or South Yorkshire [2]
8	22.3% anthropogenic VOC reduction in Nottinghamshire or South Yorkshire [2,3]
9	23.8% NO_X reduction in Nottinghamshire or South Yorkshire [2,3]
10	**No cars in the region of Rotherham/M1 [1,4]**
11	**No cars in Nottinghamshire or South Yorkshire [2,4]**

Notes [1] Region of Rotherham/M1 corresponds to the final 2 hours of the trajectory; [2] Nottinghamshire/S.Yorkshire corresponds to final 6 hours of the trajectory; [3] Level of control equates to the contribution of cars to VOC or NO_X emissions independently; [4] Control involves simultaneously reducing VOC emissions by 22.3% and NO_X emissions by 23.8%.

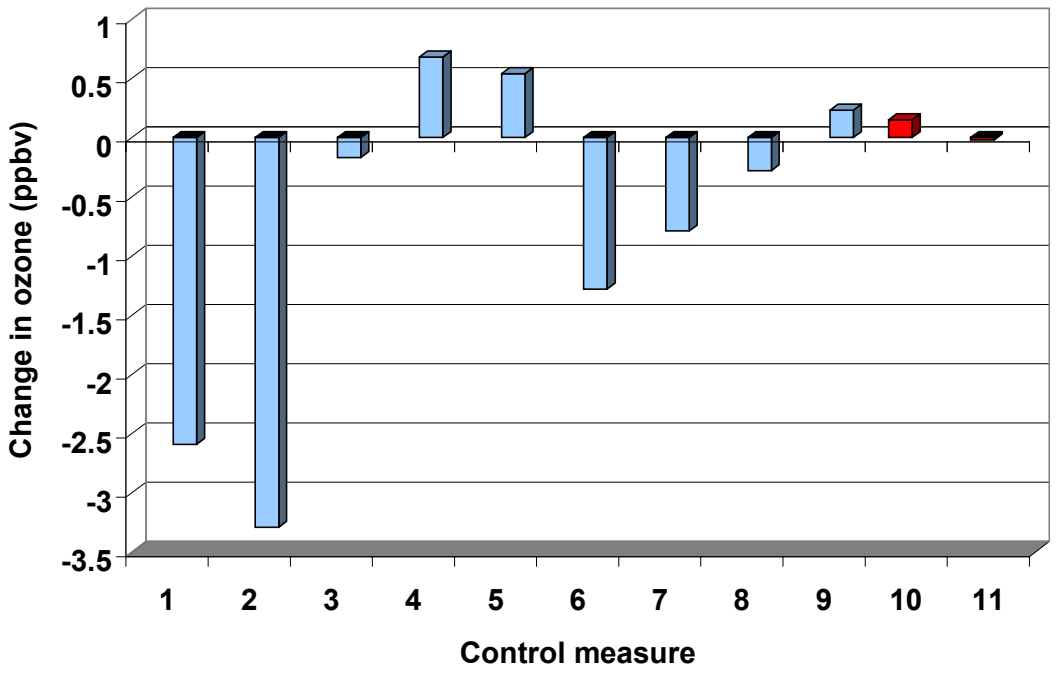

Figure 5.13 ***Illustration of the influence of the UK precursor controls listed in Table 5.3 on the simulated peak ozone level at Barnsley Gawber (1 August 1999 trajectory with assumed Friday arrival: base case ozone mixing ratio = 122.4 ppbv). Measures 1 – 9 are illustrative. Measures 10 and 11 represent a potentially achievable action.***

Figure 5.13 shows the change in the simulated ozone levels at the trajectory end point which result from the control measures listed in Table 5.3. It should be noted that none of the measures results in a large change. Even eliminating all UK anthropogenic emissions of VOC and NO_X (measure 1) only lowers the simulated mixing ratio by 2.7 ppbv. Interestingly, a similar effect is achieved by doubling UK emissions (measure 2). This is because the Barnsley Gawber site is directly downwind of Rotherham under the conditions of 1 August 1999, and the ozone level is reduced as a result of increasing the NO_X emissions shortly before the air mass

arrives at the end point. The specific influence of control measures 3, 4 and 5 involving Rotherham and the M1 (*i.e.* the final two hours of the trajectory) confirm that the airmass is strongly VOC-limited and also inhibited by elevated NO_X levels in a comparatively polluted plume. Thus removal of VOC emissions (measure 3) leads to a reduction of ozone, removal of NO_X emissions (measure 4) leads to an ozone increase, and removal of both (measure 5) leads to a smaller increase.

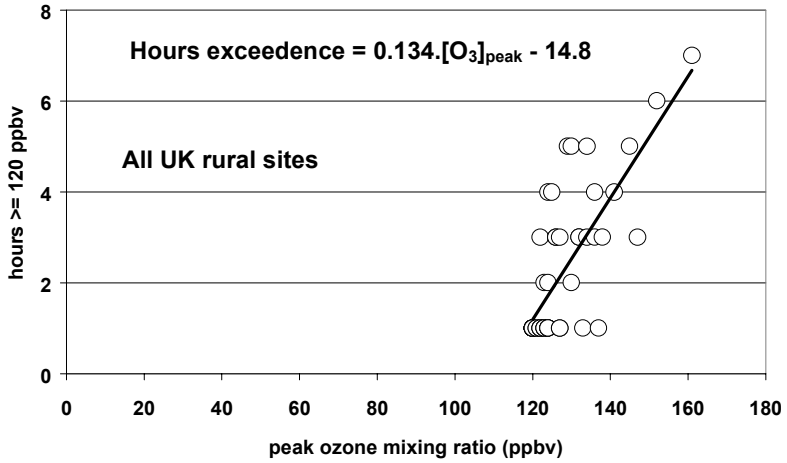

Figure 5.14 ***The observed relationship between the peak ozone mixing ratio (≥ 120 ppbv) in a given episode and the number of consecutive hours ≥ 120 ppbv, on the basis of data from all UK rural sites over the period 1989-1999. The plot has 49 data points.***

Expanding the scope of the illustrative measures to Nottinghamshire and South Yorkshire (*i.e.* the final six hours of the trajectory) leads to ozone reductions when either VOC or NO_X emissions are eliminated (measures 6 and 7). However, partial elimination of NO_X over the widened area (measure 9) still results in increased ozone.

Measures 10 and 11 represent actions which are potentially feasible. The elimination of car traffic in Rotherham and on the M1 results in a small simulated increase of 0.15 ppbv, whereas the elimination throughout Nottinghamshire and South Yorkshire leads to a very small simulated decrease of 0.02 ppbv. The magnitude and sense of the influence of these controls are logical, within the context of the effects of the illustrative measures described above.

The results of these simulations provide a series of peak ozone mixing ratios, from which it would be useful to infer the duration of the exceedence of the alert threshold. Similarly to the analysis presented in Section 5.2 (on the day-of-week variation) for the 90 ppbv information threshold, therefore, data from the air quality archive was analysed to investigate the relationship between observed peak ozone mixing ratio, and the number of consecutive hours ≥ 120 ppbv. Corresponding data for all UK rural sites over the period 1989-1999 are presented in Figure 5.14. Although the number of events is significantly lower than for the 90 ppbv threshold (Figure 5.3), the data still display a distinct relationship, suggesting the following relationship:

$$\text{Hours} \geq 120 \text{ ppbv} = 0.134(\pm 0.017).[O_3]_{peak}(\text{ppbv}) - 14.8(\pm 2.2) \qquad \text{(I)}$$

This expression implies that, on average, a peak ozone mixing ratio of 132 ppbv corresponds to 3 consecutive hours exceedence of the alert threshold. However, it is clear from the scatter in Figure 5.14 that a number of less severe events (with peak ozone ≥ 122 ppbv) have lasted for 3 or more hours, emphasising that this expression cannot be used as a strict guideline for an individual event.

Equation (I) may be used to infer the number of hours ≥ 120 ppbv that might be expected, on average, from the peak ozone mixing ratios simulated above. The base case mixing ratios of 124.0 and 122.4 ppbv, simulated for Sunday and Friday arrival, correspond to exceedence durations of 1.6 and 1.8 hours, respectively. Figure 5.15 shows the changes in inferred exceedence duration which correspond to each of the control measures listed in Table 5.3.

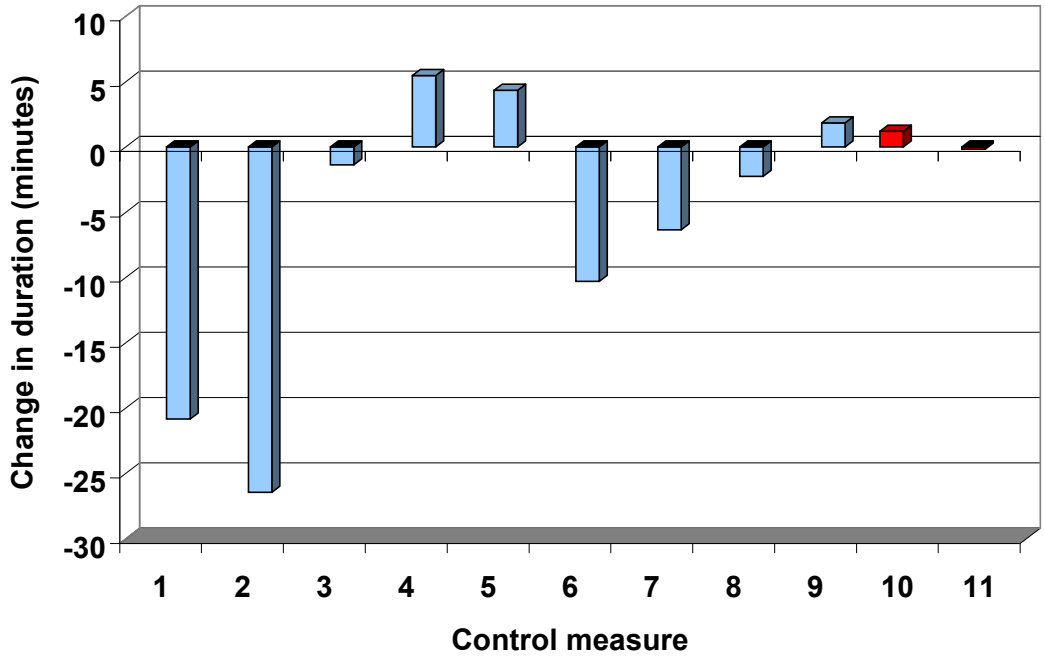

Figure 5.15 ***Illustration of the influence of the UK precursor controls listed in Table 5.3 on the inferred alert threshold exceedence duration at Barnsley Gawber (1 August 1999 trajectory with assumed Friday arrival: base case exceedence duration = 1.6 hours). Measures 1 – 9 are illustrative. Measures 10 and 11 represent a potentially achievable action.***

These suggest that none of these measures leads to changes in exceedence duration of more than 27 minutes, and the potentially achievable actions 10 and 11 would result in changes of only +70 and –10 seconds, respectively.

5.3.3 Conclusions

The above appraisal of extreme ozone events in the UK allows certain conclusions to be drawn: Monitoring data over the period 1989-1999 indicate that there is an underlying decrease in the severity and frequency of alert threshold exceedences (≥ 120 ppbv) in the UK. Although there is some year-to-year variation, six of final seven years of this period had no alert threshold exceedences of 3 or more hours (*i.e.* events for which short-term action plans would have been warranted).

The five recorded alert threshold exceedences in recent years (1997-1999), each of one hour duration, have been in eastern England (Rochester, Kent; Norwich, Norfolk; Barnsley Gawber, S.Yorkshire). The most serious was at Barnsley Gawber on 1 August 1999 (124 ppbv). The influence of a series of illustrative variations of UK emissions have been considered for this case, using the PTM. Removal of all UK anthropogenic precursor emissions resulted in a calculated

decrease in peak ozone of 2.7 ppbv, which corresponds, on average, to a reduction of approximately 22 minutes in the exceedence duration.

Potentially achievable action plans involving eliminating car use in the region of Rotherham/M1 and wider region of Nottinghamshire/S.Yorkshire resulted in simulated changes in peak ozone of +0.15 and –0.02 ppbv, respectively: these correspond, on average, to changes in exceedence duration of approximately +70 and –10 seconds, respectively.

It is difficult to identify any realistic and beneficial UK short-term actions for the type of extreme ozone events which have been recorded in the UK in recent years. In addition, the present calculations indicate that local measures can increase ozone levels under certain circumstances. It is clear from Section 8.3.2 that UK precursor controls can benefit locations further to the west of the country under typical photochemical ozone conditions. However, recorded occurrences of exceedences of 120 ppbv of three or more hours duration at sites not in the east of the country are comparatively rare, the last one being at Great Dun Fell, Cumbria on 23 May 1992.

6 Scenario Analysis and Short-term Action Plans using the Ozone Source-Receptor Model

6.1 SECTION SUMMARY

A new model - the Ozone Source-Receptor model - has been developed and applied during the present project. It is similar in concept to the ELMO model but has the advantage of higher spatial resolution, the use of realistic air mass trajectories and the option to allow the emissions to vary temporally. The model can be used to derive a range of ozone exposure metrics at 10 km resolution across the UK for different emission control scenarios.

The model was benchmarked against the PTM-MCM on a single trajectory and found to give similar concentrations for ozone and other key species involved in photochemical ozone production. The model performance was then evaluated by comparison with measurements made at UK ozone monitoring stations. The maximum hourly-mean ozone concentrations were derived for each day in 1997. The fraction of the calculated maximum daily ozone concentrations that lay within a factor of 1.5 below or 1.5 above the observed maximum ozone concentrations varied from 0.53 at Bottesford to about 0.77 at Strathvaich Dam.

Further evaluation of the OSRM performance was undertaken. The model was used to simulate the ozone, NO_x and NO_y measurements made at Lullington Heath and the nearby Barcombe Mills sites during a photochemical episode in June 2001. Model simulations were also undertaken using the PTM-CRI. The daily denuder measurements made at Barcombe Mills have provided an opportunity to test the ability of ozone photochemical models to simulate NO_y measurements. The performance of the two models is encouraging but further work is needed to optimise the formulation of the NO_y chemistry in the models. The performance of the OSRM is very comparable to that of the PTM-CRI, an accepted policy tool, for the trajectories and inventories used. Some of the discrepancy between the models will be due to the different formulation of, for example, the chemical mechanism, the photolysis processes and the parameters characterising the boundary layer. These simulations have shown that the OSRM is fundamentally robust.

AOT40 maps were prepared for the UK using the OSRM to demonstrate its capability for UK-scale modelling. Although the absolute magnitudes were overestimated, the model-derived maps give a reasonable description of the observed spatial distribution, apart from the high values on the east coast of Scotland. The AOT40 maps calculated by the OSRM for the year 1998 have significantly lower values than those shown in the corresponding 1997 maps, which was consistent with 1998 being a lower pollution year than 1997. The OSRM model is thus able to reproduce the difference caused by the changes in the meteorology from 1997 to 1998.

The OSRM was used to investigate the relative response to 30% reductions in the emissions of NO_x and VOCs. The results indicated that a 30% reduction in the NO_x emissions have a greater influence on 40 ppb exceedence days at the UK Rural Ozone Monitoring Network sites compared with 30% reduction in the VOC reduction. For the higher O_3 exceedence thresholds, the results indicate a shift towards a greater response from VOC emission control. The responses agree reasonably well with those reported using the EUROSTOCHEM model, again providing confidence in the performance of the OSRM.

6.2 INTRODUCTION

One of the major deliverables of the current programme of work is the development of a new policy modelling tool which aims to provide a more detailed description of the ozone climate of the UK than is possible with the existing Lagrangian models. This is specifically to address some of the objectives detailed in Task 3 (Scenario Analysis) and Task 4 (Real-time Ozone Forecast

Model: Short term action plans). The new source-receptor model is being constructed by building on the concepts used in existing models developed for DEFRA, in particular the Ozone Forecast Model and the ELMO model.

The Ozone Forecast Model is run routinely as part of the UK Air Pollution Forecasting Service which is provided by AEA Technology on behalf of DEFRA (Stedman and Williams, 1992; Stedman and Willis, 1996; Stedman *et al.*, 1997). The model uses real air mass trajectories arriving at a total of 20 monitoring site locations in the UK, as calculated from a combination of measured and forecast windfields. The model incorporates a highly simplified chemical scheme and uses a constant OH concentration and boundary layer height, both of which are defined by the temperature of the boundary layer. The rate of ozone production is determined from the rate of oxidation of 20 VOC by OH radicals and the ozone yield for each VOC represented by its POCP value.

The ELMO Model describes the formation and long range transport of ozone across northwest Europe to a grid of equally-spaced arrival points 10 km apart across the entire UK. The model uses idealised air mass trajectories and calculates the weighted-mean ozone concentration for 72 trajectories, each covering 96 hours travel time and spaced at 5° intervals from each other. Weighted-mean concentrations are calculated using a wind-rose appropriate to hourly mean ozone concentrations in excess of 50 ppbv during 1995. The ELMO model adopts the same chemistry and numerical methods as those used in the global STOCHEM model (Collins *et al.*, 1999, 2000; Stevenson *et al.*, 1997a, 1997b).

Broadly speaking, the new Ozone Source-Receptor Model (OSRM) is being built so that it combines the chemistry and numerical method from ELMO with the more realistic trajectory treatment of transport provided by the ozone forecast model. In addition, some features of other related atmospheric chemistry models (*i.e.,* TRACK, the Photochemical Trajectory Model, PATCHM and STOCHEM), available to the project consortium, are being used to provide the actual formulation of specific processes. The model is designed to be sufficiently flexible to incorporate alternative chemical mechanisms, if appropriate. The use of reasonably realistic chemistry and transport should enable ozone concentrations to be estimated on a day to day basis. This will allow statistics such as maximum concentrations over different averaging periods, days above limit values and AOT values to be derived directly. This facility is not currently available from existing models, which provide estimates for worst case or mean episode conditions.

6.3 MODEL DESIGN

6.3.1 Introduction

The detailed specification of the model was provided in the first annual project report (Jenkin *et al.*, 2000a), the components of which are summarised in Figure 6.1. As indicated above, many of these components are taken from, or based upon, earlier approaches:

- the chemical model is the same as used in STOCHEM and ELMO;
- the photolysis rates are calculated using the same procedure as in PATCHM;
- the trajectories are real four-day trajectories, as in the Ozone Forecasting Model;
- like the Photochemical Trajectory Model, the new model solves the differential equations using a variable-order Gear's method.

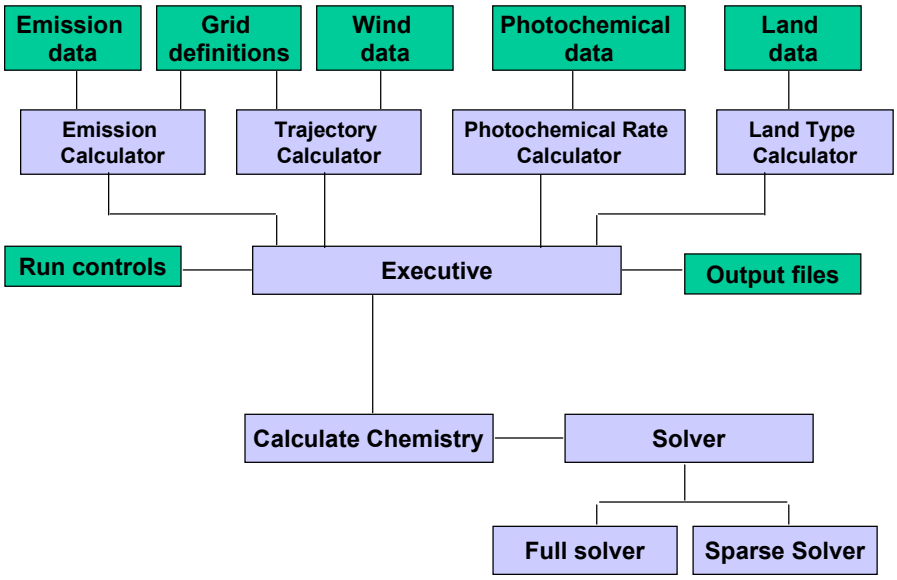

Figure 6.1 ***Schematic diagram of the components of the Ozone Source–Receptor Model.***

The model has been significantly updated during the reporting period. The following paragraphs summarise these new developments and the current status of the model.

6.3.2 Emissions

Emissions data are incorporated for CO, NO_X, SO_2 and VOC. The emissions for the whole European region are based on the EMEP 50 x 50 km grid (www.emep.int). The UK emissions are currently based on the Ordnance Survey 10 x 10km grid for the whole UK region, with the flexibility for future incorporation of finer resolution emissions (*i.e.* 1 x 1km) for selected regions.

The UK emissions have been updated to the 1998 maps defined by the NAEI, and have been aggregated to include all point sources and area sources. The current UK emissions totals are therefore: 4758 ktonne a^{-1} for CO, 1753 ktonne a^{-1} for NO_X, 1615 ktonne a^{-1} for SO_2 and 1958 ktonne a^{-1} for VOC. The emissions of each pollutant have been divided into up to 8 broad source categories, as summarised in Table 6.1, such that there are effectively 26 spatially disaggregated emissions maps superimposed for the UK region, each representing the emissions of a single pollutant is a single sector. Table 6.2 shows the fractional contribution of each sector to the emissions of each pollutant. The contribution from the maps with a common code can be scaled by factors between 0 and 1, to allow simulation of the effects of selected emissions controls.

In conjunction with the programme 'Emission Factors and Cost Curves for Air Pollutants (EPG 1/3/134)' a methodology for allowing for the temporal dependence of the emissions has been developed, as described in detail by Jenkin *et al.* (2000b). This has involved estimating the variations over the following timescales:

- Diurnal: the portion of daily emissions which occur during each hour of a typical 24 hour period have been estimated.

- Weekly: the portion of weekly emissions which occur on each day of a typical week have been estimated.
- Annual: the portion of annual emissions which occur during each month of a typical year have been estimated.

Table 6.1 ***Summary of Composite Emission Sectors for CO, NO_X, SO_2 and VOC in the OSRM, and their relation to SNAP Codes.***

OSRM code	8 composite sectors represented		SNAP code	Pollutant
01	SU	Solvent Use	6	VOC
02	RT	Road Transport	7	CO,NO_X,SO_2,VOC
03	IP	Industry/Processes	1⋆, 3, 4	CO,NO_X,SO_2,VOC
04	FF	Fossil Fuel Distribution	5	CO,NO_X,SO_2,VOC
05	DC	Domestic Combustion	2	CO,NO_X,SO_2,VOC
06	PG	Power Generation	1⋆	CO,NO_X,SO_2,VOC
07	OT	Other	8, 9	CO,NO_X,SO_2,VOC
08	NA	Natural	11	VOC
⋆ PG includes 'power stations' contribution to SNAP code 1: other contributions are in IP				

Table 6.2 ***The fractional breakdown of the total UK pollutant emissions into the composite sectors used in the OSRM.***

	CO	NO_X	SO_2	VOC
Solvent Use	-	-	-	27.2%
Road Transport	73.1%	45.5%	1.4%	26.9%
Industry/Processes	12.5%	16.4%	24.1%	15.2%
Fossil Fuel Distribution	0.1%	0.0%	0.4%	15.2%
Domestic Combustion	5.3%	6.0%	5.3%	2.1%
Power Generation	1.5%	20.7%	66.4%	0.3%
Other	7.5%	11.3%	2.4%	3.9%
Natural	-	-	-	9.1%
1998 UK total (ktonne a^{-1})	**4758**	**1753**	**1615**	**1958**

A single representative profile has therefore been defined for the diurnal, weekly and annual variations for each pollutant in up to 183 source categories in the NAEI. No attempt has been made to identify differences in the diurnal pattern of emissions on different days of the week or at different times of year. Similarly, no attempt has been made to distinguish differences in the weekly pattern of emissions at different times of year, even though it is recognised that such differences could well exist. Clearly, a fully rigorous temporal profile should therefore define the portion of emissions occurring in each hour of a given year, with the precise profile also changing from one year to the next. However, such a methodology would be impractical, and the resultant information would be difficult to use in modelling applications. The adopted approach is therefore designed to provide a practical method of defining the temporal variations in emissions.

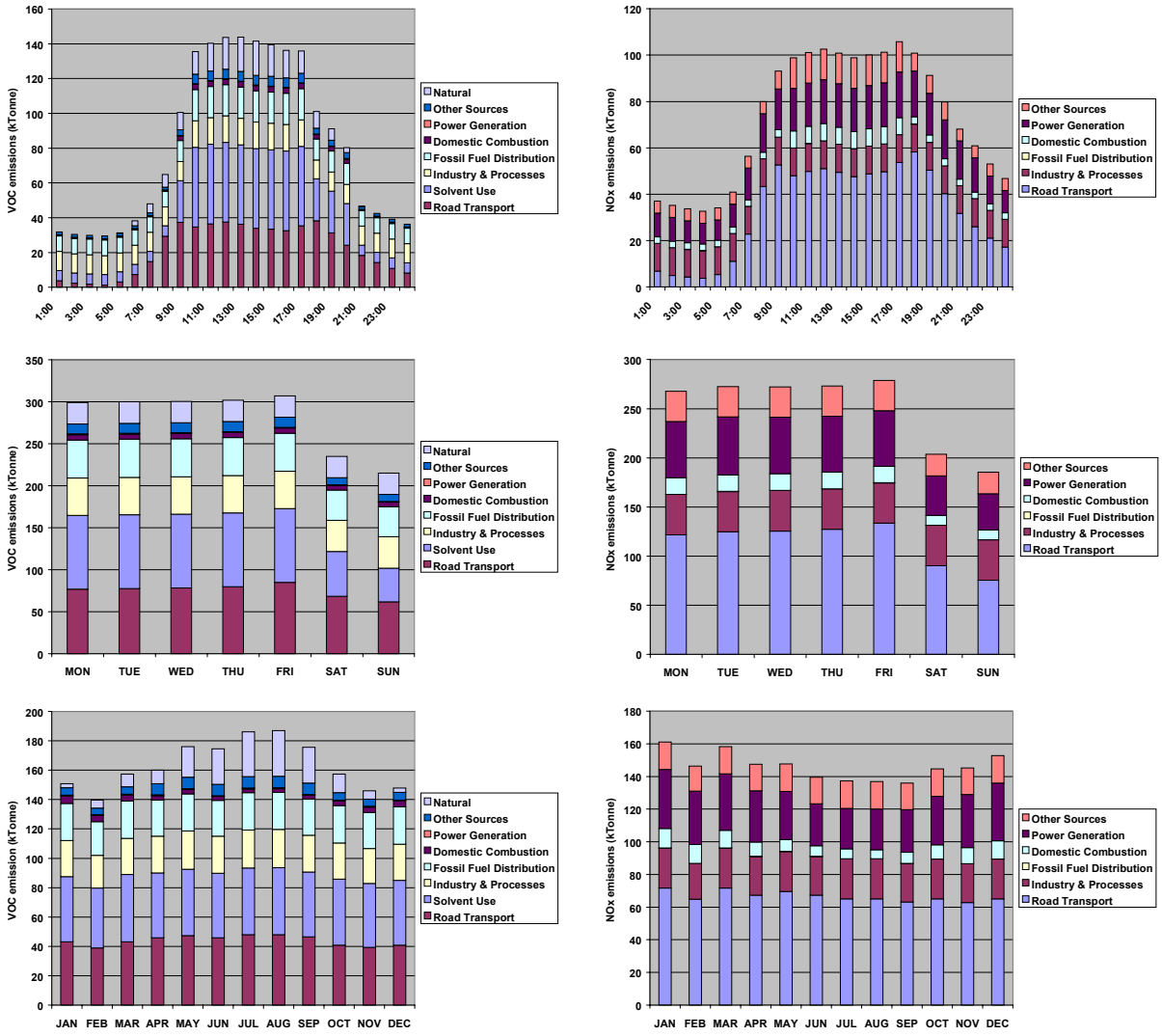

Figure 6.2 ***Variation of emissions of VOC and NO_X with month of year, day of week and hour of day, based on 1998 totals defined by the NAEI. The contributions to these totals made by a number of broad emissions categories are illustrated: solvent use (VOC only), road transport, industry/processes, natural (VOC only), fossil fuel distribution, domestic combustion, power generation and 'other' sources. A full description of the methodology of defining the temporal variations in given in Jenkin et al. (2000b). In the present application, composite temporal parameters were applied to the total emissions of anthropogenic VOC, biogenic (i.e. natural) VOC and NO_X.***

The temporal profiles were defined either on the basis of real data, or by using one of small set of default profiles. Real data (*e.g.*, fuel consumption, electricity generated, or traffic volumes, which can be related to emissions, and which are themselves temporally resolved) were used to define temporal emissions variations for road transport, power stations, domestic combustion, decorative paints and natural emissions from forests. On the basis of 1998 NAEI data, these categories collectively account for 40.3%, 70.2%, 79.7% and 71.0% of the emissions of VOC, NO_X, CO and SO_2, respectively. Default profiles have been applied to the remaining source categories, on the basis of knowledge of, and available information on, the emitting processes, and by consulting trade associations and other interested bodies.

Composite temporal profiles for each of the 26 emissions maps (each containing contributions from a number of subsectors) were defined from a weighted average of the subsector profiles, using the 1998 NAEI breakdown. The resultant temporal variation of each of the sectors for

VOC and NO_X are shown in Figure 6.2. The corresponding plots for CO and SO_2 can be found in the report by Jenkin *et al.* (2000b). On the basis of these, a series of multipliers have been defined in the OSRM which allow the average emission rate in a given sector (based on the annual total) to be scaled to provide an improved estimate of the actual emission rate of each precursor in a given hour on a given day of the week in a given month.

Whereas CO and SO_2 are unique chemical species, and NO_X is made up of two highly coupled components (NO and NO_2), the speciation of emitted VOC is extremely complex. The current NAEI VOC inventory has 569 speciated entries, each emitted to different extents in 183 source categories. In the interest of computational efficiency, however, the chemical mechanism in the OSRM represents VOC emissions in terms of 13 species and (as indicated above), it is also necessary to represent the 183 source categories by 8 broad source sectors. Where possible, each of the 569 species in the NAEI speciation was therefore assigned one of the 13 species in the chemical mechanism as a surrogate. This assignment was made on the basis of structural class, and also to ensure that the surrogate possessed a similar Photochemical Ozone Creation Potential (POCP). The resultant 13 x 8 species-source matrix (derived from the 569 x 183 species-source matrix) is shown in Table 6.3.

Table 6.3 ***The VOC 13 x 8 species-source breakdown derived from the NAEI 569 x 183 species-source matrix. Source categories are defined in Table 7.1. Assigned species are (respectively): ethane, propane, n-butane, ethene, propene, isoprene, toluene, o-xylene, methanol, formaldehyde, acetaldehyde, acetone, methylethyl ketone.***

	SU	RT	IP	FF	NA	DC	PG	OT	Total
ASSIGNED									
C_2H6	56.40	20.34	73.64	19.31	0.00	5.69	0.03	10.02	**185.42**
C3H8	35.05	0.67	26.07	31.49	0.00	2.44	0.03	7.94	**103.69**
NC4H10	223.78	181.23	71.25	234.04	0.00	17.40	0.31	23.74	**751.74**
C_2H4	4.67	31.74	14.34	0.14	0.00	2.99	0.00	3.64	**57.52**
C3H6	0.00	51.09	9.79	8.94	0.00	3.55	0.18	5.45	**79.00**
C5H8	0.32	0.00	0.00	0.05	178.00	0.00	0.00	0.36	**178.74**
TOLUEN	46.27	92.42	14.07	1.78	0.00	4.19	0.25	5.55	**164.53**
OXYL	63.02	91.90	9.88	0.23	0.00	0.14	0.72	5.14	**171.03**
CH3OH	3.70	0.00	5.39	0.00	0.00	0.00	0.00	0.13	**9.22**
HCHO	0.00	6.32	3.39	0.00	0.00	1.69	3.79	6.68	**21.86**
CH3CHO	0.00	4.02	0.59	0.00	0.00	0.08	0.00	0.95	**5.63**
ACETONE	10.93	1.46	5.92	0.00	0.00	0.03	0.02	0.38	**18.75**
CH3COE	25.30	0.00	3.45	0.00	0.00	0.00	0.00	0.03	**28.77**
	469.43	**481.19**	**237.78**	**295.98**	**178.00**	**38.19**	**5.32**	**70.02**	**1775.92**
UNASSIGNED									
Low ozone	34.35	0.00	14.29	0.00	0.00	0.03	0.00	1.06	**49.74**
Zero ozone	0.00	0.00	0.00	0.00	0.00	0.00	0.00	0.09	**0.09**
Other	28.66	46.09	46.20	2.12	0.00	1.88	1.12	6.45	**132.52**
	63.01	**46.09**	**60.49**	**2.12**	**0.00**	**1.91**	**1.12**	**7.60**	**182.35**
Total	**532.44**	**527.28**	**298.27**	**298.10**	**178.00**	**40.10**	**6.44**	**77.62**	**1958.26**

For some of the 569 species, it was not possible to assign a reasonable surrogate on the basis of the 13 available species. In some cases this is not a significant problem as the species are not potent ozone generators, and it would in fact be more erroneous to use one of the available

surrogates. As shown in Table 6.3, certain species were therefore classed as 'low ozone' (*e.g.* HCFCs) or 'zero ozone' (*e.g.* CFCs), and these are not included in the emissions totals for VOC in the model. However, approximately 7% of the speciated emissions are made up of species for which there is insufficient knowledge about their atmospheric chemistry to be able to assign a surrogate. These are classed in the category 'other' in Table 6.3. This particularly includes species containing silicon, sulphur or nitrogen. The emissions contribution from these species was therefore redistributed *pro rata* to the assigned species in each of the 8 sectors.

The emissions of CO, NO_X, SO_2 and anthropogenic VOC outside the UK are taken from EMEP (www.emep.int), with biogenic VOC emissions based on the estimates of Simpson *et al.* (1995). Anthropogenic emissions as currently assumed to have the same sectoral breakdown as for the UK (Table 6.2), and temporal variations are applied to these, and to biogenic VOC, as described above. The relative VOC speciation within each sector is also taken to be as shown in Table 6.3.

6.4 MODEL PERFORMANCE

6.4.1 Model Performance on an Idealised Trajectory

The performance of the OSRM was initially tested using the idealised Austria-UK trajectory, which leads to elevated ozone concentrations over the UK (Figure 6.3). Figure 6.4 shows a comparison of the ozone evolution along the trajectory calculated for midsummer conditions using the OSRM and the standard version of the PTM/MCM 2.0. Figure 6.5 compares the NO and NO_2 concentrations calculated using the two models. In each case, the biogenic VOC emissions have been disabled to enable the comparison.

The simulated profiles are clearly in reasonable agreement indicating that the treatment of the emissions, chemistry and deposition have been implemented successfully in the OSRM. Minor differences in the performance being attributable to the use of different chemical schemes in the two models, and to the influence of lumping VOC emissions into a limited number of representative species.

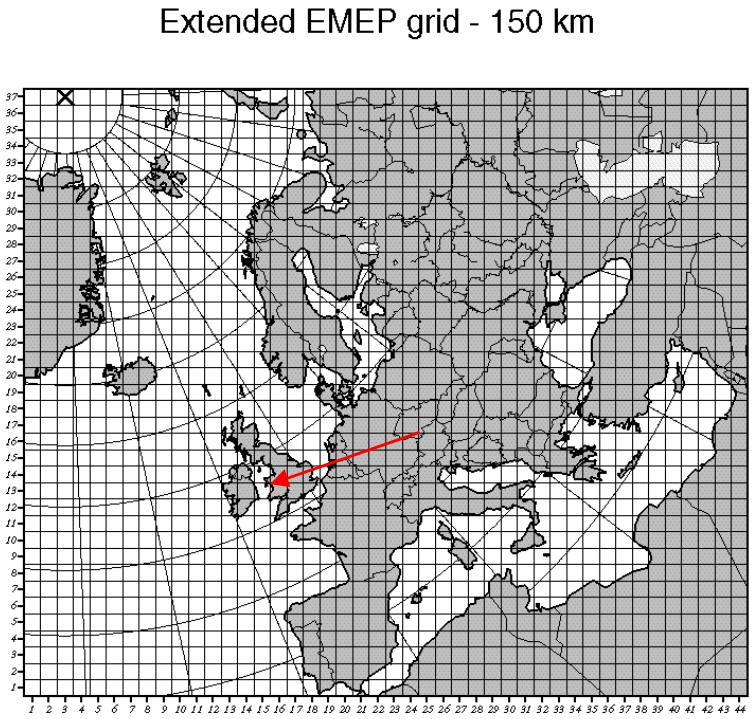

Figure 6.3 ***Idealised Trajectory leading to Elevated Ozone Concentrations over the UK.***

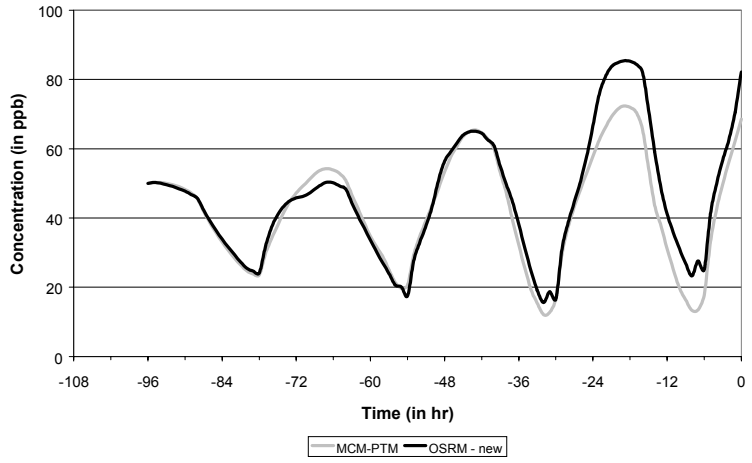

Figure 6.4 ***Comparison of ozone generation along standard Austria-UK trajectory, calculated with OSRM and PTM. Calculations were performed with biogenic VOC emissions excluded.***

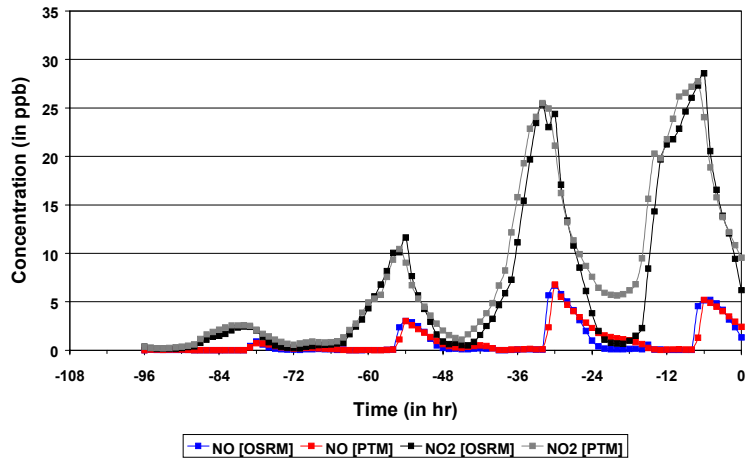

Figure 6.5 ***Comparison of the NO and NO_2 profiles along the standard Austria-UK trajectory, calculated with OSRM and PTM. Calculations were performed with biogenic VOC emissions excluded.***

6.4.2 Model Performance on OFM Trajectories

As part of the Air Quality Forecasting contract let to NETCEN by the Department, ozone concentrations are calculated along air mass trajectories arriving at 16 monitoring sites in the UK Rural Ozone Monitoring Network using an Ozone Forecasting Model (OFM) (Stedman *et al.*, 1997). The model uses 96-hour back trajectories, provided by the Met. Office, which are derived from actual and forecast wind data. The OFM is then used to predict ozone concentrations for air masses arriving at noon on the following day at the selected network sites. The ozone concentrations calculated by the Ozone Forecasting Model for 6 sites are compared with those calculated by the OSRM using the same air mass trajectories in Figure 6.6. Also shown are the measured ozone concentrations for August 1997.

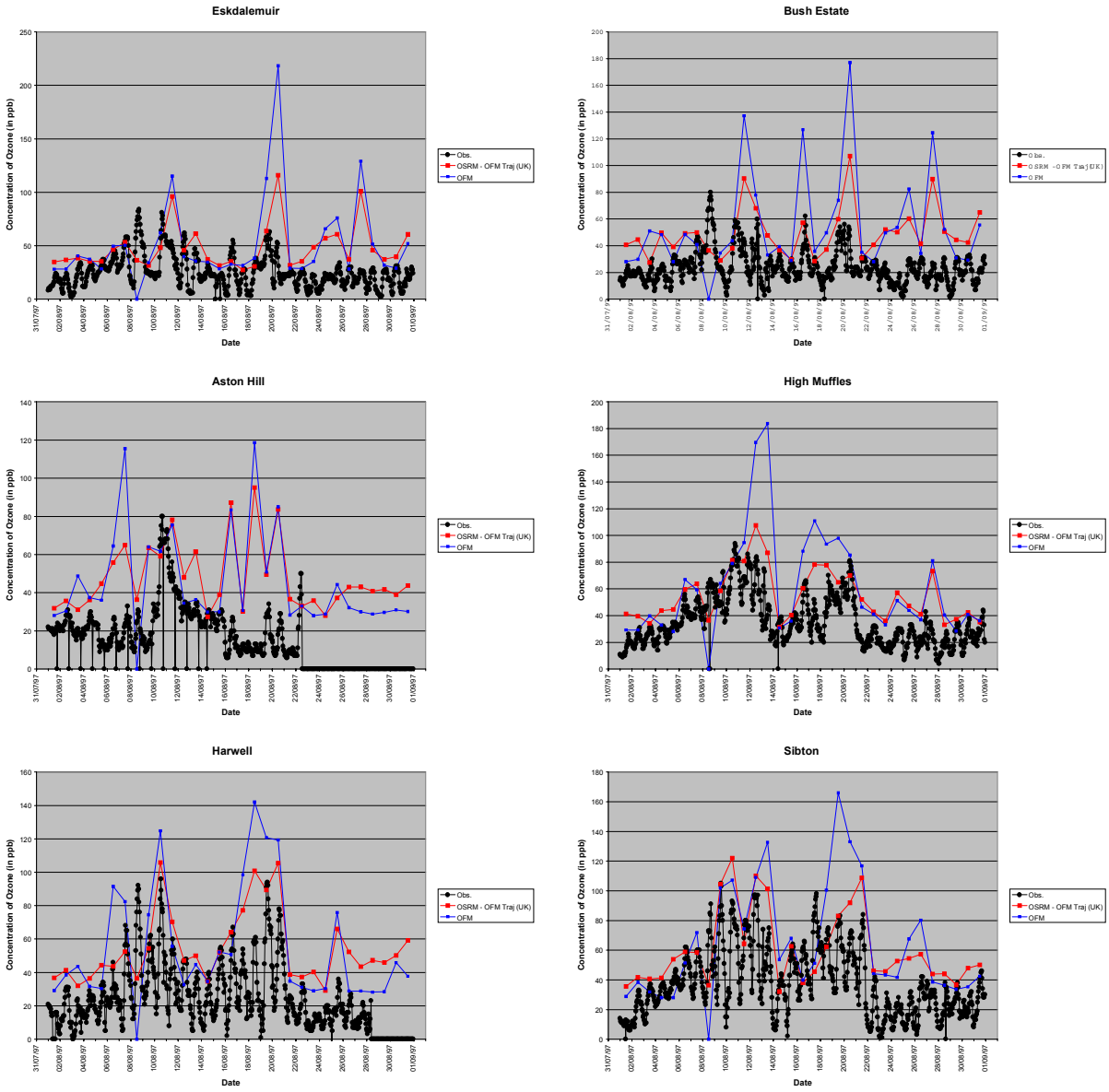

Figure 6.6 ***Comparison of the Ozone Concentrations Calculated for Midday Arrival at 6 Sites in the UK Ozone Monitoring Network Using the Ozone Forecasting and the Ozone Source-Receptor Models for the Same Air Mass Trajectories. Also shown are the Ozone Concentrations Measured at the Sites.***

As the OFM is designed to be a worse-case model and has been necessarily simplified, it will tend to overestimate ozone concentrations. Figure 6.6 shows that the OSRM, with its more realistic treatment of the chemistry, is able to give a better description of the measured ozone concentrations. For Aston Hill, both models overpredict the concentrations in the early part of August, indicating that the actual emissions and/or the air mass trajectories differed from those used in the models.

6.4.3 Model Performance using Calculated Trajectories

The Meteorological Dataset

Real air mass trajectories are calculated in the Ozone Source-Receptor Model using wind fields extracted from global meteorological dataset. Meteorological datasets have been supplied for use with the OSRM in this project by Dr Derwent for the year 1995, 1997 and 1998. The meteorological dataset is a global dataset which has been derived from a general circulation model. The dataset provides 18 meteorological parameters at a horizontal resolution of 0.83° latitude x 1.25° longitude and 11 pressure levels which represent altitudes from the surface to *ca.* 75 mbars or *ca.* 18 km. The temporal resolution is 6 hours with parameters calculated at 00:00, 06:00, 12:00 and 18:00. The parameters provided are:

- **horizontal component (u) of wind**
- **etadot** (derivative of the vertical co-ord.)
- **surface temperature**
- boundary layer depth
- **specific humidity**
- convective cloud amount
- convective cloud top number
- medium cloud amount
- convective precipitation
- **horizontal component (v) of wind**
- **temperature**
- **surface pressure**
- aerodynamic deposition
- cloud liquid water
- convective cloud base number
- low cloud amount
- high cloud amount
- dynamic precipitation

The meteorological data for a specific year was provided as 365 compressed files, one for each day of the year. As each datafile is about 120 Mbytes in size, implying that the annual dataset would need 40 Gbytes of memory, the program used to read the compressed files was adapted to create a smaller archive containing the parameters needed for the OSRM. The parameters highlighted in bold in the above list are those which used in the OSRM.

OSRM Trajectories

The air mass trajectories derived from the wind fields were compared with the air mass trajectories supplied by the Met Office to NETCEN for use in the Ozone Forecasting Model (Stedman *et al.*, 1997). In addition, trajectories can also be calculated on-line using the HYSPLIT programme on the NOAA web-site, http://www.arl.noaa.gov/ready/hysplit4.html. The period 1st August 1997 to 31st August 1997 was selected as a comparison period. During this period, there were several periods of elevated ozone concentrations, most notably on the 10th August 1997 when hourly concentrations at Rochester and Lullington Heath reached 112 and 110 ppb respectively.

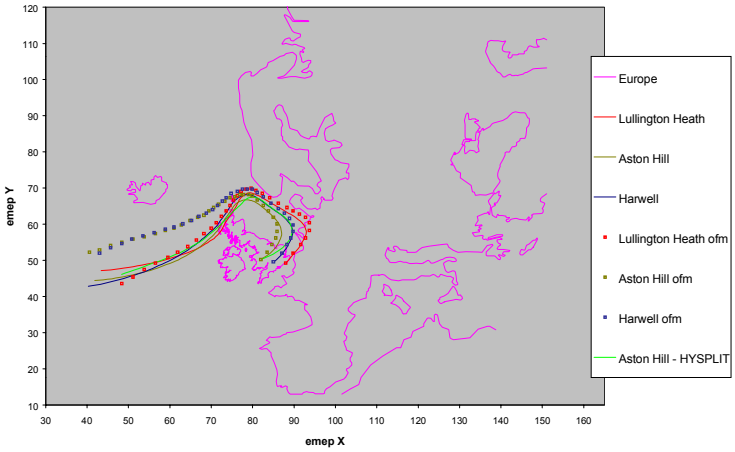

Figure 6.7 ***A Comparison of the Air Mass Trajectories Calculated by the OSRM and those used in the Ozone Forecasting Model for Midday on 5th August 1997 for Harwell (blue), Lullington Heath (red) and Aston Hill (green). For Aston Hill, the HYSPLIT trajectory is also shown.***

Figure 6.7 compares the 96-hour back trajectories arriving at three sites in the UK Rural Ozone Monitoring network - Aston Hill, Harwell and Lullington Heath - at midday on the 5th August 1997. The agreement of the trajectories is good, providing confidence in the OSRM calculations. An indication of the variation that can be expected between the different trajectory calculations can be seen for the Aston Hill trajectories where the OSRM, OFM and HYSPLIT trajectories are all included. The differences in the air mass trajectories will lead to different ozone concentrations at the arrival point, reflecting the different emission totals and hence chemistry that the air masses have experienced.

Comparison with Measured Ozone Concentrations

The OSRM has been used to calculate the hourly ozone concentrations observed in 1997 at 15 monitoring sites in the UK Rural Ozone Monitoring Network. Appendix 2.1 provides a comparison of the individual hourly concentrations calculated using OSRM and those measured. In Appendix 2.2, a comparison is made of the maximum hourly ozone concentration calculated for each day with that measured for the same 15 sites.

Figure 6.8 provides a comparison of the ozone concentrations measured between 1st and 31st August 1997 with the concentrations calculated using the OSRM. The measurements covered a photochemical episode when ozone concentrations were elevated. The model is able to capture many of the maxima and minima in the ozone concentrations although on certain days the peak ozone concentration and the strength of the ozone depletion in the shallow boundary layer at night-time is either over or underestimated.

A number of parameters were determined to evaluate the performance of the EUROSTOCHEM model (see Table 3.2 and Table 3.3 in Section 2). These were (a) *bias*; (b) *fractional bias*; (c) *fraction of model maximum daily maximum concentrations within a factor of 1.5*; and (d) *the coefficient of determination*. A similar evaluation was undertaken on the results obtained using the OSRM for the year 1997. A summary of these statistics for each of the 15 sites is presented in Table 6.4.

Table 6.4 ***Summary of the Statistics of the Comparison of the Model Calculated Maximum Hourly Ozone Concentrations with the Observations from the UK Rural Ozone Monitoring Network for 1997.***

Site	Mean of Observed Maxima	Bias (ppb)	Fractional Bias	Fraction within a factor of 1.5	Coefficient of Determination R^2
Strathvaich Dam	34.20	-3.23	-0.09	0.77	0.58
Aston Hill	36.18	-11.63	-0.28	0.60	0.49
Bush Estate	34.41	-10.89	-0.27	0.63	0.35
Eskdalemuir	35.48	-10.17	-0.25	0.68	0.60
Harwell	36.95	-12.66	-0.29	0.56	0.47
High Muffles	36.37	-10.04	-0.24	0.65	0.42
Ladybower	36.60	-10.35	-0.25	0.58	0.58
Lullington Heath	40.74	-12.21	-0.26	0.62	0.52
Narberth	38.75	-16.23	-0.35	0.58	0.65
Rochester	38.31	-8.75	-0.21	0.61	0.59
Sibton	37.70	-11.31	-0.26	0.61	0.52
Somerton	38.80	-12.35	-0.27	0.62	0.47
Yarner Wood	36.58	-14.71	-0.33	0.58	0.62
Bottesford	33.56	-13.50	-0.33	0.53	0.46
Lough Navar	31.95	-12.63	-0.33	0.65	0.38

The fraction of modelled maximum hourly mean ozone concentrations that lay within a factor of 1.5 below or 1.5 above the observed maximum ozone concentrations varied from 0.53 at Bottesford to about 0.77 at Strathvaich Dam.

6.5 OSRM APPLICATIONS

6.5.1 Modelling NO_y Concentrations

In 2000, a programme of daily measurements of gaseous and aerosol nitrate commenced at the Barcombe Mills site. The measurements were made using a denuder technique by the Centre for Ecology and Hydrology at Edinburgh as part of DEFRA's Acid Deposition Monitoring programme (see Section 4 in Hayman *et al.*, 2001). The measurement programme was stopped in November 2001.

Measurements of the hourly concentrations of ozone, NO and NO_2 are made at the nearby Lullington Heath site using automatic analysers. The two sets of measurements were analysed to identify periods when the concentrations of ozone and the nitrate components were simultaneously elevated, suggesting that the elevated nitrate concentrations could be associated with photochemical activity. Three such periods between April 2000 and July 2001 were identified, as listed in Table 6.5.

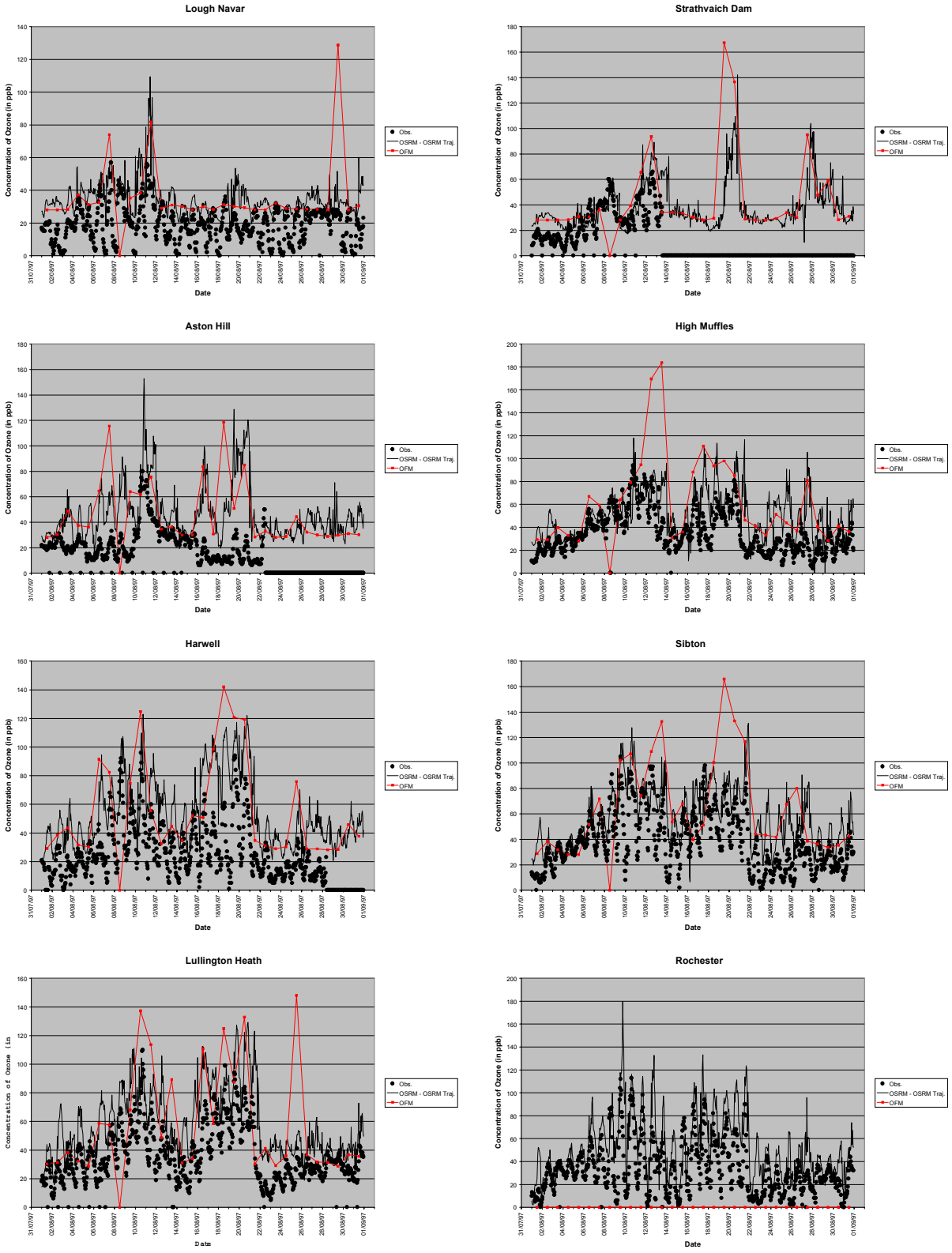

Figure 6.8 ***Comparison of the Ozone Concentrations Observed at Selected Sites in the UK Rural Ozone Monitoring Network between 1st August 1997 and 31st August 1997 with those calculated using the OSRM and OFM.***

Table 6.5 ***Simultaneous Occurrence of Elevated Concentrations of Nitric Acid, Nitrate Aerosol and Ozone Observed at the Barcombe Mills (Nitric Acid, Nitrate Aerosol) and Lullington Heath (Ozone) Sites.***

Date	Peak Concentration		
	HNO_3 (µg m^{-3})	NO_3 (µg m^{-3})	O_3 (ppb)
30 June 2000	6.03	12.48	64
25 June 2001	5.88	1.59	93
03 July 2001	3.87	1.33	86

The June 2001 episode was selected for further analysis. Back trajectories were derived from the Meteorological Archive on the NOAA HYSPLIT web-site for trajectories arriving at every hour at the Lullington Heath site from 00:00 on the 24th June to 12:00 on the 27th June 2001. Figure 6.9 shows the back trajectories arriving at the Lullington Heath Site at Midday and Midnight between 24th June and 27th June 2001. The trajectories shown for 26th June arrive off the continent from an easterly direction. Such trajectories are typically identified with elevated concentrations of photochemical pollutants.

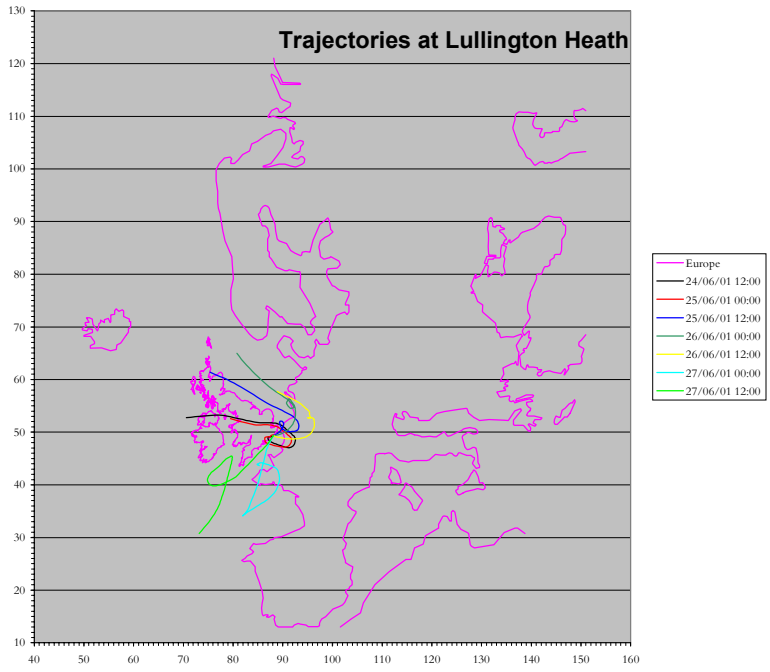

Figure 6.9 ***Back Trajectories derived from the NOAA HYSPLIT Meteorological Archive arriving at the Lullington Heath Site at Midday and Midnight between 24th June and 27th June 2001.***

The Ozone Source-Receptor model was used to simulate the period from 00:00 on the 24th June to 12:00 on the 27th June 2001. The model run used the NOAA HYSPLIT trajectories, the idealised boundary layer profile, temperatures taken from the 1997 meteorological archive and the emission inventories described in 6.3.2. The observed and modelled concentrations of ozone, NO_x (NO and NO_2) and NO_y (HNO_3 and nitrate aerosol) are shown in Figure 6.10. The hourly concentrations calculated for HNO_3 and nitrate aerosol were averaged to give a daily mean concentration for comparison with the measurements.

The OSRM provides a reasonable description of the observed ozone concentration (panel a of Figure 6.10), particularly the ozone peak on the 26th June. The red trace shown on this plot are the ozone concentrations calculated at midday using the Ozone Forecasting Model. Again, the more realistic treatment of the chemistry in the OSRM can provide a better description of the ozone behaviour.

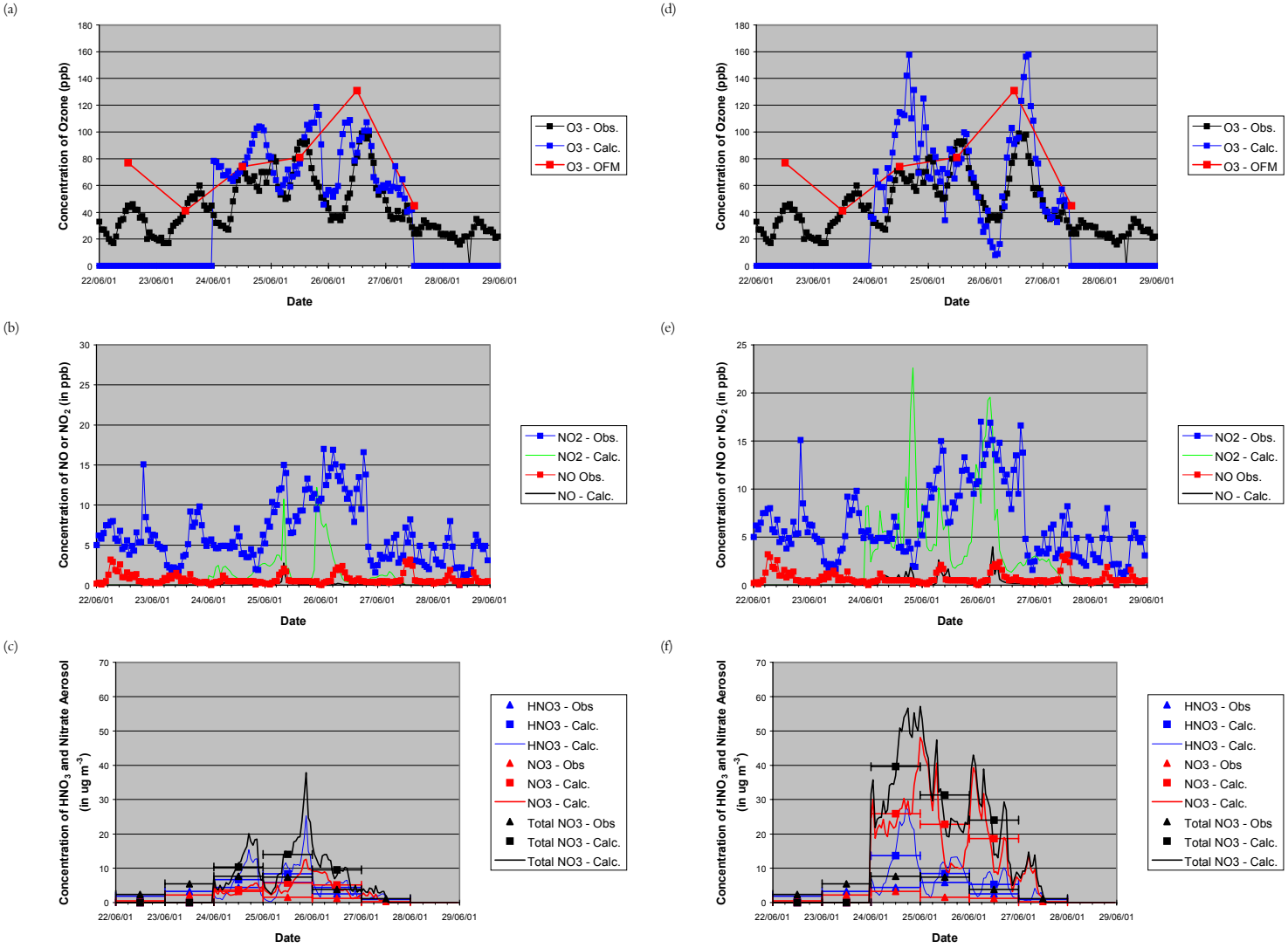

Figure 6.10 ***Comparison of the Observed and Calculated Concentrations of Ozone (Panels a and d), NO_x (Panels b and e) and Nitric Acid and Nitrate Aerosol (Panels c and f) for the Period 24th June 2001 to 27th June 2001. The Calculated Concentrations were determined using the Ozone Source-Receptor Model (Panels a-c) and the PTM-CRI (Panels d-f).***

The concentrations of NO and NO_2 are generally underestimated, as shown in panel b, although specific peaks can be reproduced. This may be a result of the limitation of the model in its treatment of the boundary layer height and its diurnal variation. By contrast, the model significantly overestimates the concentrations of nitric acid and nitrate aerosol, suggesting that the model overestimates the photochemical activity. However, it is encouraging that the model is able to reproduce these concentrations within a factor of 2.

The PTM-CRI, described in Section 7.4, was also used to simulate the concentrations of ozone, NO_x (NO and NO_2) and NO_y (HNO_3 and nitrate aerosol) during the same period. The model used the same NAEI inventory but an older EMEP inventory. The temperature profile and the diurnal variation of the boundary layer height used the values for an idealised photochemical episode in July. The photolysis parameters were derived assuming clear-sky conditions.

Panels d to f of Figure 6.10 show the observed concentrations and those calculated using the PTM-CRI for ozone (panel d), NO_x (NO and NO_2, panel e) and NO_y (HNO_3 and nitrate aerosol, panel f) during this period. The OSRM has a marginally better performance in reproducing the ozone and NO_y concentrations. Some of the differences can be attributed to the emission inventories used and the assumption of clear-sky conditions for the PTM-CRI calculations.

Two main conclusions can be drawn:

- this represents the first comparison of observed (routine) and modelled NO_y concentrations. The performance of the two models is encouraging and further work is needed to optimise the formulation of the NOy chemistry in the models;
- the performance of the OSRM is very comparable to that of the PTM-CRI, an accepted policy tool, for the trajectories and inventories used. Some of the discrepancy is clearly due to the different formulation of for example the chemical mechanism, the photolysis processes and the parameters characterising the boundary layer. This shows that the OSRM is fundamentally robust.

6.5.2 UK Scale Model Runs

The Ozone Source-Receptor model is designed to calculate ozone concentrations at a network of receptor sites. The receptor sites could be UK ozone monitoring sites (as used for the work described in Section 6.4.3) or a regular grid covering the UK, the dimensions of which the user can specify. For the UK scale modelling, the model was designed for receptor sites on a 10 km x 10 km grid (although in principle a higher resolution could be used, this would involve proportionately more trajectory calculations).

To demonstrate that the OSRM model could be used for UK scale modelling, a lower resolution network of receptor sites was used (50 km x 50 km). This reduced the number of receptor sites from nearly 3,000 to about 130 and produced a tractable computational run-time in the limited period of project time then available. Two model runs were undertaken, identical in all respects except that the 1997 meteorological dataset was used for the first run and the 1998 dataset for the second run. The model runs used the same emission inventories as the earlier model calculations and ozone concentrations were calculated at each receptor site for the calendar year.

The ozone concentrations calculated at the receptor sites were then processed to give the AOT40's for crops and for forests for the two years. The AOT40 maps are shown in Figure 6.11. shows the expected decrease in the AOT40 maps from south to north (although the reason for the high values on the east coast of Scotland has not yet been resolved).

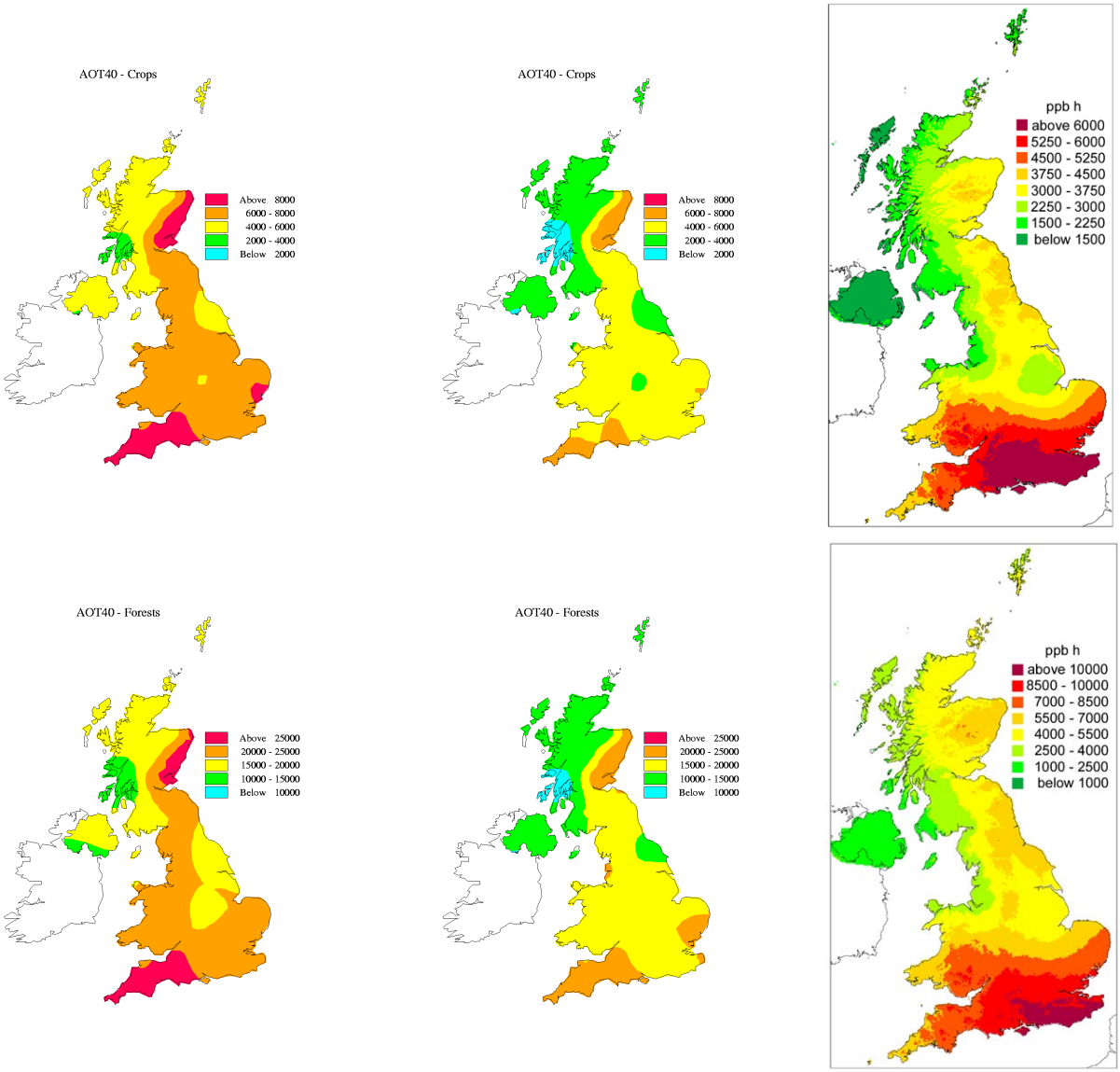

Figure 6.11 ***AOT40 Maps calculated using the Ozone Source-Receptor Model for the Protection of Crops (Left-hand Panels) and of Forests (Middle Panels) for the Years 1997 and 1998. The Right-hand Panels, taken from the NEGTAP report (2001) show the AOT40 Maps calculated for the Protection of Crops (Upper Panel) and of Forests (Lower Panel) from Ozone Measurements made in the UK between 1994 and 1998.***

Figure 6.11 also includes the AOT40 maps, taken from the NEGTAP report (NEGTAP, 2001), which have been derived from the measurements between 1994 and 1998. It is apparent that the model calculated AOT40 values are significantly higher than those derived from the measurements. This is not surprising as the annual means calculated for the UK ozone monitoring sites in 1997 were as much as 16 ppb higher than those observed. It is well known that the AOT40 parameter is extremely sensitive to systematic biases. Apart from the high values on the east coast of Scotland, the model-derived maps give a reasonable description of the observed spatial distribution. It is interesting to note that the annual mean concentrations at the

Yarner Wood and Narberth site show the largest difference between the modelled and observed values. This might explain the high values in the South West of England.

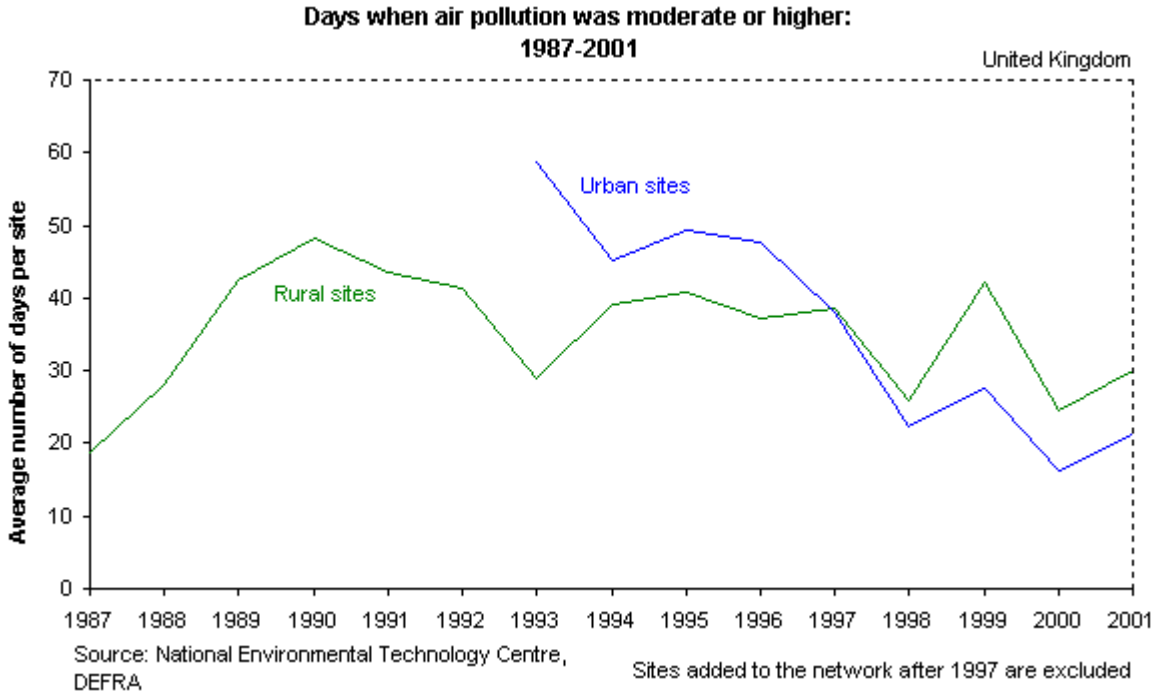

Figure 6.12 ***Trends in the Air Quality Indicator for Urban and Rural Locations showing that 1998 was a Lower Pollution Year compared to 1997.***

As shown in Figure 6.12 (taken from the DEFRA web-site, http://www.sustainable-development.gov.uk/indicators/headline/h10.htm), the air quality indicator for rural locations, which largely reflects the number of ozone exceedences, was lower in 1998 than in 1997. The AOT40 maps calculated by the OSRM for the year 1998 have significantly lower values than those shown in the corresponding 1997 maps, indicating that either dispersion was better in 1998 or that the meteorological conditions were less conducive to ozone production. The OSRM model is thus able to reproduce the difference caused by the changes in the meteorology from 1997 to 1998.

6.5.3 NO_x versus VOC Sensitivity

It is of interest in developing ozone control policy to know whether the focus should be on controlling the NO_x or VOC emissions preferentially. Model calculations presented in Figure 8.4 of Section 8.2 show that the southern half of the UK is generally VOC-limited (*i.e.*, VOC emission control will produce a greater reduction in ozone concentrations than the same control in NO_x emissions) with the northern part of the UK NO_x-limited (*i.e.*, NO_x emission control will produce a greater reduction in ozone concentrations). The model calculations used emissions appropriate to 1995 and linear easterly air mass trajectories which are typical of those found under episode conditions.

In Section 3.6, the EUROSTOCHEM model was also used to investigate the effect of separate 30% reductions to the anthropogenic emissions of VOCs and NO_x across the entire model domain. The same percentage reduction was applied across-the-board without spatial and temporal variation. The choice of this percentage reduction is arbitrary and has no regional policy significance.

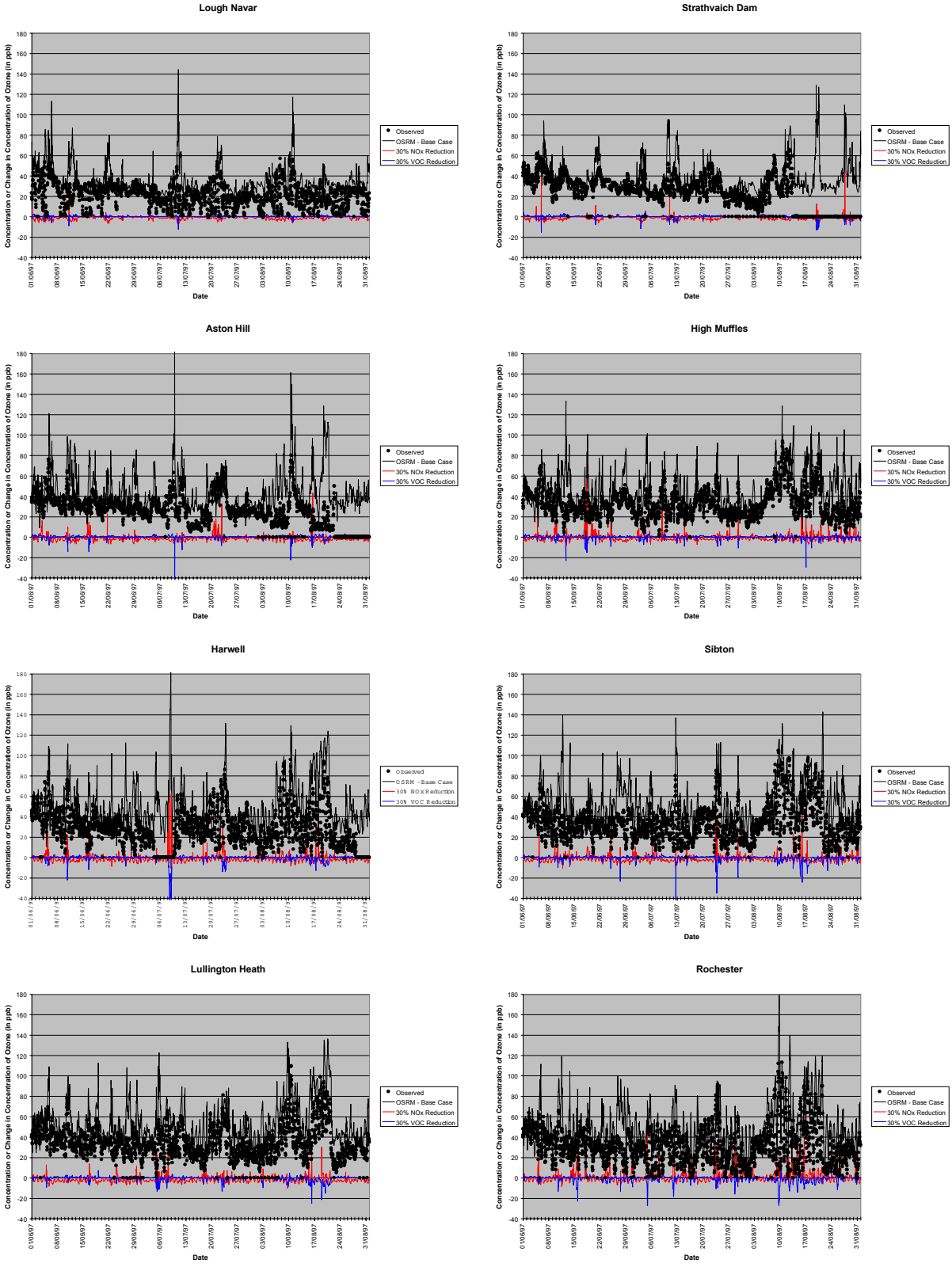

Figure 6.13 ***Plots of the Observed (circles) and the Calculated Base Case (solid black line) Ozone Concentrations for 8 UK Ozone Monitoring Sites for the Period June to August 1997. The Ozone Concentrations Calculated as a Difference from the Base Case are shown for a 30% Reduction in the Emissions of NOx (solid red line) and of VOC (solid blue line).***

In this section, these emission control scenarios were investigated using the OSRM, which incorporates more recent emission inventories and allows for the emissions to have a temporal variation. Three model runs were undertaken for the calendar year of 1997. A base case run was undertaken followed by runs in which the emissions of NO_x and VOCs were separately reduced by 30%. In Figure 6.13, the ozone concentrations calculated in the base case run are compared to the observed concentrations for 8 of the sites for the period, 1st June to 31st August 1997. The figure also includes, as the difference between the ozone concentrations calculated for the emission reduction scenario and the base case run (*i.e.*, $\Delta[O_3] = [O_3]$ scenario - $[O_3]$ base case), the results for the two emission reduction scenarios (the NOx emission reduction in red and the VOC emission reduction in blue).

As described in Section 3.6.3, if the model response to the 30% NO_x reduction is more negative than that to the 30% VOC reduction then that trajectory or day is classified as NO_x-sensitive. Conversely, if the model response to the 30% VOC reduction is more negative than that to the 30% VOC reduction then the day is classified as VOC-sensitive. Table 6.6 summarises the response to these emission reduction scenarios for (a) every hourly measurements in the year, (b) the mean of the 24 hourly measurements in each day, (c) the maximum of the 24 hourly measurements in each day and (d) the maximum of the 24 hourly measurements in each day for the period from 1st April to 31st August 1997 (which will allow comparison with the EUROSTOCHEM calculations).

The results reported in Table 6.6 indicate that a 30% reduction in the NO_x emissions have a greater influence on 40 ppb exceedence days at the UK Rural Ozone Monitoring Network sites compared with 30% reduction in the VOC reduction. For the higher O_3 exceedence thresholds, the results indicate a shift towards a greater response from VOC emission control. The responses agree reasonably well with those reported using the EUROSTOCHEM model (also shown in Table 6.6 and taken from Table 3.9) for all data and for the peak O_3 concentration but differ on occasions at the intermediate threshold levels.

As described later in Section 8.3.2, the PTM-CRI was used to investigate the response of ozone concentrations to 30% reductions in the emissions of VOC and NO_X. The PTM-CRI calculations were limited to 8 southern UK sites (Aston Hill, Harwell, Lullington Heath, Rochester, Sibton, Somerton, Wicken Fen and Yarner Wood) and to a single trajectory for each site on the 10th August 1997. The PTM-CRI model results are compared in Table 6.7 with the responses determined at the sites on this day using the OSRM.

Table 6.7 ***Comparison of sensitivity to 30% precursor reductions for 10 August 1997 episode at the 8 southern UK sites using the CRI-PTM and the OSRM. V = VOC-limited; N = NO_X-limited.***

	AH	HW	LH	RO	SI	SO	WF	YW
PTM	V	N	N	V	V	N	V	N
OSRM	V	N	N	N	V	N	V	N

The results show that the two models gave similar conclusions concerning the VOC or NO_X sensitivity at 7 of the 8 sites.

Table 6.6 ***Sensitivity to 30% NO_x and VOC Emission Reductions Determined by the OSRM and Comparison to EUROSTOCHEM Results.***

Site	Ozone Statistic	OSRM Sensitivity to 30% Emission Reduction							EUROSTOCHEM Sensitivity to 30% Emission Reduction						
		# of NOx Sensitive Values	Total # of Values	All Data	O_3 > 40 ppb	O_3 > 60 ppb	O_3 > 90 ppb	Max O_3	# of NOx Sensitive Values	Total # of Values	All Data	O_3 > 40 ppb	O_3 > 60 ppb	O_3 > 90 ppb	Max O_3
Strathvaich Dam	All Hourly Data - 1997	6341	8635	NOx	NOx	NOx	VOC	VOC							
	Mean Daily Conc - 1997	249	360	NOx	NOx	NOx	-	VOC							
	Max Daily Conc - 1997	255	360	NOx	NOx	NOx	VOC	VOC							
	Max Daily Conc - Apr-Aug 1997	131	153	NOx	NOx	NOx	VOC	VOC	128	152	NOx	NOx	VOC	VOC	NOx
Aston Hill	All Hourly Data - 1997	4510	8635	NOx	NOx	NOx	NOx	VOC							
	Mean Daily Conc - 1997	177	360	VOC	NOx	NOx	VOC	VOC							
	Max Daily Conc - 1997	205	360	NOx	NOx	NOx	-	VOC							
	Max Daily Conc - Apr-Aug 1997	109	153	NOx	NOx	NOx	NOx	VOC	101	152	NOx	VOC	VOC	VOC	VOC
Bush Estate	All Hourly Data - 1997	3824	8635	VOC	NOx	NOx	VOC	NOx							
	Mean Daily Conc - 1997	148	360	VOC	NOx	VOC	-	VOC							
	Max Daily Conc - 1997	184	360	NOx	NOx	NOx	VOC	VOC							
	Max Daily Conc - Apr-Aug 1997	108	153	NOx	NOx	NOx	VOC	VOC	123	152	NOx	NOx	VOC	VOC	NOx
Eskdalemuir	All Hourly Data - 1997	4704	8635	NOx	NOx	NOx	NOx	VOC							
	Mean Daily Conc - 1997	182	360	NOx	NOx	VOC	VOC	VOC							
	Max Daily Conc - 1997	222	360	NOx	NOx	NOx	VOC	VOC							
	Max Daily Conc - Apr-Aug 1997	123	153	NOx	NOx	NOx	VOC	VOC							
Great Dun Fell	All Hourly Data - 1997	4503	8635	NOx	NOx	NOx	VOC	VOC							
	Mean Daily Conc - 1997	180	360	-	NOx	NOx	VOC	VOC							
	Max Daily Conc - 1997	205	360	NOx	NOx	NOx	-	VOC							
	Max Daily Conc - Apr-Aug 1997	113	153	NOx	NOx	NOx	-	VOC	105	152	NOx	NOx	VOC	VOC	VOC
Harwell	All Hourly Data - 1997	3339	8635	VOC	NOx	NOx	VOC	VOC							
	Mean Daily Conc - 1997	127	360	VOC	NOx	VOC	VOC	VOC							
	Max Daily Conc - 1997	167	360	VOC	NOx	NOx	NOx	VOC							
	Max Daily Conc - Apr-Aug 1997	106	153	NOx	NOx	NOx	NOx	VOC	102	152	NOx	VOC	VOC	VOC	VOC
High Muffles	All Hourly Data - 1997	3467	8635	VOC	NOx	NOx	NOx	VOC							
	Mean Daily Conc - 1997	130	360	VOC	NOx	NOx	-	VOC							
	Max Daily Conc - 1997	162	360	VOC	NOx	NOx	VOC	VOC							
	Max Daily Conc - Apr-Aug 1997	101	153	NOx	NOx	NOx	VOC	VOC	94	152	NOx	VOC	VOC	VOC	NOx
Ladybower	All Hourly Data - 1997	2144	8635	VOC	NOx	NOx	VOC	NOx							
	Mean Daily Conc - 1997	67	360	VOC	VOC	VOC	VOC	VOC							
	Max Daily Conc - 1997	114	360	VOC	VOC	VOC	VOC	VOC							
	Max Daily Conc - Apr-Aug 1997	68	153	VOC	VOC	NOx	VOC	VOC	84	152	NOx	VOC	VOC	VOC	VOC
Lullington Heath	All Hourly Data - 1997	3403	8635	VOC	NOx	NOx	NOx	VOC							
	Mean Daily Conc - 1997	125	360	VOC	NOx	NOx	VOC	VOC							
	Max Daily Conc - 1997	164	360	VOC	NOx	NOx	NOx	VOC							
	Max Daily Conc - Apr-Aug 1997	105	153	NOx	NOx	NOx	NOx	VOC	104	152	NOx	VOC	VOC	VOC	VOC

Table 6.6 ***Sensitivity to 30% NOx and VOC Emission Reductions Determined by the OSRM and Comparison to EUROSTOCHEM Results. (cont.)***

Site	Ozone Statistic	OSRM Sensitivity to 30% Emission Reduction							EUROSTOCHEM Sensitivity to 30% Emission Reduction						
		# of NOx Sensitive Values	Total # of Values	All Data	O_3 > 40 ppb	O_3 > 60 ppb	O_3 > 90 ppb	Max O_3	# of NOx Sensitive Values	Total # of Values	All Data	O_3 > 40 ppb	O_3 > 60 ppb	O_3 > 90 ppb	Max O_3
Narberth	All Hourly Data - 1997	4982	8635	NOx	NOx	NOx	NOx	NOx							
	Mean Daily Conc - 1997	200	360	NOx	NOx	NOx	VOC	VOC							
	Max Daily Conc - 1997	226	360	NOx	NOx	NOx	NOx	NOx							
	Max Daily Conc - Apr-Aug 1997	120	153	NOx	NOx	NOx	NOx	NOx	105	152	NOx	VOC	VOC	VOC	VOC
Rochester	All Hourly Data - 1997	1794	8635	VOC	NOx	VOC	VOC	VOC							
	Mean Daily Conc - 1997	57	360	VOC	VOC	VOC	VOC	VOC							
	Max Daily Conc - 1997	98	360	VOC	VOC	VOC	VOC	VOC							
	Max Daily Conc - Apr-Aug 1997	79	153	NOx	NOx	VOC	VOC	VOC	99	152	NOx	NOx	VOC	VOC	VOC
Sibton	All Hourly Data - 1997	3010	8635	VOC	NOx	NOx	VOC	VOC							
	Mean Daily Conc - 1997	102	360	VOC	NOx	VOC	VOC	VOC							
	Max Daily Conc - 1997	138	360	VOC	NOx	NOx	VOC	VOC							
	Max Daily Conc - Apr-Aug 1997	100	153	NOx	NOx	NOx	VOC	VOC	100	152	NOx	NOx	VOC	VOC	VOC
Somerton	All Hourly Data - 1997	4224	8635	VOC	NOx	NOx	NOx	VOC							
	Mean Daily Conc - 1997	164	360	VOC	NOx	NOx	NOx	NOx							
	Max Daily Conc - 1997	198	360	NOx	NOx	NOx	NOx	VOC							
	Max Daily Conc - Apr-Aug 1997	108	153	NOx	NOx	NOx	NOx	VOC	105	152	NOx	NOx	VOC	VOC	VOC
Wharleycroft	All Hourly Data - 1997	4421	8635	NOx	NOx	NOx	VOC	VOC							
	Mean Daily Conc - 1997	176	360	VOC	NOx	NOx	VOC	VOC							
	Max Daily Conc - 1997	198	360	NOx	NOx	NOx	VOC	VOC							
	Max Daily Conc - Apr-Aug 1997	113	153	NOx	NOx	NOx	-	VOC							
Wicken Fen	All Hourly Data - 1997	2849	8635	VOC	NOx	NOx	VOC	VOC							
	Mean Daily Conc - 1997	91	360	VOC	NOx	VOC	VOC	VOC							
	Max Daily Conc - 1997	125	360	VOC	NOx	-	VOC	VOC							
	Max Daily Conc - Apr-Aug 1997	93	153	NOx	NOx	NOx	VOC	VOC							
Wray	All Hourly Data - 1997	4128	8635	VOC	NOx	NOx	NOx	VOC							
	Mean Daily Conc - 1997	163	360	VOC	NOx	VOC	VOC	VOC							
	Max Daily Conc - 1997	204	360	NOx	NOx	-	NOx	VOC							
	Max Daily Conc - Apr-Aug 1997	21	31	NOx	NOx	-	NOx	NOx							
	All Hourly Data - 1997	115	153	NOx	NOx	NOx	NOx	VOC							
Yarner Wood	Mean Daily Conc - 1997	4952	8635	NOx	NOx	NOx	NOx	VOC							
	Max Daily Conc - 1997	201	360	NOx	NOx	NOx	-	NOx							
	Max Daily Conc - Apr-Aug 1997	221	360	NOx	NOx	NOx	NOx	VOC							
	All Hourly Data - 1997	117	153	NOx	NOx	NOx	NOx	VOC	109	152	NOx	VOC	VOC	VOC	VOC
Bottesford	Mean Daily Conc - 1997	2527	8635	VOC	NOx	NOx	VOC	VOC							
	Max Daily Conc - 1997	85	360	VOC	NOx	VOC	VOC	VOC							
	Max Daily Conc - Apr-Aug 1997	119	360	VOC	NOx	VOC	VOC	VOC							
	All Hourly Data - 1997	84	153	NOx	NOx	VOC	VOC	VOC	86	152	NOx	VOC	VOC	VOC	VOC

Table 6.6 ***Sensitivity to 30% NOx and VOC Emission Reductions Determined by the OSRM and Comparison to EUROSTOCHEM Results. (cont.)***

Site	Ozone Statistic	OSRM Sensitivity to 30% Emission Reduction							EUROSTOCHEM Sensitivity to 30% Emission Reduction						
		# of NOx Sensitive Values	Total # of Values	All Data	O_3 > 40 ppb	O_3 > 60 ppb	O_3 > 90 ppb	Max O_3	# of NOx Sensitive Values	Total # of Values	All Data	O_3 > 40 ppb	O_3 > 60 ppb	O_3 > 90 ppb	Max O_3
Glazebury	Mean Daily Conc - 1997	2071	8635	VOC	NOx	VOC	VOC	VOC							
	Max Daily Conc - 1997	58	360	VOC	VOC	VOC	VOC	VOC							
	Max Daily Conc - Apr-Aug 1997	113	360	VOC	VOC	VOC	VOC	VOC							
	Daily Max Conc - April-August	71	153	VOC	VOC	VOC	VOC	VOC							
Lough Navar	All Hourly Data	6226	8635	NOx	NOx	NOx	NOx	VOC							
	Daily Mean Conc	256	360	NOx	NOx	NOx	-	NOx							
	Daily Max Conc	267	360	NOx	NOx	NOx	-	VOC							
	Daily Max Conc - April-August	137	153	NOx	NOx	NOx	NOx	VOC	137	152	NOx	NOx	NOx	VOC	VOC

7 Improvements to Chemical and Photochemical Reaction Schemes

7.1 SECTION SUMMARY

The Master Chemical Mechanism is an important component of the work to assess the contribution that individual volatile organic compounds (and hence emission sources) make to ozone formation. This will assist the development of policies to identify and target the VOCs or source sectors for control.

During the present contract, major improvements have been made to the reaction mechanisms of aromatic compounds - an important class of ozone-producing VOCs. Revision of the photolysis rates has been carried out, particularly with regard to multifunctional carbonyl products formed in the aromatic systems. The Master Chemical Mechanism has also been expanded to include the important biogenic compounds - α and β pinene. The new reaction schemes for aromatic compounds and terpenes have been tested against measurements made in chamber studies and the latest version of the Master Chemical Mechanism is able to reproduce those measurements, giving confidence in the MCM.

Using the knowledge and understanding gained from developing the MCM, a reduced mechanism - the Common Reactive Intermediate (CRI) mechanism - has been derived from the Master Chemical Mechanism. The CRI mechanism treats the degradation of methane and 120 VOC using approximately. 570 reactions of 270 species (*i.e.* about 2 species per VOC). It thus contains only 5% of the number of reactions and 7% of the number of chemical species in MCM v2, providing a computationally economical alternative mechanism for use in the Photochemical Ozone Trajectory Model. The CRI mechanism has been benchmarked against the MCM and was shown to produce almost identical concentrations for key species (O_3, OH, NO_3, RO_2 and HO_2) to those calculated using the full Master Chemical Mechanism.

The Master Chemical Mechanism continues to be widely used and is increasingly accepted as the benchmark for an explicit chemical mechanism of hydrocarbon oxidation. Version 3 and earlier versions of the MCM are available on the MCM web-site hosted by the University of Leeds.

7.2 INTRODUCTION

A key component of ozone models is a description of the sunlight-initiated chemical processing of emitted VOC and NO_X which leads to the generation of ozone in the boundary layer. The activities carried out within Task 5 therefore focus on the development of robust chemical mechanisms based on the latest information available, and the testing and validation of these mechanisms for their performance in policy related calculations. The specific activities carried out are as follows:

- Development the Master Chemical Mechanism (MCM v3).
- Development of a Common Representative Intermediates (CRI) mechanism.
- Testing and application of both the MCM and the CRI mechanism in the Photochemical Trajectory Model (PTM).

The following sections summarise the progress made on these activities during the course of the work programme, and provide recommendations for future work.

7.3 THE MASTER CHEMICAL MECHANISM, VERSION 3 (MCM V3)

7.3.1 Introduction

The Master Chemical Mechanism is a near-explicit chemical mechanism describing the detailed degradation of a large number of emitted VOC, and the resultant generation of ozone and other secondary pollutants, under conditions appropriate to the planetary boundary layer. Within the current programme, version 3 of the mechanism (MCM v3) has been completed. The mechanism describes the degradation of methane and 124 non-methane VOC (see Appendix 3), and comprises 46 inorganic reactions, 12691 organic reactions, and 4351 species. The non-methane VOC degraded in the MCM were selected on the basis of the speciation determined by the NAEI. Although the inventory currently contains over 500 entries, the 124 non methane VOC considered in the MCM give *ca.* 70% coverage of the mass emissions of unique chemical species, and are therefore believed to provide a reasonable representation of major organic compounds emitted into the boundary layer over the UK and other populated regions.

With the exception of 18 aromatic compounds, the degradation chemistry in the MCM was originally developed using a published protocol (Jenkin *et al.*, 1997). Where appropriate, this includes degradation initiated by reaction with the hydroxyl radical (OH), the nitrate radical (NO_3) and ozone, and direct photolysis. OH-initiated chemistry is important for all the VOC, and generally follows the pattern shown in Figure 7.1. This illustrates the free radical-catalysed oxidation of a given VOC into a series of first generation oxidised products, and the associated formation of ozone (O_3) as a by-product when NO_X is present. The first-generation products are further degraded to form second- and subsequent-generation products until the complete degradation to CO_2 is achieved (see Jenkin *et al.*, 1997).

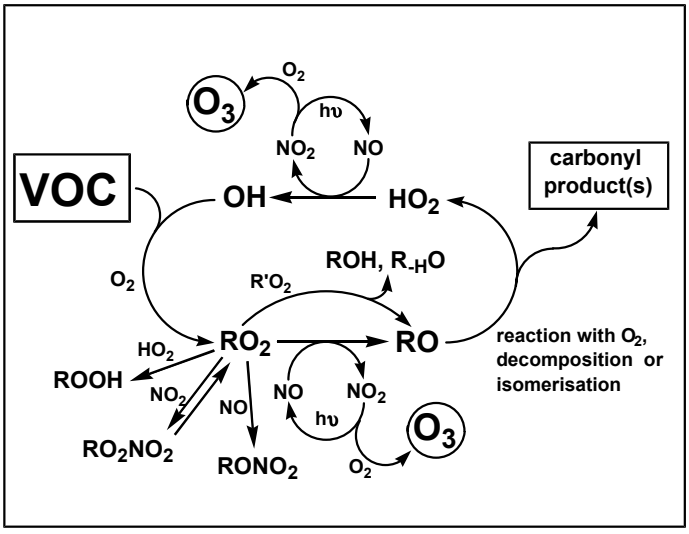

Figure 7.1 ***Schematic Representation of the OH-initiated Oxidation of a Generic VOC into its First Generation Products. The Main Free Radical-catalysed Cycle (involving OH, RO_2, RO and HO_2) Provides the Coupling with NO_X, and Leads to the Formation of Ozone as a By-product.***

The major specific improvements made to the MCM within the current work programme may be summarised as follows:

(a) Revision of the chemistry of 18 aromatic VOC

(b) Revision of the chemistry of α-pinene and inclusion of degradation schemes for β-pinene and 2,3-dimethyl-2-butene (tetramethylethene)

(c) Complete update of generic rate coefficients within the mechanism

(d) Revision of oxy radical chemistry in alkane, alkene and alcohol schemes

Further details on items (a) and (b) are provided below.

7.3.2 The MCM v3 Web-site

The MCM can be accessed from the home web page of the School of Chemistry at the University of Leeds, http://www.chem.leeds.ac.uk/Atmospheric/MCM/mcmproj.html. There is a login procedure, principally to get some idea of the interest and usefulness of the site. Since the launch in January 1997, more than 900 users from 54 countries worldwide have registered, and have had access to the MCM. The major countries are UK and USA (which have approximately 160 and 220 users, respectively), Germany and France (which have 70 and 40 users, respectively) and Canada, Sweden, Italy, Australia and Holland (which all have ≥ 22 users).

The web site provides a platform on which to make the MCM available to a wider scientific community, since a code containing thousands of lines would be impossible to publish in hard copy, and would also be very hard to read. It consists of an introduction to the project, with appropriate references, followed by a separate page describing the chemistry of each of the 124 VOC: referred to as a VOC scheme. To avoid duplicating intermediate reactions in more than one scheme, a given VOC scheme does not usually contain all the reactions necessary to describe its complete degradation in isolation. Thus to construct the complete mechanism for a given VOC, sections from several schemes invariably need to be combined. To assist this, a specially designed 'subset assembler tool' is available, which enables the user to select any number compounds from the primary VOC list, and extract a complete degradation mechanism for that subset. Options for the resultant file storage are also available, including a simple mechanism listing and FACSIMILE format.

7.3.3 Aromatic VOC: Mechanism Development Framework

Aromatic hydrocarbons are known to be of particular importance in regional-scale ozone formation in Europe, potentially making a contribution which is greater than any other class of VOC (Derwent *et al.*, 1996). However, it is also becoming increasingly well established that the detailed mechanisms by which aromatic hydrocarbons are degraded do not follow the general pattern of VOC oxidation (described above), and this is necessarily an active area of research with new information constantly emerging (*e.g.*, Bohn and Zetzsch, 1999; Moschonas *et al.*, 1999; Smith *et al.*, 1999; Ghigo and Tonachini, 1999; Berndt *et al.*, 1999; Barnes *et al.*, 2000; Volkamer *et al.*, 2000). The representation of aromatic degradation in MCM v3 has therefore been substantially revised from that in previous versions of the mechanism, to take account of information available in the literature up to the beginning of 2001.

The mechanisms for the 18 aromatic VOC in the MCM (Appendix 3) have been updated with the aim of fulfilling a number of criteria:

(a) *to represent the complete degradation*;
(b) *to give a reasonable description of known organic product formation and, where possible, yields*;
(c) *to give a description of ozone formation which is consistent with hydrocarbon/NO_X chamber observations*;
(d) *to include speciated organic products which are known to contribute to secondary organic aerosol (SOA) formation and growth.*

Some of the features are illustrated in the schematic in Figure 7.2, which emphasises the multi-step nature of the oxidation mechanisms, and the role aromatic hydrocarbons can have in the generation of ozone and SOA. Although the primary goal of the present project is to provide an

acceptable description of ozone formation, a significant proportion of the available information on speciated products, and therefore the precise oxidation pathways, comes from measurements of aerosol phase components (*e.g.* Forstner *et al.*, 1997; Kamens *et al.*, 2001). As a result, the scheme development work also provides the initial basis for representing gas-aerosol partitioning of speciated products in future work, and the role aromatic oxidation plays in fine particle formation.

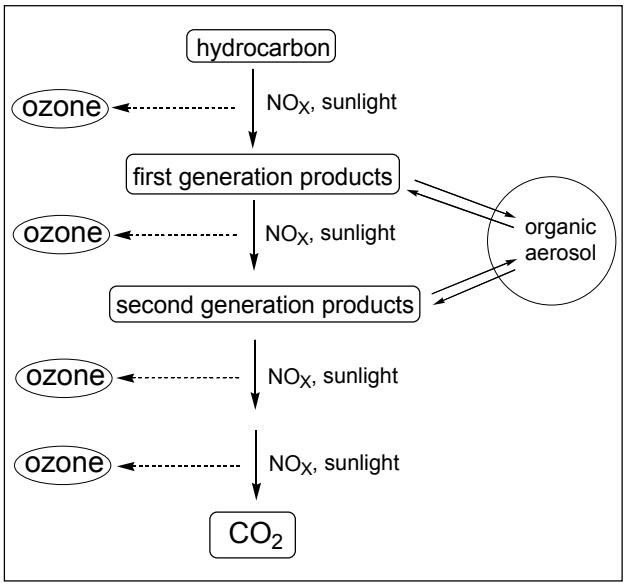

Figure 7.2 ***Simplified schematic of the complete oxidation of a hydrocarbon to CO_2 (and H_2O). The figure demonstrates that a number of oxidation steps are usually required, with ozone potentially generated at each stage. In addition, the potential for gas-aerosol partitioning exists for certain products (particularly some of the products of aromatic or terpene oxidation), with a resultant contribution to SOA formation and growth.***

A reasonable amount of quantitative information on first generation products is now available, at least for the oxidation of selected aromatics. The primary oxidation steps must include (i) minor routes to aromatic aldehydes (except in the case of benzene), (ii) routes to phenolic compounds, (iii) routes to the formation of α-dicarbonyls (and co-products) and (iv) a minor route which can lead to the subsequent formation of para-quinones. In the majority of cases for which information is available, these routes do not provide a complete carbon balance, and additional routes need to be invoked, based on other detected (but unquantified) products.

Using *p*-xylene as an example, the main features of the primary oxidation step are illustrated in Figure 7.3 to Figure 7.5. Figure 7.3 shows some of the peroxy radicals which can be generated following the attack of OH. The minor abstraction route from the methyl side group generates a conventional type of peroxy radical which, as shown in Figure 7.4, leads to the generation of the quantified aromatic aldehyde, p-tolualdehyde (*e.g.* Smith *et al.*, 1999). The sequential addition of OH and O_2 to the aromatic ring potentially generates five different hydroxy peroxy radicals, of which three are shown in the figure. These are represented by the two boxed structures, representing 1,2- and 1,4 addition. As shown in Figure 7.4, the more minor 1,4-hydroxy peroxy radical leads to the generation of a product which may be further oxidised to the observed para-quinone, 2,5-dimethyl-1,4-benzoquinone (*e.g.* Smith *et al.*, 1999).

The majority of the OH attack generates the 1,2-hydroxy peroxy radical, the subsequent chemistry of which is summarised in Figure 7.5. This shows the routes to the generation of 2,5-dimethylphenol (**I**), and via the 'peroxide-bridged' intermediates to the C_2 and C_3 ring-opened α-dicarbonyls, glyoxal and methyl glyoxal (and co-products), the yields of which are reasonably well quantified. The balance of the reaction is assumed to proceed via an epoxy-oxy radical to yield an epoxydicarbonylene (**IV**). Evidence for this route has been reported (Jeffries *et al.*, 1995), although the yield of the epoxy product has not been quantified. The broken arrows in Figure 7.5 show additional routes which have been postulated but which are not currently

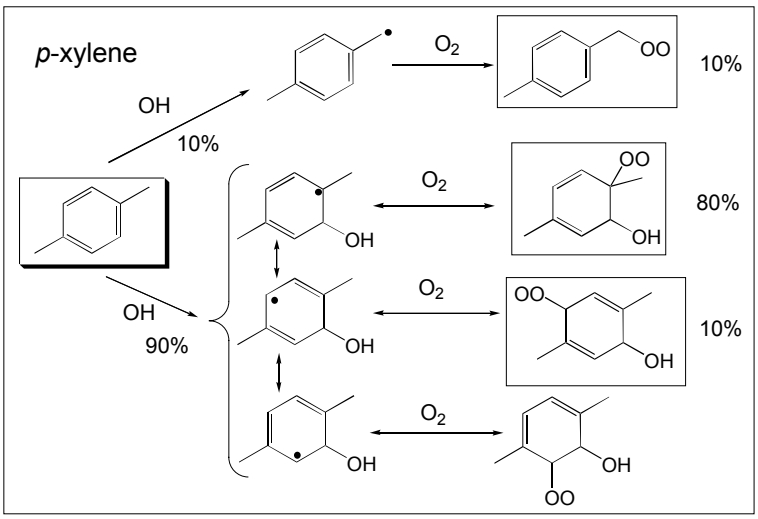

Figure 7.3 ***Schematic representation of the peroxy radicals generated from the OH initiated oxidation of p-xylene. Radicals resulting from addition of OH to the aromatic ring are only shown for one of the two possible attack positions. Boxed species are representatives of all possible peroxy radicals, as used in scheme development (see text).***

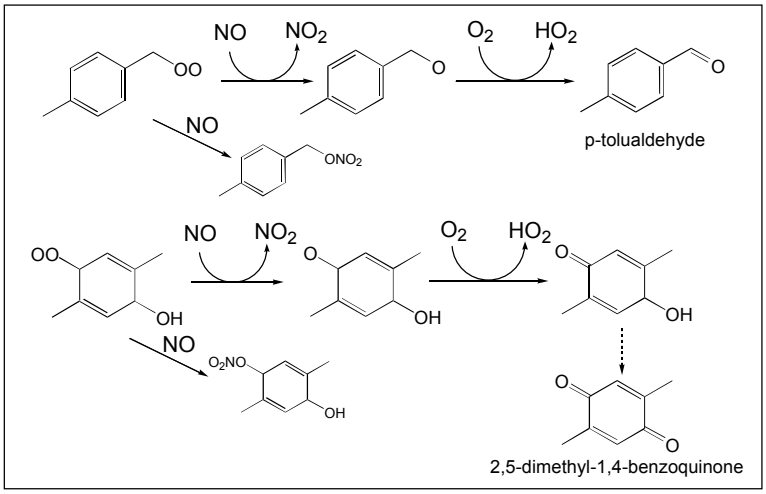

Figure 7.4 ***Schematic representation of the subsequent chemistry of the minor peroxy radicals generated from the OH initiated oxidation of p-xylene, as shown Figure 7.3 (see text). Chemistry following reaction with NO is shown. Chemical schemes also include competing reactions for peroxy radicals, as shown in Figure 7.1.***

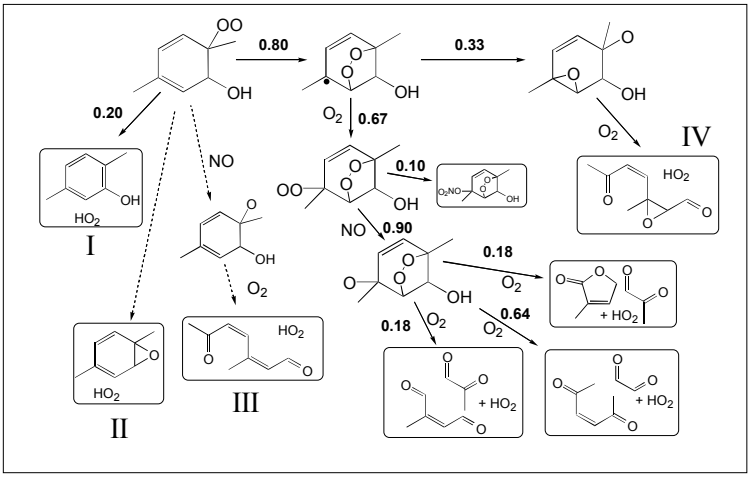

Figure 7.5 ***Schematic representation of the subsequent chemistry of the major peroxy radical generated from the OH initiated oxidation of p-xylene, as shown Figure 7.3. Details of the subsequent chemistry are discussed in the text. Peroxy radical reactions with NO are shown. Competing reactions are included where appropriate.***

represented in the mechanism. The route to yield 3-methyl-6-oxo-hepta-2,4-dienal (**III**) via direct reaction of the peroxy radical with NO almost certainly does not compete, because the yields of the α-dicarbonyl products (formed following isomerisation of the peroxy radical), are invariant over a wide range of NO. The route to the aromatic oxide/oxepin (**II**) is currently excluded, because significant inclusion of this route appears to be inconsistent with recent chamber observations. However, the required chemistry has been developed previously and will be re-incorporated if future experimental or theoretical results provide compelling evidence for its occurrence in any of the aromatic systems under consideration.

The assigned branching ratios for the various reaction channels given in Figure 7.3 to Figure 7.5 are consistent with the first generation product yields presented in Table 7.1, under conditions where there is sufficient NO_X present for the displayed chemistry to dominate. The branching ratios were optimised to give a good description of the p-xylene product yields in NO_X-present experimental studies, which are also shown in the table. A similar procedure has been carried out for all the other aromatic VOC for which the experimental data are available. In each case, the mechanisms have been optimised to provide a good description of the quantified first generation products. It must be noted, however, that a notable proportion of the reaction in each case has to be assumed to yield detected (but not quantified) products, such as the epoxydicarbonylenes, and other likely products formed in conjunction with those detected, but which have currently not been detected (*e.g.* co-products of the α-dicarbonyls; organic nitrates formed from the alternative channels of the reactions of the various peroxy radicals with NO). The mechanisms for those aromatics for which no product data exist are defined by analogy (*e.g.* the branching ratios for *p*-ethyl toluene are assumed equivalent to those for *p*-xylene).

Table 7.1 ***Yields of the major first generation products of the OH-initiated oxidation of p-xylene under NO_X-present conditions (see discussion in text).***

Oxygenated product	Calculated (%)[1]	Observed (%)[2]
p-tolualdehyde	9.0	8.4
2,5-dimethylphenol	16.0	15.9
glyoxal	24.7	24.4
methyl glyoxal	13.9	13.8
2-methyl butenedial[3]	6.9	7.1
hexene-2,5-dione[4]	24.7	22.1
epoxydicarbonylene[5]	22.1	-
cyclic hydroxycarbonyldiene[6]	9.0	-
3-methyl-5H-furan-2-one[3]	6.9	-

Notes: [1] Molar yield calculated on the basis of the branching ratios given in Figure 7.3 to Figure 7.5. [2] Mean of reported molar yields in experimental studies in the presence of NO_X: Tuazon *et al.*, 1984; Bandow and Washida, 1985; Atkinson *et al.*, 1991; Smith *et al.*, 1999; [3] C_5 co-product of methyl glyoxal (see Figure 7.3). [4] C_6 co-product of glyoxal (see Figure 2.9) [5] Product has been observed (Jeffries *et al.*, 1995), but not quantified. [6] Precursor to 2,5-dimethyl-1,4-benzoquinone (see Figure 7.4).

The subsequent degradation of the first generation products is largely defined by the mechanism construction protocol used previously for the MCM as a whole (Jenkin *et al.*, 1997). However, some special consideration is being given to selected classes of product showing combinations of functional groups which are unlike those considered previously. For example, there is experimental evidence that certain α,β-unsaturated-1,4-dicarbonyls (formed as co-products of the α-dicarbonyls) are partially oxidised to generate cyclic anhydride products known as furandiones (Bierbach *et al.*, 1994), and these secondary products have been detected in the observed speciation of SOA in chamber experiments (Forstner *et al.*, 1997). Consequently, the generation of furandiones is being fully represented in the current mechanism construction. Furthermore, the photolysis rates for the α,β-unsaturated-1,4-dicarbonyls have been found to be exceptionally rapid, and therefore potent radical generators in aromatic systems. The rates of these processes are therefore based on the available data of Sørensen *et al.* (1998).

We have demonstrated in a previous report (Jenkin *et al.*, 2000a) that the perceived propensity of an aromatic hydrocarbon to generate ozone upon degradation is strongly dependent on the relative importance assigned to the possible reaction channels. The POCP values for five

postulated channels were shown to cover the range 15.1–111.0, using 1,3,5-trimethylbenzene as an example. In particular, the POCP values for all aromatics calculated with MCM v2 were found to be consistently about 60% of those calculated with MCM v1. In the absence of definitive published information on the elementary processes involved, the representation in MCM v1 was comparatively simple, and effectively followed the most efficient ozone-generating route via the peroxide bridged intermediates to form the α-dicarbonyls and co-products. The chemistry in MCM v2 was developed to explore a proposed degradation route involving the formation of 'aromatic oxide/oxepin' intermediates (Klotz *et al.*, 1997; 1998), as also partly illustrated in Figure 7.5 for *p*-xylene. The lower POCP values for these mechanisms resulted from partial conversion of the oxepin intermediates into phenolic species which, as discussed previously, tend to have a significant inhibiting influence on ozone formation (Jenkin *et al.*, 2000a). In addition, schemes involving the formation of the oxepin intermediates have been found to provide a very poor description of ozone formation in hydrocarbon/NO_X chamber experiments, with a significant time lag before ozone is generated. As shown in Figure 7.6, the ozone generated by the MCM v3 mechanism for toluene, under illustrative chamber conditions, lies intermediate to MCM v1 and MCM v2, and does not show the significant time lag before the onset of ozone formation occurs. Although there are still areas of uncertainty in explaining the precise time dependence of ozone formation in aromatic hydrocarbon/NO_X chamber experiments (*e.g.* Wagner *et al.*, 2002), available indications are that the MCM v3 mechanisms provide a significantly more reliable description of ozone formation from aromatic hydrocarbons than those in MCM v1 or MCM v2.

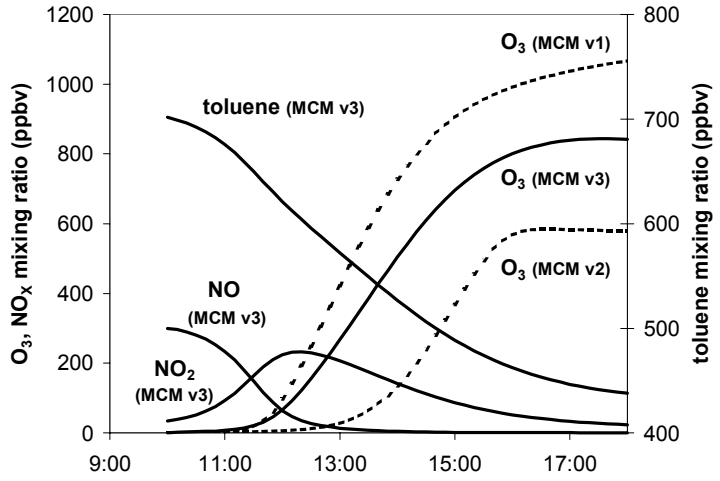

Figure 7.6 ***The simulated generation of ozone in an illustrative smog chamber experiment in which 700 ppbv toluene and 335 ppbv NO_X (90 % NO) were irradiated.***

7.3.4 The Monoterpenes α- and β-pinene

It is well established that the oxidation of monoterpenes in the troposphere plays a potentially important role in the generation of ozone and secondary organic aerosols (*e.g.*, Went, 1960; Rasmussen, 1972; Trainer *et al.*, 1987; Jacob and Wofsy, 1988; Andreae and Crutzen, 1997), and increasing attention has therefore been given in recent years to elucidating the oxidation mechanisms of monoterpenes known to be emitted into the troposphere in substantial quantities (Atkinson and Arey, 1998; Calogirou *et al.*, 1999). Much emphasis has been placed on α- and β-pinene, since measurements of monoterpene speciation suggest that these make a particularly significant contribution to monoterpene emissions (*e.g.*, Guenther *et al.*, 1994 and references therein), and also because they are representative of classes of monoterpene having either a endocyclic double bond (in the case of α-pinene) or an exocyclic double bond (in the case of β-pinene). Particular progress has been made in defining the kinetics and mechanisms of the early stages of the gas-phase degradation chemistry of α-pinene initiated by reaction with OH

radicals, NO_3 radicals and ozone (*e.g.*, Arey *et al.*, 1990; Hakola *et al.*, 1994; Wangberg *et al.*, 1997; Berndt and Boge, 1997; Aschmann *et al.*, 1998; Alvarado *et al.*, 1998a; Noziere *et al.*, 1999a), and the further oxidation of the major first generation product, pinonaldehyde (*e.g.*, Glasius *et al.*, 1997; Hallquist *et al.*, 1997; Alvarado *et al.*, 1998b; Noziere *et al.*, 1999a,b).

The degradation of α-pinene was represented in MCM v2 (Jenkin *et al.*, 1999). The chemistry has been updated within MCM v3 to reflect subsequent improvements in the database, particularly with regard to the formation of the multifunctional acids, pinonic acid, pinic acid and 10-hydroxypinonic acid, which are now well-established as degradation products (*e.g.*, Christoffersen *et al.*, 1998; Hoffmann *et al.*, 1998; Glasius *et al.*, 1999; Kamens *et al.*, 1999). The initial oxidation step initiated by reaction with O_3 is represented schematically in Figure 7.7. The degradation of β-pinene is also fully treated in MCM v3, and consistent with recently published data relevant to its oxidation chemistry (Christoffersen *et al.*, 1998; Winterhalter *et al.*, 2000), including the formation of pinic acid. The complete degradation mechanism for α- and β-pinene involves *ca.* 1500 reactions of *ca.* 500 species.

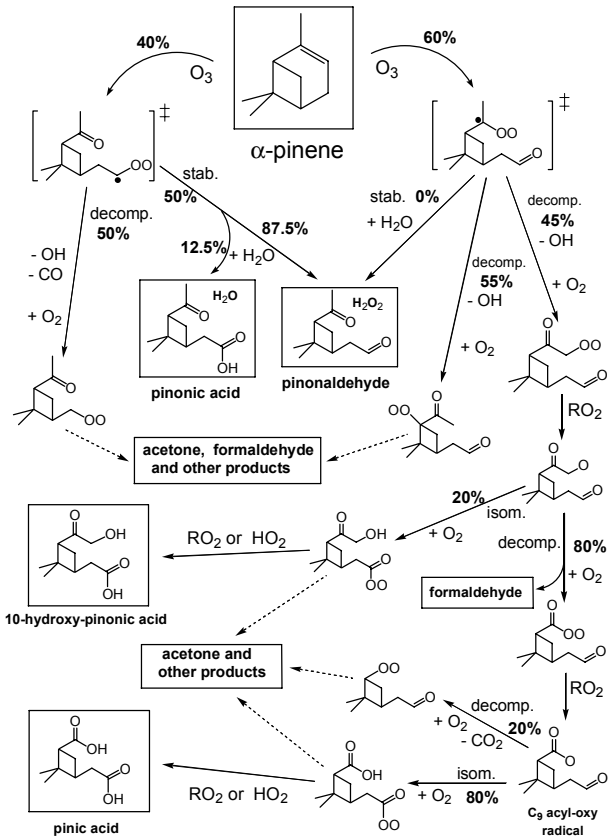

Figure 7.7 ***Schematic overview of some of the features of the initial step of the ozonolysis of α-pinene, as represented in MCM v3 Broken lines indicate multistep pathways initiated by the reaction of the given peroxy radical. The mechanism provides yields of the boxed products which are consistent with the range of reported values in the literature.***

As shown in Figure 7.8, the updated a-pinene scheme has been found to provide an excellent description of the oxidation of NO to NO_2 and associated O_3 formation in experiments performed in the European Photoreactor (EUPHORE) as part of the EU project OSOA (Origin and Formation of Secondary Organic Aerosol). Similarly to the situation for the aromatic VOC, a significant proportion of the available information on speciated products, and therefore the precise oxidation pathways, has come from measurements of species either entirely in the aerosol phase or partitioned between the gaseous and aerosol phases. Consequently, the scheme development work for α- and β-pinene also provides the initial basis for representing gas-aerosol partitioning of speciated products in future work, and for describing the important role played by monoterpenes in fine particle formation.

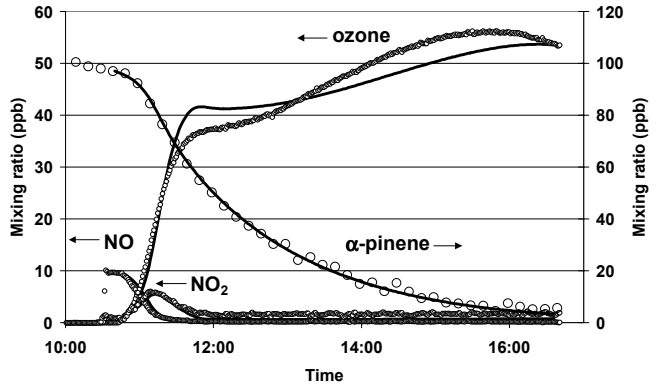

Figure 7.8 ***Observed time dependences of α-pinene, NO_X and O_3 during a photo-oxidation experiment at EUPHORE (performed as part of the EU OSOA project), and those simulated with the MCM v3 α-pinene scheme (lines).***

7.4 THE COMMON REPRESENTATIVE INTERMEDIATES (CRI) MECHANISM

7.4.1 Introduction

The MCM is a near-explicit mechanism which represents a direct method of utilising and applying the results of studies of elementary chemical processes, and is conceptually simple, since it aims to represent that actual reactions that are occurring. As a result, however, it contains many thousands of chemical species and reactions, and it is recognised the development of less-detailed schemes is necessary for some applications where greater computational efficiency is required. A reduced mechanism to describe the formation of ozone from VOC oxidation has therefore been developed as part of the current programme, using MCM v2 as a reference benchmark. The 'Common Representative Intermediates' (CRI) mechanism treats the degradation of methane and 120 VOC using *ca.* 570 reactions of *ca.* 250 species (*i.e.* approximately 2 species per VOC). It thus contains only *ca.* 5% of the number of reactions and *ca.* 7% of the number of chemical species in MCM v2, providing a computationally economical alternative.

7.4.2 Quantifying Ozone Formation from VOC degradation

The complete oxidation of a given VOC though to CO_2 and H_2O normally proceeds via a series of intermediate oxidised products. At each stage, the chemistry is propagated by reactions of free radicals leading to the oxidation of NO to NO_2 and resultant formation of O_3 as a by-product, following the photolysis of NO_2:

$$NO_2 + h\nu\ (\lambda < 420\ nm) \rightarrow NO + O(^3P) \quad (7.1)$$

$$O(^3P) + O_2\ (+M) \rightarrow O_3\ (+M) \quad (7.2)$$

The total quantity of O_3 potentially generated is therefore dependent on the number of NO to NO_2 conversions which can occur during the degradation, but is restricted by the time available for the chemistry to occur. Consequently, the O_3 forming ability of VOC has sometimes been expressed in terms of 'kinetic' and 'mechanistic' or 'structure-based' components (*e.g.* Carter, 1994; Derwent *et al.*, 1998).

On the basis of understanding of the detailed chemistry for simple hydrocarbons such as methane, ethane and ethene, the total quantity of O_3 potentially formed as a by-product of the complete OH-initiated and NO_X-catalysed oxidation to CO_2 and H_2O can be represented by the following overall equations:

$$CH_4 + 8O_2 \rightarrow CO_2 + 2H_2O + 4O_3 \quad (7.3)$$
$$C_2H_6 + 14O_2 \rightarrow 2CO_2 + 3H_2O + 7O_3 \quad (7.4)$$
$$C_2H_4 + 12O_2 \rightarrow 2CO_2 + 2H_2O + 6O_3 \quad (7.5)$$

In the case of ethane, for example, this is based on the oxidation via CH_3CHO, HCHO and CO as intermediate oxidised products, as shown in Figure 7.9. According to equations (7.3) - (7.5), therefore, the complete oxidation of one molecule of each of these compounds leads to the production of 4, 7 and 6 molecules of O_3 respectively. Logically, the number of O_3 molecules produced in each case (*i.e.* the number of NO to NO_2 conversions) is equivalent to the number of reactive bonds in the parent molecule, that is the number of C-H and C-C bonds which are eventually broken during the complete oxidation to CO_2 and H_2O.

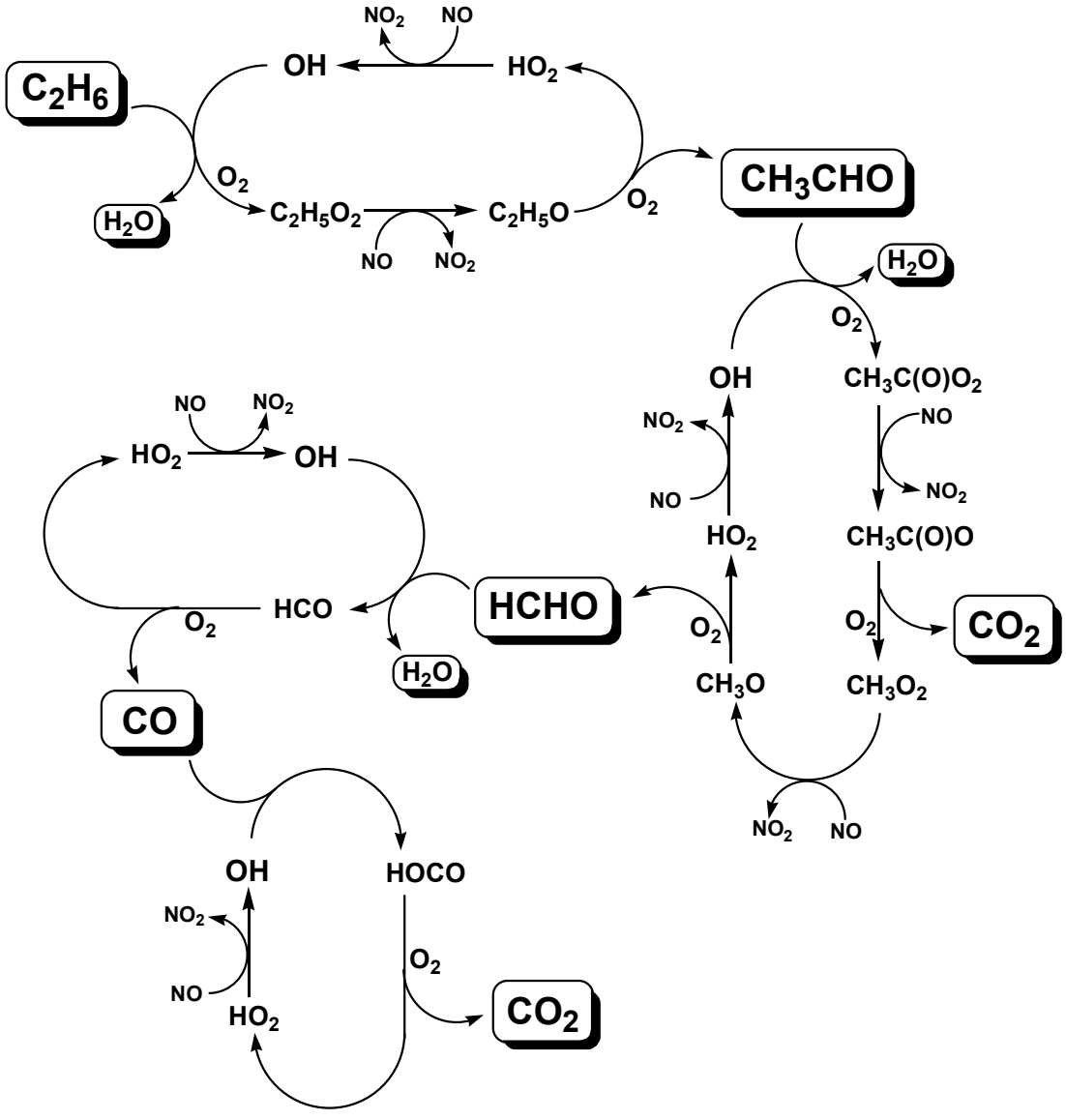

Figure 7.9 ***Schematic representation of the reactions involved in the OH initiated, NO_X catalysed oxidation of ethane to CO_2. The reaction sequence shows the formation of acetaldehyde (CH_3CHO), formaldehyde (HCHO) and CO as intermediate oxidised products. The complete sequence results in 7 NO to NO_2 conversions. Subsequent photolysis of NO_2 regenerates NO and leads to ozone formation (reactions (1) and (2)), with the net overall chemistry as shown in reaction (4). (N.B. The oxidation of CO to CO_2 partially proceeds via OH + CO → H + CO_2, followed by H + O_2 + M → HO_2 + M, which has the same overall chemistry as that displayed above, i.e. OH + CO + M → HOCO + M, followed by HOCO + O_2 → HO_2 + CO_2).***

7.4.3 Construction of the CRI Mechanism

As described in detail by Jenkin *et al.* (2002a), this simple rule is used in the CRI mechanism, to define a series of generic intermediate radicals and products, which mediate the breakdown of larger VOC into smaller fragments (*e.g.*, HCHO, CH_3CHO), the chemistry of which is treated explicitly. Some of the degradation chemistry is illustrated schematically in Figure 7.10.

This shows the major oxidation pathway following the attack of OH for a number of VOC. Using this approach, a comparatively small set of generic radicals and molecular products can be used to represent the intermediates formed from many VOC. In each case, however, the initial oxidation step is included explicitly, such that the removal kinetics for each individual VOC are fully represented. It should also be noted that Figure 7.10 shows only the major radical-propagated oxidation pathway, initiated by reaction with OH. Competing reactions for the intermediate peroxy radicals are included (leading particularly to the formation of nitrates, $RONO_2$, and hydroperoxides, ROOH, as shown in Figure 7.1) throughout the mechanism and, where appropriate, chemistry initiated by reaction with O_3, NO_3 and direct photolysis is also represented.

7.4.4 Testing and Optimisation of the CRI Mechanism

The performance of the CRI mechanism was compared with the MCM v2 using the Photochemical Trajectory Model (PTM), described below in Section 7.5.2, operating on an idealised linear trajectory originating in Austria on day 1 and terminating in the southern UK on day 5. The two mechanisms were found to generate levels of ozone which agreed to within 5% along the entire trajectory. The agreement was optimised by varying slightly the rate coefficients for the reactions of OH with the limited number of generic intermediate carbonyl compounds(*e.g.* CARB11 in Figure 7.10) to minimise the square deviation between the two mechanisms, with the result as shown in Figure 7.11.

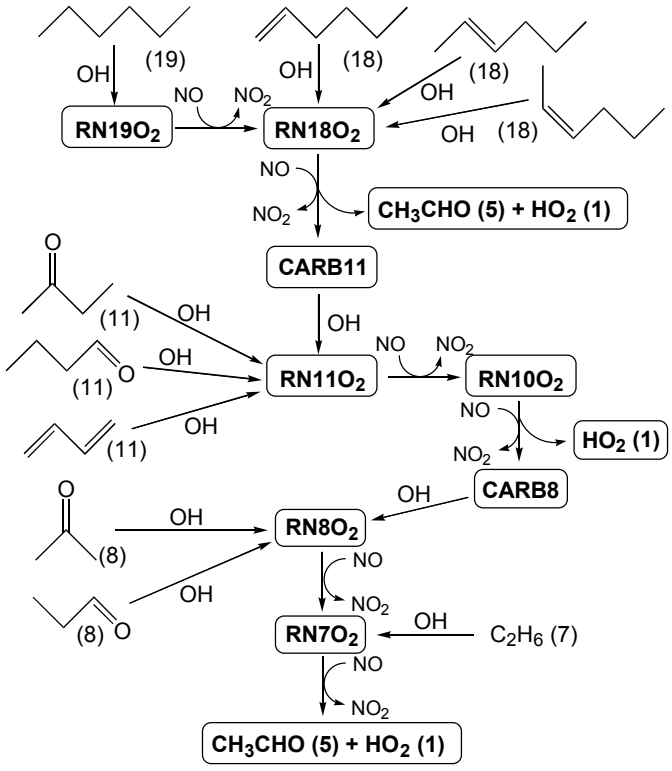

Figure 7.10 ***Schematic representation of some of the degradation chemistry in the CRI mechanism. The index assigned (in brackets) to each VOC is the total number of C-H and C-C bonds it contains. The indices within the generic radicals and carbonyls (e.g. '19' in $RN19O_2$ and '11' in CARB11), represent the number of NO-to-NO_2 conversions (i.e. number of O_3 molecules) which can result from the subsequent complete degradation. HO_2 is assigned an index of 1, since a single NO-to-NO_2 conversion regenerates OH, which initiated the reaction sequence.***

Figure 7.11 also demonstrates that the concentration-time profiles for a number of key species involved in ozone formation (OH, peroxy radicals, NO, NO_2,) are in good agreement, indicating that the mechanism construction methodology in the CRI mechanism successfully captures the salient features of the ozone formation process as represented in the MCM.

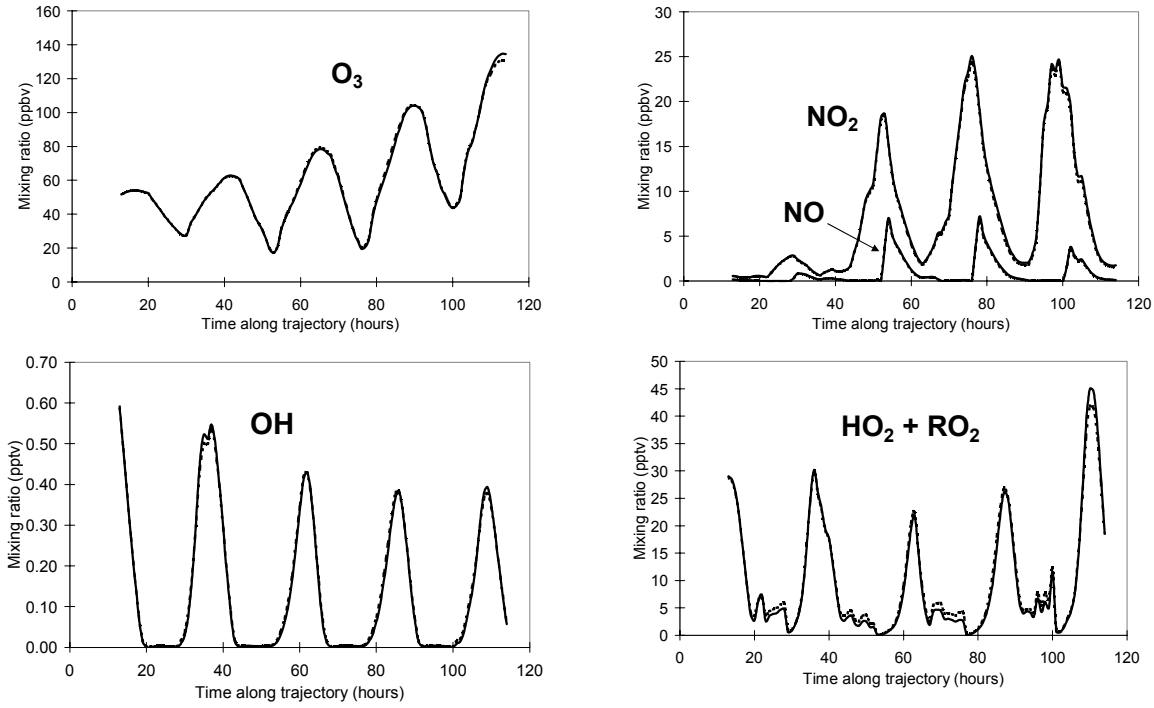

Figure 7.11 ***Comparison of mixing ratios of O_3, NO_x, OH and total peroxy radicals simulated along the idealised linear trajectory using the CRI mechanism (solid lines) and MCM v2 (broken lines).***

7.5 PHOTOCHEMICAL OZONE CREATION POTENTIALS

7.5.1 Introduction

There are many hundreds of organic compounds emitted into the atmosphere, each reacting at different rates, by different chemical mechanisms, to produce different amounts of ozone (Bowman and Seinfeld, 1994). Those organic compounds that produce a significant amount of ozone are often termed 'highly reactive' and those that produce little or none at all are termed 'less reactive' or 'unreactive'. There is currently no widely accepted reactivity scale that applies under all conditions and in all locations to quantify the role played by each organic compound in ozone formation (Dimitriades, 1996). This is because reactivity values depend not only the intrinsic properties of the individual organic compounds but they also depend on the environmental conditions under which the organic compounds react in the atmosphere (Carter, 1994a). However, for the development of cost-effective ozone control policies, some practical means of quantifying reactivity is essential for policy-makers.

In Europe, the VOC Protocol to the international convention on Long-range Transboundary Air Pollution specifically recommends the focussing of control policy actions on those organic compounds that contribute most to ozone formation and its long-range transport (UNECE 1991). To this end, the Photochemical Ozone Creation Potential (POCP) concept has been

developed to describe the relative contributions made by a large number of organic compounds to regional scale ozone formation in NW Europe.

7.5.2 The Photochemical Trajectory Model

POCP values are calculated using a Photochemical Trajectory Model (PTM), which has been widely applied to the simulation of photochemical ozone formation in north-west Europe (*e.g.*, Derwent *et al.*, 1996; 1998). The PTM simulates the chemical development in a boundary layer air parcel travelling along pre-selected trajectories over Europe. The air parcel thus picks up emissions of NO_X, CO, SO_2, methane, non-methane VOC and biogenic isoprene (based on inventories from EMEP, EC CORINAIR and the UK NAEI), which are processed using an appropriate description of the chemical and photochemical transformations leading to ozone formation. As described in detail previously (Derwent *et al.*, 1996), diurnal variations in atmospheric boundary layer depth, windspeeds, temperatures and humidities are represented as climatological means over a number of photochemical episodes.

7.5.3 The definition of POCP

POCP values are usually defined from calculations performed using an idealised linear trajectory (Derwent *et al.*, 1998). A boundary layer air parcel is followed from a release point in Austria with subsequent passage over Germany and Belgium prior to arriving in the southern UK on the fifth day. This trajectory describes a highly idealised anticyclonic meteorological situation of easterly winds, leading to a broad air flow carrying photochemically-aged polluted air masses out of mainland Europe towards the UK, and is broadly representative of trajectory paths which are frequently associated with elevated ozone concentrations in the southern UK (Jenkin *et al.*, 2002b). The production of ozone on this and similar trajectories has previously been shown to display some sensitivity to the availability of VOC (Derwent *et al.*, 1998; Jenkin *et al.*, 2002a). Consequently, the chosen trajectory is appropriate for the definition of a comparative ozone formation index for VOC.

The POCP for a particular VOC is determined by quantifying the effect of a small incremental increase in its emission on ozone formation along the trajectory, relative to that resulting from an identical increase in the emission (on a mass basis) of a reference VOC, which is taken to be ethene. Thus, the POCP for the given VOC 'i' is defined by equation (i),

$$POCP_i = \frac{\text{ozone increment with the } i\text{th VOC}}{\text{ozone increment with ethene}} \times 100 \qquad \text{(i)}$$

with the value for ethene being 100 by definition. The POCP is calculated from the results of separate model experiments. A base case scenario is initially run, followed by model runs in which the emission term of the selected VOC and of ethene are, in turn, incremented by *ca.* 1 kg km^{-2} day^{-1} across the entire model domain. The extra VOC emission stimulates additional ozone formation over the base case, and this incremental quantity of ozone can be defined for a particular point along the trajectory or integrated over the entire trajectory length. POCP values published previously for methane and 119 non-methane VOC using MCM v1 (Derwent *et al.*, 1998), and those reported below, are based on the integrated incremental ozone formation.

In addition to being an index to assist policy development, the POCP is effectively a single number descriptor for a given VOC degradation mechanism under the selected conditions, the value of which may be sensitive to particular features of the mechanism. It therefore provides a useful method of comparing the performance of different degradation mechanisms, and an

indication of whether the mechanisms are likely to perform comparably in policy calculations of precursor emissions controls.

7.5.4 Summary of POCP results

During the current programme a number of sets of POCP calculations have been performed, both to assist comparison of mechanism performance, and to update information on the relative ozone forming abilities of emitted VOC.

(a) POCP values for non-aromatic VOC calculated with MCM versions: POCP values have been calculated using both MCM v2 and MCM v3 for comparison with those reported previously with MCM v1 (Derwent *et al.*, 1998). The results are presented for selected VOCs in Figure 7.12.

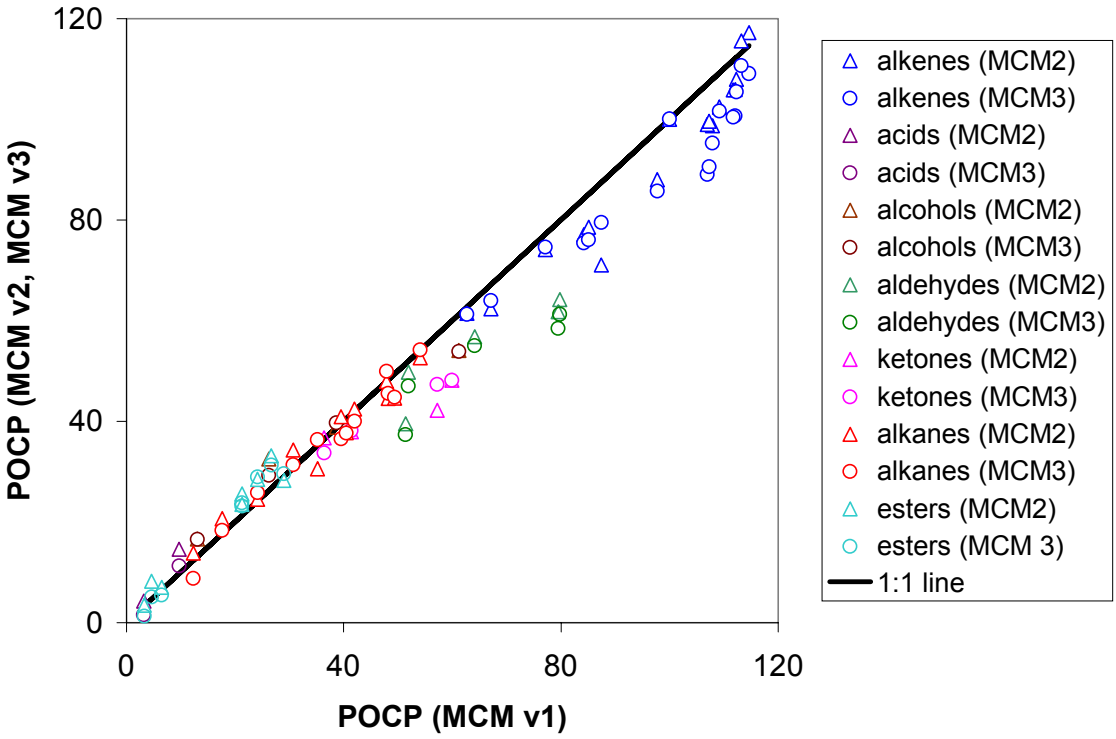

Figure 7.12 ***Comparison of POCP values calculated with versions of the MCM.***

It is apparent that the results obtained with all three versions of the mechanism show a high degree of correlation broadly indicating good agreement for all non-aromatic VOC. In particular, the values obtained with MCM v2 and MCM v3 are in excellent agreement. In some instances, these values are notably lower than those calculated with MCM v1. The largest percentage discrepancies are observed for the carbonyl compounds, in particular the longer chain aldehydes and some ketones. This results from the thermal decomposition rate of peroxyacyl nitrates being updated subsequently to MCM v1, such that these species are more stable. Since peroxyacyl nitrates are formed in the primary oxidation step from the OH-initiated oxidation of aldehydes $\geq C_2$ (and to a lesser extent from ketone photolysis), this has a resultant increased inhibiting influence on ozone formation in the later mechanisms through the increased sequestering of free radicals and NO_X in an inactive form. As a result, POCP values for longer chain carbonyl compounds

are now up to 25% lower than previously reported. Those for small carbonyls (*e.g.* formaldehyde) remain almost unchanged. The POCP values calculated for some larger alkenes in MCM v2 and MCM v3 are also lower than those calculated with MCM v1 by virtue of a secondary influence of forming larger carbonyls in high yield.

(b) POCP values for non-aromatic VOC calculated with CRI mechanism and MCM v2: POCP values calculated for a series of non-aromatic VOC classes with the CRI mechanism are compared with those calculated with MCM v2 in Figure 7.13.

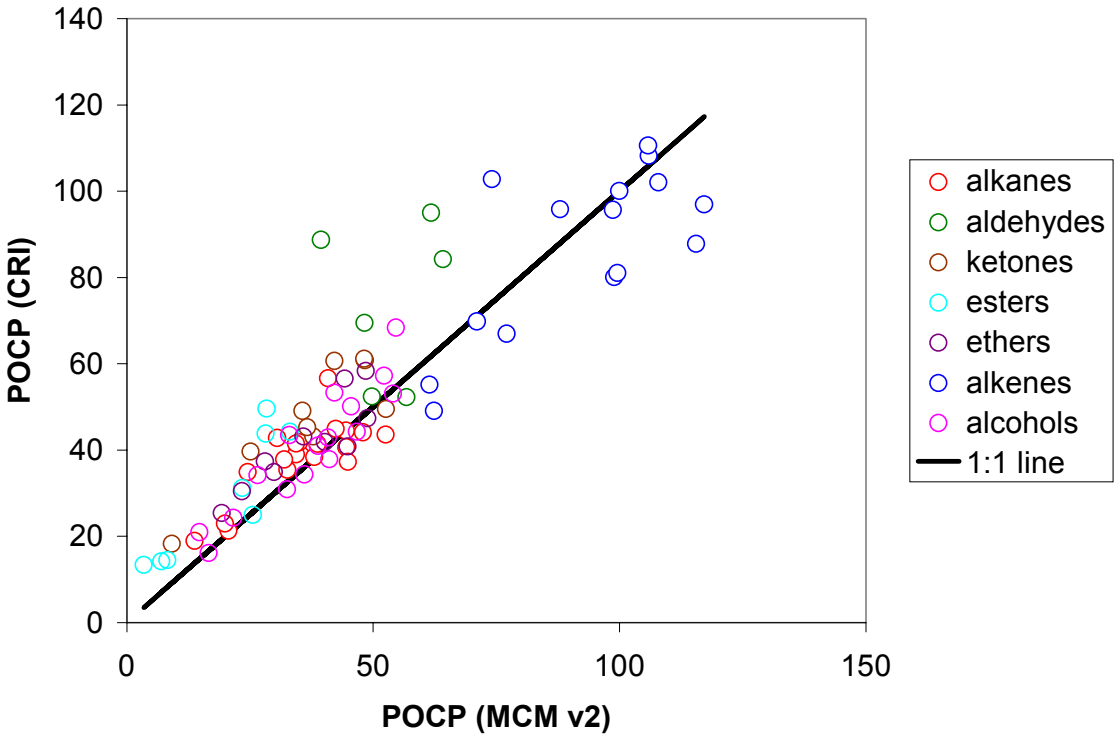

Figure 7.13 ***Comparison of POCP values calculated with the CRI mechanism and MCM v2.***

Clearly the two mechanisms show a reasonable correlation for a diverse series of VOC. Although the CRI mechanism does not recreate all the subtleties of ozone formation which can be represented in a near-explicit mechanism, the general variation of ozone forming ability within these classes of compound is adequately described by the simplified mechanism. The most notable discrepancies are once again observed for the carbonyl compounds, because the simplified representation of their degradation in the CRI mechanism does not include formation of $\geq C_3$ peroxy acyl nitrates. Consequently, the POCP values calculated for the larger aldehydes and ketones are significantly greater than those determined with the MCM v2. Despite this systematic difference, however, the relative variation of POCP along the series of carbonyl compounds is generally consistent with that calculated with the detailed representation in MCM v2.

The CRI mechanism has therefore been shown to provide a description of ozone formation, under simulated photochemical episode conditions, which is comparable with that of MCM v2. The POCP values determined using the CRI mechanism generally show a variation from compound to compound which is remarkably consistent with that calculated with the detailed representation in MCM v2. This confirms that the mechanism

construction methodology not only captures the salient features of the ozone formation process in general, but also how this varies from one VOC to another. This results from inclusion of features which are able to represent both the 'kinetic' and the 'mechanistic' or 'structure-based' contributions to ozone formation. The former is achieved by the explicit inclusion of initiation reactions and rate coefficients for all 120 VOC. The latter results from use of generic intermediates which are selected on the basis of ozone forming potential rather than other factors such as carbon number.

(c) POCP values for aromatic VOC calculated with MCM versions: POCP values calculated for aromatic VOC with the three versions of the MCM are shown in Figure 7.14. These clearly demonstrate how our perception of the ability of these compounds to form ozone has varied with our understanding of the chemistry of their degradation. With the

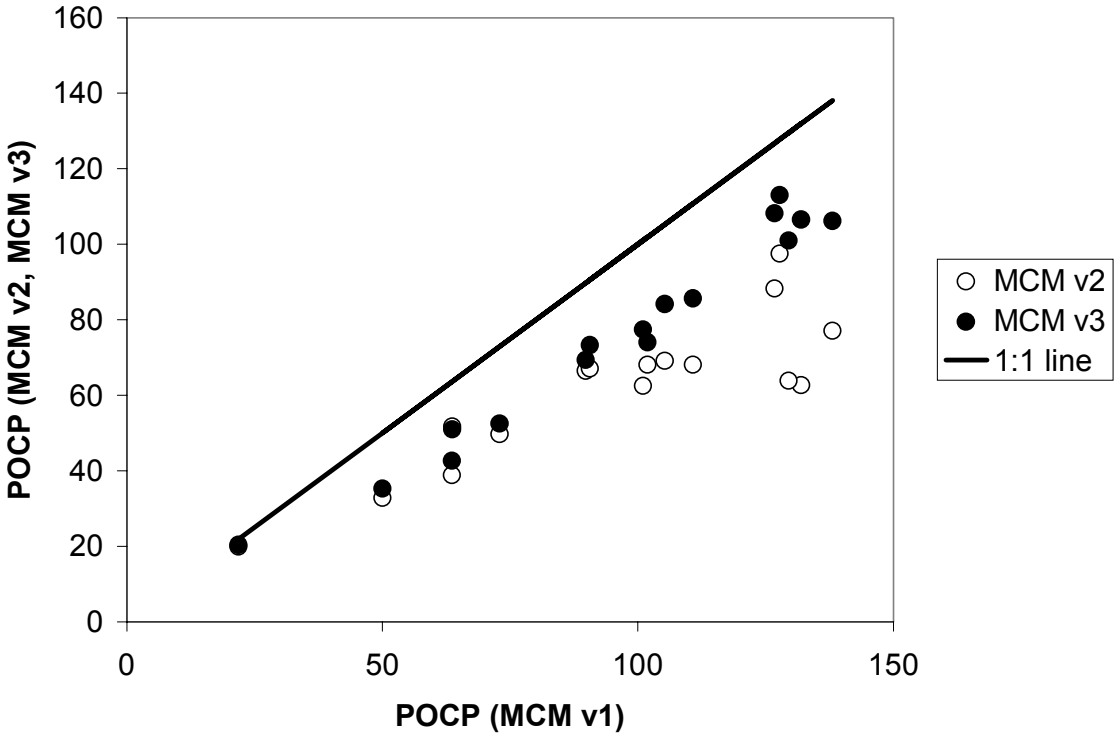

Figure 7.14 ***Comparison of POCP values calculated for aromatic VOC with MCM versions.***

comparatively simple representation of the degradation in MCM v1, half the aromatic VOC were calculated to have POCP values in excess of 100, identifying them as the most potent ozone forming VOC class. The degradation chemistry in MCM v2, based on the proposed formation of 'aromatic oxide/oxepin' intermediates (Klotz *et al.*, 1997; 1998), resulted in much reduced POCP values, with the values for all aromatic VOC being less than 100. On the basis of this assessment, therefore, aromatic VOC were regarded as being less potent at making ozone than alkenes. However, these schemes also provided an extremely poor description of ozone formation in hydrocarbon/NO_X chamber experiments. The degradation chemistry in MCM v3 provides a more acceptable description of the chamber data, although there are still areas of uncertainty in explaining the precise time dependence of ozone formation (*e.g.* Wagner *et al.*, 2002). The corresponding POCP values generally lie above those calculated with MCM v2, but consistently 15-20 POCP units below those calculated originally with MCM v1, and provide the best assessment to date of the relative ozone forming abilities of these compounds under photochemical episode conditions. On the

basis of this assessment, aromatic VOC are generally comparable with alkenes in their ability to generate ozone.

(d) New POCP values: POCP values have also been calculated with MCM v3 for the monoterpenes, α- and β-pinene, and for the branched alkene, 2,3-dimethyl-2-butene. The values for all three VOC are comparable (57.5, 62.1 and 56.4, respectively), and are consistent with the trend observed for other unsaturated hydrocarbons. The values are comparatively high by virtue of all these VOC being very reactive, but are substantially lower than those for smaller reactive alkenes (*e.g.*, $POCP_{ethene}$ = 100) because of significant generation of acetone during the degradation. Acetone is very unreactive, and previous work has shown that its formation has a significant influence on the ability of the precursor VOC to generate ozone on the necessary timescale (Jenkin and Hayman, 1999).

(e) POCP values under North American conditions: As described in detail by Derwent *et al.* (2001), additional POCP calculations have also been performed for the single day, highly polluted conditions typical of North American cities to allow direct comparison of the POCP scale with the widely accepted Maximum Incremental Reactivity (MIR) scale, developed in the USA. These were carried out using MCM v2, and corresponding POCP values were determined for 101 non-aromatic VOC. The POCP values were found to correlate linearly with reported MIR values for 86 VOC for which both POCP and MIR values are available. The linear relationship is in contrast with the curvilinear dependence of European POCP values on MIR value, as reported previously (contract EPG 1/3/70). This emphasises that less reactive VOC have a relatively heightened contribution to ozone formation under the multi day scenario used for the European calculations. We conclude that choice of policy focus between single day and multi day conditions is important for establishing a quantitative reactivity scale, particularly for less reactive VOC classes, such as alkanes, alcohols, esters and ethers.

7.6 APPLICATION AND TESTING OF MCM V3

7.6.1 Introduction

Additional calculations have been performed using MCM v3 in a version of the Photochemical Trajectory Model (PTM) with updated emissions and VOC speciation. The main objective of this work is to test the performance of the model under idealised photochemical episode conditions by comparing the simulated levels of ozone and speciated hydrocarbons generated with those typically observed. The model is also used to determine the absolute contribution to ozone formation made by each of the 124 non-methane VOC in MCM v3.

7.6.2 Emissions

The PTM utilises emission inventories at various spatial resolutions to estimate the instantaneous emissions at any point in time along the trajectory path, as described previously (Derwent *et al.*, 1996). At the widest spatial scales, European emissions of SO_2, NO_x, VOCs and isoprene are taken at 150 km x 150 km for 1991 from Tuovinen *et al.* (1994). For the countries of the European Union closest to the United Kingdom, emissions of SO_2, NO_x, VOCs and methane are taken at 50 km x 50 km from CORINAIR 1990 (McInnes, 1994). For the United Kingdom, all emissions data for 1991 were taken at 10 km x 10 km resolution from Eggleston and Goodwin (1994). For the present study, the emissions of all pollutants in each grid squares were then updated to 1999 values using the EMEP emission inventories for each of their base years and for 1999 (http://www.emep.int/index.html).

An important issue in this study has been the speciation of the VOC emission inventory and this has been based on the speciation used for the National Atmospheric Emissions Inventory (NAEI). This speciation depends upon the conversion of NAEI estimates of emissions of non-methane VOC (NMVOC) into estimates of the emissions of individual hydrocarbons and other organic species using source-specific profiles for each source. The profiles consist of estimates of the proportion of total NMVOC emissions which are emitted as each organic species. A full description of the profiles has been given elsewhere (Passant, 2002).

The NAEI profiles are taken from four main sources:

(1) literature values, especially those given in the EMEP/CORINAIR Emission Inventory Guidebook (EMEP-CORINAIR, 1996) and United States Environmental Protection Agency's Speciation manual (US EPA, 1995);

(2) estimates provided by UK industry representatives;

(3) data available for individual UK industrial processes via regulatory bodies such as the UK Environment Agency and local government bodies;

(4) data obtained from measurements carried out as part of the research programme of the UK Department for Environment, Food and Rural Affairs.

Table 7.2 summarises how these four sources of data have contributed to the development of the NAEI profiles. In total, 86 profiles are used to speciate the VOC inventory and the final speciated inventory includes 536 compounds or groups of compounds. Although the speciated VOC inventory currently contains over 500 entries, the 124 non methane VOC considered in MCM v3 place emphasis on those with greater emissions such that about 69% coverage of the mass emissions of unique chemical species is achieved. MCM v3 is therefore believed to provide a reasonable representation of the processing of major organic compounds emitted into the boundary layer over the UK and other populated regions of north west Europe.

Table 7.2 ***Summary of data used in the development of VOC species profiles.***

SNAP Code[a]	VOC sources	% of UK emissions[b]	Main sources for profiles[c]
01, 02, 03	Stationary combustion	3	1
04	Production processes	12	1, 3
05	Extraction/distribution of fossil fuels	12	1,4
06	Solvents	25	2,3,4
07	Road transport	35	1,4
08	Other transport	3	1
09	Waste treatment & disposal	2	1
10	Agriculture	1	NA
11	Nature	7	NA
Notes: [a] Standardised Nomenclature for Air Pollution given at the lowest level of detail. [b] Values for 1991 taken from the 1999 update of the NAEI (Goodwin *et al.*, 2001). [c] See text for description of sources 1-4. NA indicates that no detailed speciation is available for these sources in the NAEI.			

7.6.3 Verification of the Model Results with Ambient Observations.

The modified PTM was run on the standard Austria-UK trajectory. For a small number of species, concentrations were initialised at realistic tropospheric baseline levels for a polluted boundary layer situation (NO, 2 ppb; NO_2, 6 ppb; SO_2, 5 ppb; CO, 120 ppb; methane, 1700 ppb; formaldehyde, 2 ppb; ozone, 50 ppb; hydrogen 550 ppb). Ozone concentrations

calculated in the base case therefore started off at 50 ppb, and rose to 54 ppb during the first afternoon, as shown in Figure 7.15. On subsequent days, significant ozone production ensued and the mid-afternoon maxima rose from 57 ppb, to 63 ppb, 72 ppb and to 86 ppb on the fifth day by which time the air parcel had reached the England-Wales border. To have confidence in the results concerning ozone formation from individual organic compounds, the photochemical trajectory model needs verification and evaluation over a wide range of species. These evaluation studies are described briefly in the following paragraphs.

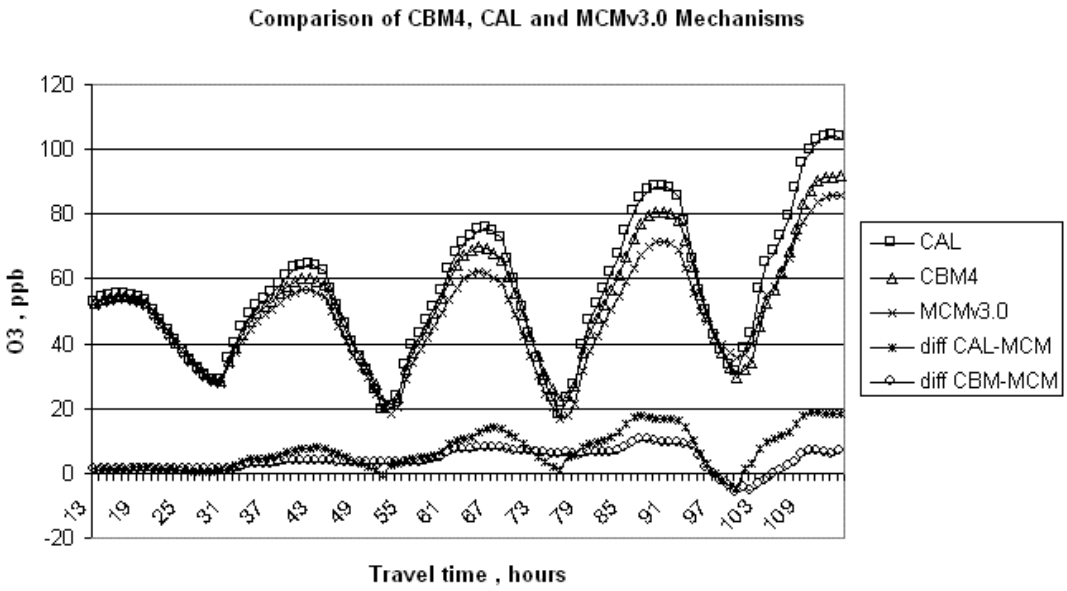

Figure 7.15 ***Time development of ozone in the UK Photochemical Trajectory Model using 1999 emissions and three different chemical mechanisms, together with the differences in ozone concentrations between them.***

The peak ozone concentration of 86 ppb reached on the fifth day of the base case model experiment can be compared with observations from the UK rural ozone monitoring network for the Aston Hill site in the England-Wales borders. Over the period from 1986-1997, the maximum 1-hour ozone concentration recorded was 125 ppb during 1996 (UK PORG 1997). Previous and subsequent annual maximum values lie in the range 76-110 ppb, illustrating a high degree of year-on-year variability, with evidence of a clear downwards trend during the 1990s. The base case model experiment produces peak ozone concentrations within a few ppb of those observed during regional scale photochemical ozone episodes.

In previous work, the ozone concentrations calculated in an air parcel travelling along this same five day trajectory with previous versions of the MCM, together with the two main chemical mechanisms derived from smog chamber studies, Carbon-Bond IV (Gery *et al.*, 1989) and CAL (Lurmann *et al.* 1987) have been compared. The ozone concentrations calculated with all three chemical mechanisms and 1999 emissions agreed closely throughout the five day's photochemistry as is shown in Figure 7.15. Differences appeared to be within 10–18 ppb with the two USA mechanisms generally producing more ozone than the MCM v3. These differences are not thought to be significant and are within the uncertainty ranges implicit in smog chamber studies under the low NO_x conditions implied in Figure 7.15.

An important aspect of the model performance in this study is its ability to describe quantitatively the impact of the emissions of VOC on the formation of photochemical ozone. Clearly the adequacy of the model treatment of VOC will be a crucial issue in assigning

confidence in the model predictions. To this end, the model VOC concentrations have been carefully compared against the observations from the Automatic Hydrocarbon monitoring network operated on behalf of DEFRA by AEA Technology. The observations of 21 hydrocarbons have been assembled for the month of July 2000 for the rural site at Harwell in Oxfordshire and the mean, maximum and minimum hourly concentrations have been determined. These have been compared with the mean concentrations of each VOC species in the last day of the base case model experiment and the results are shown in Figure 7.16. The observations are shown on a logarithmic scale as the three parallel traces (fine lines) and the model results as the thick line. The VOCs are ordered with increasing elution time in the gas chromatography procedures employed in the observations.

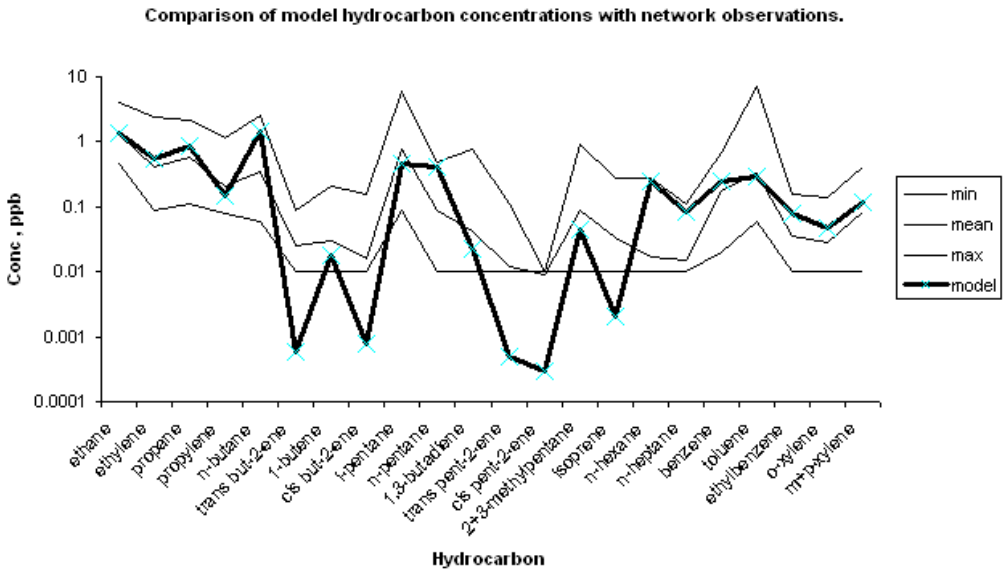

Figure 7.16 ***A comparison of the model calculated and observed hydrocarbon concentrations for Harwell, Oxfordshire.***

The results of the comparison reveal a strikingly similar pattern of concentrations in the observations and model calculations. The peaks and troughs in the three parallel traces are followed closely by the thick model line showing that the model is well able to describe the broad distribution of the VOC classes: alkanes, alkenes and aromatics. For the large majority of the VOC, the model line is close to the mean of the observations. The exceptions are: n-butane, benzene, and ethylbenzene, where the model is close to the maximum in the observations and *cis* but-2-ene, 1,3-butadiene, *trans* pent-2-ene and *cis* pent-2-ene where the model is close to the minimum in the observations. Altogether then the level of agreement found in Figure 7.16 across the 21 VOC species between observations and model calculations is considered entirely satisfactory.

7.6.4 The Contribution to Photochemical Ozone Formation from each VOC

The PTM was set up as in the base case and rerun 124 times with the emission of each VOC species set to zero, in turn. The difference in ozone concentrations between each of runs and the base case was taken as an indication of the contribution to ozone formation from that VOC species. The results have been tabulated in Table 7.3 in rank order. *n*-butane appears to be the most prolific ozone-forming VOC species, contributing over 4 ppb, closely followed by ethene with slightly over 3 ppb. In third and fourth places are ethanol and toluene, with ethanol, the highest ranking oxygenated organic compound. The top-20 most prolific ozone-forming VOC

species contain 8 aromatic hydrocarbons, 8 aliphatic hydrocarbons, two olefinic and two oxygenated compounds. Because the list refers only to man-made organic compounds, isoprene is found at rank 88th in the list.

The total of the individual contributions in Table 7.3 across the 124 organic compounds amounted to 36.82 ppb. This appears to be a measure of the photochemical ozone formation potentials of the man-made organic compounds. Assuming this stands on top of the initial global tropospheric ozone concentration of 50 ppb, a peak ozone concentrations of 86.82 ppb would be anticipated at the trajectory end point. The peak concentration on the last day was found to be 85.9 ppb in close agreement with the sum of the photochemical ozone potentials. The agreement is better than expected and shows that under the 1999 emission conditions, there is little apparent non-linearity in the oxidation of the organic compounds.

Table 7.3 ***Ozone Formation from the Photochemical Oxidation of Each Individual Organic Compound Using 1999 Emissions and the Master Chemical Mechanism v3.0.***

Rank	Organic Compound	O_3 Contribution (ppb)	Rank	Organic Compound	O_3 Contribution (ppb)	Rank	Organic Compound	O_3 Contribution (ppb)
1	n-butane	4.31	43	acetylene	0.11	85	2,2-dimethylpentane	0.02
2	ethylene	3.13	44	cyclohexane	0.09	86	sec-butylacetate	0.02
3	ethanol	2.74	45	cyclohexane	0.09	87	1-methoxy-2-propanol	0.02
4	toluene	2.49	46	m-ethyltoluene	0.08	88	isoprene	0.02
5	i-pentane	1.91	47	propylbenzene	0.07	89	methyl-t-butylether	0.02
6	propylene	1.83	48	propionaldehyde	0.07	90	methylpropylketone	0.02
7	n-pentane	1.78	49	2-butoxyethanol	0.07	91	methylacetate	0.01
8	n-hexane	1.76	50	cis pent-2-ene	0.06	92	trans dichloroethylene	0.01
9	m-xylene	1.68	51	dimethylether	0.06	93	2-methyl-2-butanol	0.01
10	1,2,4-trimethylbenzene	1.50	52	methyl-t-butylketone	0.06	94	i-propylbenzene	0.01
11	o-xylene	0.96	53	cis but-2-ene	0.05	95	methylchloroform	0.01
12	i-butane	0.84	54	pentanaldehyde	0.05	96	tetrachloroethylene	0.01
13	p-xylene	0.80	55	benzaldehyde	0.05	97	diacetone alcohol	0.01
14	n-heptane	0.76	56	acetic acid	0.05	98	cyclohexanone	0.01
15	propane	0.68	57	propylene glycol	0.04	99	3,5-dimethylethylbenzene	0.01
16	ethylbenzene	0.67	58	trans pent-2-ene	0.04	100	3-pentanol	0.00
17	formaldehyde	0.65	59	i-butanol	0.04	101	ethyl-t-butylether	0.00
18	1,3,5-trimethylbenzene	0.50	60	n-dodecane	0.04	102	2-methylbut-1-ene	0.00
19	n-octane	0.47	61	p-ethyltoluene	0.04	103	2-methylbut-2-ene	0.00
20	benzene	0.45	62	formic acid	0.04	104	methyl-i-butylketone	0.00
21	trichloroethylene	0.41	63	cyclohexanol	0.03	105	i-propylacetate	0.00
22	butylene	0.38	64	diethylketone	0.03	106	3,5-diethyltoluene	0.00
23	methylethylketone	0.36	65	ethylene glycol	0.03	107	hexan-3-one	0.00
24	n-decane	0.34	66	dimethoxymethane	0.03	108	1-butoxy-2-propanol	0.00
25	1,3-butadiene	0.34	67	3-methylbut-1-ene	0.03	109	t-butyl acetate	0.00
26	methanol	0.33	68	butyraldehyde	0.03	110	neopentane	-0.01
27	ethane	0.32	69	i-propionaldehyde	0.03	111	butanol	-0.01
28	but-1-ene	0.31	70	methyl chloride	0.03	112	3-methyl-1-butanol	-0.01
29	1,2,3-trimethylbenzene	0.31	71	hex-1-ene	0.03	113	di-isopropylether	-0.01
30	ethylacetate	0.24	72	2-methyl-1-butanol	0.03	114	t-butanol	-0.02
31	acetaldehyde	0.23	73	alpha-pinene	0.03	115	propanol	-0.02
32	n-nonane	0.21	74	2,3-dimethylpentane	0.02	116	diethylether	-0.02
33	1-pentene	0.21	75	cis dichloroethylene	0.02	117	methyl-i-propylketone	-0.02
34	2-methylpentane	0.18	76	n-propylacetate	0.02	118	2-methoxyethanol	-0.02
35	acetone	0.17	77	hexan-2-one	0.02	119	beta-pinene	-0.02
36	2-methylhexane	0.16	78	2-ethoxyethanol	0.02	120	methylene dichloride	-0.02
37	sec-butanol	0.15	79	chloroform	0.02	121	propanoic acid	-0.02
38	3-methylhexane	0.14	80	trans but-2-ene	0.02	122	trans hex-2-ene	-0.03
39	butylacetate	0.14	81	o-ethyltoluene	0.02	123	methyl formate	-0.03
40	n-undecane	0.13	82	styrene	0.02	124	cis hex-2-ene	-0.04
41	i-propanol	0.13	83	3-methyl-2-butanol	0.02			
42	3-methylpentane	0.11	84	dimethoxycarbonate	0.02			
	Total							36.82

8 Policy Support - National Plan for VOCs/Ozone

8.1 SECTION SUMMARY

As part of Task 6 of the present programme (policy support - national plan for VOCs/ozone), different versions of the photochemical trajectory model containing either the CRI or MCM mechanisms have been used to investigate the influence of a series of ozone precursor emissions controls on peak ozone levels typical of a UK photochemical episode.

Peak ozone concentrations have been simulated using the PTM-CRI for a series of year 2010 emissions scenarios related to the EU NECD, allowing the effectiveness of the different measures to be compared. Using an ozone episode occurring on the 31st July 1999 for this study, the influence of a series of the emissions scenarios on simulated peak ozone at the 8 southern UK sites was determined. The present investigation of ozone precursor control scenarios using a representative case study allowed a number of conclusions can be drawn:

- Reductions in UK precursor emissions from 1998 to 2010 reference levels are calculated to have little or no effect on peak episodic ozone levels at locations to the east of the UK. Greater influences (up to 11% reduction) are calculated for locations on the west of the UK, or specific locations which are downwind of regions with particularly high UK emissions;

- Additional VOC reductions in the UK (1252 to 1200 kt a^{-1}) to meet the NECD target may have a small additional influence on selected downwind locations: further proposed reductions (1200 to 1150 kt a^{-1}) appear unlikely to have a major effect on peak episodic ozone levels. However, achievement of NECD targets throughout the EU (together with projected reductions in non-EU countries) were calculated to lead to a reduction of 20-25% in peak episodic ozone levels in the UK.

- The reduction of precursor emissions from 1998 to 2010 levels will be accompanied by a significant shift towards NO_X-limited conditions for episodic ozone formation.

It is likely that the actions taken to implement the United Nations Economic Commission for Europe VOC Protocol through EU Directives on motor vehicle emission controls has led to a reduction in the emissions of certain individual VOC species. In a separate modelling study undertaken in the project (see Section 7.6.4), a combination of the highly sophisticated Master Chemical Mechanism and speciated VOC inventories was used in the PTM for the standard Austria-UK trajectory. Ozone concentrations were calculated over a five day travel time in an air parcel which arrived at the England-Wales border. The peak ozone concentration calculated for the fifth and last day was 85.9 ppb. The UK PTM model was then rerun a further 124 times with the emission of each VOC species set to zero in turn. The difference in ozone concentrations was taken as an indication of the contribution to ozone formation of that VOC species. Some of the VOC species identified in motor vehicle emissions were found to be among the most prolific of all the VOC species in forming ozone.

If the contribution of each VOC to ozone production is combined with the observed trends in VOC concentrations, a downward trend in episodic peak ozone concentrations in north west Europe would have been expected during the 1990s. The present analyses should be extended to address the quantitative origins of the elevated ozone concentrations in terms of the VOC emissions from individual stationary source categories and the National Plan for VOCs and ozone.

8.2 OZONE CONTROL STRATEGIES USING THE UK PTM

The broader picture of the sensitivity of ozone formation to VOC or NOx emission reductions under photochemical episode conditions has also been investigated using the UK PTM. Straight line trajectories were set up to run to the centres of each of the Ordnance Survery 100km x 100km grid squares. Straight line trajectories were followed for 96 hours arriving at each grid square centre at 18:00z. One trajectory only was followed into each arrival point with a bearing of 100 degrees from true North, simulating the broad easterly flows associated with regional scale ozone episodes. The emissions employed in the base case experiment were the standard values appropriate to the base year of 1995. The model employed the chemical mechanism MCMv2.0 and described the chemistry of 123 emitted VOC species. In these experiments, ozone precursor emission reductions are applied 'across-the-board', that is, with the same percentage reduction irrespective of source and location, whether in the UK or in the rest of Europe.

The ozone distribution with base case emissions is illustrated in Figure 8.1 and shows a steady progression in peak ozone levels from 40 ppb in the far north of Scotland to 130 ppb in south-west Wales. In Figure 8.2, we have plotted the total oxidised nitrogen NO_z concentrations in each of the air parcels from the final concentrations of nitric acid, nitrate aerosol and the sum of over 190 peroxyacyl nitrate species. The NO_z concentrations vary over the range ppb across the British Isles. The ratio of the final ozone to NO_z concentrations defines the ozone-sensitivity indicator ratio $[O_3]/[NO_z]$ and this is plotted out in Figure 8.3. This indicator has been defined by the studies of Sillman *et al.* (1997) to indicate the likely ozone-sensitivity of an air mass, such that:

- $[O_3]/[NO_z] > 12$, then the air parcel is NO_x-sensitive, and
- $[O_3]/[NO_z] < 12$, then the air parcel is VOC-sensitive.

In this context, NO_x-sensitive means that the air parcel shows a greater reduction in ozone concentrations in response to a reduction in NO_x emissions than to a reduction in VOC emissions, and vice versa for VOC-sensitive.

In Figure 8.4, the model results are shown of the NO_x or VOC-sensitivity of each parcel. The final ozone concentrations in the base case model experiments were compared directly with those from model experiments with 30% reductions in NO_x emissions and in VOC emissions. If the ozone response, base case - reduction case, was larger with 30% NO_x emission reductions than with 30% VOC emission reductions, then the air parcel was termed NO_x-sensitive. If the ozone response, base case - reduction case was larger with 30% VOC emission reductions than with 30% NO_x emission reductions, then the air parcel was termed VOC-sensitive. The map then shows 'V' for the VOC sensitive air parcels and 'N' for the NO_x-sensitive air parcels.

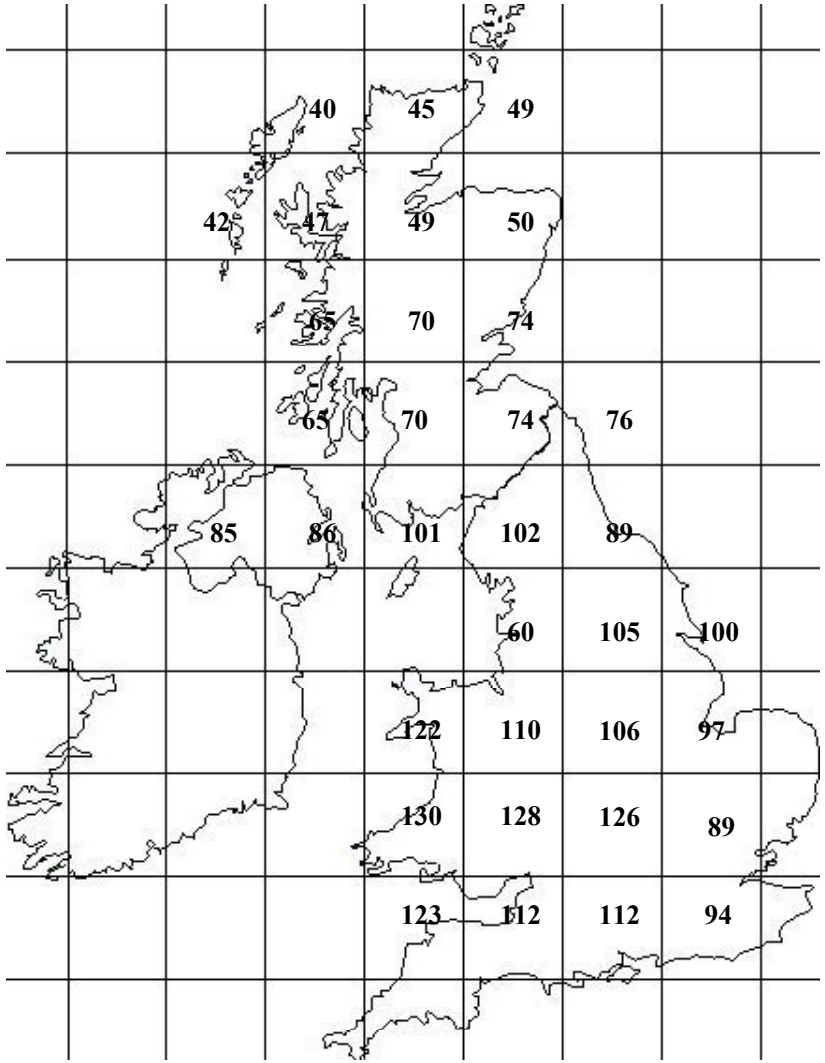

Figure 8.1 ***UK PTM model calculated ozone concentrations in the base case model experiment in ppb.***

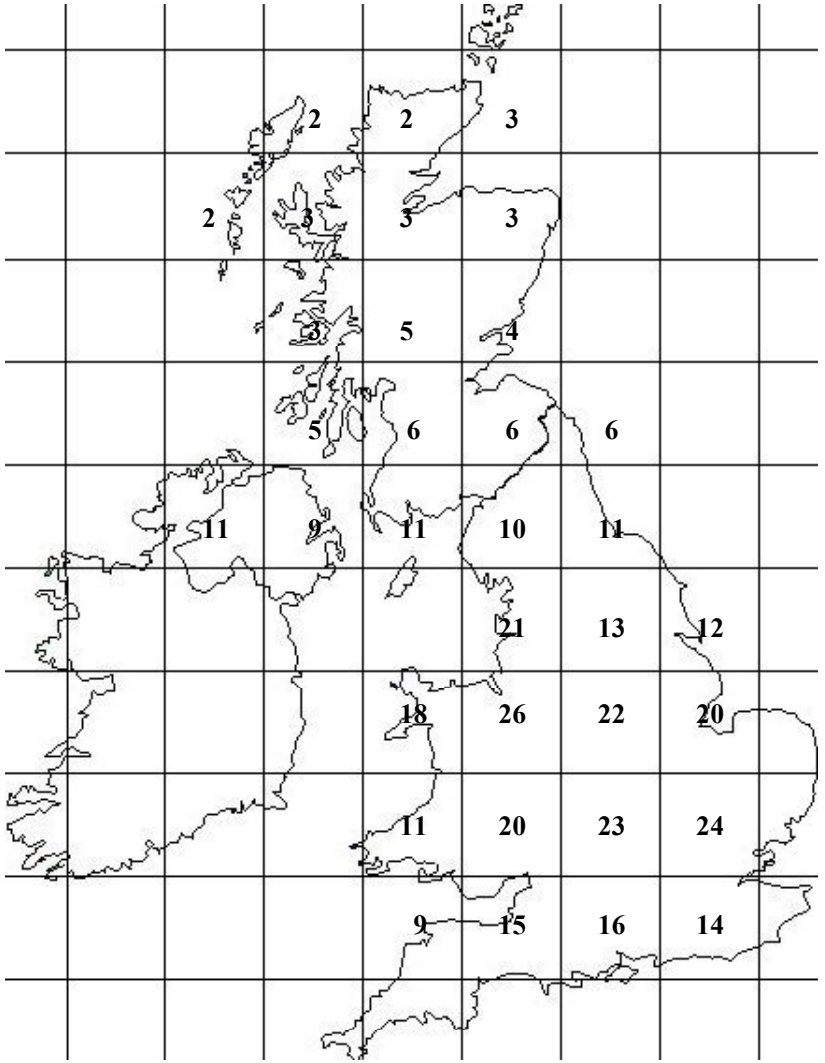

Figure 8.2 ***Concentrations of NO_z = HNO3 + nitrate aerosol + sum of PANs in the Base Case Model Experiment in ppb.***

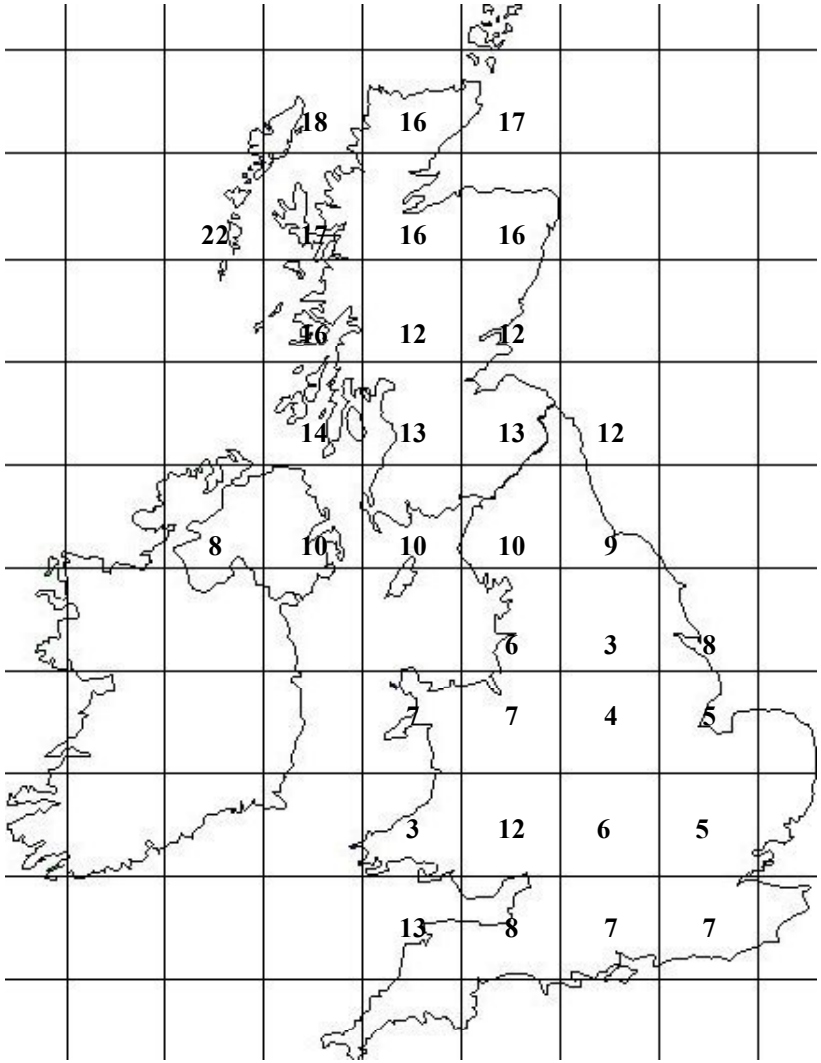

Figure 8.3 ***Ozone-sensitivity Indicator Ratios, $[O_3]/[NO_2]$ in the Base Case Model Experiment.***

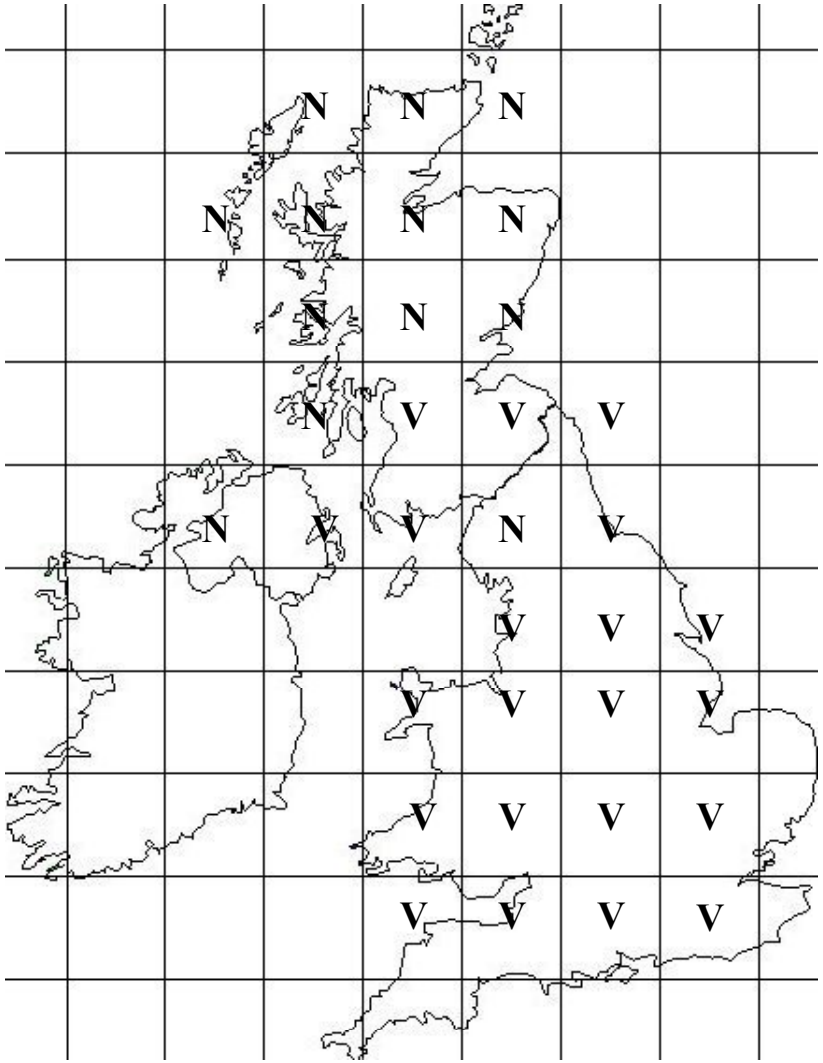

Figure 8.4 ***VOC- (V) or NOx-Sensitivity (N) across the British Isles as shown by the UK PTM.***

In Figure 8.5, we tie together the model ozone responses to NO_x and VOC emission reductions with the $[O_3]/[NO_z]$ indicator ratios. In this plot, a pair of points is plotted for each air parcel, showing the ozone responses for NO_x and VOC controls against the indicator ratio in the base case experiment. On the left hand side of the diagram, the ozone responses to VOC control, open squares, tend to be higher than those responses to NO_x control, plus signs. On the right hand side of the diagram, the ranking of the symbols changes, with the plus signs, placed above the open squares. Clearly then, there is a changeover from VOC control responses being larger than NO_x control responses to NO_x control responses being larger than VOC control responses. There is therefore a changeover from VOC- to NO_x-sensitivity with increasing $[O_3]/[NO_z]$ ratio exactly as predicted by theory. VOC-sensitivity is indicated by low indicator ratios and NO_x-sensitivity by higher indicator ratios. This gives a measure of support to the application of the UK PTM to the quantitative assessment of ozone control strategies.

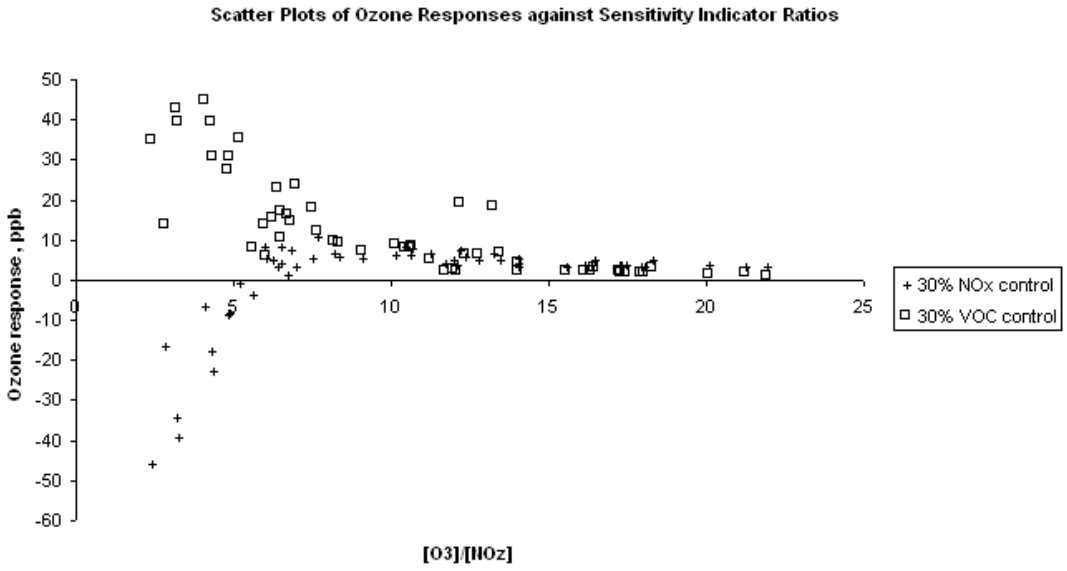

Figure 8.5 ***Scatter plots of Ozone Responses to 30% NOx controls (+) and to 30% VOC controls (squares) against the Ozone Sensitivity Indicator Ratios $[O_3]/[NO_z]$ in the Base Case Model Experiment.***

8.3 OZONE BENEFITS ACCRUING FROM THE UN ECE PROTOCOLS AND THE NATIONAL EMISSIONS CEILINGS DIRECTIVE

8.3.1 Introduction

The UNECE, through its Convention on Long Range Transport of Air Pollution (LRTAP), has concluded negotiations on a protocol to address the issues of acidification, eutrophication and ground-level ozone (the Gothenburg Protocol). Emission reduction targets for European countries have been defined for sulphur oxides, nitrogen oxides, VOC and ammonia. Further action is being considered under the EU draft Directives on 'National Emission Ceilings for Certain Atmospheric Pollutants' and 'Ozone in Ambient Air' (COM(1999) 125 final). The former is commonly referred to as the 'National Emissions Ceilings Directive (NECD)', and includes the setting of emissions ceilings for ozone precursors for 2010. The latter proposes an obligation for member states to implement short term action plans where there is a risk of

exceedence of the alert threshold (120 ppbv) for three or more hours at sites representative of a zone or agglomeration, or to demonstrate that realistic action plans would be ineffective.

As part of Task 6 of the present programme (policy support - national plan for VOCs/ozone), the PTM/CRI mechanism has been used to investigate the influence of a series of ozone precursor emissions controls on peak ozone levels typical of a UK photochemical episode, in relation to the two policy issues described above. First, peak ozone concentrations have been simulated with a series of year 2010 emissions scenarios related to the EU NECD, allowing the effectiveness of the different measures to be compared. Secondly, the severity and frequency of extreme ozone events (≥ 120 ppbv) in the UK has been examined, and the influence of a series of illustrative UK action plans has been simulated to investigate the possible impact on the duration or severity of the most severe recent event.

8.3.2 National Emissions Ceilings Directive (NECD)

Emissions Scenarios

The ozone episode case study (31 July 1999), as described in Sections 5.2.4 and 5.3.2, was extended to investigate the influence of a series of emissions scenarios on simulated peak ozone at the 8 southern UK sites. The emissions scenarios are summarised in Table 8.1. The '1998 ref' scenario is that which was applied in the investigation presented in Section 5.2.4 (complete with temporal variations), such that the ozone levels simulated with this base case are the same as those given in Figure 5.6.

Table 8.1 ***Summary of NECD-related emissions scenarios used for investigation of the influence of precursor emission controls on episodic ozone levels.***

Abbreviation	Description	UK VOC and NO_X totals
1998 ref (base case)	1998 UK emissions of CO, NO_X, SO_2 and VOC as defined by NAEI[1]. Other relevant country total scaled to latest EMEP values[2].	VOC: 1958 kt a^{-1} NO_X: 1753 kt a^{-1}
2010 UK ref	2010 UK emissions of CO, NO_X, SO_2 and VOC as projected by NAEI[3]. Emissions outside UK unchanged from 1998 ref.	VOC: 1252 kt a^{-1} NO_X: 1167 kt a^{-1} (NECD)
2010 UK 1200	UK VOC emissions reduced to meet NECD according to NAEI scenario[3]. Emissions outside UK unchanged from 1998 ref.	VOC: 1200 kt a^{-1} (NECD) NO_X: 1167 kt a^{-1} (NECD)
2010 UK 1150	UK VOC emissions further reduced according to NAEI scenario[3]. Emissions outside UK unchanged from 1998 ref.	VOC: 1150 kt a^{-1} NO_X: 1167 kt a^{-1} (NECD)
2010 NECD	As 2010 UK 1200, with other EU country totals set at NECD values. Other relevant country totals set to EMEP 2010 projection[2].	VOC: 1200 kt a^{-1} (NECD) NO_X: 1167 kt a^{-1} (NECD)

Notes: [1] 1998 emissions available from National Atmospheric Emissions Inventory, NAEI (http://www.aeat.co.uk/netcen/airqual/). [2] EMEP website (http://www.emep.int/index.html) accessed August 2000. 'Latest' values generally corresponded to 1997. Projections for 2010 based on reduction plans in force at that time. 3 NAEI 2010 reference scenario supplied by J. Goodwin, AEA Technology; VOC reduction scenarios based on cost curve analysis supplied by N. Passant and J. Goodwin, AEA Technology.

Simulated Influence on Peak Ozone Mixing Ratios

The model was used to simulate the chemical development over a 96 hour period along the 8 trajectories arriving at the southern UK sites at 1600 hr (Figure 5.4). The calculation was carried out with the arrival day corresponding, in turn to each day of the week, and the complete set of calculations was repeated for each of the emissions scenarios summarised in Table 8.1. The simulated ozone mixing ratios at the end points are presented in Figure 8.6.

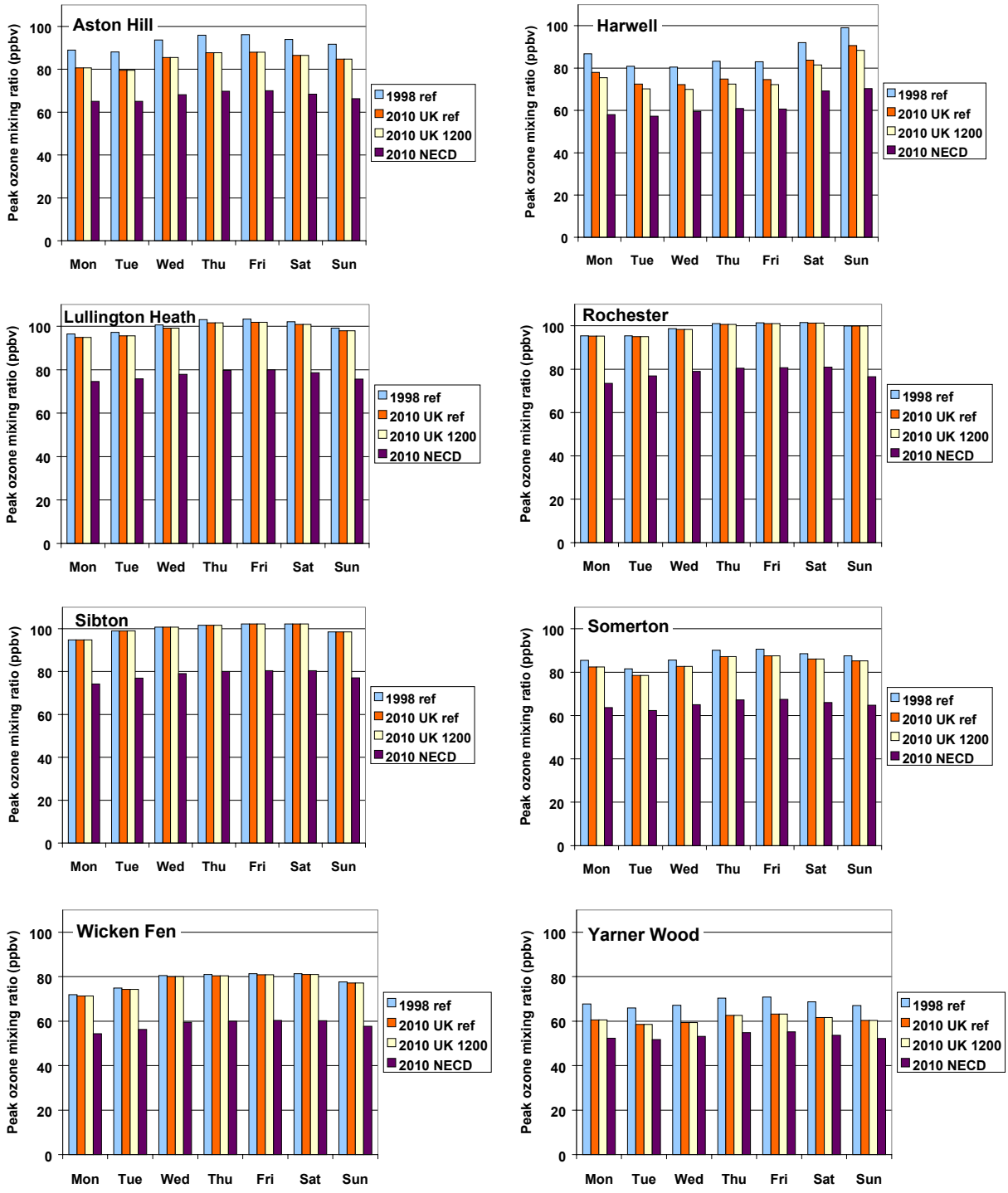

Figure 8.6 ***Variation of simulated peak ozone mixing ratios at 8 southern UK sites with day of week. Results are shown for the emissions scenarios given in Table 8.1. The results simulated using 2010 UK 1150 were identical to those with 2010 UK 1200.***

The influence of the changing emissions scenarios is reasonably independent of day of week, but shows some variability from one site to another, particularly for those scenarios in which only UK controls are implemented. Figure 8.7 summarises the information in terms of the percentage reduction in simulated peak ozone at each site, relative to the 1998 reference, with each of the scenarios (averaged over all 7 days). The sites are presented in order of location from west to east to emphasise the geographical dependence of the effectiveness of the control

measures. Relative to the 1998 reference, there is generally a clear decreasing trend in percentage ozone reduction from west to east as a result of purely UK measures, reflecting that the prevailing airflow is broadly from the east. In the limit, Sibton is totally unaffected by any UK reductions under the meteorological conditions of the present case study. Harwell is an exceptional case, in that the corresponding trajectory passes directly over London prior to arrival (Figure 5.4), and therefore receives substantial UK emissions. As a result, the simulated influence of UK reductions is significantly greater than for sites further west (*e.g.* Aston Hill). Under the precise conditions of 31 July 1999, Harwell may be regarded as being representative of sites directly downwind of major UK population centres during an ozone episode.

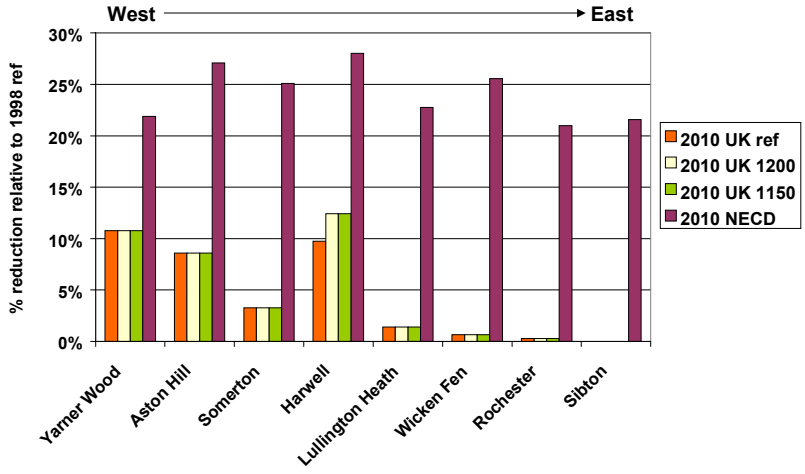

Figure 8.7 ***The percentage reduction in simulated peak ozone at each site, relative to the 1998 reference, for each of the scenarios in Table 8.1. Results represent the average of the results for each day of the week (Figure 8.6).***

The reduction of VOC emissions from '2010 UK ref' to '2010 UK 1200' (*i.e.* 1252 to 1200 kt a^{-1}) is only calculated to have an effect at Harwell, and the further reduction from '2010 UK 1200' to '2010 UK 1150' (*i.e.* 1200 to 1150 kt a^{-1}) has no simulated influence at any of the sites. The main reason for the limited influence is the nature of the specific reduction measures defined by the cost-curve analysis. The reduction from 1252 to 1200 kt a^{-1} involves control measures which mainly target oil refineries (Passant, 2000), such that only trajectories which pass over these specific point sources are influenced. The measures include the Coryton and Shell Haven refineries on the north of the Thames estuary and therefore specifically influence the trajectory to Harwell in the present case study. The reduction from 1200 to 1150 kt a^{-1} involves control measures which mainly target crude oil loading (Passant, 2000). This largely occurs in Scotland (*e.g.* Edinburgh Hound Point), although some measures are further south (*e.g.* North Tees, Hamble). The specific locations do not influence any of the trajectories considered in this study.

Figure 8.6 and Figure 8.7 demonstrate that the reduction of precursor emissions to the 2010 NECD scenario (involving controls throughout Europe) is accompanied by notable reductions (*ca.* 20-25%) in the simulated peak ozone mixing ratios at all 8 southern UK sites. This emphasises the transboundary nature of the ground level ozone problem, and the importance of internationally co-ordinated strategies. The results indicate that the influence of the agreed precursor controls outside the UK has a greater influence on the simulated peak ozone than those within the UK at all 8 sites, and that controls outside the UK are essential for any significant reduction in peak values at locations to the east/south east of the country.

The relationship between peak ozone mixing ratio and number of hours exceedence of the 90 ppbv threshold (Figure 5.7) was once again used to infer the number of hours ≥ 90 ppbv at each of the 8 sites for each of the emissions scenarios. Figure 8.8 shows the combined results for the

6 sites where the 90 ppbv threshold was calculated to be achieved on at least one day of the week in the base case. This shows that the UK reductions typically lead to some reduction in the total number of hours ≥ 90 ppbv, particularly on the days where the exceedences are more prevalent in the base case. However, the achievement of the NECD targets throughout the EU (and associated projections in non-EU countries) is calculated to reduce peak ozone levels sufficiently that no hours ≥ 90 ppbv are predicted to occur at any of the 8 sites under the conditions of this case study.

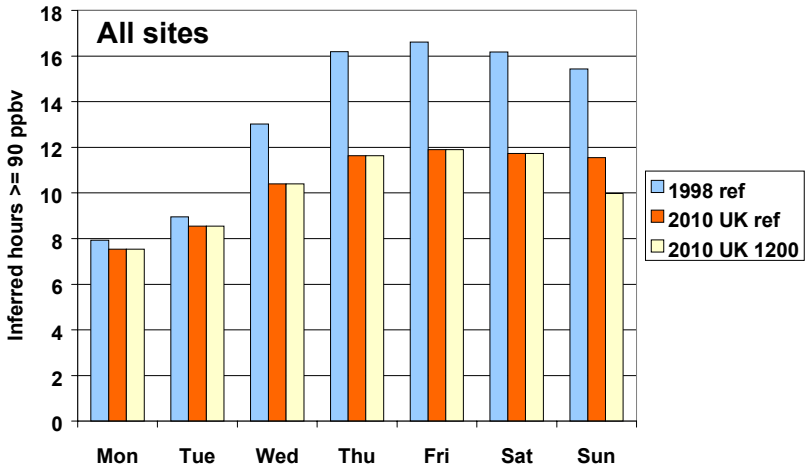

Figure 8.8 ***Variation of inferred number with hours ≥ 90 ppbv ozone with day of week at all considered sites. Results are shown for the emissions scenarios given in Table 8.1. The results for 1998 ref are the same as shown in Figure 5.8. The results simulated using 2010 UK 1150 were identical to those with 2010 UK 1200. The 2010 NECD scenario led to no exceedences of 90 ppbv.***

Sensitivity to VOC and NO_X Reductions

The ozone formation characteristics along the trajectories to all the sites were investigated by performing additional calculations in which the emissions of anthropogenic VOC and NO_X were reduced, in turn, by 10% throughout the whole model domain. This was carried out with both the 1998 ref scenario and the 2010 NECD scenario, to explore changes in the precursor sensitivity arising from the agreed reductions.

Figure 8.9 shows the influence of the 10% precursor reductions, with arrival on Saturday. The results were found to be very insensitive to changes in arrival day, such that the results in Figure 8.9 are typical of any day of the week. The results using the 1998 ref scenario show clearly that the trajectory to Harwell is strongly VOC-limited, with a significant decrease in the calculated ozone concentration when VOC emissions are reduced, and a significant increase when NO_X emissions are reduced. The other sites are less sensitive to the controls, although Rochester and Sibton also display a marginal increase when NO_X is controlled indicative of notable VOC-limitation. The remaining five sites all show modest reductions in ozone when either precursor is reduced, with VOC reductions having a slightly greater effect in three of the five cases. This suggests that the southern UK tends to be more VOC-limited under the 1998 ref scenario, since the majority of sites show greater ozone reductions when VOC emissions are reduced.

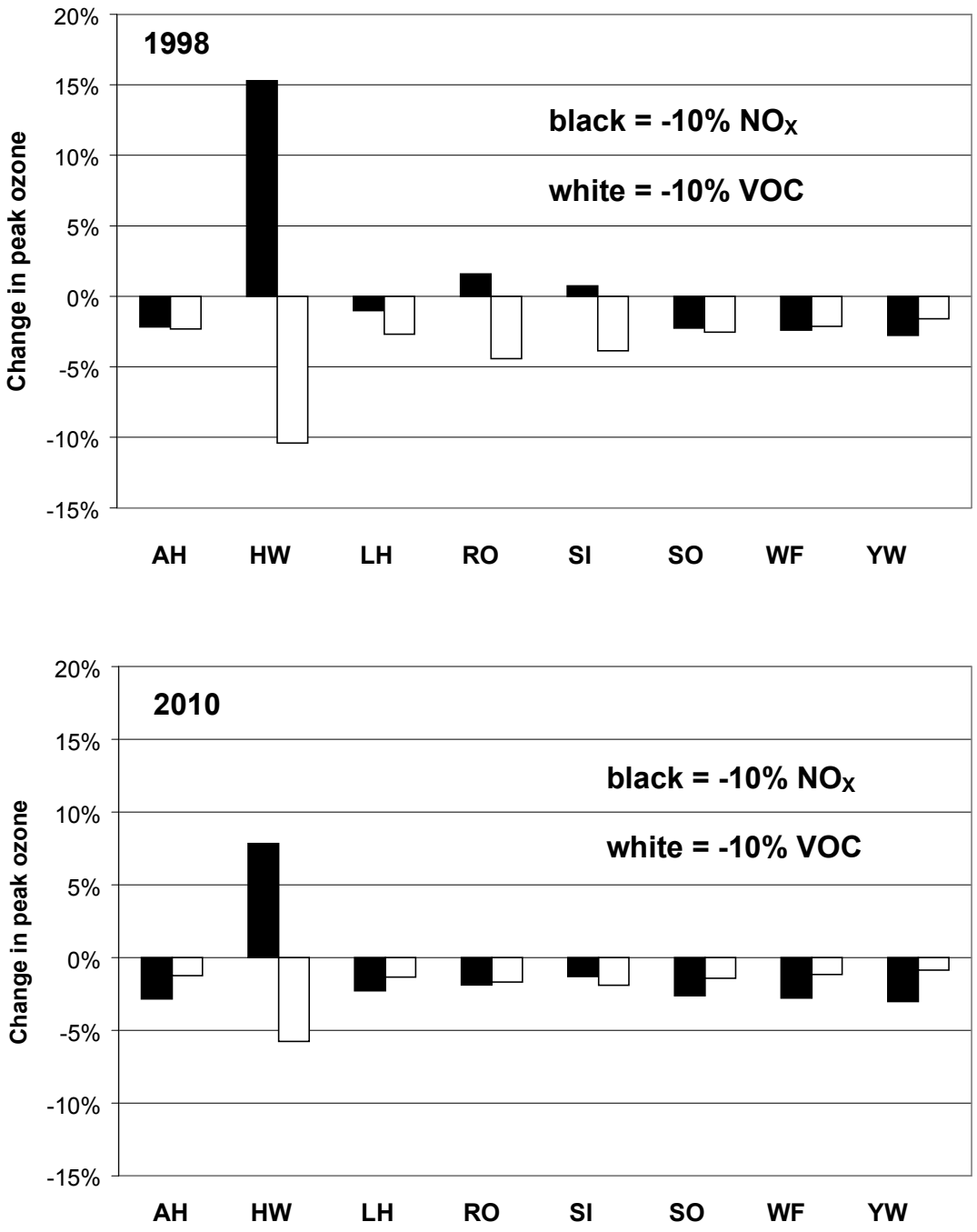

Figure 8.9 ***Percentage change in the simulated peak ozone mixing ratios at 8 southern UK sites with 10% reductions in VOC or NO_X emissions throughout Europe, for the meteorological conditions of 31 July 1999 (Saturday arrival). Simulations were carried out using the 1998 ref scenario, and the 2010 NECD scenario (see Table 8.1). AH – Aston Hill; HW – Harwell; LH – Lullington Heath; RO – Rochester; SI – Sibton; SO – Somerton; WF – Wicken Fen; YW – Yarner Wood.***

With the 2010 NECD scenario, the trajectory to Harwell is still clearly VOC-limited, although the relative effectiveness of a 10% VOC reduction is reduced by a factor of about two compared with the 1998 ref scenario. The other sites all show reductions in ozone when either precursor is reduced, with NO_X reductions having a greater effect in all but one case. A significant shift toward NO_X-limitation is therefore observed with the 2010 NECD scenario.

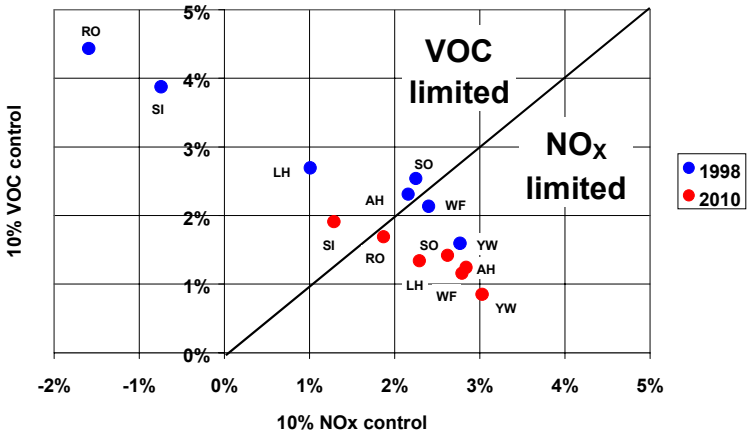

Figure 8.10 ***Percentage reduction in the simulated peak ozone resulting from 10% reductions in VOC or NO_X emissions throughout Europe, with either 1998 ref or NECD 2010 scenarios (see Figure 8.9 caption for key to sites). Harwell is strongly VOC-limited with both scenarios and is off scale.***

This is also apparent from Figure 8.10, which presents the results for both emission scenarios on a single 'scatter' plot. This shows the percentage reduction in peak ozone resulting from a 10% reduction in NO_X (on the x-axis) and a 10% reduction of VOC (on the y-axis). The 1:1 line therefore represents the division between VOC-limitation and NO_X limitation. Whereas 6 of the 8 sites fall in the VOC-limited region with the 1998 ref scenario, the shift towards NO_X-limitation results in only 2 of the 8 sites being VOC-limited with the 2010 NECD scenario.

To investigate inter-episode variability, the CRI-PTM with 1998 ref scenario has also been used to provide an analysis of a widespread photochemical ozone episode on the 10 August 1997. The model is able to recreate adequately the peak the levels of ozone observed at the same series of 8 southern UK sites. Once again, the sensitivity to reductions of precursor NO_X and VOC emissions throughout the model domain has been performed. With 10% reductions, 5 of the 8 sites show a greater response to VOC than to NO_X, as shown in Figure 8.11. This result is similar to that from analysis of the 31 July 1999 episode (Figure 8.9), in which 6 of the same 8 sites showed a greater response to VOC control. However, although the picture is broadly similar, the distribution of sites showing NO_X and VOC limitation clearly differs in the 2 episodes, emphasising that the influence of emissions controls at a particular site depends on the precise conditions of the episode. To enable comparison with calculations performed with the OSRM, the influence of 30% reductions in the precursor emissions was also investigated for the 10 August 1997 episode. As shown in Figure 8.11, this provided a similar picture to the 10% reduction calculations, but with a marginal shift towards NO_X limitation at all sites, such that 4 of the 8 sites showed a greater response to VOC reduction, and the other 4 a greater response to NO_X reduction. This result is similar to the conclusions of an analysis with the OSRM which demonstrated comparable effects of VOC and NO_X controls at these sites for 10 August 1997 (see Table 8.2 and Section 6.5). As shown in the table, the conclusions concerning VOC or NO_X sensitivity differ at only one site.

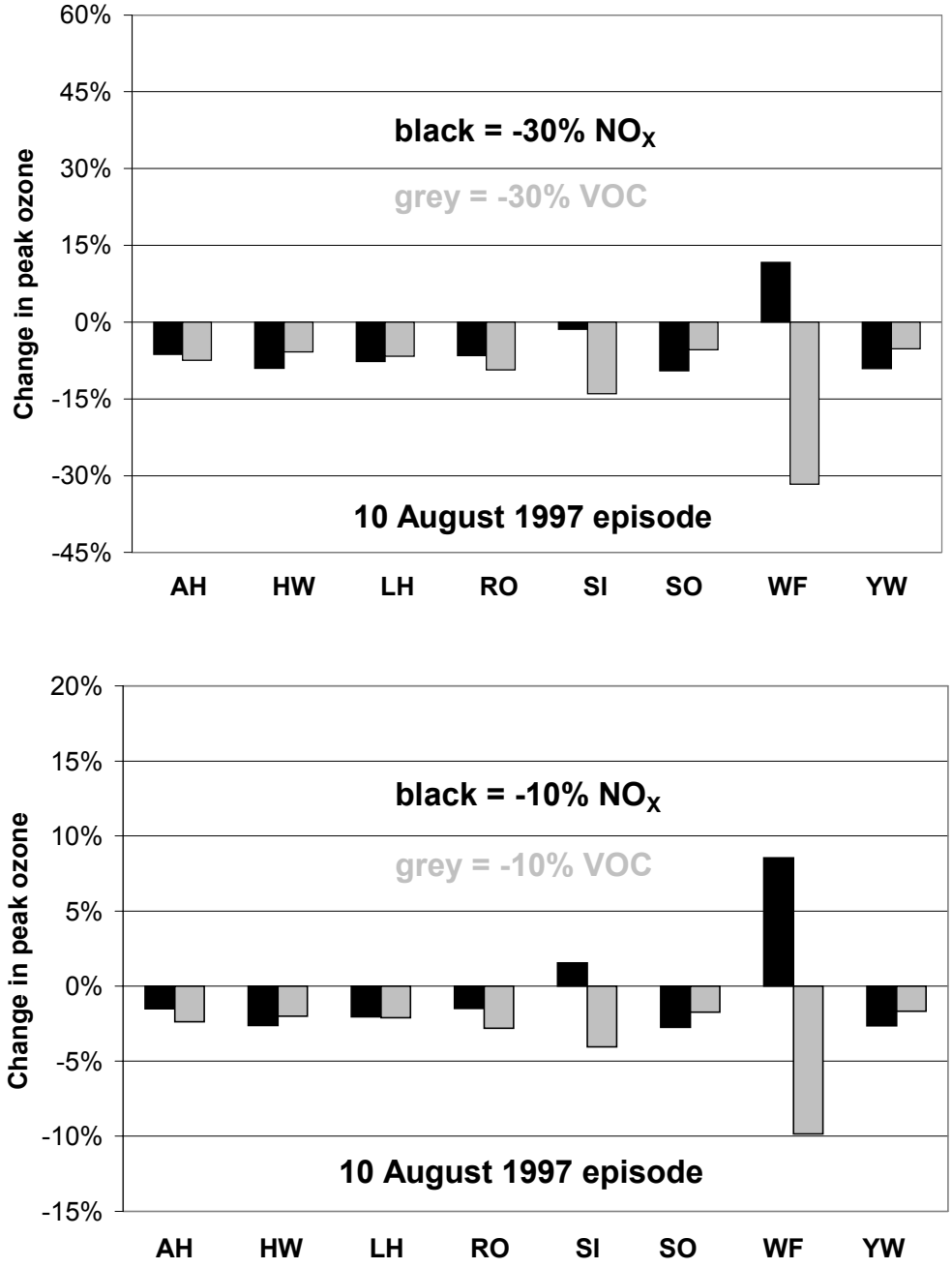

Figure 8.11 ***Percentage change in the simulated peak ozone mixing ratios at 8 southern UK sites with 10% and 30% reductions in VOC or NO_X emissions throughout Europe, for the meteorological conditions of 10 August 1997 (Sunday arrival). Simulations were carried out using the 1998 ref scenario (see Table 8.1). AH – Aston Hill; HW – Harwell; LH – Lullington Heath; RO – Rochester; SI – Sibton; SO – Somerton; WF – Wicken Fen; YW – Yarner Wood.***

Table 8.2 ***Comparison of sensitivity to 30% precursor reductions for 10 August 1997 episode at the 8 southern UK sites using the CRI-PTM and the OSRM. V = VOC-limited; N = NO_X-limited.***

	AH	HW	LH	RO	SI	SO	WF	YW
PTM	V	N	N	V	V	N	V	N
OSRM	V	N	N	N	V	N	V	N

Conclusions

The present investigation of ozone precursor control scenarios using a representative case study allows a number of conclusions can be drawn:

- Reductions in UK precursor emissions from 1998 to 2010 reference levels are calculated to have little or no effect on peak episodic ozone levels at locations to the east of the UK.

- Greater influences (up to 11% reduction) are calculated for locations on the west of the UK, or specific locations which are downwind of regions with particularly high UK emissions.

- Additional VOC reductions (1252 to 1200 kt a^{-1}) to meet the NECD target may have a small additional influence on selected downwind locations: further proposed reductions (1200 to 1150 kt a^{-1}) appear unlikely to have a major effect on peak episodic ozone levels.

- Achievement of NECD targets throughout the EU (together with projected reductions in non-EU countries) are calculated to lead to a reduction of 20-25% in peak episodic ozone levels in the UK.

- The reduction of precursor emissions from 1998 to 2010 levels will be accompanied by a significant shift towards NO_X-limited conditions for episodic ozone formation.

8.3.3 Evaluation of the Ozone Benefits Accruing from the Implementation of the UNECE VOC Protocol

In Europe, member states have agreed within the aegis of the United Nations Economic Commission for Europe to reduce emissions of volatile organic compounds (UN ECE 1991) and nitrogen oxides (UN ECE 1988) so as to limit ozone formation and its transboundary transport. At the time these agreements were reached, it was widely understood that their emission reduction would be largely met by the widespread implementation of three-way catalyst exhaust and evaporative emission controls on petrol-engined motor vehicles (NORDIC, 1991). The uptake of these pollution control technologies has been made mandatory in the European Union through a series of motor vehicle emission control Directives.

In this study, the UK Photochemical Trajectory Model and the Master Chemical Mechanism v3.0 are used to identify those organic compounds that are responsible for the bulk of the photochemical ozone formation. Observational data are then reviewed to assess the likely impact of motor vehicle emission controls on the urban concentrations of the most prolific ozone forming compounds. The observed trends of the most prolific ozone forming organic compounds and the computer modelling studies of their ozone formation potential are then used to deduce trends in peak ozone concentrations. These deduced trends are then compared with ozone observations to see if the expectations of the policy-makers have been realised with respect to photochemical ozone formation and its control.

Details of how the UK Photochemical Trajectory Model was set up to use a highly speciated emission inventory and the Master Chemical Mechanism v3.0 are given above in Section 7.6. Using the standard Austria-UK trajectory, ozone concentrations were calculated over a five day travel time in an air parcel which arrived at the England-Wales border. The peak ozone

concentration calculated for the fifth and last day was 85.9 ppb. The UK PTM model was then rerun a further 124 times with the emission of each VOC species set to zero in turn. The difference in ozone concentrations was taken as an indication of the contribution to ozone formation of that VOC species as discussed in Section 7.6.4 above. Table 7.3 tabulated the absolute ozone forming potentials of the 124 VOC species in rank order.

Figure 8.12 presents the observed trends in the 90-day running mean concentrations of six of the more important VOC species identified in Table 7.3 at an urban background location in central London over the period 1994-2000. The observed trends are statistically significant and range between –4.5 and –12.0 % year^{-1} for the VOC species plotted. At the chosen location, motor vehicle traffic dominates as the major source of the observed VOC species. Clear downwards trends are observed for the predominantly motor vehicle exhaust species: ethylene, propylene, toluene, *m*+*p*-xylene and the predominantly petrol evaporative species: *n*-butane and *i*-pentane.

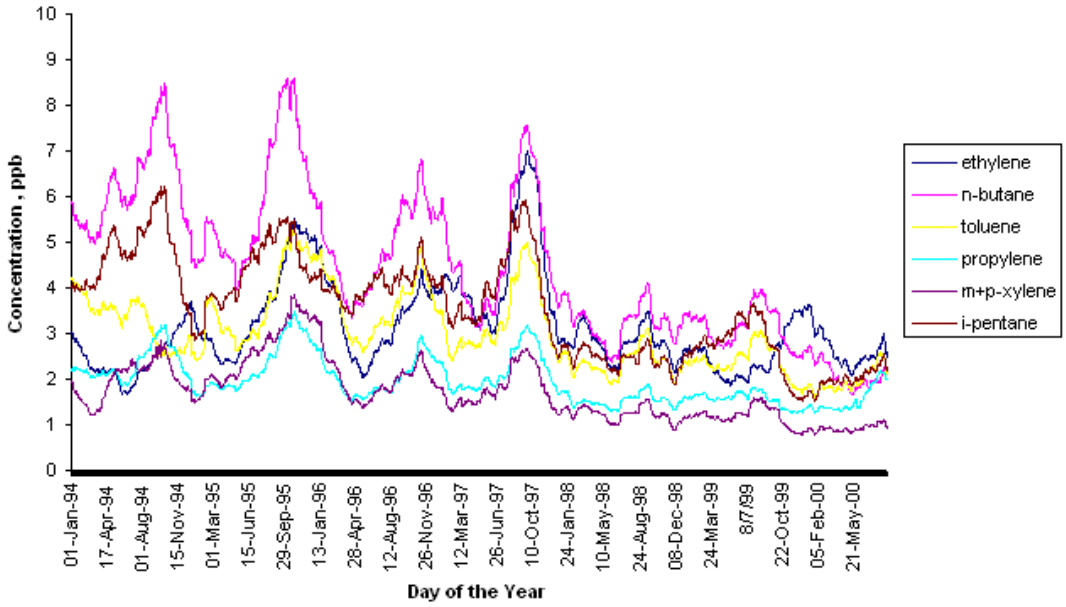

Figure 8.12 ***Time Series of the 90-day Running Mean Concentrations of Six Selected VOC Species at an Urban Background Location in Central London over the Period 1994-2001.***

Table 8.3 presents the estimated absolute reactivities and the observed trends for each VOC species at the urban background location in central London. If is assumed that that observed VOC concentration trends reflect emissions more widely in north west Europe, then these concentrations trends should drive a reduction in photochemical ozone formation. An indication of the magnitude of this reduction in ozone formation should be given by the product of the reactivity and the observed ozone trend. These derived ozone reductions driven by each VOC species are also tabulated in Table 8.3. As is apparent, some of the most prolific ozone-forming VOC species are showing large and highly significant downward trends. The estimated downwards trends in peak ozone concentrations due solely to the VOC species for which there are trend data available amounts to a concentration trend of -2.2 ppb year^{-1}, as shown in Table 8.3.

Table 8.3 ***The Percentage by Mass in Emissions, the Contribution made to Peak Ozone Levels, their Observed Urban Concentration Trends and the Resulting Trend induced in Ozone for a Selection of Volatile Organic Compounds.***

Rank	Volatile Organic Compound	% by Mass Emission	Peak Ozone Formation (ppb)	Observed VOC Trend, (% year^{-1})	Resulting Peak Ozone Trend (ppb year^{-1})
1	n-butane	8.7	4.31	-10.8	-0.47
2	ethylene	2.7	3.13	-4.5	-0.14
3	ethanol	5.6	2.74		
4	toluene	4.0	2.49	-8.6	-0.21
5	i-pentane	4.0	1.91	-10.0	-0.19
6	propylene	1.5	1.83	-5.6	-0.10
7	n-pentane	3.7	1.78	-8.4	-0.15
8	n-hexane	3.0	1.76	-4.4	-0.08
9	m-xylene	1.7	1.68	-12.0	-0.20
10	1,2,4-trimethylbenzene	1.1	1.50		
11	o-xylene	0.9	0.96	-12.3	-0.12
12	i-butane	2.3	0.84	-10.5	-0.09
13	p-xylene	0.8	0.80	-12.0	-0.10
14	n-heptane	1.3	0.76	-8.4	-0.06
15	propane	3.0	0.68	-3.7	-0.03
16	ethylbenzene	1.1	0.67	-12.3	-0.08
17	formaldehyde	1.4	0.65		
18	1,3,5-trimethylbenzene	0.4	0.50		
19	n-octane	0.9	0.47		
20	benzene	1.7	0.45	-11.4	-0.05
25	1,3-butadiene	0.4	0.34	-10.3	-0.04
27	ethane	2.6	0.32	+4.1	+0.01
28	but-1-ene	0.2	0.31	-10.5	-0.03
34	2-methylpentane	0.3	0.18	-6.7	-0.01
42	3-methylpentane	0.2	0.11	-6.7	-0.007
43	acetylene	0.9	0.11	-11.4	-0.01
50	cis pent-2-ene	0.02	0.06	-10.5	-0.006
53	cis but-2-ene	0.04	0.05	-7.4	-0.004
58	trans pent-2-ene	0.05	0.04	-10.5	-0.004
88	isoprene	0.002	0.02	-10.7	-0.002
	Total		**36.8 ppb**		**-2.2 ppb yr^{-1}**

The VOC species profiles for motor vehicle exhaust emissions and petrol evaporation in the speciated inventory, point to there being significant downwards trends in the emissions of a small number of additional VOC species for which comparable monitoring data to that used in Table 8.3 are not available. If it is assumed that all of these species currently exhibit comparable downwards trends of –10% year^{-1}, then these non-monitored VOC species would account for an additional -0.7 ppb year^{-1} downwards trend in episodic peak ozone concentrations. The largest contributing non-monitored species appear to be the trimethylbenzenes and C_8 alkanes.

Over the time period covered by the UN ECE VOC Protocol, emissions of acidifying and eutrophying agents have been reduced under the framework of the Convention on Long Range Transboundary Air Pollution. Furthermore, the pollution control measures implemented under the UN ECE VOC Protocol and their underpinning Commission of the European Communities directives have reduced the emissions of carbon monoxide (CO). Although they are not commonly considered ozone precursors, CO and SO_2 act together with NO_x and VOCs in the presence of sunlight to drive photochemical ozone formation. As a result, it is possible that the simultaneous reductions in emissions of CO, NO_x and SO_2 across Europe will have confounded the attribution of the observed trends in episodic peak ozone to the UN ECE VOC Protocol.

The UK PTM model has therefore been used to investigate how reductions in CO emissions may have influenced photochemical ozone formation in north west Europe. The model responses to the current annual trends in CO were estimated by performing a base case model run using 1999 emissions taken from EMEP (2001) and a sensitivity case was run with emissions reduced by the annual trend in CO emissions. The differences in the time development of the ozone concentrations between these two cases are then displayed in Figure 8.13.

The time development of the ozone response to one year's worth of the annual trend in CO emissions appears to build up steadily throughout the trajectory, reaching eventually about –0.35 ppb at the end of the fifth day. This shows that reducing CO emissions decreases episodic peak ozone formation, a model response entirely analogous to that of the VOCs. The response appears to accumulate along the trajectory because of the intrinsic low reactivity of CO, giving a timescale for its oxidation of several days under photochemical episode conditions. The current annual decline in European CO emissions should on this basis be contributing on the order of –0.35 ppb year^{-1} to the trends in episodic peak ozone concentrations.

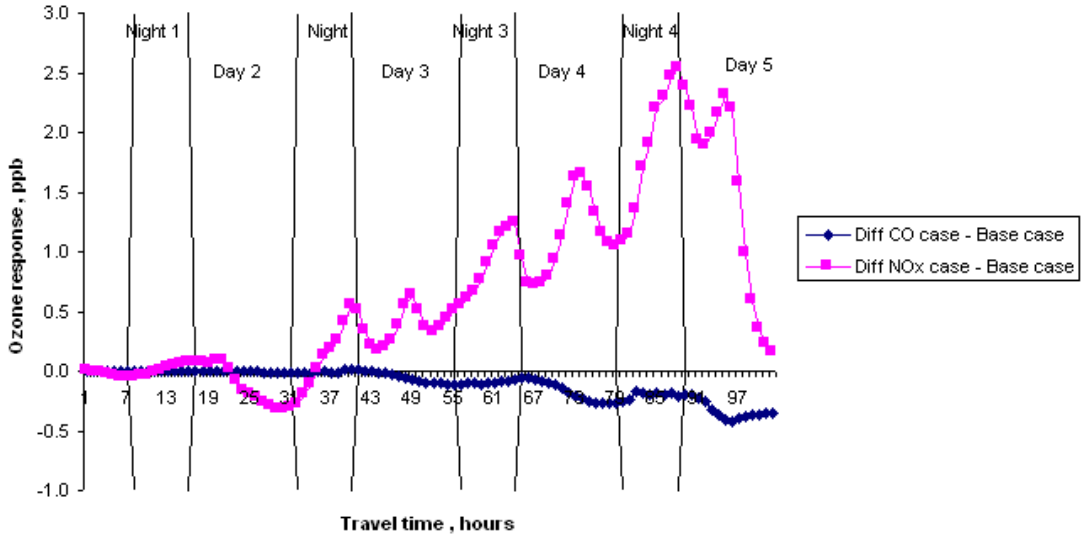

Figure 8.13 ***Time Development of the Ozone Responses to the Annual Trends in European CO and NO_x Emissions Calculated in a Trajectory Model.***

The UK PTM model was then used to investigate how reductions in NO_x emissions may have influenced photochemical ozone formation in north west Europe by modelling the ozone response to one year's worth of the current annual trends in NO_x emissions. The base case model run was performed using 1999 emissions taken from EMEP (2001) and a sensitivity case was run with emissions reduced by the annual trend in NO_x emissions. The difference in the time development of the ozone concentrations between these two cases is also displayed in Figure 8.13.

In contrast, the model ozone response to one year's worth of the annual trend in NO_x emissions is much larger and is of opposite sign to that for CO. That is to say, ozone concentrations generally increase along the trajectory in response to the decreasing NO_x emissions. The model response to NO_x emissions is however much more complex than that of CO or indeed, VOCs.

In this figure, three regimes can be identified in the model response to the NO_x emission reductions relative to the base case, as follows:

- during night-time, ozone concentrations tend to increase quite sharply due to decreased NO_x titration through the reaction $NO + O_3 \rightarrow NO_2 + O_2$,

- during the morning and early afternoons, ozone concentrations grow more quickly due to decreased NOx inhibition of the fast photochemistry and increased hydroxyl (OH) radical oxidation of the VOCs through the competition between the reactions of OH with NO2 and VOCs,

  i.e., $OH + NO_2 + M \rightarrow HNO_3 + M$
  vs. $OH + VOC \rightarrow HO_2 +$ carbonyl products

- during the afternoon, ozone concentrations decline mush more strongly due to increased NO_x loss that dramatically reduced the photochemical ozone production efficiency through increased radical loss through the competition between the reactions of peroxy radicals with NO and HO_2:

  i.e., $RO_2 + NO \rightarrow NO_2 + HO_2 +$ carbonyl products
  vs. $RO_2 + HO_2 \rightarrow ROOH + O_2$

In the earlier section of the trajectory, the decreased NO_x emissions reduce the ability of NO_x to inhibit ozone formation and ozone concentrations build-up faster than in the base case during the mornings. At these times, the fast photochemistry is VOC-limited because of the fresh injections of NO_x and VOCs during the early mornings. However by the mid-afternoon much of the NO_x is oxidised away and nitric oxide (NO) concentrations fall to levels where the chemistry becomes NO_x-limited. Ozone production falls relative to the base case because with the reduced NO_x emissions, NO_x-limiting conditions are reached earlier in the afternoon. By the time the 5th day is reached, the NO_x-limiting conditions are reached close to midday and during the entire afternoon ozone production falls along way below the levels achieved in the base case. By the time the end point of the trajectory is reached with reduced NO_x emissions, almost all the extra ozone found in the VOC-limited region has been lost in the NO_x-limited region.

Considering only the trajectory endpoint then, the current annual decline in European NO_x emissions should on this basis be contributing on the order of +0.16 ppb year^{-1} to the trends in episodic peak ozone concentrations and up to +2.5 ppb year^{-1} for areas closer to the main sources of ozone precursors.

Close in to the main ozone precursor source areas of north west Europe, the response of the episodic peak ozone concentrations to the reductions in European NO_x emissions is likely to have been complex. For those photochemical episodes characterised by intense, local production under VOC-limited conditions, it is likely that some areas will have experienced increased episodic peak ozone concentrations due to NO_x emission reductions whilst at the same time decreased episodic peak ozone concentrations due to VOC emission reductions, as shown by the model responses on the third and fourth days. However, for those photochemical episodes characterised by long range transport from more distant sources and ozone production under NO_x-limited conditions, episodic peak ozone concentrations may have been relatively weakly influenced by NO_x emission reductions, as shown by the model responses on the fifth

day. In the more remote regions of north west Europe, after several days of long-range transport under NO_x-limited conditions, it is likely that ozone concentrations will have decreased significantly because of the NO_x emission reductions. However, ozone concentrations steadily decline during long range transport due to efficient dry deposition and so these reductions in ozone concentrations will be apparent in concentrations that are well below their episodic peak levels.

Sulphur dioxide (SO_2) is photochemically oxidised in pollution episodes to sulphuric acid and sulphate aerosols by hydroxyl radicals in the reactions below:

$$\begin{aligned} OH + SO_2 + M &\rightarrow HOSO_2 + M \\ HOSO_2 + O_2 &\rightarrow HO_2 + SO_3 \\ HO_2 + NO &\rightarrow NO_2 + OH \end{aligned}$$

In this way, the oxidation of SO_2 behaves like the oxidation of VOCs, leading to the conversion of nitric oxide (NO) to nitrogen dioxide (NO_2) and hence the production of ozone. SO_2 therefore behaves as a VOC precursor and the reduction of European SO_2 emissions during the 1980s and 1990s should in principle have contributed to a reduction in the formation of episodic peak ozone concentrations. However, because of the low reactivity of SO_2 compared with most VOC species, this contribution might well be small.

The UK PTM model has therefore been used to investigate how reductions in SO_2 emissions may have influenced photochemical ozone formation in north west Europe. The model responses to one year's worth of the current annual trends in SO_2 emissions were estimated by performing a base case model run using 1999 emissions taken from EMEP (2001) and a sensitivity case was run with emissions reduced by the annual trend in SO_2 emissions. Ozone concentrations were slightly lower in the case with reduced SO_2 emissions showing that currently SO_2 emission reductions are contributing to the trends in episodic peak ozone concentrations to the extent of –0.11 ppb $year^{-1}$.

An important question then is the extent to which European photochemical episodes sit on top of this increasing baseline. If this baseline ozone plays no part in the fast photochemistry occurring in the photochemical episodes than it could be envisaged that all percentiles in the cumulative frequency distribution should experience this same trend. Any trend in the ozone production capacity in Europe would then have to have this increasing baseline trend folded in to produce the overall trend in episodic peak ozone concentrations. In this case, the baseline trend would act as a confounding influence in the determination of the impact of the UN ECE VOC Protocol.

The impact of the increasing trend in global ozone baseline concentrations on the European regional distribution of ozone has been analysed using the EUROSTOCHEM model in Section 3.5 above. There, it is concluded that it is likely that the observed downwards trends in episodic peak ozone concentrations anticipated during the 1990s have not been confounded significantly by the observed +0.5 ppb $year^{-1}$ increase in baseline ozone levels, at least in the more photochemically-active regions of north west Europe. However, for the more remote fringes of Europe, the baseline ozone increase may well have offset any small decrease in photochemical ozone formation within Europe that has occurred as a result of regional pollution control.

It is likely that the actions taken to implement the United Nations Economic Commission for Europe VOC Protocol through the Commission of the European Communities directives on motor vehicle emission controls has led to a reduction in the emissions of certain individual VOC species. Some of these VOC species have been identified using a combination of speciated VOC inventories and a highly sophisticated Master Chemical Mechanism, to be among the most prolific ozone forming of all the VOC species. On this basis, a downwards trend in episodic peak ozone concentrations in north west Europe is to be expected during the 1990s, as shown in Figure 8.14.

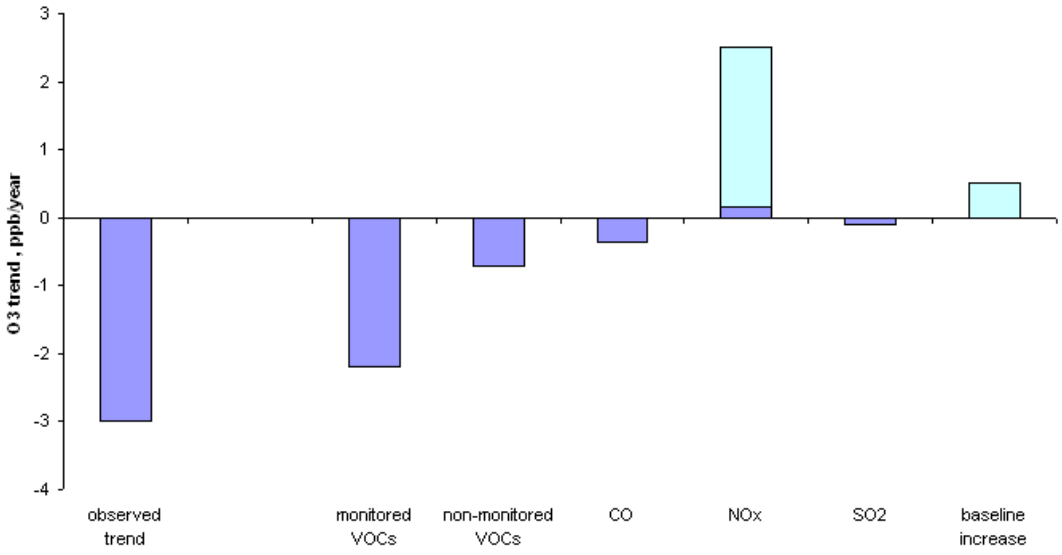

Figure 8.14 ***Overall Summary of the Observed Trends in Episodic Peak Ozone Concentrations in North West Europe and their likely Attribution.***

Figure 8.15 presents the observed trends in the maximum 8-hour mean ozone concentrations recorded for four illustrative rural locations in the United Kingdom that are broadly representative of north west Europe. Also presented are the trends in the number of days in each year when at least one 8-hour period exceeded 50 ppb. Whatever the index of episodic peak ozone chosen and whichever location was chosen, statistically significant downward trends have been observed. Indeed, annual maximum 8-hour mean ozone concentrations declined at between –1.9 and –2.9 ppb year^{-1} between the years 1990 and 2000 across the four locations.

Fowler *et al.* (NEGTAP, 2001) report a large decline in the annual maximum 1-hour mean ozone concentrations observed across the United Kingdom between the decades 1982-1991 and 1992-2000. At four of the UK rural locations, annual maxima are decreasing currently at over –3 ppb year^{-1} over the period from 1988-2000 and these trends are statistically significant. At a further 4 sites the decreases have been between –1.5 and –3 ppb year^{-1}.

In Figure 8.14, the observed ozone trends and the postulated trends due to VOC, NO_x, CO and SO_2 controls evaluated with the UK PTM and the possible baseline influence from EUROSTOCHEM are all plotted out. Within the likely uncertainty ranges, (shown as open columns) the observed trends in episodic peak ozone concentrations on the left hand side of Figure 8.14 can be reconciled with the sum of the postulated influences on the right hand side. Of the postulated trends, those in the VOC species are undoubtedly the largest.

It is likely that the action taken to implement the United Nations Economic Commission for Europe VOC Protocol has brought about the observed downwards trends in the episodic peak ozone concentrations in north west Europe during the 1990s.

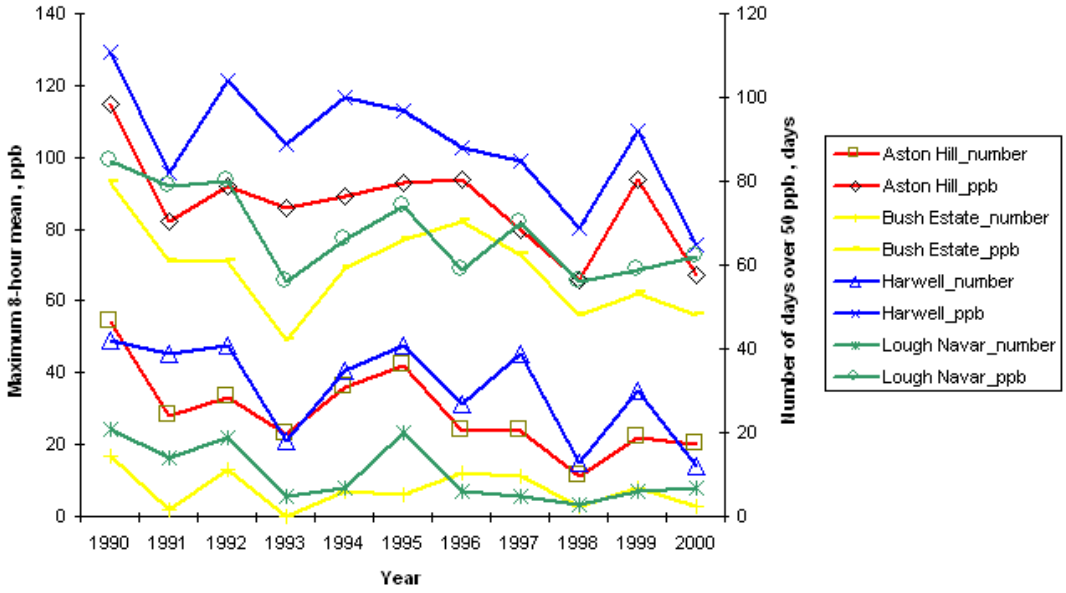

Figure 8.15 ***Time Series of the Maximum 8-hour Mean Ozone Concentration and the Number of 50 ppb 8-hour Mean Ozone Concentration Exceedence Days at Four Illustrative Sites across the British Isles between 1990 and 2000.***

8.3.4 Maximising Ozone Benefits Accruing from the Implementation of the National Emissions Ceilings Directive in the UK

By using the UK PTM, the detailed NAEI speciated VOC inventory and the Master Chemical Mechanism v3.0, it has been possible evaluate the impacts of the UNECE VOC Protocol as described in the Section 8.3.3 above. This evaluation depends crucially on access to an accurately speciated VOC inventory and a chemical mechanism that adequately treats the chemical degradation of the most prolific ozone-forming species. The success of the evaluation reflected the fact that the motor vehicle exhaust and evaporative emissions sources controlled by the UNECE VOC Protocol have been accurately handled in the speciated VOC inventory and that the olefinic and aromatic hydrocarbons controlled are among the most prolific ozone-forming species.

It is clear that any assessment of the ozone benefits from the implementation of the EU National Emissions Ceilings Directive should adopt a similar procedure as that employed to assess the UNECE VOC Protocol as in Section 8.3.3 above. The National Emissions Ceilings Directive addresses a number of stationary VOC sources whose VOC species profiles are dramatically different to those of the motor vehicle exhaust and evaporative sources controlled by the UNECE VOC Protocol. Furthermore, the overlap between the VOC species profiles for these stationary sources and the MCM v3.0 species is by no means as favourable as it has been for the motor vehicle sources. Indeed, the MCM v3.0 only address 69% of the mass emission in the NAEI speciated inventory with the entire shortfall falling in the stationary sources.

Although the combination of the NAEI inventory and the MCM v3.0 is the only means of accurately assessing the likely ozone benefits from the implementation of the EU National

Emissions Ceiling Directive, further progress will have to be made to address the shortfall between the 69% of the mass emissions handled by the MCM v3.0. Although the shortfall is described here in mass terms, in species terms the shortfall is even larger. The NAEI currently handles over 500 VOC species whereas the MCM v3.0 describes the degradation of only 124 species.

Further work is required to bridge the gap between the NAEI speciated VOC inventory and the MCM v3.0 before the UK PTM can be employed to evaluate the ozone benefits from the EU NECD.

8.3.5 Updating the UK Strategy to Reduce Emissions of Volatile Organic Compounds

In formulating the UK strategy to reduce emissions of volatile organic compounds, policy advice has largely rested on a bottom-up analysis of the likely trends in emissions of each of the stationary and mobile source categories. This analysis comprises the UK VOC Strategy and it underpins the VOC emission projections.

It should be a straightforward matter to employ the UK PTM with the MCM v3.0 to evaluate the ozone benefits from each of the likely trends in each of these source categories. However, such an analysis can only be performed thoroughly when the work has been completed to bridge the gap between the NAEI speciated inventory and the MCM v3.0.

9 Ozone Exposure Metrics

9.1 INTRODUCTION

The accumulated exposure above a threshold concentration of 40 ppb (AOT40), or 60 ppb (AOT60) is widely used as a measure of the exposure of ecosystems to ozone. Current environmental quality standards for the protection of crops, semi-natural vegetation and forests are framed in terms of the AOT40 (*e.g.*, the environmental quality standards for the protection of crops is set as an AOT40 of 3,000 ppb-hours).

The AOT metric is adequate as a measure for indicating duration and exposure levels of events when concentrations of ozone are well above 40 (or 60) ppb. The problem with the AOT index is that it shows high sensitivity with respect to concentration changes close to the threshold. This unstable response makes its application problematic, as it is difficult to compare values that have a corresponding high sensitivity. There are other exposure indices but these are not used in setting ecosystem exposure standards.

A paper by Sofiev and Tuovinen (2001) has been published on the factors determining the robustness of AOT40 and other ozone exposure indices. The paper considers the stability of the AOT index and also derives a universal stability criterion for a general time-integrating index function (*i.e.* an index like the AOT index). Other exposure indices are evaluated in the context of the universal stability criterion. Finally, a modification of the AOT index is presented, which shows a limited sensitivity.

9.2 STABILITY OF THE AOT FUNCTION

The AOT index, A, for the threshold level, L (AOT-L) can be written as

$$A = \int_0^T (\xi - L)\Theta(\xi - L).dt \tag{9.1}$$

where ξ is the time-dependent ozone concentration, T is the integration period and $\Theta(\xi\text{-}L)$ is the Heaviside function.

$$\Theta(\xi - L) = \begin{cases} 1 & \xi \le L \\ 0 & \xi > L \end{cases} \tag{9.2}$$

Whilst this seems a reasonable approach to take, the reliance on the factor $(\xi\text{-}L)$ gives rise to a discontinuity in the sensitivity of the index at $\xi = L$. This can be seen in the example of the response of A_L, r, to a 10% increase in ξ.

$$r = \frac{A_L(1.1\xi) - A_L(\xi)}{A_L(\xi)} \times 100\% \tag{9.3}$$

The plot of the response against ozone concentration is shown in Figure 9.1.

Figure 9.1 illustrates the problem with the AOT index around the threshold value, where the break in the plot indicates a discontinuity in the response, *i.e.*, an unstable response. It is clear that this response makes comparing AOT calculations with ambient monitoring data around the

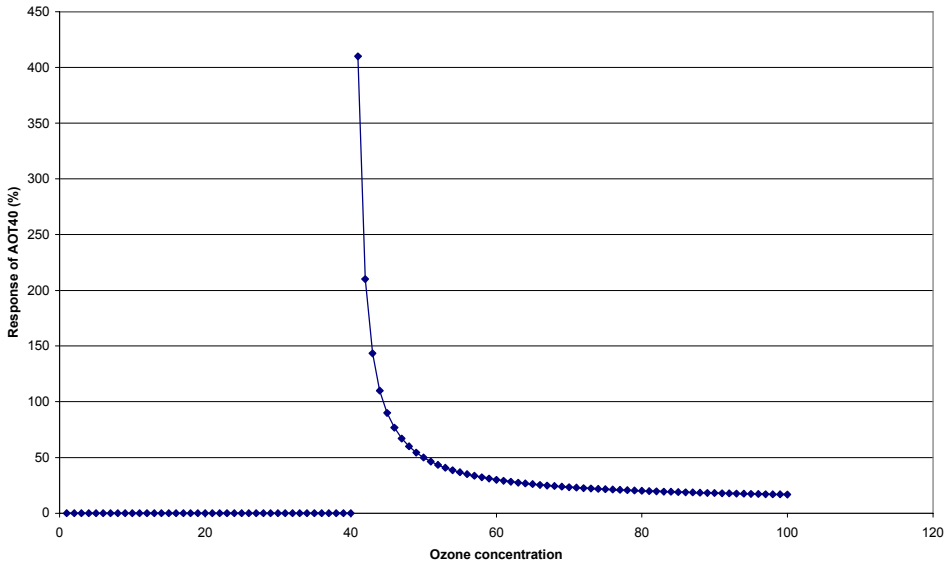

Figure 9.1 ***Response of AOT40 to a 10% Change in ξ, the Ozone Concentration.***

critical level very difficult. The concern is well founded as the inherent uncertainties in monitoring and modelling ozone as well as in determining the threshold value, are larger than 10%. This behaviour is a problem, particularly if a large fraction of the concentrations are in the neighbourhood of the threshold value; this is often the case in remote Northern European locations. From figure 1, it is clear that in such a data set, a small change in the value of the data could result in a large response in the AOT-L index.

The instability problem was investigated through use of the mathematical expectation, MA, and the relative sensitivity, S, of the index.

$$MA = \int_{-\infty}^{\infty} (\xi - L)\Theta(\xi - L)\, p(\xi).d\xi \tag{9.4}$$

Where ξ is a stochastic process with a probability density function p(ξ), *i.e.*, ξ is a collection of random variables, {ξ(t), t$\in$T} such that for each t in the index set T, ξ(t) is a random variable (p.41 Ross, 1996), with probability density function (p.d.f.) p(ξ). The p.d.f., p, is non-negative for all ξ and equal to zero outside the range [a,b], inside the range (a,b), p is analytic (*i.e.* p is defined and has a derivative at every point in (a,b), (p. 132 Stephenson, 1992)). For tropospheric ozone, a is 0 ppb and b ~ 100 – 1000 ppb.

The relative sensitivity is defined as

$$S \equiv \frac{\Delta MA / MA}{\Delta L / L} = \frac{L}{MA}\frac{\partial MA}{\partial L} \tag{9.5}$$

In the Appendix to the paper, it is shown that

$$S \propto \frac{1}{b - L}, \text{ as } L \to b^{-0} \tag{9.6}$$

This means that as L approaches b from the L<b side, that the relative sensitivity will tend to infinity. This is because the denominator, b-L approaches zero and so S approaches a division by zero, *i.e.*, infinity. Therefore, if the threshold value is near the upper limit of tropospheric ozone concentration, the relative sensitivity of the AOT index tends to infinity.

The aim of modified AOT-L functions would be to have a sensitivity that is limited, *i.e.* does not tend to infinity at any point. The criteria, which are necessary and sufficient to determine the stability, are considered in the following section.

9.3 STABILITY OF A GENERAL TIME-INTEGRATING INDEX

The necessary and sufficient conditions for the properties of the relative sensitivity are shown in Theorem 1.

Theorem 1

It is necessary and sufficient for the relative sensitivity to be limited, $|S| \leq S_{max} < \infty$, that the filter function, *f*, is limited in[a,b] and separated from zero in any sub-range of [a,b], except a zero-metric set Z (if any)

There exists such f_{MAX} that $f(\xi) \leq f_{MAX}$ for any $\xi \in$ [a,b] and for any $\varepsilon > 0$,
there exists such $f_{MIN}(\varepsilon) > 0$ that $f(\xi) \geq f_{MIN}$ for any $\xi \in$ [a+ε, b-ε]\Z, $\int_Z d\xi = 0$

The first point means that for any value of the concentration, ξ in the range of concentrations, [a,b] the corresponding value of the filter function, $f(\xi)$ will always be less than or equal to another value of the filter function. This implies that the filter function has an upper bound and therefore will not tend to infinity for any $\xi \in$ [a,b]. This refers to the problem of the filter function tending towards infinity when the concentration ξ is close to the threshold level, L, where $a \leq L \leq b$. This response was shown in Figure 9.1. The second point means that the filter function is positive for any ξ in a sub-range of [a,b]. This means that the filter function has a lower bound over the range [a,b] and that this lower bound is greater than zero. The AOT-L index violates this requirement by setting the index equal to zero for $\xi < L$, which means the index has a discontinuous jump at the threshold level, which makes it unstable.

9.4 EVALUATION OF DIFFERENT STABILITY INDICES

The criteria outlined above were applied to various other exposure indices to evaluate whether their response was any more consistent than that of the AOT-L index. The stability of the other indices was evaluated, as shown in Table 9.1.

Table 9.1 ***Ozone Exposure Indices and their Stability.***

Index	Stability	Filter Function
SUM-*L*	Unstable	$f(\xi) = \xi\Theta(\xi - L)$
PER-*n*	N/A (since no time integration involved)	
AOT-*L*	Unstable	$f(\xi) = (\xi - L)\Theta(\xi - L)$
NUM-*L*	Unstable	$f(\xi) = \Theta(\xi - L)$
SIG-*M,k*	Stable	$f(\xi) = \xi[1 + M\exp(-k\xi)]$
AL-*i,j*	Stable	$f(\xi) = \xi(\xi/j)^i$

Therefore, it would seem that it is possibly more sensible to use either the SIG or AL indices. However, it can be expected that when the relative sensitivity of AOT40 exceeds 5, other indices will also show high sensitivity. This sensitivity may still be too high to draw firm

conclusions whether the exposure of an area is below or above the ecological targets. The high sensitivity coupled with the fact that the values of the other indices are not comparable to those of the AOT40 indicates the usefulness of a modified AOT functional, rather than a completely different index. The modified function would not have the instability of the original function, but would provide values that are comparable to the original, which would be useful to maintain consistency in the regulation standards.

9.5 A MODIFIED AOT FUNCTION

An example of a modified AOT functional, $\varphi(\xi)$ is given below

$$\varphi(\xi) = \exp\left(-0.1\frac{L^2}{(\xi-a)^2}\right)\begin{cases}\xi - L & \xi \geq \varepsilon_1 + L \\ \varepsilon_1\left(\dfrac{\varepsilon_1}{2\varepsilon_1 - \xi + L}\right)^n & a \leq \xi < \varepsilon_1 + L \\ 0 & \xi < a\end{cases} \qquad (9.7)$$

The exponential part ensures compatibility to the values of the original AOT index and does not affect the stability. The division of the function into three sections removes the discontinuity from the function, since the ranges for each part are dependent on ε_1, where $\varepsilon_1 << b-a$.

By a considered choice of the parameters, *n* and ε_1, the sensitivity of the modified function can be smaller than that of the original function, and the value of the index is similar to the original function. The modified AOT function was tested at two stations, Rörvik (Sweden) and Deuselbach (Germany). The Rörvik site has exposure estimates that are considerably lower than those at Deuselbach. This means the modification of the AOT function has a stronger effect at Rörvik as a greater proportion of the data are in the range $[a, L+\varepsilon_1]$.

9.6 CONCLUSIONS FROM THE PAPER

The practical conclusions that can be drawn from the paper are:

- The AOT40 index is adequate for the majority of situations, but it fails in the critical region of the concentration threshold value. This is a major shortcoming, as it is around the crucial area where ecosystem exposure standards can be met or violated. Therefore, there is a need for an alternative to be investigated
- Since the AOT40 index is well established it is desirable for the alternative index to be comparable to the AOT40 index. The modified AOT40 index achieves this for particular choice of the parameters ε and n. Other indices that could be used instead, such as the SIG and AL indices are not comparable to the AOT40 scale.
- The modified AOT index generally has lower relative sensitivity values than the original index, with particular effect in remote areas. This indicates that the modified index would be better to use. The fact that it is effective in remote areas is important as it is here that the concentrations are around the threshold value and where the original AOT40 index had particular problems.
- A potential problem with the modified AOT index surrounds the choice of ε and n. Whilst the formulae provided give some guidance on their value, their exact value will vary from location to location and possibly from time to time. With this variation, is it then possible

to compare the modified AOT indices amongst themselves if different ε and n have been used? Also, is it possible to compare the indices against ambient monitoring or modelling data if various values of ε and n are required for the benefits of the modified formula to be seen?

9.7 PRACTICAL APPLICATION

Some exposure indices listed in the paper were tested using Excel. The indices chosen were the standard AOT40, the SIG and AL indices and the modified AOT40 index (MODAOT40). The SIG and AL indices were chosen, as they were the two found to be stable by Sofiev and Tuovinen. The filter functions used for the indices were taken from the paper, as shown in equation 8.1 and Table 9.1. The indices were calculated by summing the results of the filter function for the hours between 8 am and 8 pm. It was decided not to investigate the other indices SUM-*L* and PER-*n* because the filter function for the SUM-*L* index is very similar to that of the AOT40 index and the PER-*n* index does not rely on time integration. Equation 8.7 was used for the MODAOT40 function.

9.7.1 Parameter Choice

For the SIG and AL indices, the values for the parameters shown in were used.

Table 9.2 ***Parameter Values for SIG and AL Indices.***

Index	Parameter	Value
SIG-*M,k*	M	100
SIG-*M,k*	K	500
AL-*i,j*	I	2
AL-*i,j*	J	120

These were selected somewhat arbitrarily from the values given in Table 3 of the paper by Sofiev and Tuovinen (2001), since no information was given on how the combinations of parameters were chosen. Different parameter values were tried in Excel, but made little change to the SIG index, and whilst there were substantial changes to the value of the AL index, it was not clear what this change implied.

The choice of parameters for the MODAOT40 index also proved difficult. In Section 5 of the paper, *n* is recommended to be between 1 and 2 and since little other guidance was given, *n* was arbitrarily chosen to be 1.5. ε is recommended to be around 0.05-0.1(b-a), where b is the upper limit of ozone concentrations and a, the lower limit of ozone concentrations. However, this recommendation is then contradicted by the sentence '*As the actual concentration range (b-a) ~ 10^2 ppb, a value of ε ~ 10 ppb should be taken*'. Since the first formula for ε will generally result in a negative value for ε, it was decided to use the second method, *i.e.* ε ~ 0.1(b-a). In the investigation, a and b were taken as the minimum and maximum of the range of ozone concentrations in the data set.

9.7.2 Results

The indices were investigated for 6 UK sites, which were selected as interesting ozone measurements had been made. The sites are listed in Table 9.3.

Generally the MODAOT40 index was less spiky than the standard AOT40 index. This is shown for the Yarner Wood site in Figure 9.2a-d. The fewer spikes suggests that the MODAOT40 copes better with values near the 40 ppb threshold. The alternative indices SIG-100,500 and AL-2,120 were also smoother than the AOT40 index, as shown in Figure 9.2b and Figure 9.2c.

Table 9.3 ***Sites used to Investigate the Different Ozone Exposure Indices.***

Site name	OS Grid reference	Monitoring Network
Yarner Wood	SX786789	Rural
Lullington Heath	TQ538016	Rural
London Bloomsbury	TQ302820	Urban Centre
Strath Vaich	NH347750	Rural
Harwell	SU474863	Rural
Sibton	TM364719	Rural

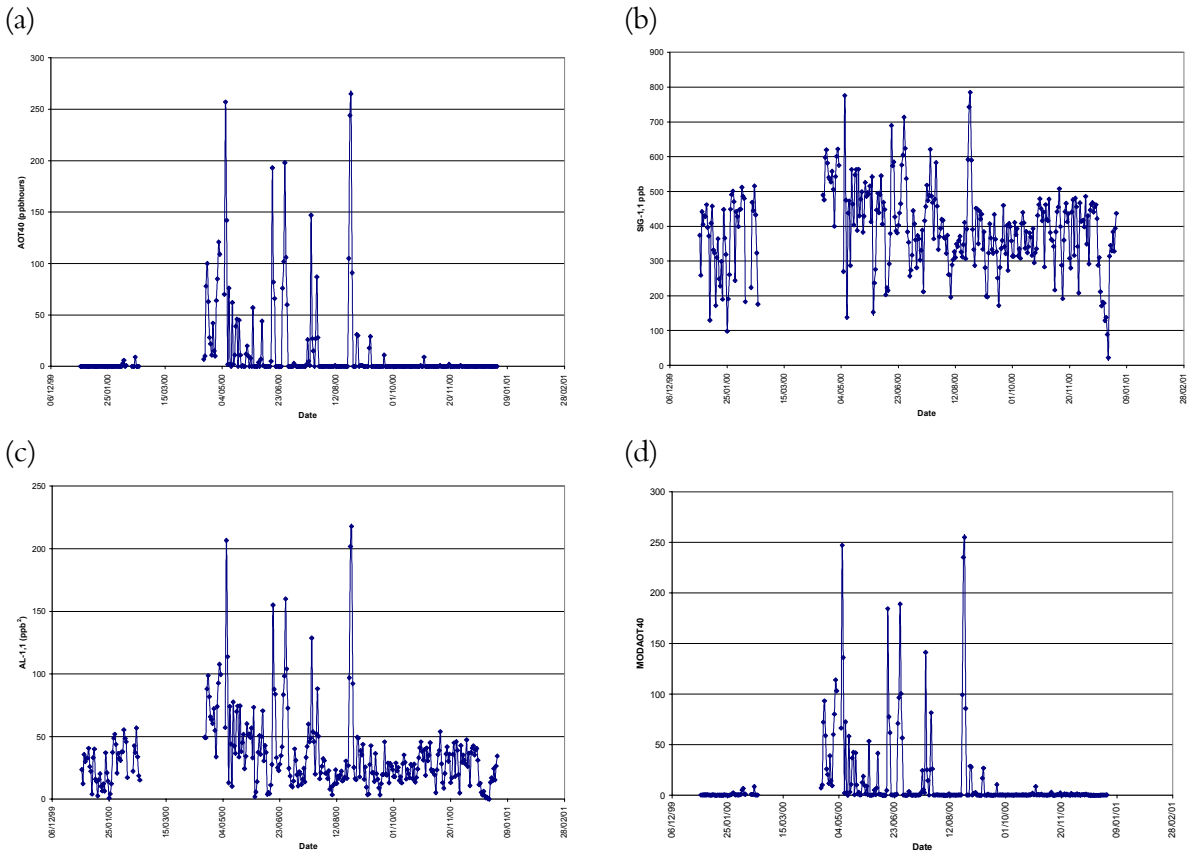

Figure 9.2 ***Ozone exposure indices for Yarner Wood (2000). (a) AOT40, (b) SIG-100,500, (c) AL-2,120 and (d) MODAOT40.***

The fact that the baseline cluster of values for SIG (~400 ppb) and AL (~25 ppb^2) indicates the effort that would be involved with applying these indices to ozone guidelines that already exist, based on AOT40. For the indices to be transferable, this baseline would need to be near zero to mimic the properties of the AOT40 index, the alternative being a complete change guidelines for ozone.

This pattern of response in the ozone exposure indices is seen in a number of sites, namely Lullington Heath, London Bloomsbury, Harwell, Strath Vaich and Sibton. London

Bloomsbury particularly highlights the compatibility between the AOT40 and the MODAOT40 indices, as shown in Figure 9.3. Also of interest is the similarity between the AOT40 and the AL index, as shown in Figure 9.3a and Figure 9.3c. The SIG index remains incompatible with the AOT40 index.

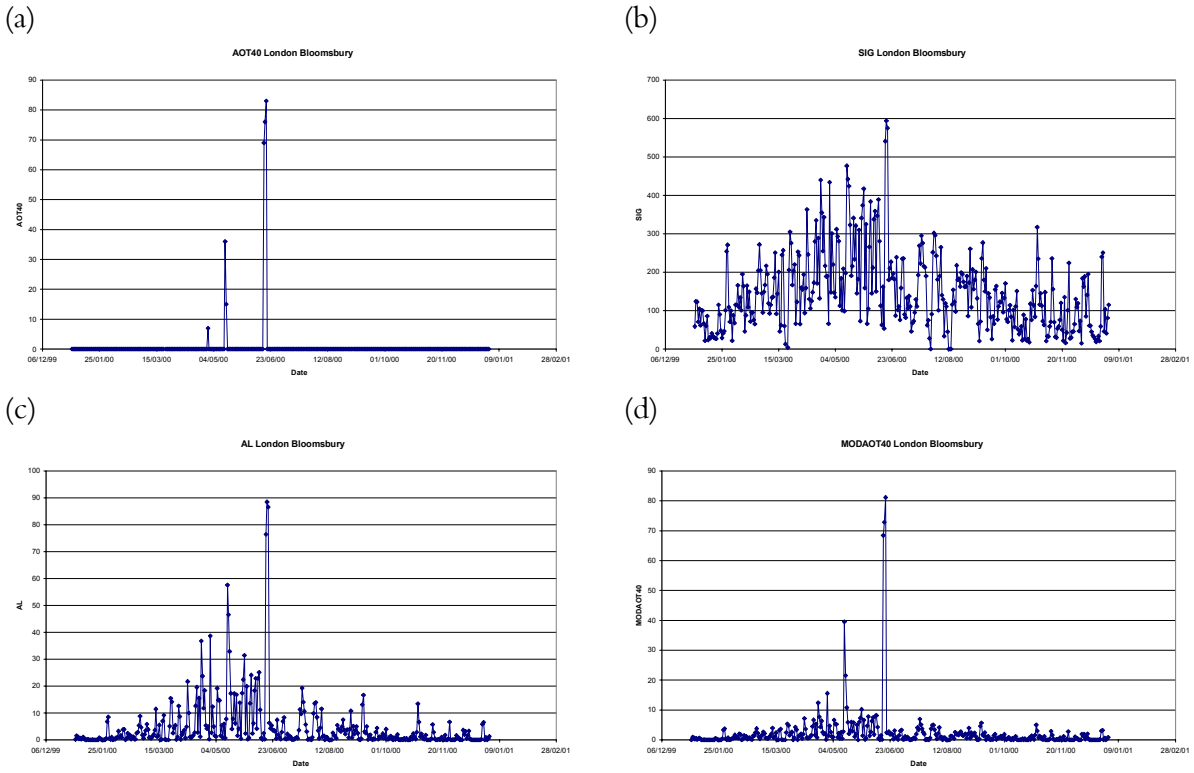

Figure 9.3 ***Ozone Exposure Indices for London Bloomsbury (2000). (a) AOT40, (b) SIG-100,500, (c) AL-2,120 and (d) MODAOT40.***

The results for London Bloomsbury show the difference between rural and urban ozone concentration patterns.

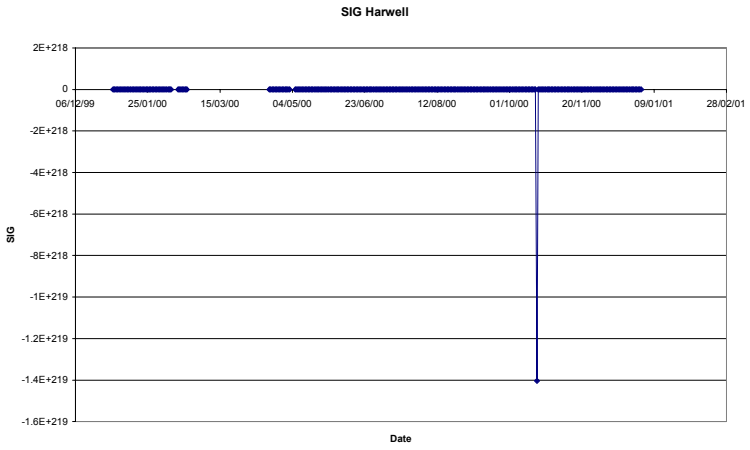

Figure 9.4 ***The SIG-100,500 Ozone Exposure Index for Harwell (2000).***

Further to the general compatibility of AOT40 and MODAOT40 at Harwell, this site also showed a weakness in the SIG index in the handling of poor data. In the Harwell records, an ozone concentration of –1 ppb is recorded during 20/10/00. The other indices seem robust

against the spurious data, but it dominates the response from the SIG-100,500 index. This is shown in Figure 9.4.

9.7.3 Sensitivities

The sensitivities for the AOT40 and MODAOT40 indices were calculated for the Yarner Wood and Strath Vaich sites to give an idea of the stability of the responses of the respective indices. The sensitivities for the SIG and AL indices were given in the paper and are specific to the choice of parameters. These sensitivities are shown in Table 9.4.

Table 9.4 ***Sensitivities of the AOT40 , MODAOT40, SIG and AL indices for Yarner Wood and Strath Vaich.***

Site	Index	Sensitivity
Yarner Wood	AOT40	α = 0.028571
	MODAOT40	0.742727
Strath Vaich	AOT40	α = 0.034483
	MODAOT40	0.824192
All sites	SIG-100,500	3.5
	AL-2,120	2.7

The small sensitivities of the MODAOT40 index are probably due to the large range of concentrations in ozone sampled throughout the year. This has the effect of averaging the concentrations away from the 40 ppb threshold; the area where high sensitivities are expected. Only proportional sensitivities are given for the AOT40 index due to the complexity in the calculation of the actual sensitivity, which depends on equations 8.4, 8.5 and 8.6.

The choice of parameters, ε and n has a large effect on the sensitivity of the MOD AOT40 index, and indeed the degree of compatibility between the AOT40 index and itself. This is show in Figure 9.5. The aim would be to arrive at a MODAOT40, which has a baseline of results on the 0 ppb line, so mimicking the AOT40 index. It is also desirable to have a sensitivity less than around 5, as mentioned in the paper. These points would have to be borne in mind if the MODAOT40 index was to be used. It is likely that different parameters would need to be used for different locations and therefore, some decision process would need to be formulated. The guidance given in the paper to assist with the choice of ε and n was not detailed enough to be able to confidently use the MODAOT40 without first thorough investigation into the choice of the parameters.

Plots of the response (equation 8.3) of the AOT40 and MODAOT40 indices were attempted for a 10 % increase in ozone concentration data. However, these plots were thought to be misleading since a substantial proportion of the AOT40 indices went from 0 to a positive AOT40 index after the increase of 10 % in concentration. In some cases this increase was large, going from 0 to 12 with a 10 % increase in concentration. In these cases, the response function, as given in equation 3 becomes meaningless as it results in a division by zero. Other response indicators were investigated, such as the variance between the before and after AOT40 values, and the simple difference between the two values, but none were found to be particularly helpful.

(a) ε=7.5, n=1.5, sensitivity = 0.738

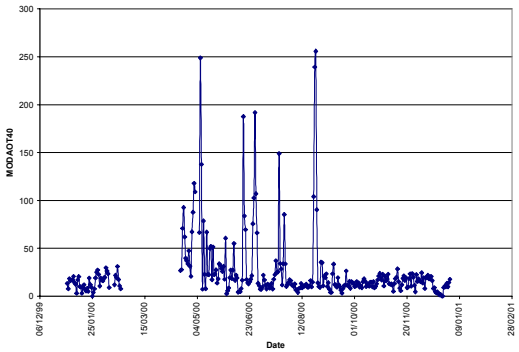

b) ε=2, n=1.5, sensitivity = 2.77

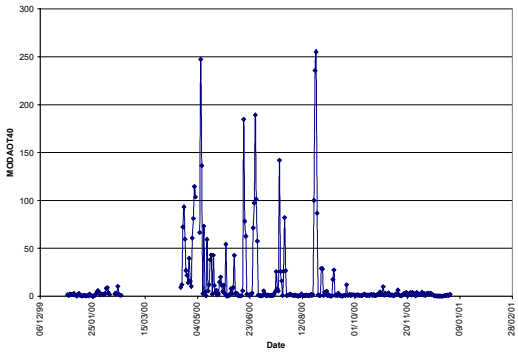

(c) ε=7.5, n=2, sensitivity = 9.834

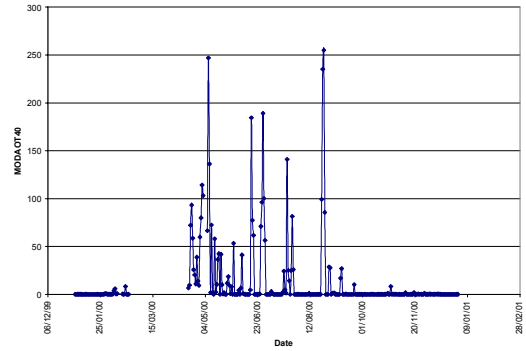

d) ε=7.5, n=1, sensitivity = 4.91

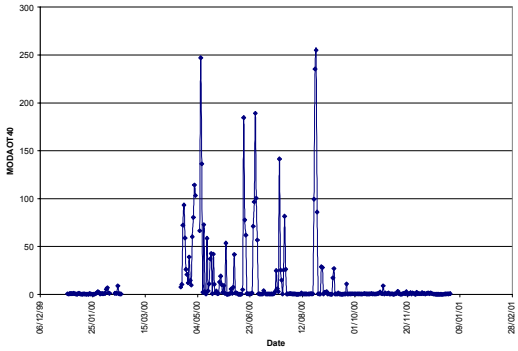

Figure 9.5 ***The changing sensitivity and response of the MODAOT40 index to different parameters ε and n at the Yarner Wood site in 2000. a) MODAOT40, ε=7.5 , n=1.5 , b) MODAOT40, ε=2 , n=1.5, c) MODAOT40, ε=7.5 , n=2 and d) MODAOT40, ε=7.5 , n=1.***

A simple test of the sensitivity, similar to that shown in Figure 9.1 was carried out to investigate the general response of the MODAOT40 index. This was conducted on false data, which ran monotonically from 1 ppb to 100 ppb, and then increased by 10 %. The results of these plots are shown in Figure 9.6.

(a)

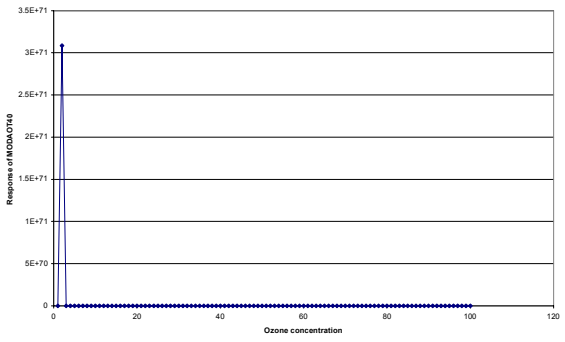

(b)

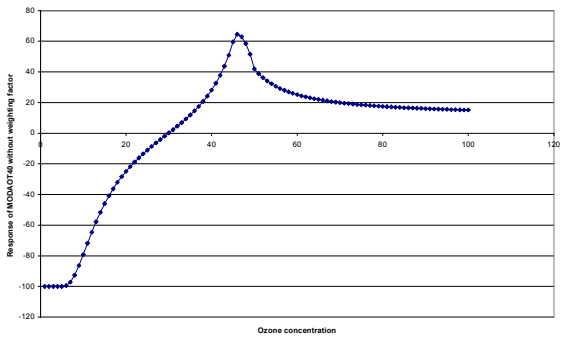

Figure 9.6 ***Response of the MODAOT40 Index of the Range 1 ppb to 100 ppb. (a) MODAOT40 Index with the Exponential Weighting Function, (b) MODAOT40 Index without the Exponential Weighting Function.***

From these plots, it is obvious that the response of the MODAOT40, as given in equation 8.7, has problems too, particularly around the minimum of the range of ozone concentrations. From Figure 9.6b, it appears that this problem is caused by the choice of the exponential weighting factor in the filter function. This is discussed further in the following section.

9.7.4 Filter Function

An area also requiring further investigation is the choice of the filter function used in the MODAOT40 formula. The one used in the investigation is that given in the paper, and in equation 8.7. The method of selection for this function is complex and is not outlined in the paper, however, its choice is crucial and governs the effectiveness of the MODAOT40 index. A major flaw with the filter function in equation 8.7 occurs when ξ = a, *i.e.* the measured ozone concentration, ξ equals the minimum ozone concentration in the data set. This event leads to a division by zero in the exponential part of the equation and renders the filter function for that particular time null. The MODAOT40 index is arrived at by summing the filter function results over the period of interest and therefore the MODAOT40 index is also null. The exponential part of the filter function also has trouble when the concentrations are close to the minimum of the range, where very small number s are in the denominator, this is seen in Figure 9.6a. This major shortcoming compromises the achievements of the MODAOT40 index in this case and if the MODAOT40 index were to be used extensively, a different filter function would need to be devised.

9.7.5 Conclusions from the Practical Application of the Paper

The indices tested, the SIG, AL and MODAOT40 show a different approach to the problem of quantifying ozone exposure to the standard AOT40 index. The SIG index was probably the least useful as its results were in no way comparable to that of the AOT40 index, and it also had trouble dealing with spurious data. The AL index showed greater compatibility with the AOT40 index, although this wasn't as a strong a relationship as that achieved by the MODAOT40 index. This could perhaps be improved upon with greater understanding of this index and the role of its parameters i and j. The paper did not expand on the properties of this index. The MODAOT40 index has potential to overcome the problems presented by the AOT40 index, namely the infinite sensitivities of the AOT40 index around the threshold of 40 ppb. However, extensive work is required. Firstly a choice of filter function would need to be made and this filter function should make the MODAOT40 results compatible with the AOT40 index and it should be defined for all likely values of ozone concentration. Secondly, greater understanding on the choice of the parameters ε and n is required. This understanding then needs to be developed into a framework so that the parameters can be selected for different areas of the country consistently, whilst maintaining the compatibility of the MODAOT40 index to the AOT40 index, and also keeping a reasonable level of sensitivity.

9.8 POSTER

A poster on this work was presented at the 15th Task Force Meeting of the UN/ECE ICP on Vegetation, which was held in Trier, Germany during February 2002. A copy of the poster can be found in Appendix 4.

10 Publications

In the following sections, peer-reviewed papers and conference proceedings which have been published or submitted for publication are listed. Relevant presentations are also listed.

10.1 PEER-REVIEWED PUBLICATIONS

M.E. Jenkin and K.C. Clemitshaw (2000) **Ozone and Other Secondary Photochemical Pollutants: Chemical Processes governing their Formation in the Planetary Boundary Layer**. Atmospheric Environment, **34**, 2499-2527.

Carslaw N., Creasey D.J., Harrison D., Heard D.E., Hunter M.C., Jacobs P.J., Jenkin M.E., Lee J.D., Lewis A.C., Pilling M.J., Saunders S.M. and Seakins P.W. (2001) **OH and HO_2 Radical Chemistry in a Forested Region of North-western Greece**. Atmospheric Environment **35**, 4725-4737.

Derwent R.G., Jenkin M.E., Saunders S.M. and Pilling M.J. (2001) **Characterisation of the Reactivities of Volatile Organic Compounds using a Master Chemical Mechanism**. Journal of Air and Waste Management Association **51**, 699-707.

Clapp L.J. and Jenkin M.E. (2001) **Analysis of the Relationship between Ambient Levels of O_3, NO_2 and NO as a function of NO_X in the UK**. Atmospheric Environment **35**, 6391-6405.

Jenkin M.E., Davies T.J. and Stedman J.R. (2002) **The Origin and Day-of-week Dependence of Photochemical Ozone Episodes in the UK**. Atmospheric Environment **36**, 999-1012.

Jenkin M.E., Saunders S.M., Derwent R.G. and Pilling M.J. **Development of a Reduced Speciated VOC Degradation Mechanism for Use in Ozone Models**. Atmospheric Environment (submitted).

Derwent R.G., Collins W.J., Johnson C.E., Stevenson D.S. **A Nested Model Study of the Coupling between Global and European Regional Ozone Distributions at Present and in the Future**. Journal of Atmospheric Chemistry (submitted).

Metcalfe S.E., Whyatt J.D., Derwent R.G., O'Donoghue ?. The Regional Distribution of Ozone across the British Isles and its Response to Control Strategies. Atmospheric Environment (submitted).

10.2 OTHER PUBLICATIONS

Jenkin M.E., Saunders S.M. and Derwent R.G. (2000) **Photochemical Ozone Creation Potentials for Aromatic Hydrocarbons: Sensitivity to Variations in Kinetic and Mechanistic Parameters**. Proceedings of the International Workshop on Aromatic Hydrocarbons, Valencia, Spain. August 2000.

Jenkin M. (2000) **Development and Application of Detailed Chemical Mechanisms for the Gas-phase Oxidation of VOC**. CMD Annual Report '99, pp. 47-51. EUROTRAC-2, International Scientific Secretariat, Munich, Germany, (2000).

Jenkin M.E., Saunders S.M. (2001) **Development and Application of Detailed Chemical Mechanisms for the Gas-phase Oxidation of VOCs**. EUROTRAC-2 Annual Report 2000: CMD, Chemical Mechanism Development subproject. International Scientific Secretariat, GSF-Forschungszentrum fuer Umwelt und Gesundheit GmbH, Munich, Germany.

Bell N., Carslaw N., Creasey D., Derwent R., Heard D., Jenkin M., Lee J., Lewis A., McQuaid J., Pilling M.J., Pascoe S., Saunders S.M. and Seakins P. (2000) **Development and Applications of a Master Chemical Mechanism**. CMD Annual Report '99, pp. 72-75. EUROTRAC-2, International Scientific Secretariat, Munich, Germany, (2000).

Jenkin M.E. (2001) **Master Chemical Mechanisms: Comparison with the Real World**. Proceedings from the EUROTRAC-2 symposium 2000. Eds P.M. Midgley, M. Reuther and M. Williams. Sringer-Verlag.

10.3 PRESENTATIONS

Conference and workshop presentations on work relevant to this contract were made as follows:

S.M. Saunders, N. Carslaw, S. Pascoe, M.J. Pilling, M.E. Jenkin and R.G. Derwent. **Development of the Master Chemical Mechanism (MCMv2.0) Web site and Recent Applications of its Use in Tropospheric Chemistry Models**. Presented at the US/German workshop on fine particle and oxidant formation, Riverside, CA, October 4-6, 1999.

N. Carslaw and M.J. Pilling. **Simulations of EUPHORE And Field Experiments Using a Master Chemical Mechanism**. Presented at the US/German workshop on fine particle and oxidant formation, Riverside, CA, October 4-6, 1999.

R.G. Derwent, M.E. Jenkin, S.M. Saunders and M.J. Pilling. **Modelling Ozone Formation with a Master Chemical Mechanism**. Presented at the US/German workshop on fine particle and oxidant formation, Riverside, CA, October 4-6, 1999.

M.E. Jenkin, S.M. Saunders and R.G. Derwent. **Photochemical Ozone Creation Potentials for Aromatic Hydrocarbons: Sensitivity to Variations in Kinetic and Mechanistic Parameters**. Presented at International Workshop on Aromatic Hydrocarbons, Valencia, February 27-29 2000.

M.E. Jenkin. **Master Chemical Mechanisms: Comparison with the Real World**. Presented at EUROTRAC-2 Symposium 2000, Garmisch-Partenkirchen, March 27-31 2000.

M.E. Jenkin. **Polluted Troposphere**. Invited seminar at the Royal Meteorological Society, Leicester, April 2000.

Saunders S.M., Pascoe S., Johnson A.P., Pilling M.J. and Jenkin M.E. (2000) **Development and Preliminary Test Results of an Expert System for the Automatic**

Generation of Tropospheric VOC Oxidation Schemes. Presented at EC/EUROTRAC-2 CMD workshop, Lausanne, Switzerland, September 2000.

Clapp L.J. and Jenkin M.E. **Analysis of the Relationship between Ambient levels of O_3, NO_2 and NO as a function of NO_X in the UK**. Presented at workshop of Emissions, Roadway and Tunnel Studies, Vienna, Austria, October 2000.

Jenkin M.E. **Mechanisms of Photo-oxidation Processes in the Atmosphere**. Presented at the COACh International Research School on Atmospheric Chemistry 'Chemical, Physics and Biogenic Processes in the Atmosphere', Obernai, France, March 2001.

Saunders S.M., Pascoe S., Johnson A.P., Pilling M.J. and Jenkin M.E. (2001) **Preliminary Test Results of an Expert System for the Automatic Generation of Tropospheric VOC Oxidation Schemes**. Presented at EGS XXVI General Assembly, Nice, France, March 2001.

Brady C., Hayman G.D. **Review and Application of Current and Suggested Ozone Exposure Metrics**. Poster presented at the 15th Task Force Meeting of the UN/ECE ICP on Vegetation, Trier, Germany, February 2002.

11 Summary, Policy Implications and Recommendations

The detailed project objectives addressed a series of issues relating to:

Task 1. Global/regional modelling
Task 2. Urban ozone/nitrogen dioxide
Task 3. Scenario analysis
Task 4. Real-time ozone forecast model - short-term action plans
Task 5. Improvements to chemical and photochemical reaction schemes
Task 6. Policy support - national plan for VOCs/ozone

The key highlights and policy implications are summarised below:

Task 1: Global/Regional Modelling

To improve previous predictions on the impact of climate change on regional-scale ozone concentrations, a nested model (EUROSTOCHEM) has been developed to calculate ozone concentrations over Europe at higher spatial and temporal resolutions than those achieved using the STOCHEM model.

The performance of the EUROSTOCHEM model has been assessed by comparing the model output with ozone measurements made at UK and European ozone monitoring sites. The EUROSTOCHEM model can reproduce the maximum hourly ozone concentrations observed daily at each site but was less successful at simulating the full diurnal behaviour. The model performance was generally found to be very good against a range of quantitative measures. The model exhibited the expected behaviour when the NO_x and VOC emissions used were separately reduced.

The modelling work has shown that much of the day-to-day variability in the maximum hourly mean ozone concentrations observed at a wide range of sites across Europe and across the British Isles is controlled by the global distribution and circulation of tropospheric ozone.

In general, the future global ozone build-up due to climate change will exert a major influence on the ozone concentrations around the median levels in the distribution of ozone hourly concentrations, with decreasing influences towards the minimum and maximum levels. In contrast, regional pollution control measures will tend to exert their major influence on the peak concentrations. Thus, for ozone concentrations close to median levels, the global build-up and regional pollution controls are calculated to affect the mean ozone concentrations by similar but opposite amounts. However, regional pollution controls were calculated to reduce maximum ozone concentrations significantly more than they were increased by the global-scale build-up.

Recommendation: There is a continued need for global modelling to investigate the linkage between regional and global-scale ozone and to assess the implication of climate change on the effectiveness of ozone policy control measures.

Task 2: Urban Ozone/Nitrogen Dioxide

Regional and/or global changes in ozone will affect local concentrations of O_3 and NO_2. There are air quality standards for NO_2 and NO_2, as a secondary pollutant, will respond in a non-linear manner to control of the NO_x precursor emissions. It is important to define the NO_x-NO_2-O_3 relationship so that the level of emission reduction to achieve the required air quality standard can be determined.

Measurement data taken from ozone monitoring sites in London and the South East have been analysed to understand the NO_x-NO_2-O_3 relationship. The results indicate that there is a linear relationship between the concentrations of oxidant and NO_x. The intercept can be identified with the initial regional oxidant input while the slope was found to reflect the input of additional oxidant locally. Possible local sources were identified as direct emissions of NO_2, photochemical and thermal processes.

An analysis of the maximum hourly NO_2 concentrations observed each day at the Marylebone Road site in 1999 confirmed that elevated regional scale oxidant formation can contribute to exceedences of the 105 ppb standard for NO_2 during summer months. The analysis clearly showed that such summertime exceedences can be well correlated with levels of oxidant at Rochester (the nearest rural site to London), and such an analysis provides a possible basis for improved prediction of such exceedences.

The relationship between annual mean concentrations of NO_x-NO_2-OX were analysed for 4 different site types (Central London background, Central London roadside, London suburbs and sites outside of London). The expressions derived for urban centre and background central London sites and sites outside central London are consistent with the expressions of Stedman (2001), with the inferred NOx thresholds which correspond to an annual mean NO_2 mixing ratio of 21 ppb consistently lying slightly higher. A number of sites were classified as 'intermediate', as they have partial roadside character, due to the influence of nearby roads. As expected, the expressions derived for these sites lie between the generic expressions derived for the urban centre and background sites and those derived for roadside sites. This analysis could also be used to assess the impact of climate change on the achievement of the annual air quality standard for NO_2. For every 0.1 ppb increase in background O_3 concentrations, an additional 0.12-0.22 ppb reduction would be needed in NO_x concentrations to achieve the NO_2 air quality standard.

The London Routine Column Trajectory Model was used to show that future annual mean NO_2 concentrations in central London will remain above the 21 ppb annual mean air quality target despite future planned reductions in road transport NO_x emissions. Furthermore, should global tropospheric ozone concentrations continue to increase, the annual mean air quality target will prove even more difficult to meet.

Recommendation: There is a need for detailed modelling of urban NO_2 and ozone using new approaches. The semi-empircal approach described above combined with regional scale modelling provides a possible way forward.

Task 3: Scenario Analysis and Task 4: Real-time Ozone Forecast Model - Short-term Action Plans (Using the PTM-CRI).

An analysis of the ozone concentration measurements made in 1988 and 1989 had previously shown that episodes of elevated concentrations of ozone over the UK were associated with air masses which had passed over continental Europe. For such air masses, the study concluded that

about 50% of the ozone could be attributed to emissions from sources on mainland Europe. Therefore, control of ozone concentrations over the UK would require concerted international action. The analysis has been extended in the present project to take account of the larger dataset now available. Using ozone measurements made at 20 UK sites between 1992 and 1999, the present study provided further confirmation that episodes of elevated concentrations of ozone over the UK were associated with photochemically-aged air masses arriving in the UK from a broadly easterly or south-easterly direction, after passing over mainland Europe for a period of several days.

Analysis of monitoring data from the same sites over the period 1989-1999 demonstrate that ozone episodes are more prevalent at the end of the week, with the greatest numbers of hours ≥ 90 ppbv occurring on Fridays. ***This has clear implications in terms of exposure and policy control***. Using the Photochemical Trajectory Model with the Common Reactive Intermediate mechanism (PTM-CRI), a likely explanation for the observed day-of-week dependence is the temporal dependence in the emissions of the ozone precursor species (VOC and NO_X) (which are greater on weekdays) and the multi-day timescale required for chemical processing and transport that lead to elevated ozone levels under photochemical episode conditions in the UK.

Many of the assessment models assume that the annual emission is released at a constant rate. The neglect of the variation in the temporal emission rates could compromise the ability of such models to reproduce the observed ozone behaviour. However, as a result of progressive changes in working practices and social habits, this effect may become less marked in the future, with the consequence that weekly cycles of pollution may become less noticeable.

The PTM-CRI was also applied to investigate the effectiveness of UK Short-term Action Plans. The design of the model is such that only a limited number of trajectories could be investigated. An episode occurring on 1st August 1999 at Barnsley Gawber (124 ppbv) was selected for investigation from the limited number of extreme ozone events now occurring. A number of possible emission control options were assessed. Removal of all UK anthropogenic precursor emissions resulted in a calculated decrease in peak ozone of 2.7 ppbv corresponding to a reduction of approximately 22 minutes in the exceedence duration. Potentially achievable action plans involving eliminating car use in the region of Rotherham/M1 and wider region of Nottinghamshire and South Yorkshire only resulted in small changes in the peak ozone concentration. The study concluded that it was difficult to identify any realistic and beneficial UK short-term actions for the type of extreme ozone events which have been recorded in the UK in recent years.

Task 3: Scenario Analysis and Task 4: Real-time Ozone Forecast Model - Short-term Action Plans (Using the OSRM).

A new model - the Ozone Source-Receptor model - has been developed and applied during the present project. It is similar in concept to the ELMO model but has the advantage of higher spatial resolution, the use of realistic air mass trajectories and the option to allow the emissions to vary temporally. The model can be used to derive a range of ozone exposure metrics at 10 km resolution across the UK for different emission control scenarios.

The model was benchmarked against the PTM-MCM on a single trajectory and found to give similar concentrations for ozone and other key species involved in photochemical ozone production. The model performance was then evaluated by comparison with measurements made at UK ozone monitoring stations. The maximum hourly-mean ozone concentrations were derived for each day in 1997. The fraction of the calculated maximum daily ozone

concentrations that lay within a factor of 1.5 below or 1.5 above the observed maximum ozone concentrations varied from 0.53 at Bottesford to about 0.77 at Strathvaich Dam.

Further evaluation of the OSRM performance was undertaken. The model was used to simulate the ozone, NO_x and NO_y measurements made at Lullington Heath and the nearby Barcombe Mills sites during a photochemical episode in June 2001. Model simulations were also undertaken using the PTM-CRI. The daily denuder measurements made at Barcombe Mills have provided an opportunity to test the ability of ozone photochemical models to simulate NO_y measurements. The performance of the two models is encouraging but further work is needed to optimise the formulation of the NO_y chemistry in the models. The performance of the OSRM is very comparable to that of the PTM-CRI, an accepted policy tool, for the trajectories and inventories used. Some of the discrepancy between the models will be due to the different formulation of, for example, the chemical mechanism, the photolysis processes and the parameters characterising the boundary layer. These simulations have shown that the OSRM is fundamentally robust.

AOT40 maps were prepared for the UK using the OSRM to demonstrate its capability for UK-scale modelling. Although the absolute magnitudes were overestimated, the model-derived maps give a reasonable description of the observed spatial distribution, apart from the high values on the east coast of Scotland. The AOT40 maps calculated by the OSRM for the year 1998 have significantly lower values than those shown in the corresponding 1997 maps, which was consistent with 1998 being a lower pollution year than 1997. The OSRM model is thus able to reproduce the difference caused by the changes in the meteorology from 1997 to 1998.

The OSRM was used to investigate the relative response to 30% reductions in the emissions of NO_x and VOCs. The results indicated that a 30% reduction in the NO_x emissions have a greater influence on 40 ppb exceedence days at the UK Rural Ozone Monitoring Network sites than a 30% reduction in the VOC reduction. For the higher O_3 exceedence thresholds, the results indicate a shift towards a greater response from VOC emission control. The responses agree reasonably well with those reported using the EUROSTOCHEM model, again providing confidence in the performance of the OSRM.

Recommendation: The Ozone Source-Receptor Model (OSRM) is a powerful tool for assessing UK and European emission reduction strategies as it uses realistic air mass trajectories. It should be applied to investigate various UK and European emission reduction scenarios.

Task 5: Improvements to Chemical and Photochemical Reaction Schemes

The Master Chemical Mechanism is an important component of the work to assess the contribution that individual volatile organic compounds (and hence emission sources) make to ozone formation. This will assist the development of policies to identify and target the VOCs or source sectors for control.

During the present contract, major improvements have been made to the reaction mechanisms of aromatic compounds - an important class of ozone-producing VOCs. Revision of the photolysis rates has been carried out, particularly with regard to multifunctional carbonyl products formed in the aromatic systems. The Master Chemical Mechanism has also been expanded to include the important biogenic compounds - α and β pinene. The new reaction schemes for aromatic compounds and terpenes have been tested against measurements made in chamber studies and the latest version of the Master Chemical Mechanism is able to reproduce those measurements, giving confidence in the MCM.

Using the knowledge and understanding gained from developing the MCM, a reduced mechanism - the Common Reactive Intermediate (CRI) mechanism - has been derived from the Master Chemical Mechanism. The CRI mechanism treats the degradation of methane and 120 VOC using approximately 570 reactions of 270 species (*i.e.* about 2 species per VOC). It provides a computationally-efficient mechanism for use in the Photochemical Ozone Trajectory Model. The CRI mechanism has been benchmarked against the MCM and was shown to produce almost identical concentrations for key species (O_3, OH, NO_3, RO_2 and HO_2).

The Master Chemical Mechanism continues to be widely used and is increasingly accepted as the benchmark for an explicit chemical mechanism of hydrocarbon oxidation. Version 3 and earlier versions of the MCM are available on the MCM web-site hosted by the University of Leeds.

Recommendations:

(a) ***Maintenance of the Master Chemical Mechanism:*** The chemistry of the existing 124 VOC in MCM v3 should be maintained to ensure that it incorporates the latest available information. A continued area of emphasis would necessarily be aromatic VOC for which new information is constantly becoming available.

(b) ***Maintenance of the MCM website***: The MCM website provides the opportunity to make the MCM available to the wider community. This allows independent testing and validation, and provides independent feedback on the performance of the mechanism. The website should therefore should be updated periodically in line with developments in the mechanism.

(c) ***Expansion of the MCM***: The MCM should be expanded to include a number of additional VOC which potentially make an important contribution to ozone formation, and which cannot be reasonably represented by an existing VOC in the mechanism. This should include additional major biogenic VOCs. In conjunction with this, it is recommended that an improved representation of biogenic emissions (magnitude and speciation) is required for the UK and NW Europe.

(d) ***Revision of Photolysis Rates***: Although some appraisal and revision of photolysis rates has been carried out within the present programme, particularly with regard to multifunctional carbonyl products formed in aromatic systems, a complete review of the basis of photolysis rates should be carried out to reflect improvements in the database.

(e) ***Inclusion of Organic Aerosol Formation Processes***: For large, cyclic, unsaturated VOC (such as aromatics and monoterpenes), it is well established that secondary organic aerosol (SOA) is formed in conjunction with ozone. The inclusion of routes to the formation of secondary organic aerosol (SOA) should therefore be considered. This will assist the validation of schemes using chamber data (where SOA formation influences the time dependence of the gas phase species) and will also allow any impact of SOA formation on ambient ozone generation to be assessed.

(f) ***Development and Application of Related Chemical Mechanisms***: In addition to work on the MCM, the current programme has led to associated improvements in other schemes used in ozone models (*e.g.* STOCHEM) and the development of the CRI mechanism. The CRI mechanism should be updated, and a method should be developed for improving the representation of aromatic degradation. The CRI mechanism methodology also provides a basis for representing the chemistry of a large number of hydrocarbons in the speciated

inventory which individually make small contributions, but which collectively represent a significant proportion of the 30% not currently covered by the MCM.

Task 6 : Policy Support

As part of Task 6, different versions of the photochemical trajectory model containing either the CRI or MCM mechanisms have been used to investigate the influence of a series of ozone precursor emissions controls on peak ozone levels typical of a UK photochemical episode.

Peak ozone concentrations have been simulated using the PTM-CRI for a series of year 2010 emissions scenarios related to the EU NECD, allowing the effectiveness of the different measures to be compared. Using an ozone episode occurring on the 31st July 1999 for this study, the influence of a series of the emissions scenarios on simulated peak ozone at 8 southern UK sites was determined. The present investigation of ozone precursor control scenarios using a representative case study allowed a number of conclusions can be drawn:

- Reductions in UK precursor emissions from 1998 to 2010 reference levels are calculated to have little or no effect on peak episodic ozone levels at locations to the east of the UK. Greater influences (up to 11% reduction) are calculated for locations on the west of the UK, or specific locations which are downwind of regions with particularly high UK emissions;
- Additional VOC reductions in the UK (1252 to 1200 kt a^{-1}) to meet the NECD target may have a small additional influence on selected downwind locations: further proposed reductions (1200 to 1150 kt a^{-1}) appear unlikely to have a major effect on peak episodic ozone levels. However, achievement of NECD targets throughout the EU (together with projected reductions in non-EU countries) were calculated to lead to a reduction of 20-25% in peak episodic ozone levels in the UK.
- The reduction of precursor emissions from 1998 to 2010 levels will be accompanied by a significant shift towards NO_X-limited conditions for episodic ozone formation.

It is likely that the actions taken to implement the United Nations Economic Commission for Europe VOC Protocol through EU Directives on motor vehicle emission controls has led to a reduction in the emissions of certain individual VOC species. In a separate modelling study undertaken in the project, a combination of the highly sophisticated Master Chemical Mechanism and speciated VOC inventories was used in the PTM for the standard Austria-UK trajectory. Ozone concentrations were calculated over a five day travel time in an air parcel which arrived at the England-Wales border. The peak ozone concentration calculated for the fifth and last day was 85.9 ppb. The UK PTM model was then rerun a further 124 times with the emission of each VOC species set to zero in turn. The difference in ozone concentrations was taken as an indication of the contribution to ozone formation of that VOC species. Some of the VOC species identified in motor vehicle emissions were found to be among the most prolific of all the VOC species in forming ozone.

If the contribution of each VOC to ozone production is combined with the observed trends in VOC concentrations, a downward trend in episodic peak ozone concentrations in north west Europe would have been expected during the 1990s. The present analyses should be extended to address the quantitative origins of the elevated ozone concentrations in terms of the VOC emissions from individual stationary source categories and the National Plan for VOCs and ozone.

Recommendation: There will be a continued need to use numerical models containing a detailed description to simulate ozone formation from each of the stationary VOC source categories.

12 Acknowledgements

The authors gratefully acknowledge the support provided by the Department for Environment, Food and Rural Affairs for this work under contract EPG 1/3/143. Additional technical input and support for the development of the Master Chemical Mechanism was provided by the projects commissioned by the European Union on the *Effects of the Oxidation of Aromatic Compounds in the Troposphere* (EVK2-1999-00332) and *Origin and Formation of Secondary Organic Aerosol* (EVK2-CT-1999-00016).

13 References

AQS (2000) **The Air Quality Strategy for England, Scotland, Wales and Northern Ireland**. Department of the Environment, Transport and the Regions, Scottish Executive, National Assembly for Wales, Department of the Environment for Northern Ireland. CM 4548, SE2000/3, NIA7 Jan 2000, ISBN 0 10 145482-1 (http://www.environment.detr.gov.uk/airquality/index.htm).

Altshuler S.L., Arcado T.D., Lawson D.R. (1995) **Weekday *vs*. Weekend Ambient Ozone Concentrations: Discussion and Hypotheses with Focus on Northern California**. Journal of the Air and Waste Manage ment Association, **45**, 967-972.

Alvarado A., Tuazon E.C., Aschmann S.M., Atkinson R., Arey J., (1998a) **Products of the Gas-phase Reactions of O(^{3}P) atoms and O_3 with α-pinene and 1,2-dimethyl-1-cyclohexene**. Journal of Geophysical Research, **103**, 25541 -25551.

Alvarado A., Arey J., Atkinson R. (1998b) **Kinetics of the Gas-phase Reactions of OH and NO_3 Radicals and O_3 with the Monoterpene Reaction products Pinonaldehyde, Caronaldehyde and Sabinaketone**. Journal of Geophysical Research, **103**, 25541 - 25551.

Andreae M.O., Crutzen P.J. (1997) **Atmospheric Aerosols: Biogeochemical Sources and Role in Atmospheric Chemistry**. Science, **276**, 1052-1058.

Arey J., Atkinson R., Aschmann S.M. (1990) **Product Study of the Gas-phase Reactions of Monoterpenes with the OH Radical in the Presence of NO_x**. Journal of Geophysical Research, **95**, 18539 -18546.

Aschmann S.M., Reissel A., Atkinson R., Arey J., (1998) **Products of the Gas-phase Reaction of the OH radical with α- and β-Pinene in the Presence of NO_x**. Journal of Geophysical Research, **103**, 25553 -25561.

Ashworth J.R. (1929) **The Influence of Smoke and Hot Gases from Factory Chimneys on Rainfall**. Quarterly Journal of the Royal Meteorological Society, **55**, 341-350.

Atkinson, R. (1994) **Gas-phase Tropospheric Chemistry of Organic Compounds**. Journal of Physical Chemistry Reference Data, Monograph 2, 1-216.

Atkinson, R. (1998) **Gas-phase Degradation of Organic Compounds in the Troposphere**. Pure and Applied Chemistry **70** (7), 1327-1334.

Atkinson, R., Arey, J., (1998) **Atmospheric Chemistry of Biogenic Organic Compounds**. Accounts of Chemical Research, **31**, 574-583.

Atkinson R., Aschmann S.M. and Arey J. (1991) **Formation of Ring-retaining Products from the OH radical initiated reactions of o-, m- and p-xylene**. International Journal of Chemical Kinetics, **23**, 77-97.

Bandow, H., Washida, N. (1985). **Ring-cleavage Reactions of Aromatic Hydrocarbons Studied by FT-IR spectroscopy. II. Photo-oxidation of o-, m- and p-xylenes in the NO_x-air System**. Bulletin of the Chemical Society of Japan, **58**, 2541-2548.

Barnes I., Thomas W., Becker K.H. (2000) **Atmospheric Chemistry of Organic Tricarbonyl Compounds: Detection in the Photo-oxidation of Aromatic Hydrocarbons**. Proceedings of the workshop on 'Chemical Behaviour of Aromatic Hydrocarbons in the Troposphere', ed. K.H. Becker. Valencia, Spain, February 2000.

Berndt T., Boge O. (1997) **Products and Mechanism of the Gas-phase Reaction of NO_3 radicals with α-pinene**. Journal of the Chemical Society, Faraday Transactions, **93**, 3021-3027.

Berndt T., O. Boge, H. Herrmann (1999) **On the formation of Benzene Oxide/Oxepin in the Gas-phase Reaction of OH Radicals with Benzene**. Chem.Phys.Lett., **314**, 435-442.

Bierbach A., Barnes I., Becker K.H., Wiesen E. (1994) **Atmospheric Chemistry of Unsaturated Dicarbonyls: Butenedial, 4-oxo-2-pentenal, 3-hexene-2,5-dione, Maleic Anhydride, 3H-furan-2-one and 5-methyl-3H-furan-2-one**. Environmental Science and Technology, **29**, 715-729.

Bohn B., C. Zetzsch (1999) **Gas-phase reaction of the OH-benzene Adduct with O_2: Reversibility and Secondary Formation of HO_2**. Physical Chemistry Chemical Physics, **1**, 5097-5107.

Bower J.S., Broughton G.F., Dando M.T., Stevenson K.J., Lampert J.E., Sweeney B.P., Parker V.J., Driver G.S., Clark A.G., Waddon C.J., Wood A.J., Williams M.L. (1989) **Surface Ozone Concentrations in the UK in 1987-1988**. Atmospheric Environment, **23** (9), 2003-2016.

Bower, J.S., Broughton, G.F.J, Stedman, J.R., Williams, M.L. (1994) **A Winter NO_2 Smog episode in the UK**. Atmospheric Environment **28** (3), 461-475.

Bowman F.M., Seinfeld J.H. (1994) **Ozone Productivity of Atmospheric Organics**. J. Geophys. Res., **99**, 5309-5324.

Broennimann S., Neu U. (1997) **Weekend-weekday Differences on Near-surface Ozone Concentrations in Switzerland for Different Meteorological Conditions**. Atmospheric Environment, **31** (8), 1127-1135.

Burgess R.A., Penkett S.A. (1993**) Ground-based Non-methane Hydrocarbon Measurements in England**. Proceedings of the EUROTRAC'92 Symposium, Garmisch-Partenkirchen, March 1992. Academic Publishing, The Hague, The Netherlands, pp.165-169.

Calogirou A., Larsen B.R., Kotzias D. (1999) **Gas-phase Terpene Oxidation Products: A Review**. Atmospheric Environment, **33**, 1423-1439.

Carslaw D.C, S.D. Beevers, G. Fuller (2001) **An Empirical Approach for the Prediction of Annual Mean Nitrogen Dioxide Concentrations in London**. Atmospheric Environment, **35**, 1505-1515.

Carter W.P.L. (1994) **Development of Ozone Reactivity Scales for Volatile Organic Compounds**. J. of the Air and Waste Man. Assoc., **44**, 881-899.

Christoffersen T.S., Hjorth J., Horie O., Jensen H.R., Kotzias D., Molander L.L., Neeb P., Ruppert L., Winterhalter R., Virkkula A. Wirtz K., Larsen B.R. (1998) ***Cis*-pinic acid, A Possible Precursor for Organic Aerosol Formation from Ozonolysis of α-pinene**. Atmospheric Environment, **32**, 1657-1661.

Clapp, L.J., Jenkin, M.E. (2001) **Analysis of the Relationship between Ambient Levels of O_3, NO_2 and NO as a function of NO_X in the UK**. Atmospheric Environment **35**, 6391-6405.

Collins W.J., Stevenson D.S., Johnson C.E., Derwent R.G. (1997) **Tropospheric Ozone in a Global-scale Three-dimensional Lagrangian model and its Response to NO_x Emission Controls**. Journal of Atmospheric Chemistry, **26**, 223-274.

Collins W.J., Stevenson D.S., Johnson C.E., Derwent R.G. (1999) **The Role of Convection in determining the Budget of Odd Hydrogen in the Upper Troposphere**. Journal of Geophysical Research, **104**, 26,927-26,941.

Collins W.J., Stevenson D.S., Johnson C.E., Derwent R.G. (2000) **The European Regional Ozone Distribution and its Links with the Global Scale for the Years 1992 and 2015**. Atmospheric Environment, **34**, 255-267.

Derwent R. G. (1999a) **Oxides of Nitrogen and Ozone in the London Routine Column Trajectory model**. Climate Research Division, Meteorological Office, Bracknell.

Derwent R.G. (1999b) **The Potential Influence of any Future Increase in Global Ozone Concentrations on Nitrogen Dioxide Concentrations in London**. Climate Research Division, Meteorological Office, Bracknell.

Derwent R.G., Middleton D.R., Field R.A., Goldstone M.E., Lester J.N., Perry R. (1995) **Analysis and Interpretation of Air Quality Data from an Urban Roadside Location in Central London over the Period from July 1991 to July 1992**. Atmospheric Environment, **29** (8), 923-946.

Derwent R.G., M.E. Jenkin, S.M. Saunders (1996) **Photochemical Ozone Creation Potentials for a Large Number of Reactive Hydrocarbons Under European Conditions**. Atmospheric Environment, **30**, 181-199.

Derwent R.G., Jenkin M.E., Saunders S.M., Pilling M.J. (1998) **Photochemical Ozone Creation Potentials for Organic Compounds in North West Europe Calculated with a Master Chemical Mechanism**. Atmospheric Environment, **32**, 2419-2441.

Derwent R.G., Jenkin M.E., Saunders S.M., Pilling M.J. (2001) **Characterisation of the Reactivities of Volatile Organic Compounds using a Master Chemical Mechanism**. Journal of Air and Waste Management Association **51**, 699-707.

Diem J.E. (2000) **Comparisons of Weekday-weekend Ozone: Importance of Biogenic Volatile Organic Compound Emissions in the Semi-arid Southwest USA**. Atmospheric Environment, **34**, 3445-3451.

Dimitriades B. (1996) **Scientific Basis for the VOC Reactivity Issues raised by Section 183(c) of the Clean Air Act Amendments of 1990**. Journal of the Air and Waste Management Association, **46**, 963-970.

Eggleston H.S., Goodwin J. (1994) **National Atmospheric Emissions Inventory**. NETCEN, Culham Laboratory, Oxfordshire, UK.

EMEP (2001) **Transboundary Acidification, Eutrophication and Ground-level Ozone in Europe**. EMEP summary report 2001. EMEP Report 1/2001, DNMI Research Report 124, Det Norske Meteorologiske Institutt, Oslo, Norway.

EMEP-CORINAIR (1996) **Atmospheric Emission Inventory Guidebook**. Edited by G McInnes.

EPAQS (1994) **Ozone**. The Expert Panel on Air Quality Standards. ISBN 0-11-752873-0, The Stationery Office, 1994.

EPAQS (1996) **Nitrogen Dioxide**. The Expert Panel on Air Quality Standards. ISBN 0-11-753352-1, The Stationery Office, 1996.

EU (1992) **Council Directive 92/72/EEC of 12 September 1992 on Air Pollution by Ozone**. Official Journal of the European Communities, N° L297, Vol 34.

Elkus B., Wilson K.R. (1977) **Photochemical Air Pollution: Weekend-weekday Differences**. Atmospheric Environment, **11**, 509-515.

Forstner H.J.L., Flagan S.C., Seinfeld J.H. (1997) **Secondary Organic Aerosol from the Photo-oxidation of Aromatic Hydrocarbons: Molecular Composition**. Environmental Science and Technology, **31**, 1345-1358.

Ghigo G., G. Tonachini (1999) **From Benzene to Muconaldehyde: Theoretical Mechanistic Investigation on some Tropospheric Oxidation Channels**. Journal of the American Chemical Society, **121**, 8366-8372.

Glasius M., Calogirou A., Jensen N.R., Hjorth J., Nielsen C.J. (1997) **Kinetic Study of the Gas-phase Reactions of Pinonaldehyde and Structurally-related Compounds**. International Journal of Chemical Kinetics, **29**, 527-533.

Glasius M., Lahaniati M., Calogirou A., Di Bella D., Jensen N.R., Hjorth J., Kotzias D., Larsen B.R. (1999) **Carboxylic Acids in Secondary Aerosols from the Oxidation of Cyclic Monoterpenes by Ozone**. Environmental Science and Technology.

Graedel T.E., Farrow L.A., Webster T.A. (1977) **Photochemistry of the "Sunday Effect"**. Environmental Science and Technology, **11**, 690-694.

Gery M.W., Whitten, G.Z., Killus, J.P., Dodge, M.C. (1989) **A Photochemical Kinetics Mechanism for Urban- and Regional-scale Computer Modelling**. Journal of Geophysical Research, **94**, 12925-12956.

Goodwin, J.W.L., Salway, A.G., Murrells, T.P., Dore, C.J., Passant, N.P., King, K.R., Coleman, P.J., Hobson, M.M., Pye, S.T., Watterson, J.D. (2001) **UK Emissions of Air Pollutants 1970-1999.** A Report (AEAT/ENV/R/0798) of the National

Atmospheric Emission Inventory prepared for the Department for Environment, Food and Rural Affairs, ISBN 1-85580-031-4.

Gordon C. *et al.* (2000) **The Simulation of SST, Sea Ice Extents and Ocean Heat Transports in a Version of the Hadley Centre Coupled Model without Flux Adjustments**. Climate Dynamics, **16**, 147-168.

Guenther A., Zimmerman P., Wildermuth M. (1994) **Natural Volatile Organic Compound Emission Rate Estimates for US Woodland Landscapes**. Atmospheric Environment, **28**, 1197-1210.

Hallquist M., Wangberg I., Ljungstrom E. (1997) **Atmospheric Fate of Dicarbonyl Products Originating from α-pinene, and Δ^3-Carene: Determination of Rate of Reaction with OH and NO_3 Radicals, UV Absorption Cross Sections and Vapor Pressures**. Environmantal Science and Technology, **31**, 3166-3172.

Hakola H., Arey J., Aschmann S.M., Atkinson R. (1994) **Product Formation from the Gas-phase Reactions of OH Radicals and O_3 with a series of Monoterpenes**. Journal of Atmospheric Chemistry, **18**, 75-102.

Hayman G.D. (1997) **Effects of Pollution Control on UV Exposure**. Final Report (Reference AEA/RCEC/22522001/R/002 ISSUE1) prepared for the Department of Health on Contract 121/6377.

Hayman, G.D, Hasler S., Vincent K., Baker S., Donovan B., Smith M., Davies M., Sutton M., Tang Y.S., Dragosits U., Love L., Fowler D., Sansom L. and Page H. (2001) **Operation and Management of the UK Acid Deposition Monitoring Networks: Data Summary for 2000**. AEA Technology Report AEAT/ENV/R/0740 Issue 1. AEA Technology plc, E5 Culham, Abingdon, OX14 3ED.

Heywood (1988) **Internal Combustion Engine Fundamentals**. McGraw-Hill, New York.

Hjellbrekke, A.-G. (1999) **Ozone Measurements 1997**. Norwegian Institute for Air Research, EMEP/CCC-Report 2/99, Kjeller, Norway.

Hoffmann T., Bandur R., Marggraf U., Linscheid M. (1998) **Molecular Composition of Organic Aerosols formed in the α-pinene/O_3 Reaction: Implications for New Particle Formation Processes**. Journal of Geophysical Research, **103**, 25,569-25,578.

Jacob D. , Wofsy S. (1988) **Photochemistry of Biogenic Emissions over the Amazon Forest**. Journal of Geophysical Research, **93**, 1477-1486.

Jang M., Kamens R.M. (2001) **Characterisation of Secondary Aerosol from the Photooxidation of Toluene in the presence of NO_X and 1-propene**. Environmental Science and Technology, **35**, 3626-3639.

Jeffries, H.E., Yu, J., Bartolotti, L. (1995) **Theoretical and Analytical Advances in Understanding Aromatics Atmospheric Oxidation Mechanisms**. Workshop on 'Chemical mechanisms Describing Oxidation Processes in the Troposphere'. Valencia, Spain.

Jenkin M.E., G.D. Hayman (1999) **Photochemical Ozone Creation Potentials for Oxygenated Organic Compounds: Sensitivity to Variations in Kinetic and Mechanistic Parameters**. Atmospheric Environment, **33**, 1275-1293.

Jenkin M.E., Clemitshaw K.C. (2000) **Ozone and Other Secondary Photochemical Pollutants: Chemical Processes governing their Formation in the Planetary Boundary Layer**. Atmospheric Environment, **34**, 2499-2527.

Jenkin M.E., Saunders S.M., Pilling M.J. (1997) **The Tropospheric Degradation of Volatile Organic Compounds: A Protocol for Mechanism Development**. Atmospheric Environment, **31**, 81-104.

Jenkin M.E., Hayman G.D., Derwent R.G., Saunders S.M., Carslaw N., Pilling M.J. (1999) **Tropospheric Chemistry Modelling: Improvements to Current Models and Application to Policy Issues**. Final Report (Reference AEAT-4867/20150/R004 Issue 1) prepared for the Department of the Environment, Transport and the Regions on Contract EPG 1/3/70. March 1999.

Jenkin M.E., Davies, T.J., Hayman, G.D., Stedman, J.R., Thetford, R., Fitzgerald, P.L., Derwent, R.G., Collins, W.J., Saunders, S.M., Pilling, M.J. (2000a) **Modelling of Tropospheric Ozone Formation**. First Annual Report on the DETR contract EPG 1/3/143. Report AEAT/R/ENV/0099 Issue 1.

Jenkin M.E., Murrells T.P., Passant N.R. (2000b) **The Temporal Dependence of Ozone Precursor Emissions: Estimation and Application**. AEA Technology report AEAT/R/ENV/0355 Issue 1. Prepared for Department of the Environment, Transport and the Regions.

Jenkin M.E., Clapp, L.J., Davies, T.J., Hayman, G.D., Stedman, J.R., Thetford, R., Fitzgerald, P.L., Derwent, R.G., Collins, W.J., Saunders, S.M., Pilling, M.J. (2001) **Modelling of Tropospheric Ozone Formation**. Second Annual Report on the DETR contract EPG 1/3/143. Report AEAT/R/ENV/0485 Issue 1.

Jenkin, M.E., Saunders, S.M., Derwent, R.G., Pilling, M.J. (2002a) **Development of a Reduced Speciated VOC Degradation Mechanism for Use in Ozone Models**. Submitted to Atmospheric Environment.

Jenkin M.E., Davies T.J., Stedman J.R. (2002b) **The Origin and Day-of-week Dependence of Photochemical Episodes in the UK**. Atmospheric Environment **36**, 999-1012.

Johnson C.E., Derwent R.G. (1996) **Relative Radiative Forcing Consequences of Global Emissions of Hydrocarbons, Carbon Monoxide and NO_x from Human Activities estimated with a Zonally-averaged Two-dimensional Model**. Climate Change, **34**, 439-462.

Kamens R., Jang M., Chien C.J., Leach K. (1999) **Aerosol Formation from the Reaction of α-pinene and Ozone using a Gas-phase Kinetics-Aerosol Partitioning Model**. Environmental Science and Technology, **33**, 1430-1438.

Karl T.R. (1978) **Day of Week Variations of Photochemical Pollutants in the St. Louis Area**. Atmospheric Environment, **12**, 1657-1667.

Klotz B.G., Bierbach A., Barnes I. Becker K.H., Golding B.T. (1997) **Atmospheric Chemistry of Benzene Oxide/Oxepin**. J.Chem. Soc. Faraday Trans. **93**, 1507.

Klotz B.., Barnes I., Becker K.H. (1998) **New Results on the Atmospheric Photo-oxidation of Simple Alkylbenzenes**. Chem. Phys., **231**, 289-301.

Kurtenbach R., Becker K.H., Gomes J.A,G., Kleffmann J., Loerzer J.C., Spittler M., Wiesen P. , Ackermann R., Geyer A., Platt U. (2001) **Investigations of Emissions and Heterogeneous Formation of HONO in a Road Traffic Tunnel**. Atmospheric Environment **35**, 3385-3394.

Leighton P.A. (1961) **Photochemistry of Air Pollution**. Academic Press, New York.

Lurmann F.W., Carter W.P.L., Coyner L.A. (1987) **A Surrogate Species Chemical Mechanism for Urban-scale Air Quality Simulation Models**. US EPA Report EPA/600/3-87/014, United States Environmental Protection Agency, Research Triangle Park, North Carolina.

Martinez-Villa G., Clemitshaw K.C., Marsh A.R. (2000**) Observations of Nitrous Acid at a Kerbside Site in Central London**. Presented at workshop on traffic emissions, roadway and tunnel studies, Vienna University of Technology, October 1-3, 2000.

McInnes G. (1994) **CORINAIR 1990**. European Environment Agency, Copenhagen, Denmark.

McLaren R., Singleton D.L., Lai J.Y.K., Khouw B., Singer E., Wu Z., Niki H. (1996) **Analysis of Motor Vehicle Sources and their Contribution to Ambient Hydrocarbon Distributions at Urban Sites in Toronto during the Southern Oxidants Study**. Atmospheric Environment, **30** (12), 2219-2232.

Monks P.S. (2000) **A Review of the Observations and Origins of the Spring Ozone Maximum**. Atmospheric Environment, **34**, 3545-3561.

Moschonas N., D. Danalatos, S. Glavas (1999) **The effect of O_2 and NO_2 on the Ring-retaining Products of the Reaction of Toluene with Hydroxyl Radicals**. Atmospheric Environment, **33**, 111-116.

Murphy, D.M., Fahey, D.W. (1994) **An Estimate of the Flux of Stratospheric Reactive Nitrogen and Ozone into the Troposphere**. Journal of Geophysical Research, **99**, 5325-5332.

Nakicenovic N.J., *et al.* (2000) **Emissions Scenarios**. A Special Report of Working Group III of the Intergovernmental Panel on Climate Change, Cambridge University Press.

NORDIC (1991) **Photochemical Oxidants in the Atmosphere**. Nordic Council of Ministers, NORD 1991:7, Copenhagen, Denmark.

Noziere B., Barnes I., Becker K.H. (1999a) **Product Study of the Reactions of α-Pinene and of Pinonaldehyde with OH radicals**. Journal of Geophysical Research, in press.

Noziere B., Spittler M., Ruppert L., Barnes I., Becker K.H., Pons M., Wirtz K. (1999b) **Kinetics of the Reactions of Pinonaldehyde with OH Radicals and with Cl Atoms**. International Journal of Chemical Kinetics, 104, 23645-23656.

NEGTAP (2001) **Transboundary Air Pollution: Acidification, Eutrophication and Ground-level Ozone in the UK.** Report prepared by the National Expert Group on Transboundary Air Pollution on behalf of the Department for Environment, Food and Rural Affairs and the Devolved Administrations (ISBN 1 870393 61 9).

Parrish, D.D., Holloway, J.S., Trainer, M., Murphy, P.C., Forbes, G.L., Fehsenfeld F. (1993) **Export of North American Ozone Pollution to the North Atlantic**. Science, **259**, 1436-1439.

Passant N.R. (2000). AEA Technology. Private communication.

Passant N.R. (2002) **Speciation of UK Emissions of Non-methane Volatile Organic Compounds**. AEA Technology Report ENV-0545, Culham, Abingdon, United Kingdom.

Pont V., Fontan J. (2001) **Comparison between Weekend and Weekday Ozone Concentration in Large Cities in France**. Atmospheric Environment, **35**, 1527-1535.

Pryor S.C., Steyn D.G. (1995) **Hebdomadal and Diurnal Cycles in Ozone Time Series from the Lower Fraser Valley, BC**. Atmospheric Environment, **29** (9), 1007-1019.

PORG (1993) **Ozone in the United Kingdom**. Third report of the UK Photochemical Oxidants Review Group, Department of the Environment, London. Published by Institute of Terrestrial Ecology, Bush Estate, Penicuik, Midlothian, EH26 0QB, UK. ISBN: 0 7058 1683 4, and available at www.aeat.co.uk/netcen/airqual/reports/home.html.

PORG (1997) **Ozone in the United Kingdom**. Fourth report of the UK Photochemical Oxidants Review Group, Department of the Environment, Transport and the Regions, London. Published by Institute of Terrestrial Ecology, Bush Estate, Penicuik, Midlothian, EH26 0QB, UK. ISBN: 0-870393-30-9, and available at www.aeat.co.uk/netcen/airqual/reports/home.html.

QUARG (1993) **Urban Air Quality in the United Kingdom**. First report of the Quality of Urban Air Review Group. Prepared at the request of the Department of the Environment, London.

Rasmussen R.A. (1972) **What do the Hydrocarbons from Trees Contribute to Air Pollution?** Journal of Air Pollution Control Association, **22**, 537-543.

Reimann S., Calanca P., Hofer P (2000) **The Anthropogenic Contribution to Isoprene Concentrations in a Rural Atmosphere**. Atmospheric Environment, **34**, 109-115.

Ross S. (1996) **Stochastic Processes**. Second Edition, John Wiley and Sons, New York.

Ryall, D.B., Maryon, R.H. (1998) **Validation of the UK Meteorological Office's NAME Model against the ETEX Dataset**. Atmospheric Environment **32**, 4265-4276.

Saunders S.M., M.E. Jenkin, R.G. Derwent and M.J. Pilling (1997) **Report Summary: World Wide Web site of a Master Chemical Mechanism (MCM) for use in Tropospheric Chemistry Models**. Atmospheric Environment, **31**, 1249-1250.

Sillman S. (1999) **The Relationshp between Ozone, NO_X and Hydrocarbons in Urban and Polluted Rural Environments**. Atmospheric Environment, **33** (12), 1821-1845.

Sillman S., He, D., Cardelino, C., Imhoff, R.E. (1997) **The Use of Photochemical Indicators to Evaluate Ozone-NO_x-hydrocarbon sensitivity: Case Studies from Atlanta, New York, and Los Angeles**. Journal of the Air and Waste Management Association, **47**, 1030-1040.

Simmonds P.G., Derwent, R.G., McCulloch, A., O'Doherty, S., Gaudry, A. (1996) **Long-term Trends in Concentrations of Halocarbons and Radiatively-active Trace Gases in Atlantic and European Air Masses Monitored at Mace Head, Ireland from 1987-1994**. Atmospheric Environment, **30**, 4041-4063.

Simpson, D., Guenther, A., Hewitt, C.N., Steinbrecher, R. (1995) **Biogenic Emissions in Europe 1. Estimates and Uncertainties**. Journal of Geophysical Research, **100**, 22875-22890.

Smith D.F., T.E. Kleindienst, C.D. McIver (1999) **Primary Product Distributions from the Reaction of OH with m-, p-Xylene, 1,2,4- and 1,3,5-trimethylbenzene**. Journal of Atmospheric Chemistry, **34**, 339-364.

Sofiev M., Tuovinen J-P. (2001) **Factors determining the Robustness of AOT40 and Other Ozone Exposure Indices**. Atmospheric Environment **35**, 3521-3528.

Sørensen, S., Barnes, I., Becker, K.H. (1998) **Photolysis of Unsaturated 1,4-dicarbonyls under Atmospheric Conditions in the European Photo Reactor (EUPHORE)**. Environmental Science and Pollution Research, **5**, 159.

Stedman J. R. (1999) **Site-specific Projections of NO_X and NO_2 Concentrations for the UK**. AEA Technology, National Environmental Technology Centre. Report AEAT – 5850, available at (www.aeat.co.uk/netcen/airqual/reports/home.html).

Stedman J.R. (2001). AEA Technology Environment. Personal Communication.

Stedman J., Williams M.L. (1991) **A Trajectory Analysis of the Relationship between Ozone in the United Kingdom and Precursor Emissions**. Warren Spring Laboratory report LR 768 (AP).

Stedman, J.R., Williams, M.L. (1992) **A Trajectory Model of Relationship between Ozone and Precursor Emissions**. Atmospheric Environment, **26A**, 1271-1281.

Stedman, J.R., Willis, P.G. (1996) **Air Quality Forecasting in the United Kingdom, 1995**. Report AEA/RAMP/20008001/002 Culham: AEA Technology, National Environmental Technology Centre.

Stedman, J. R., Espenhahn, S. E., Willis, P. G., Jenkin, M.E. (1997) **Air Quality Forecasting in the United Kingdom: 1996**. AEA Technology, National Environmental Technology Centre. Report AEA/RAMP/20008001/004. AEAT-1693.

Stedman J.R., Bush T., King K. (1998) **An Empirical Model for Estimating Roadside Nitrogen Dioxide Concentrations in the UK**. AEA Technology, National Environmental Technology Centre. Report AEAT-4291, available at www.aeat.co.uk/netcen/airqual/reports/home.html.

Stedman J.R., Bush T., Linehan E.B. (2000) **The 10-year Transport Plan. Site-specific Analyses of Ambient NO_2 and PM_{10} Concentrations**. AEA Technology, National Environmental Technology Centre Report AEAT/R/ENV/0166, available at www.aeat.co.uk/netcen/airqual/reports/home.html.

Stephenson G. (1992) **Mathematical Methods for Science Students**. Second Edition, Longman, London.

Stevenson, D.S., Collins, W.J., Johnson, C.E., Derwent, R.G (1997a) **Tropospheric Ozone in a Global-Scale Three-Dimensional Lagrangian Model and its Response to NO_x Emission Control**. Journal of Atmospheric Chemistry, **26**, 223-274.

Stevenson, D.S., Collins, W.J., Johnson, C.E., Derwent, R.G (1997b) **The Impact of Aircraft Nitrogen Oxide Emissions on Tropospheric Ozone Studied with a 3D Lagrangian Model including Fully Diurnal Chemistry**. Atmospheric Environment, **31**, 1837-1850.

Trainer M., Williams E., Parrish D., Burhr M., Allwine E., Westberg H., Fehsenfeld F., Liu S. (1987) **Models and Observations of the Impact of Natural Hydrocarbons on Rural Ozone**. Nature, 705-707.

Tuovinin J.-H, Barrett K., Styve H. (1994) **Transboundary Acidifying Pollution in Europe: Calculated Fields and Budgets 1985-1993**. EMEP/MSC-W Report 1/94. Norwegian Meteorological Institute, Oslo, Norway.

UN ECE (1988) **Protocol to the 1979 Convention on Long-range Transboundary Air Pollution Concerning the Control of Emissions of Nitrogen Oxides Compounds or their Transboundary Fluxes.** United Nations Economic Commission for Europe, Geneva, Switzerland.

UN ECE (1991) **Protocol to the 1979 Convention on Long-range Transboundary Air Pollution Concerning the Control of Emissions of Volatile Organic Compounds or their Transboundary Fluxes. ECEIEB.AIR/30**. United Nations Economic Commission for Europe, Geneva, Switzerland.

UN ECE (1992) **Air Pollution Studies 8: Impacts of Long-range Transboundary Air Pollution**. Published by United Nations.

UN ECE (1993) **Air Pollution Studies 9: The State of Transboundary Air Pollution 1992 Update**. Published by United Nations.

UN ECE (1994) **Environmental Conventions**. Published by United Nations.

US EPA (1995) **Compilation of Air Emission Factors, Volume 1, 5th Edition**. United States Environment Protection Agency, Report AP-42, North Carolina, USA.

Volkamer, R. Platt, U., Wirtz, K., (2001) **Primary and Secondary Glyoxal Formation from Aromatics: Experimental Evidence for the Bicycloalkyl-radical Pathway from Benzene, Toluene, and *p*-Xylene**. J. Phys. Chem. A **105**, 7865-7874.

Volz, A., Kley, D. (1988) **Evaluation of the Montsouris Series of Ozone Measurements made in the Nineteenth Century.** Nature, **332**, 240-242.

Wagner V., Jenkin M.E., Saunders S.M., Stanton J., Wirtz K., Pilling M.J. (2002) **Modelling of the Photooxidation of Toluene: Conceptual Ideas for Validating Detailed Mechanisms**. In preparation.

Wangberg I, Barnes I, Becker K.H. (1997) **Product and Mechanistic Study of the Reaction of NO_3 radicals with α-pinene**. Environmental Science and Technology, **31**, 2130-2135.

Went F.W. (1960) **Blue Hazes in the Atmosphere**. Nature, **187**, 641-643.

WHO (1994) **Updating and Revision of the Air Quality Guidelines for Europe**. Report of the WHO working group on ecotoxic effects. Les Diablerets, Switzerland, 22-23 September 1993. World Health Organisation, Copenhagen, Denmark.

WHO (1995) **Updating and Revision of the Air Quality Guidelines for Europe**. Meeting of the WHO working group on 'classical air pollutants'. Bilthoven, the Netherlands, 11-14 October 1994. World Health Organisation, Copenhagen, Denmark.

Wilby R.L., Tomlinson O.J. (2000) **The 'Sunday Effect' and Weekly Cycles of Winter Weather in the UK**. Weather, **55**, 214-222.

Winterhalter R., Neeb P., Grossmann D., Kollof A., Horie O., Moortgat G.K. (2000) **Products and Mechanism of the Gas-phase Reaction of Ozone with β-pinene**. Journal of Atmospheric Chemistry, **35**, 167-197.